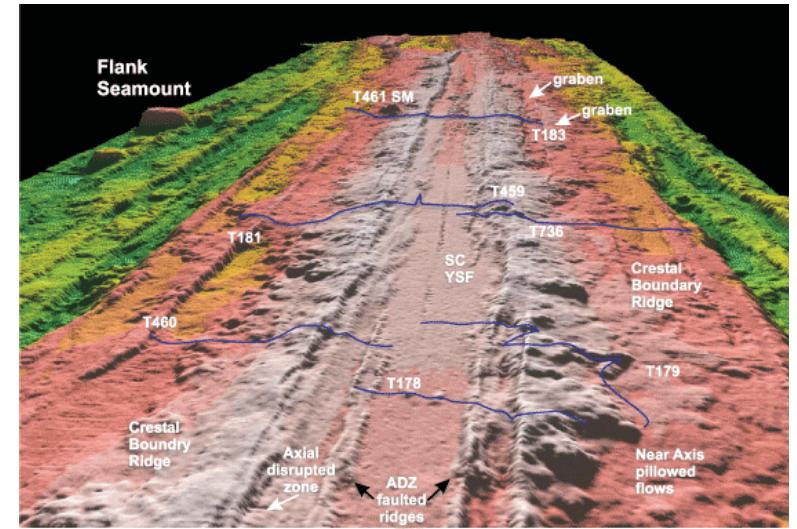


Mineral Physics 1: Earth Mineralogy and Phase Diagrams

June 27, 2016 CIDER



Jennifer M. Jackson,

Natalia V. Solomatova, PhD student
Seismological Laboratory
Geological and Planetary Sciences
California Institute of Technology

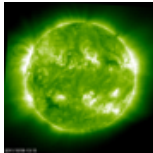


Outline

1. Basic Compositional Constraints
2. Building Minerals
3. Coordination environments
4. Substitution Mechanisms
5. Two Component Phase Diagrams, including
Partial Melting
6. Additional slides on single crystal elasticity,
composites, and thermal equations of state

Compositional constraints for Earth's interior

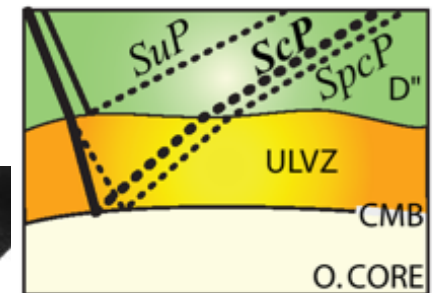
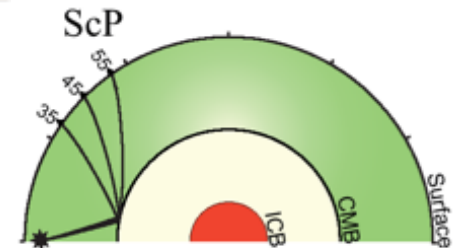
- Solar atmospheric analyses



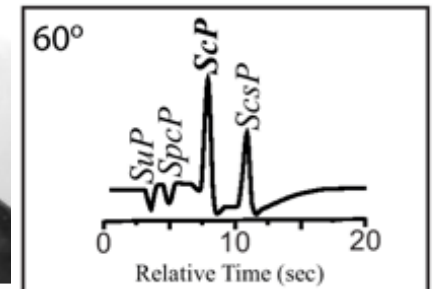
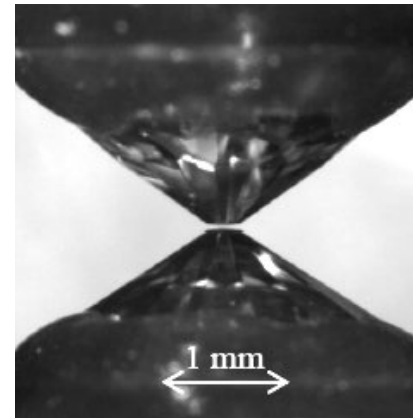
Kola Superdeep Borehole
12.262 km (Kola 1989)

- **Mineralogy and (isotope) geochemistry**

- Drill cores, mantle xenoliths, meteorites



diamond-anvil cells



- **Going deeper**

- Geophysical observations, seismology, gravity
- Extreme conditions: theory and experiments

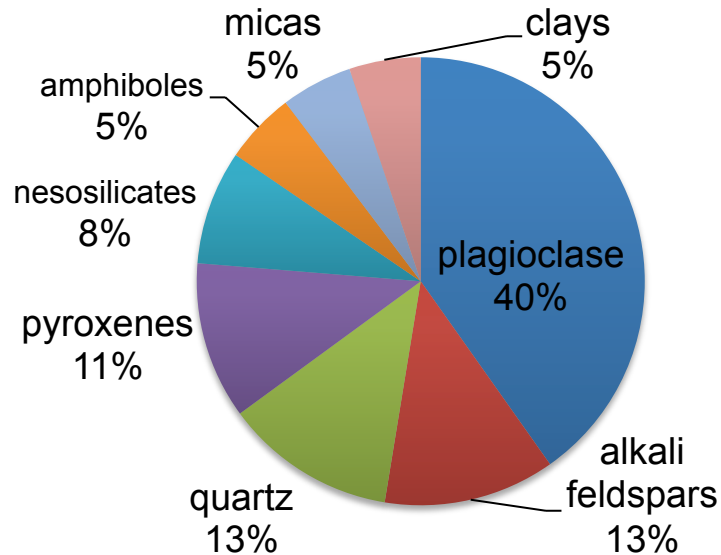


Earth Chemistry (in general)

Element Name	Symbol	Weight% crust	Weight% Whole Earth (approx.)
Oxygen	O ²⁻	45.2	30
Silicon	Si ⁴⁺	27.2	15
Aluminum	Al ³⁺	8.0	1
Iron	Fe ^{0,2+,3+}	5.8	34.5
Calcium	Ca ²⁺	5.1	1
Magnesium	Mg ²⁺	2.8	12.5
Sodium	Na ⁺	3.2	<1
Potassium	K ⁺	1.7	<1
Nickel	Ni ²⁺	<1	4
Sulfur	S	<1	2

Where these elements reside dictates elastic and transport properties

Abundance of the major minerals on the surface of the Earth (crust)



Role of atomic structure:

Solids: crystalline vs. amorphous

Regular array of atoms lowers the systems energy.

Competition between attractive (binding) and repulsive (electrostatic) forces.

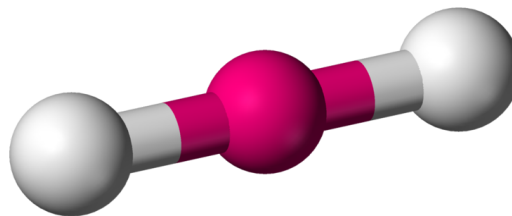
Structure plays a major role in determining physical properties of materials.

Determination: X-ray and neutron diffraction, ab initio (bulk). TEM, EBSD, AFM (surface).

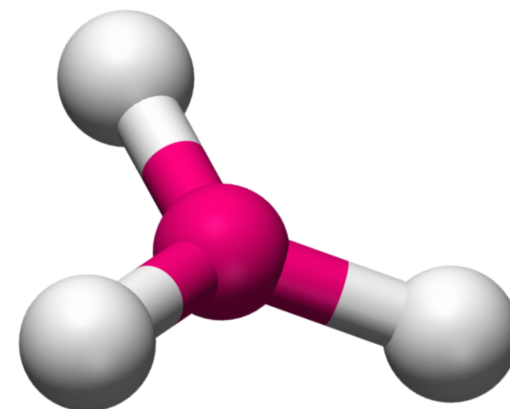
Deviations: perfect crystals do not exist. Many key properties depend on deviations: defects (exception = silicon), phonons (lattice vibrations, atoms are moving, no single lattice at any given instant), surface (finite size effects)

Common Coordination Environments

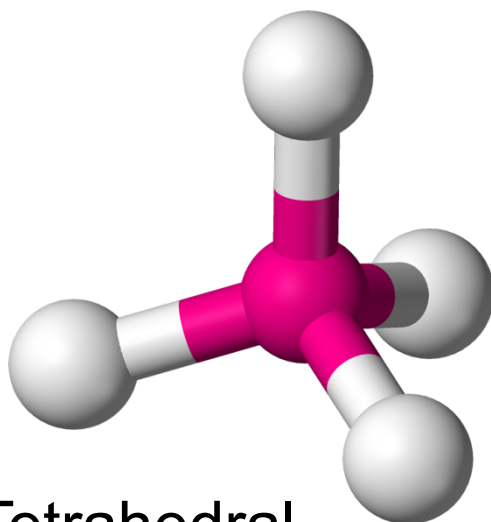
Coordination number (CN)
= # of nearest neighbors



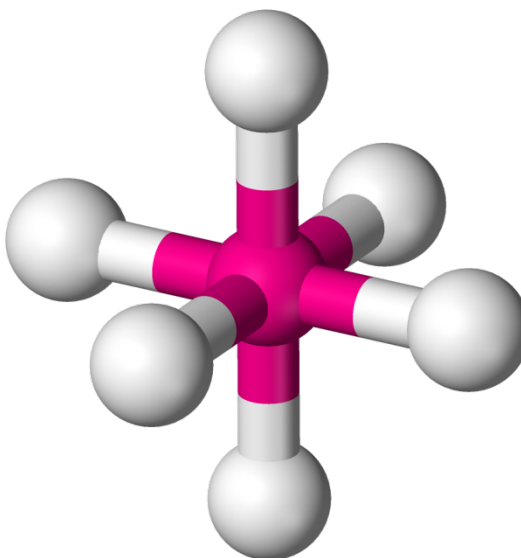
Linear
(CN=2)



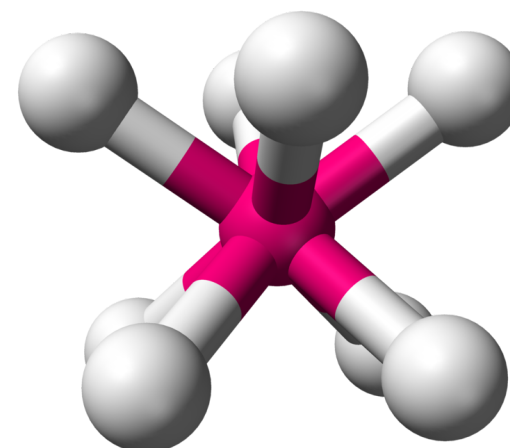
Triangular (CN=3)



Tetrahedral
(CN=4)



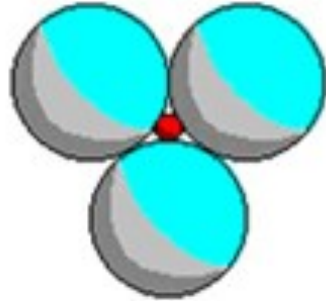
Octahedral (CN=6)



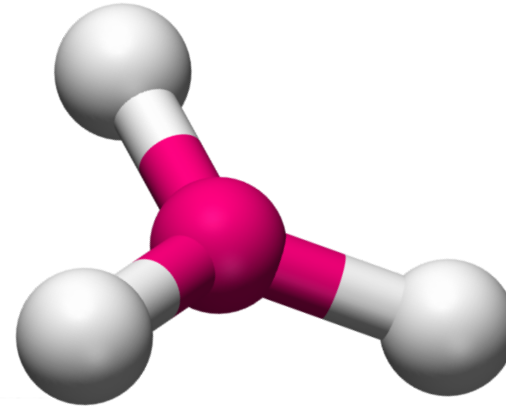
Cubic (CN=8)

Common Coordination Environments

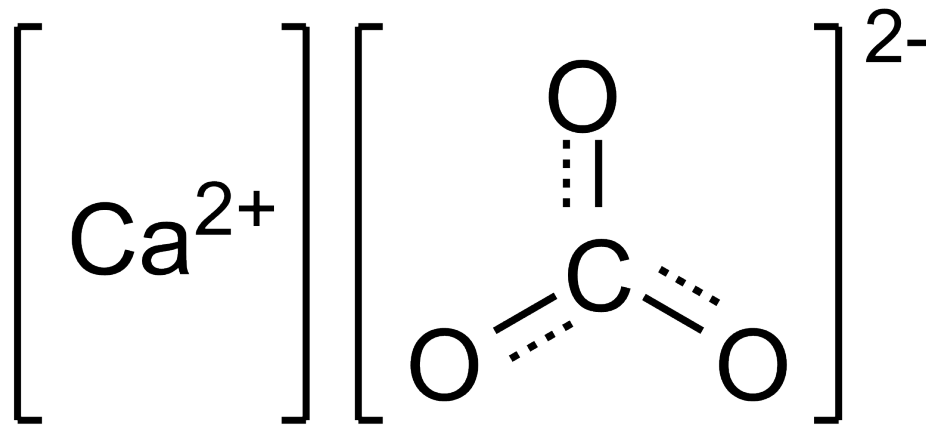
3-fold



Triangular



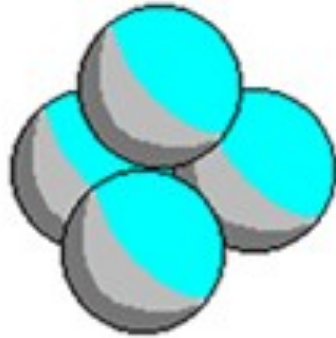
Triangular (CN=3)



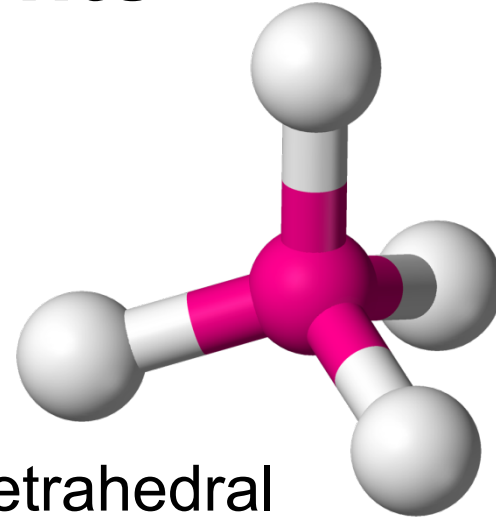
Calcite
(CaCO₃)

Common Coordination Environments

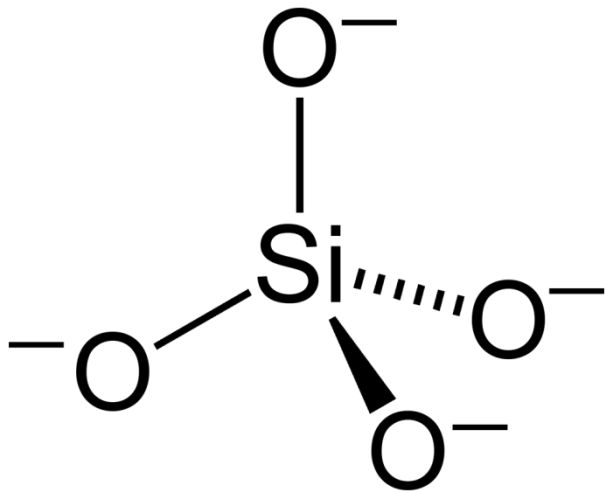
4-fold



Tetrahedral



Tetrahedral
(CN=4)

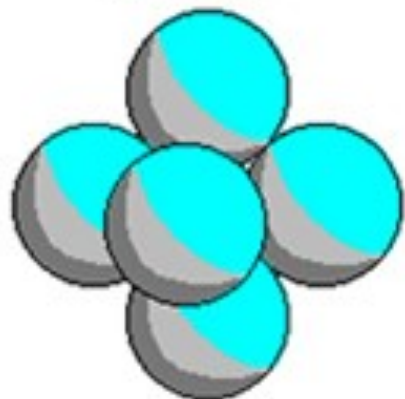


Quartz
(SiO₂)

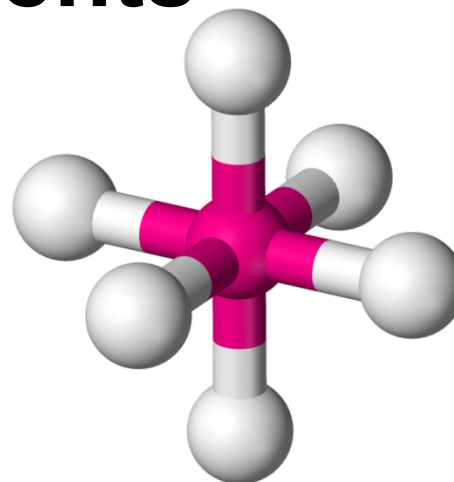


Common Coordination Environments

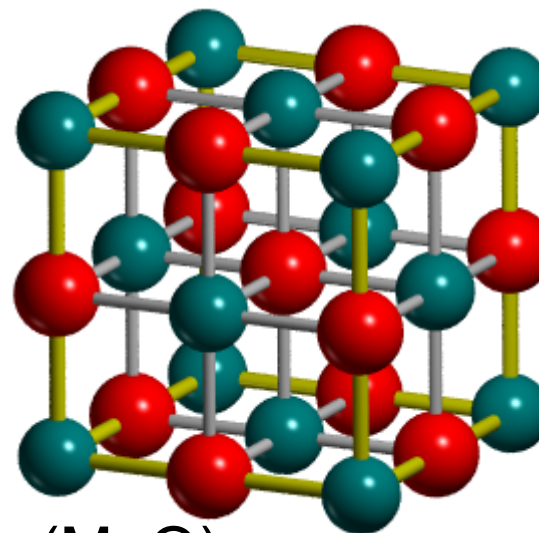
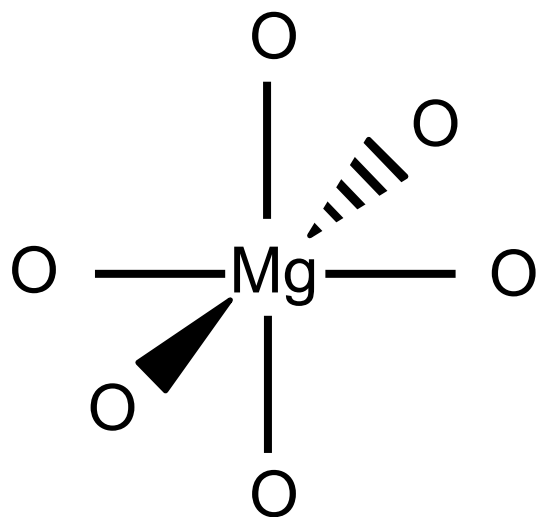
6-fold



Octahedral



Octahedral (CN=6)

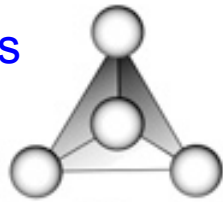


Periclase (MgO)
(NaCl structure)

Silicate classification, based on connectivity

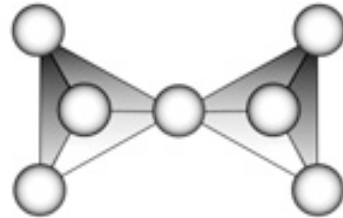
Nesosilicates:

Olivine
Garnets



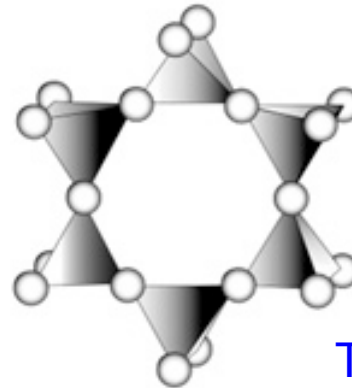
Isolated Tetrahedron
(SiO₄)⁴⁻

Sorosilicates:
Hemimorphite



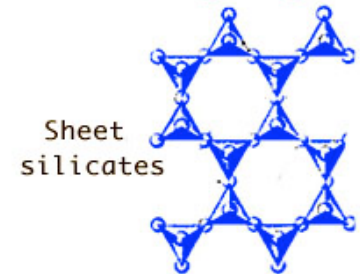
Double Tetrahedra
(Si₂O₇)⁶⁻

Cyclosilicates:
Beryl



Tetrahedral
ring (6-fold):
(Si₆O₁₈)¹²⁻

Phyllosilicates:
Micas (Si₂O₅)²⁻



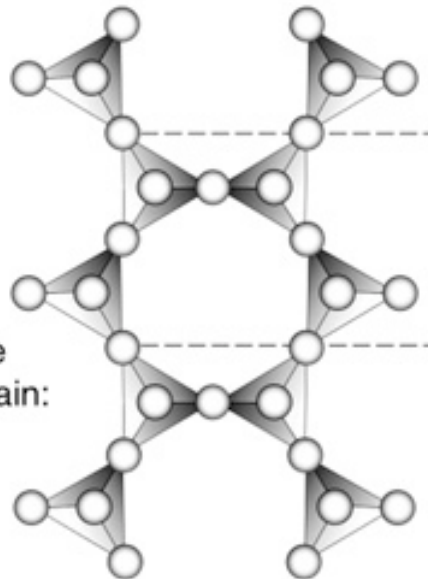
Sheet
silicates

Inosilicates:
Pyroxenes



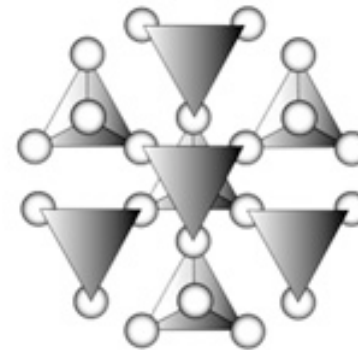
Infinite, single
tetrahedral chain:
(Si₂O₆)⁴⁻

Inosilicates:
Amphibole



Infinite, double
tetrahedral chain:
(Si₄O₁₁)⁶⁻

Tectosilicates:
Quartz, Feldspars



Infinite tetrahedral
network:
(SiO₂)⁰

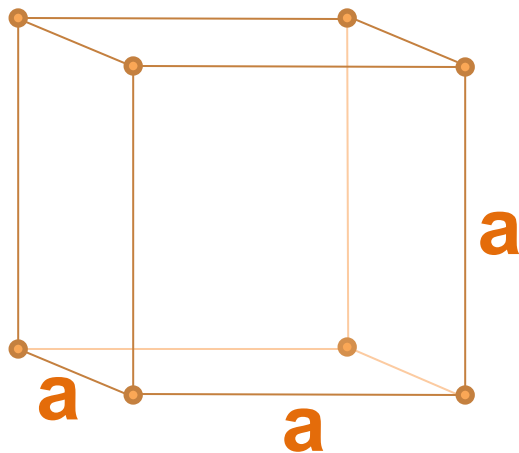
Unit Cells

- There are 7 lattice systems
- The lattice systems are characterized by the relative lengths of the cell edges (a, b, c) and the angles between them (α, β, γ)
- These lattice systems can be further subdivided into 14 Bravais lattices

Cubic Lattice System

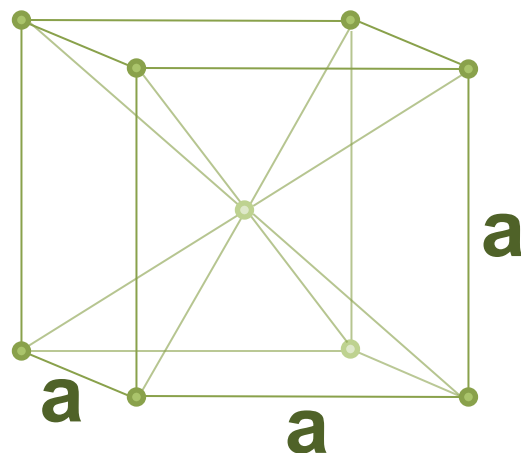
P

primitive
“simple cubic”



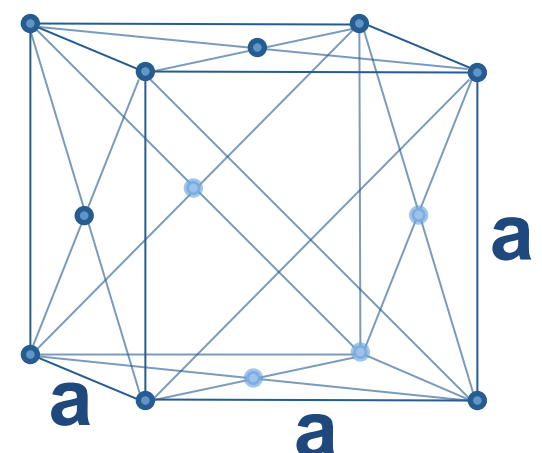
I

body-centered
“bcc”



F

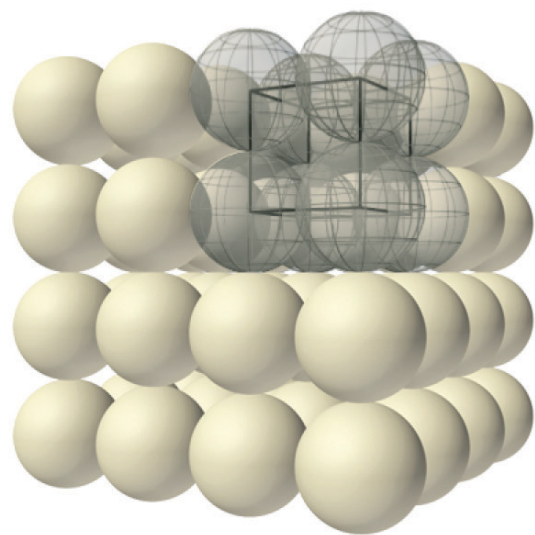
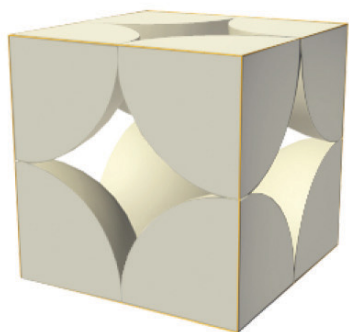
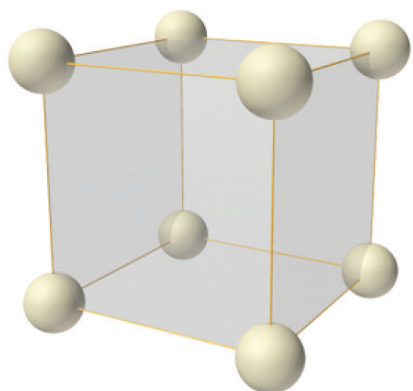
face-centered
“fcc”



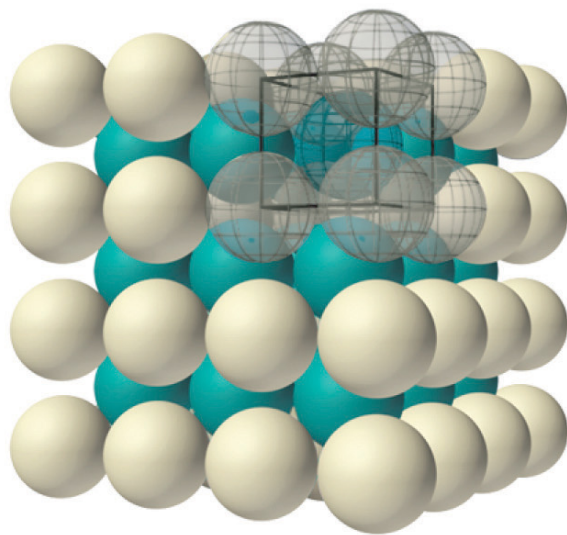
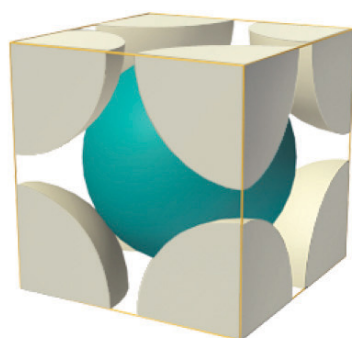
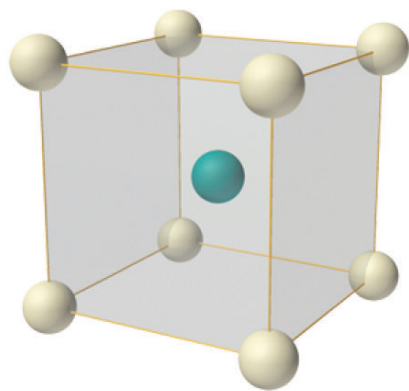
$$a = b = c$$

$$\alpha = \beta = \gamma = 90^\circ$$

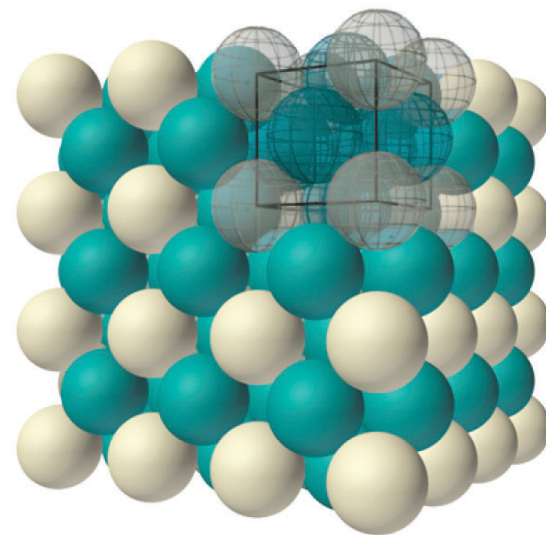
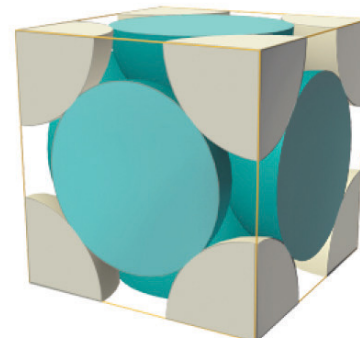
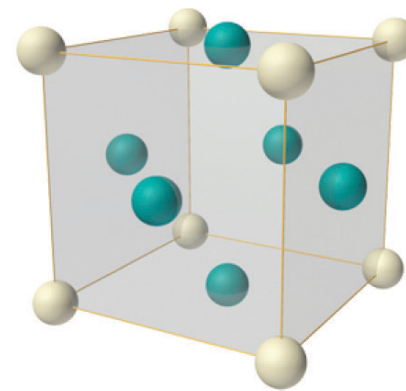
(a) Simple cubic



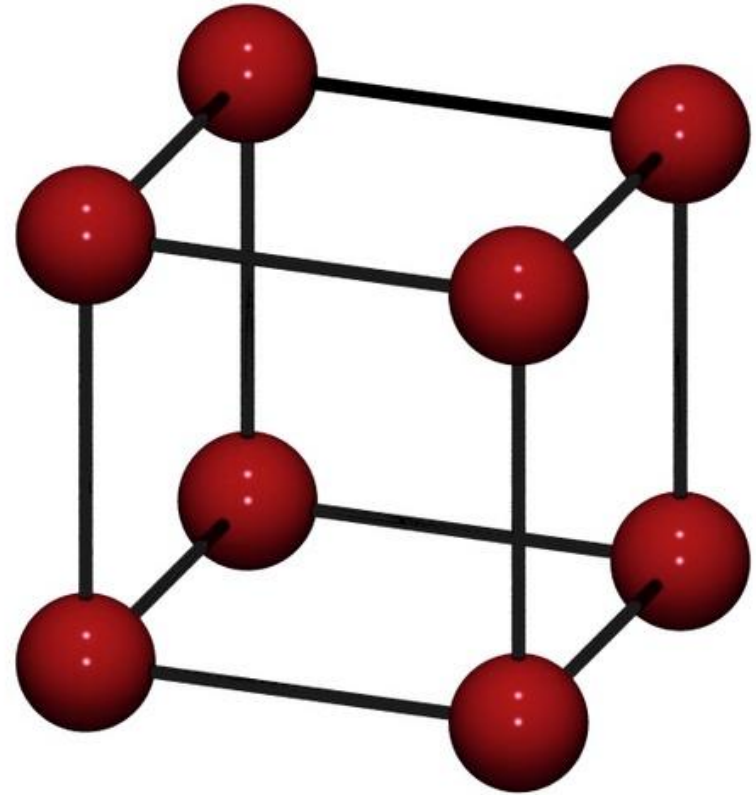
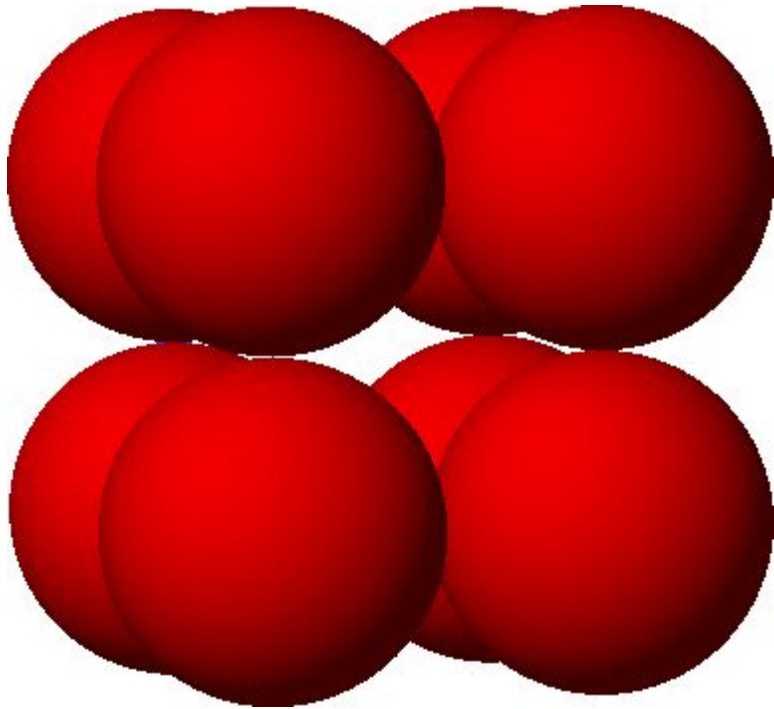
(b) Body-centered cubic



(c) Face-centered cubic

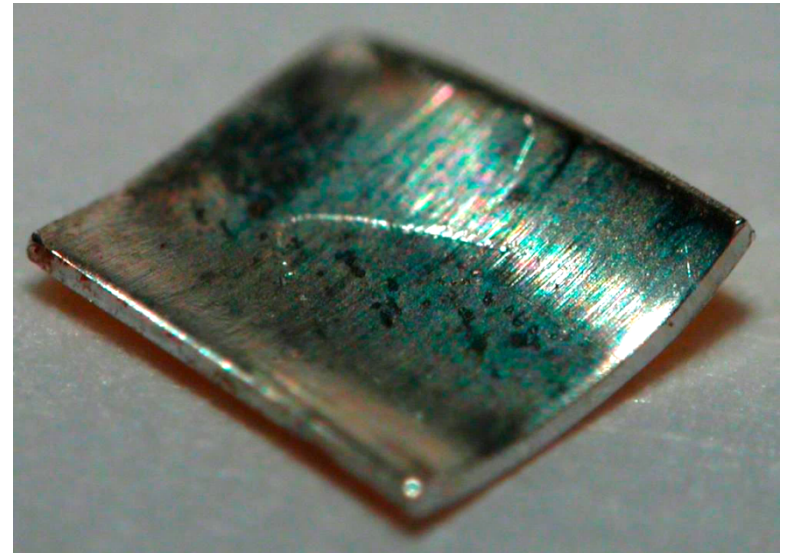
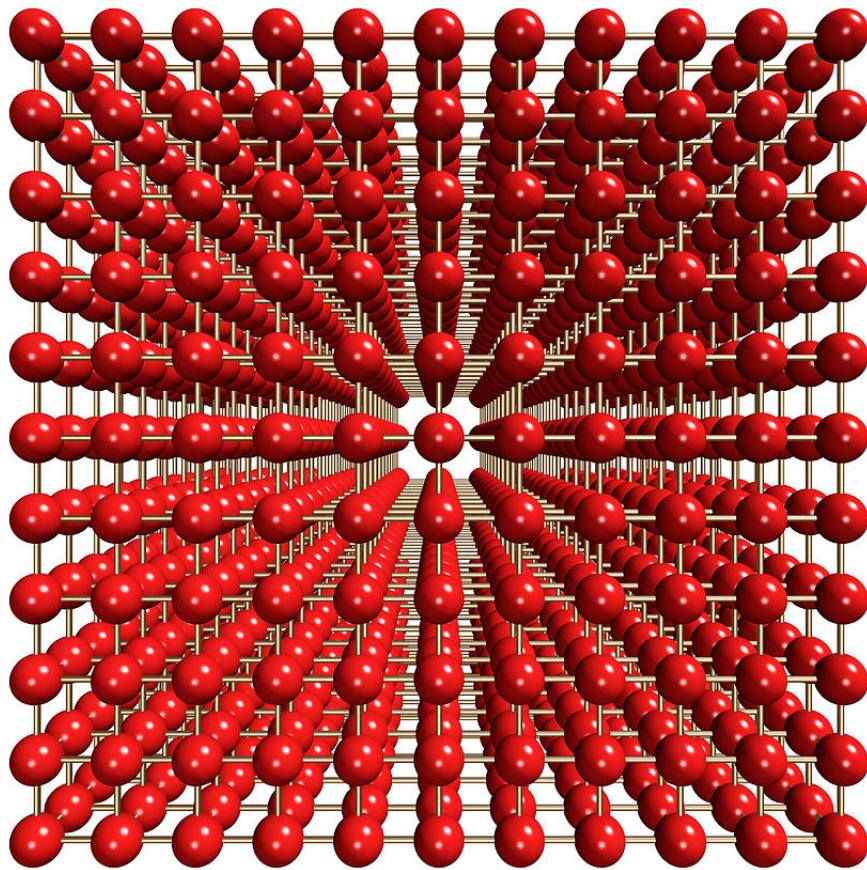


Primitive Cubic (Simple Cubic)



Primitive Cubic (Simple Cubic)

Very rare in metals (not efficient).
Example: Polonium metal.

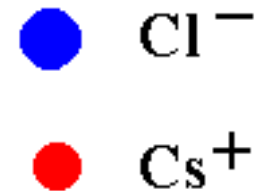
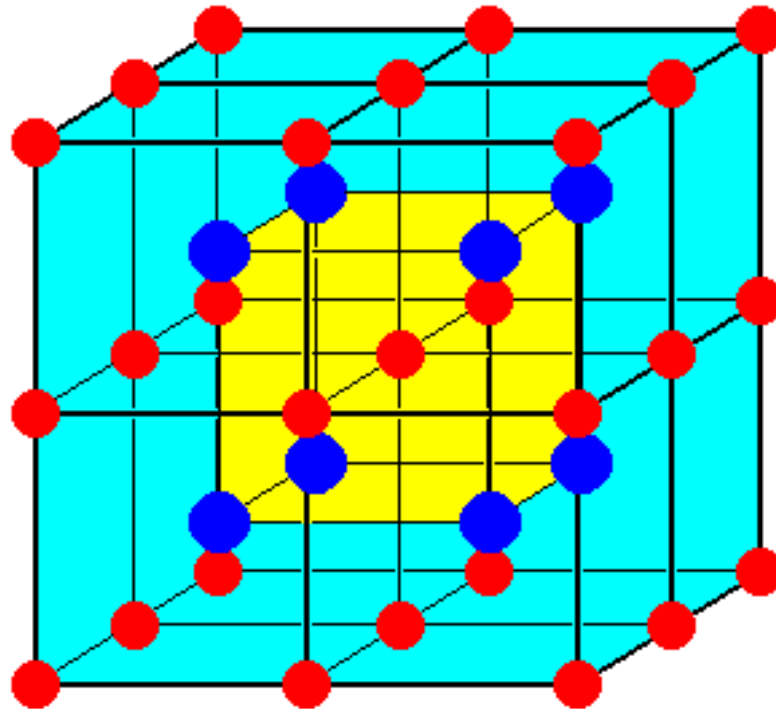


Theodore W. Gray (2003)

Primitive Cubic (Simple Cubic)

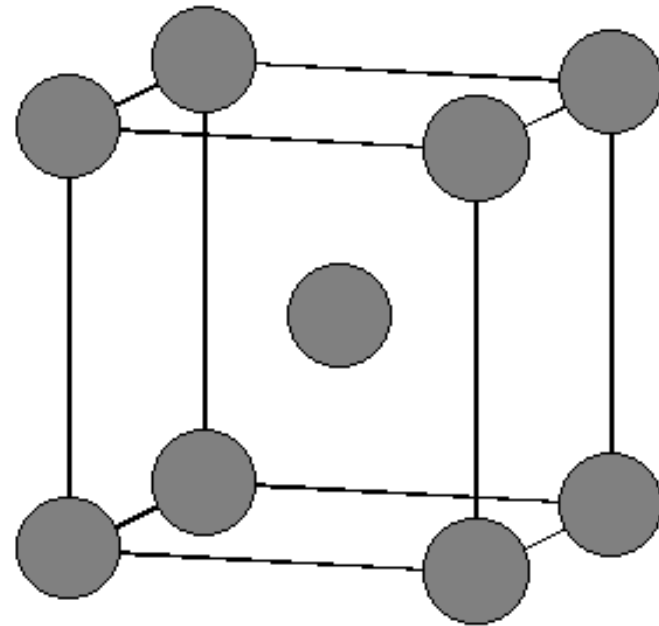
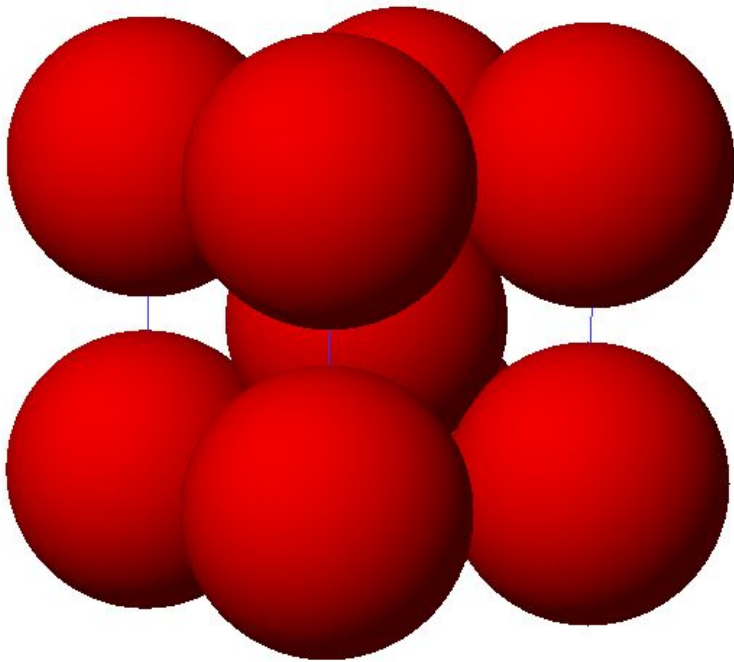
Minerals with more than one atom type can have the primitive cubic structure.

Example:
cesium
chloride



Body Centered Cubic

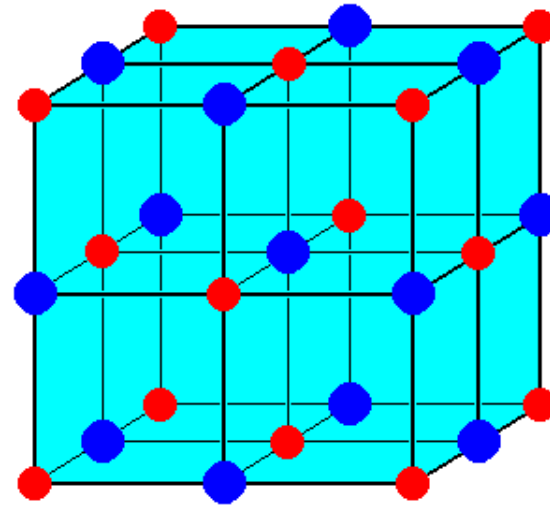
Many metals have the BCC structure: iron, lithium, sodium, potassium, chromium, barium, vanadium.



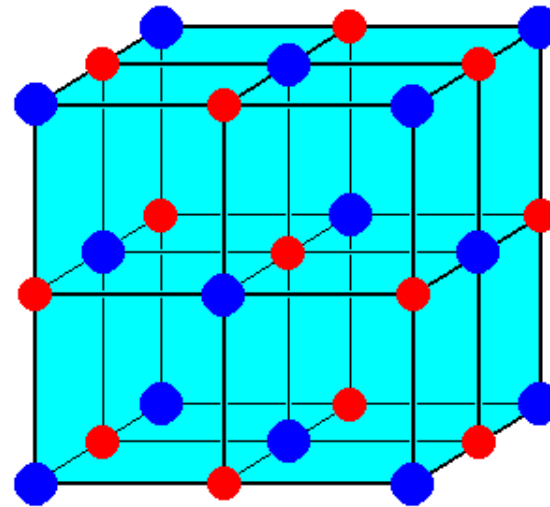
Face Centered Cubic



Halite – NaCl
(fcc)

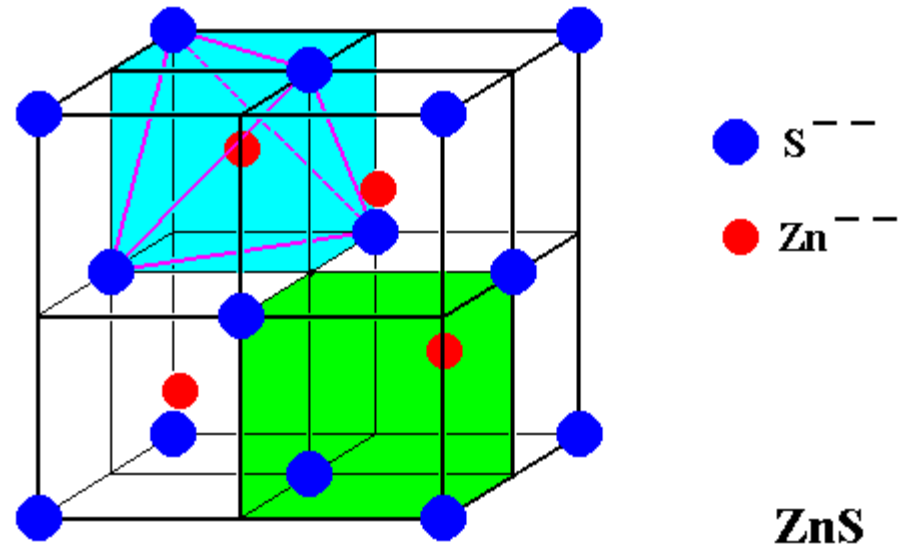


NaCl



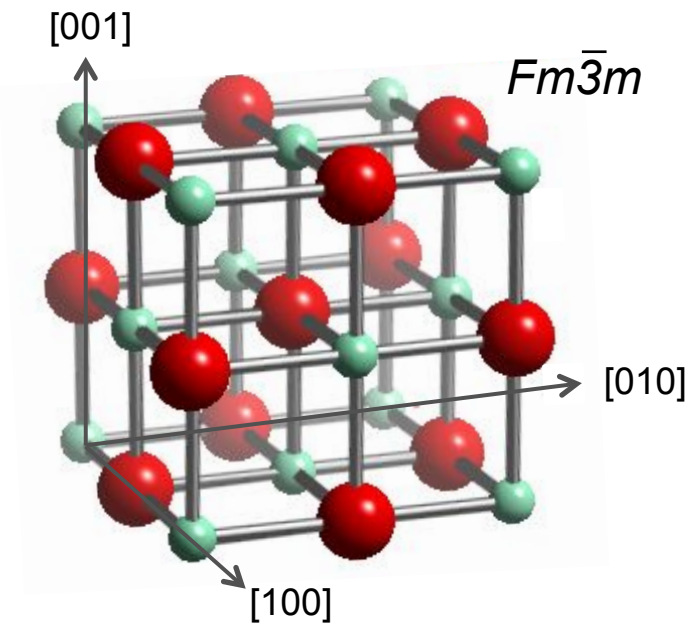
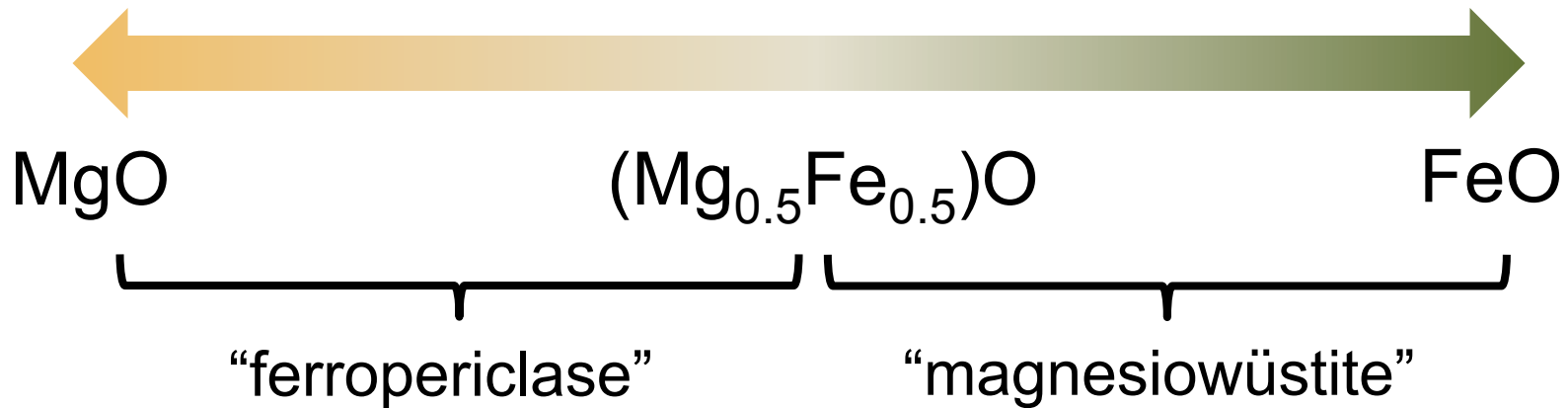
NaCl

Face Centered Cubic



Sphalerite - (Zn,Fe)S
(fcc)

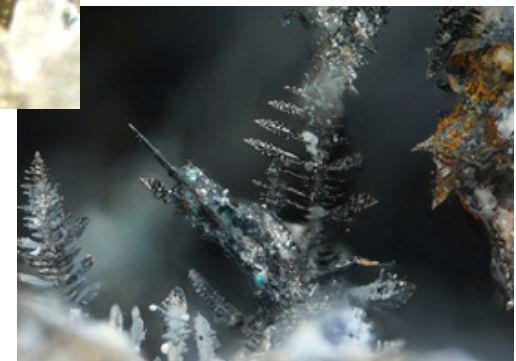
Periclase-Wüstite Solid Solution



B1 phase



periclase



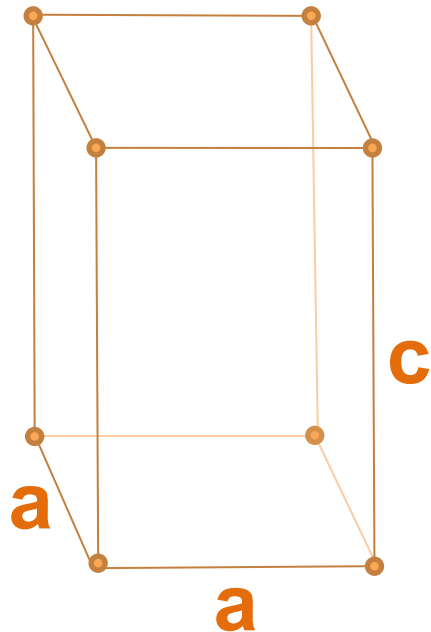
wüstite

Tetragonal Lattice System

P

primitive

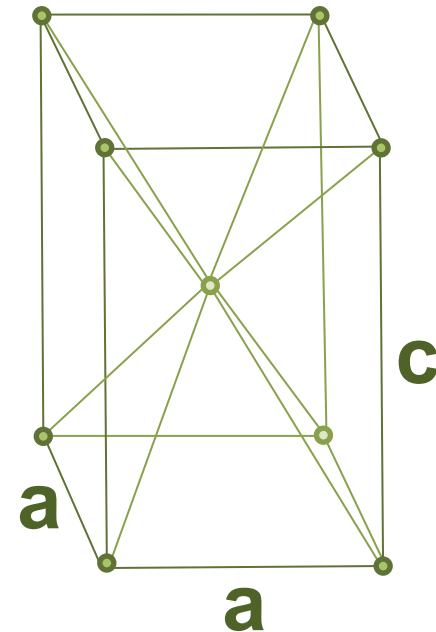
“simple tetragonal”



I

body-centered

“centered tetragonal”



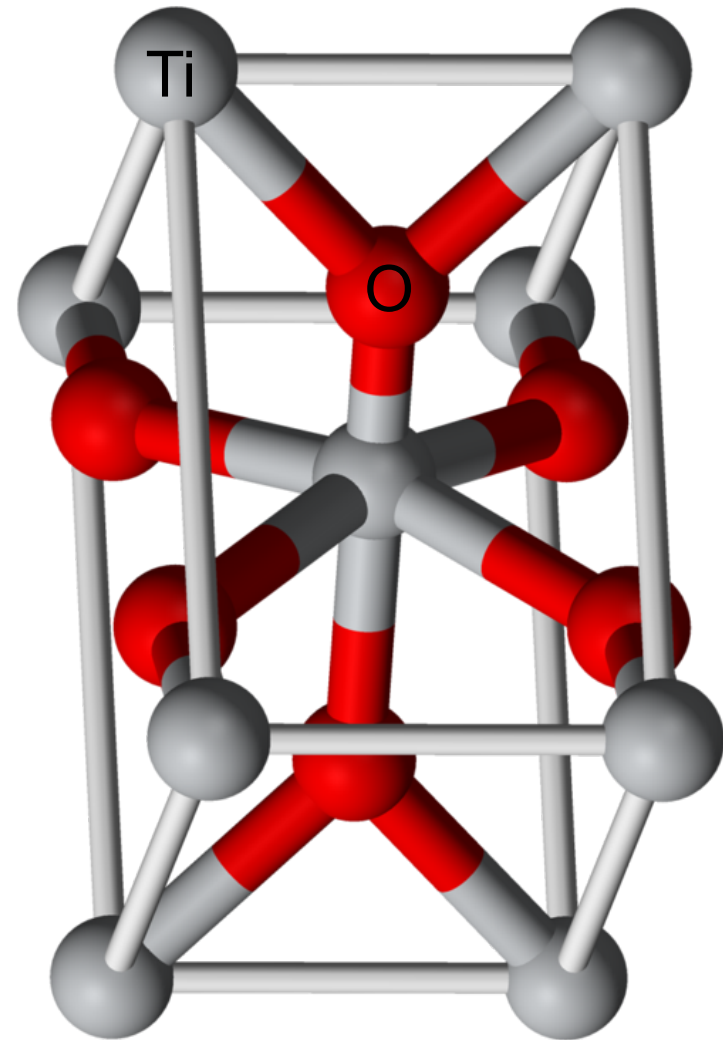
$$a = b \neq c$$

$$\alpha = \beta = \gamma = 90^\circ$$

Example of Tetragonal Lattice



<http://www.minfind.com/mfthumbs>

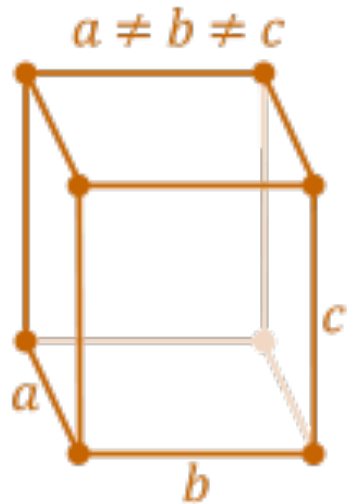


Rutile – TiO₂

Orthorhombic Lattice System

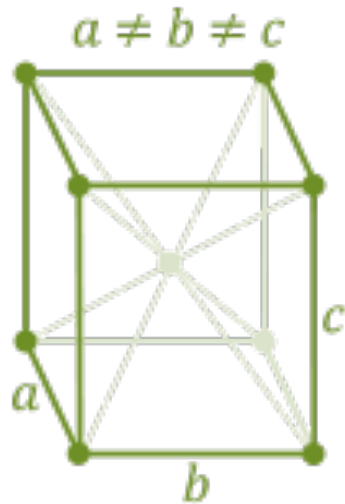
P

primitive



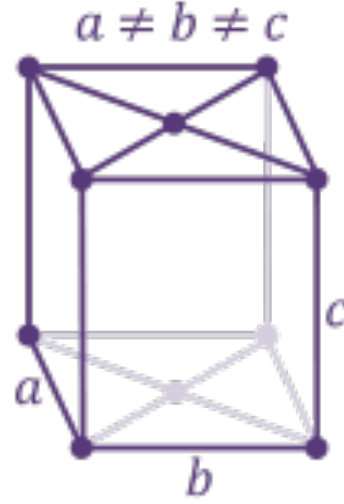
I

body-centered



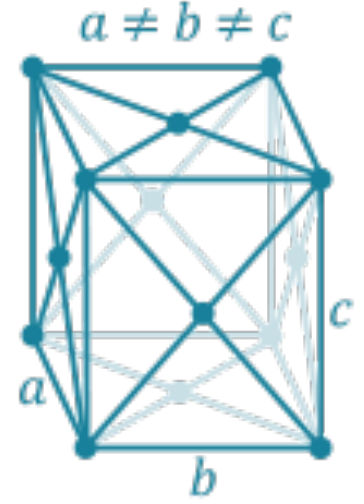
A, B, C

base-centered



F

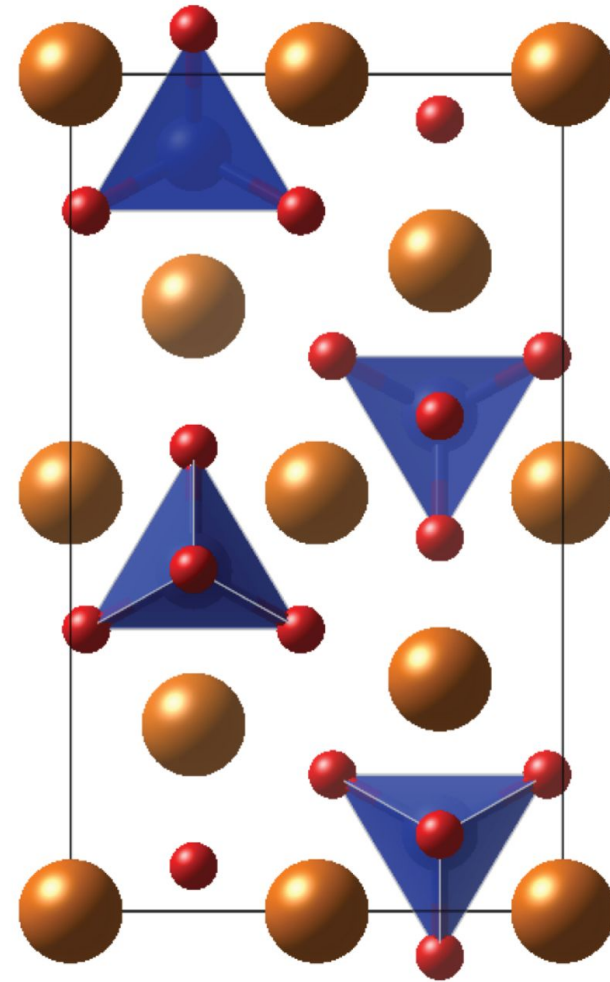
face-centered



$$a \neq b \neq c$$

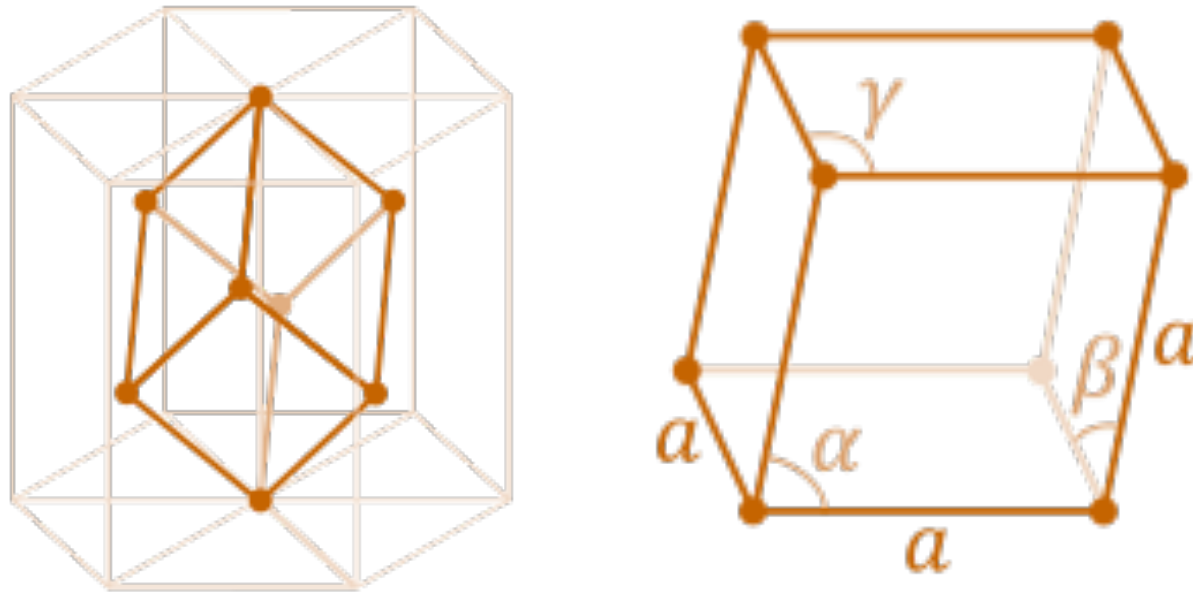
$$\alpha = \beta = \gamma = 90^\circ$$

Example of Orthorhombic Lattice



Olivine – Mg_2SiO_4

Rhombohedral Lattice System

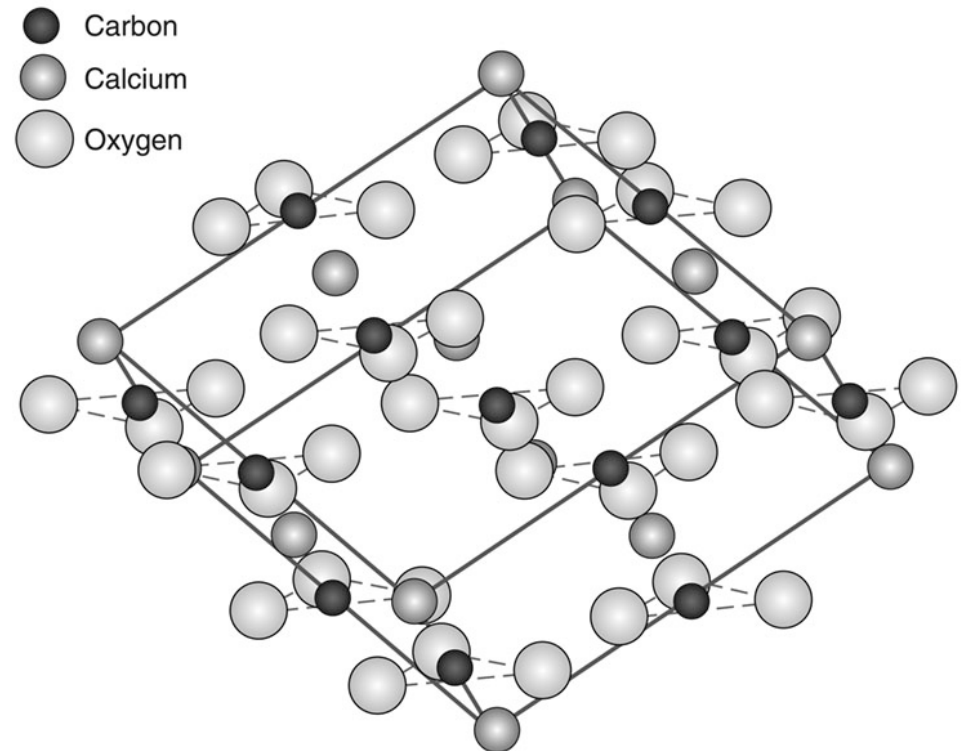


$$a = b = c$$

$$\alpha = \beta = \gamma \neq 90^\circ$$

The rhombohedral lattice is combined with the hexagonal lattice, grouped under the hexagonal family because the same hexagonal unit cell can be used for both.

Example of Rhombohedral Lattice



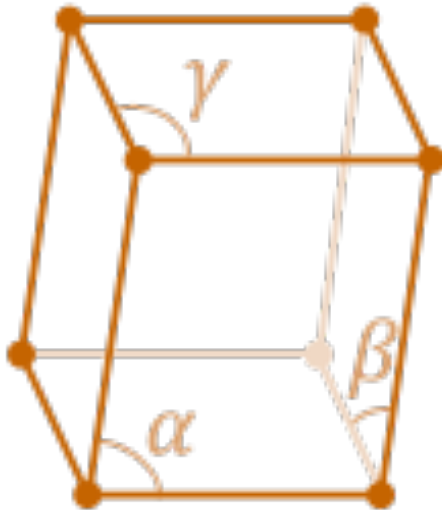
Calcite – CaCO_3

<http://geophysics.ou.edu/geol1114/notes/minerals/calcite.jpg>

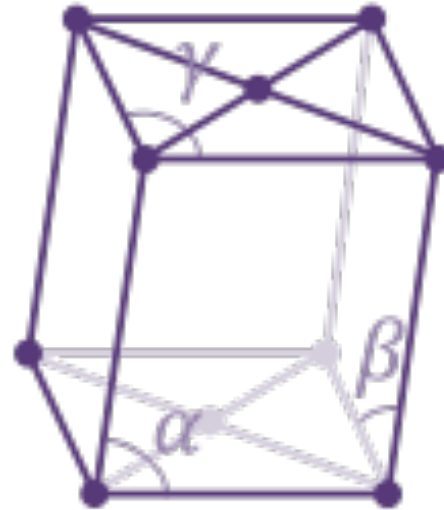
http://igs.indiana.edu/images/rocksandminerals/CalciteArticle_Figure2.jpg

Monoclinic Lattice System

P
primitive



C
base-centered



$$a \neq b \neq c$$
$$\alpha = \gamma, \beta \neq 90^\circ$$

Monoclinic Lattice System

Diopside-
hedenbergite
 $\text{Ca}(\text{Mg,Fe})\text{Si}_2\text{O}_6$



Orthoclase
 KAlSi_3O_8



Pyroxenes



Photo by Rob Lavinsky

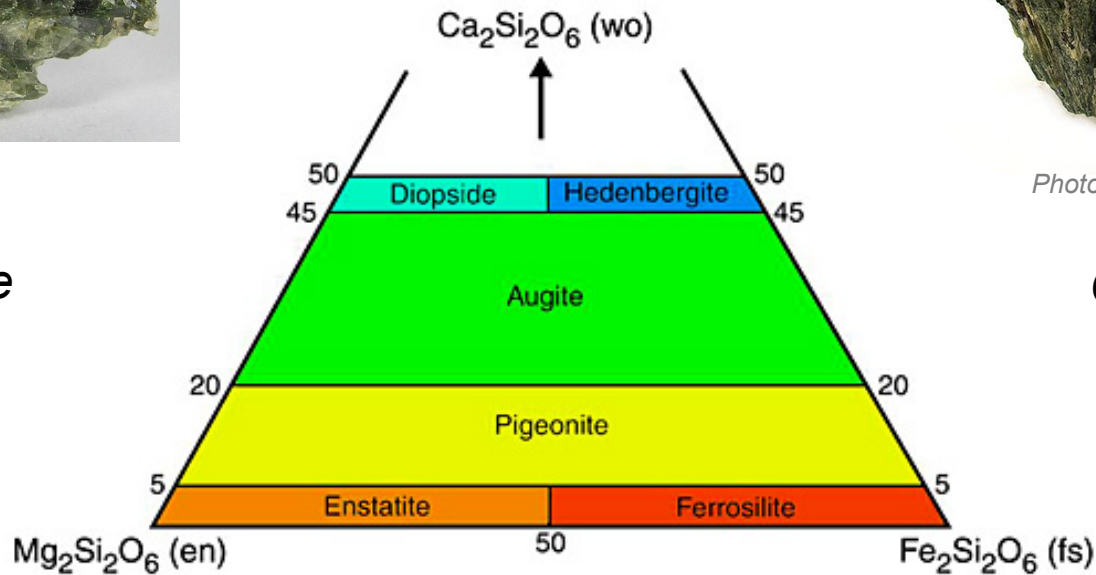
Diopside
CaMg-pyroxene



Photo by Rob Lavinsky

Hedenbergite
CaFe-pyroxene

← monoclinic →



Enstatite
Mg-pyroxene

Ferrosilite
Fe-pyroxene



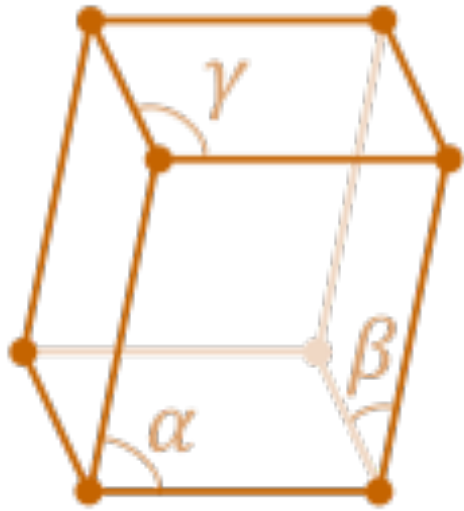
Photo by Stephan Wolfried

← orthorhombic →



johnbetts-fineminerals.com

Triclinic Lattice System



P

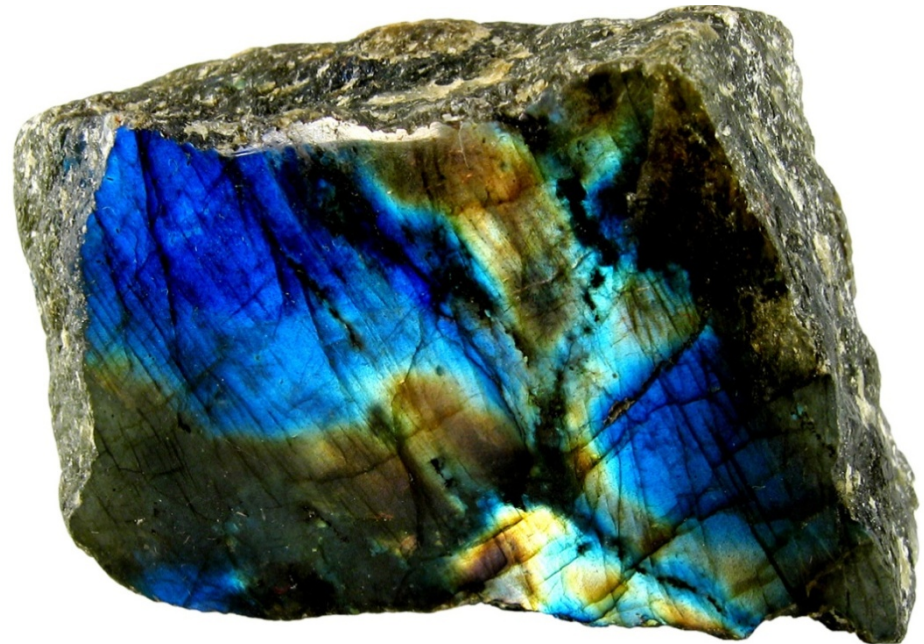
primitive

$$a \neq b \neq c$$

$$\alpha \neq \beta \neq \gamma \neq 90^\circ$$

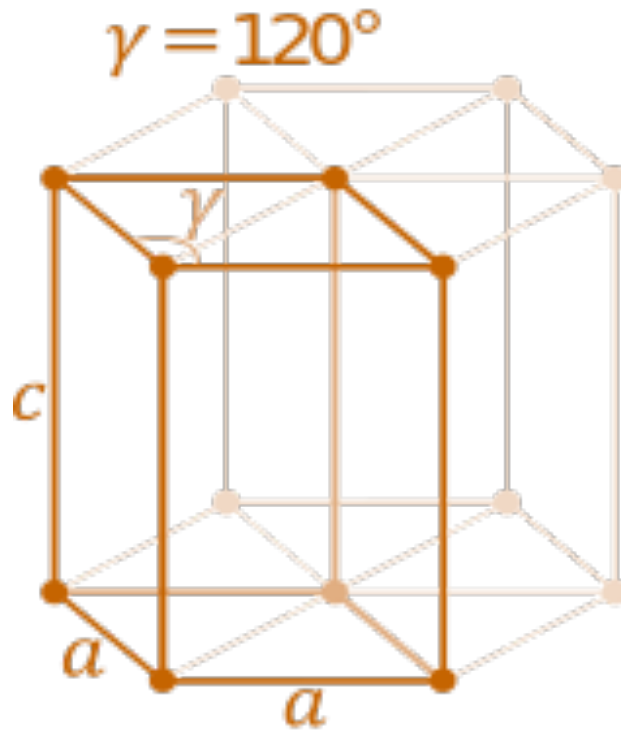
Plagioclase (feldspar)

Example: Labradorite, $(\text{Ca}, \text{Na})\text{Al}_2\text{Si}_2\text{O}_8$
 $\text{Ca}/(\text{Ca} + \text{Na}) = 50 - 70\%$



Hexagonal Lattice System

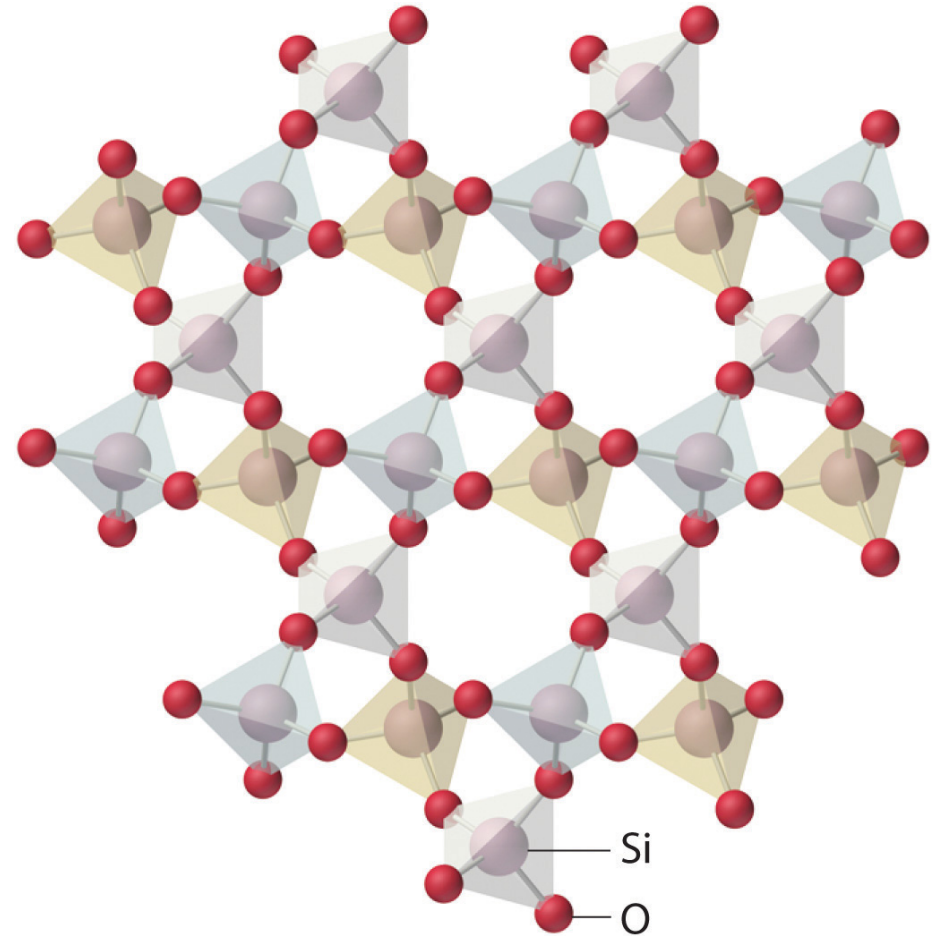
P
primitive



$$a = b \neq c$$

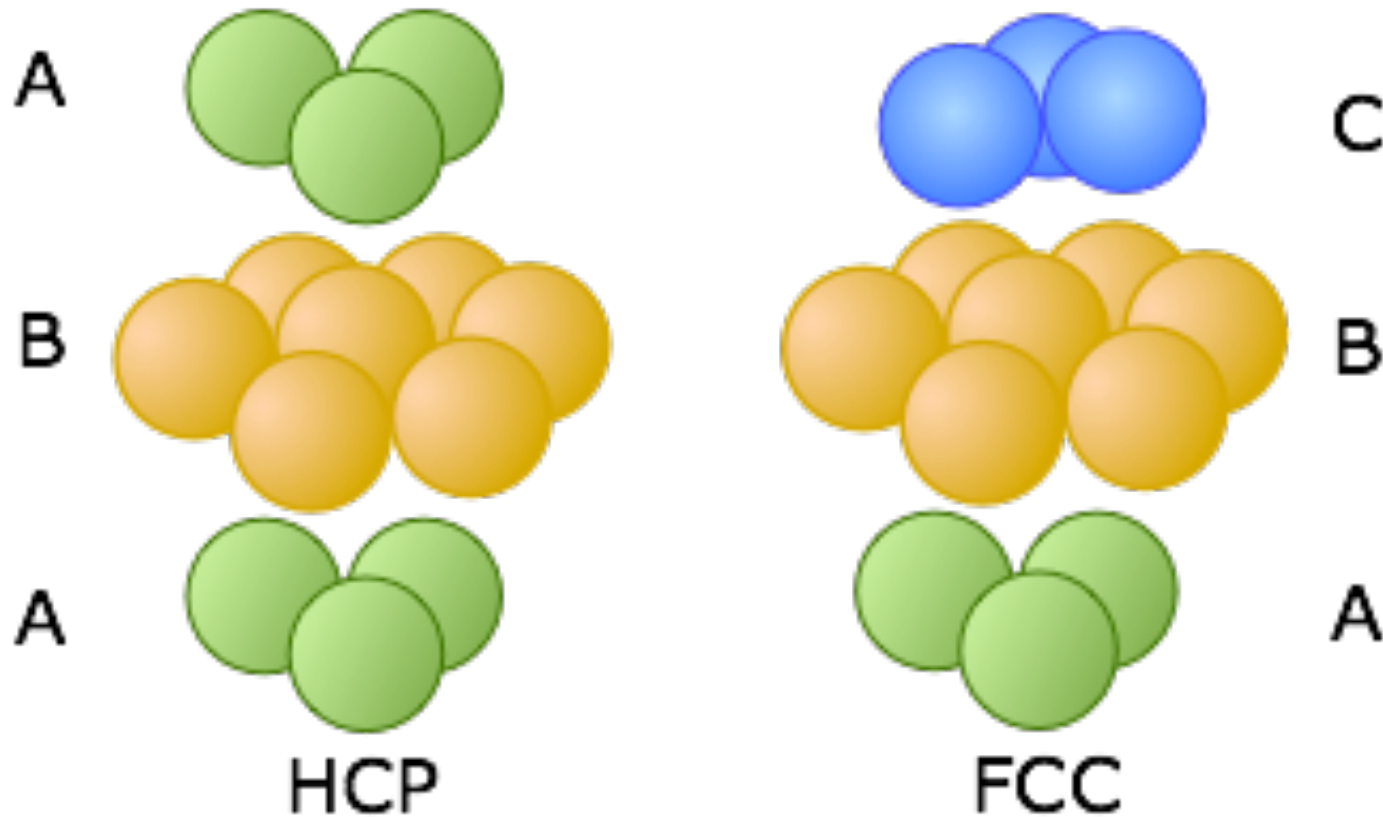
$$\alpha = \beta = 90^\circ, \gamma = 120^\circ$$

Example of Hexagonal Lattice

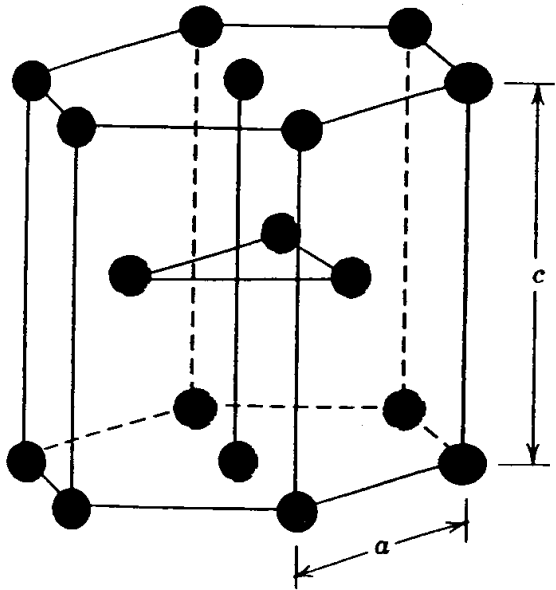


Quartz – SiO_2

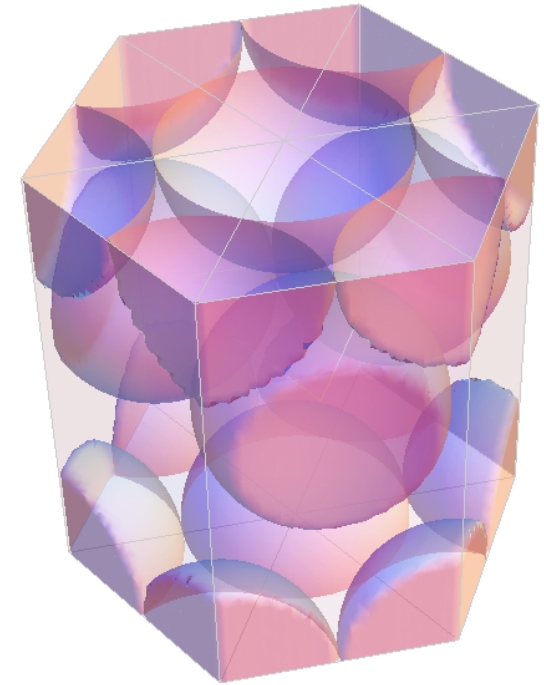
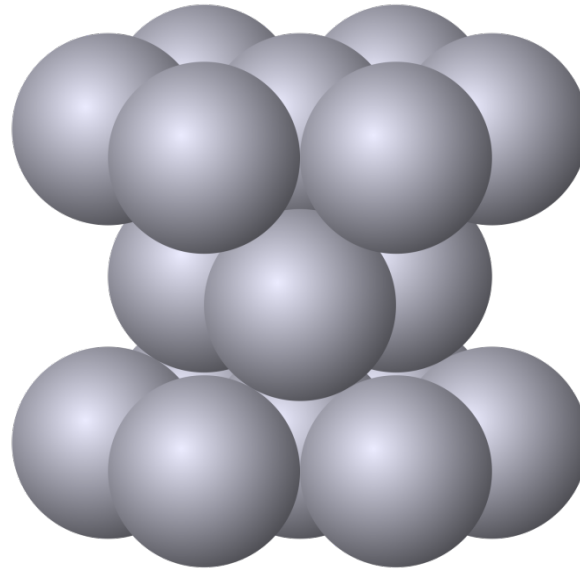
Hexagonal Close Packing compared with Face-Centered Close Packing



Hexagonal Close-Packing (HCP)



HCP

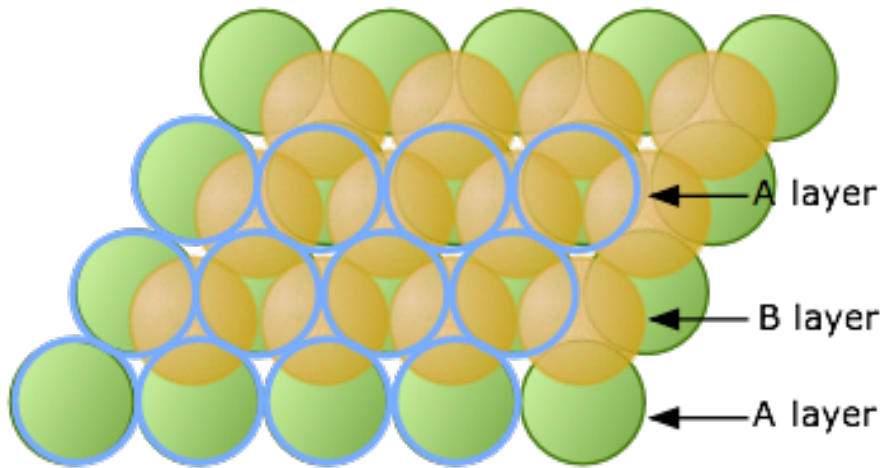
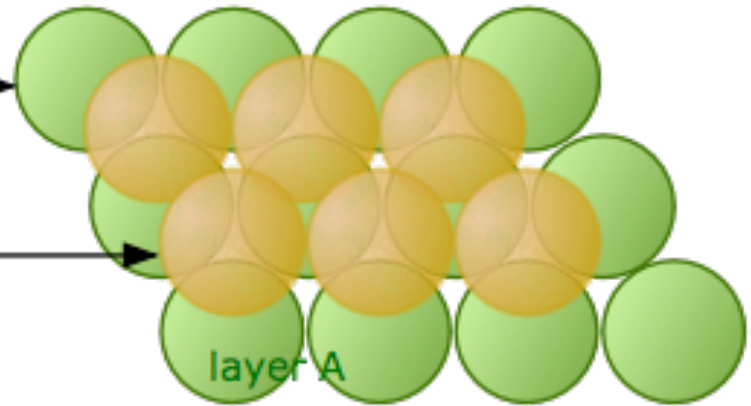
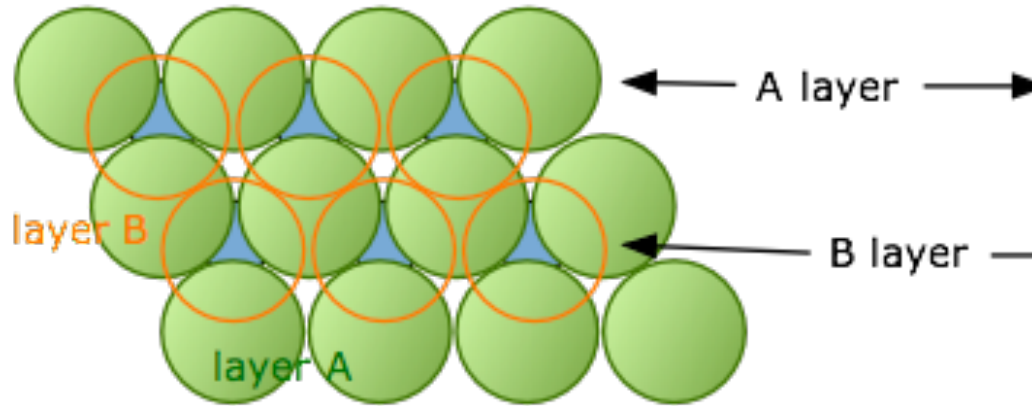


Beryllium, magnesium, zinc, cadmium, titanium metals. *Iron at large compressions*

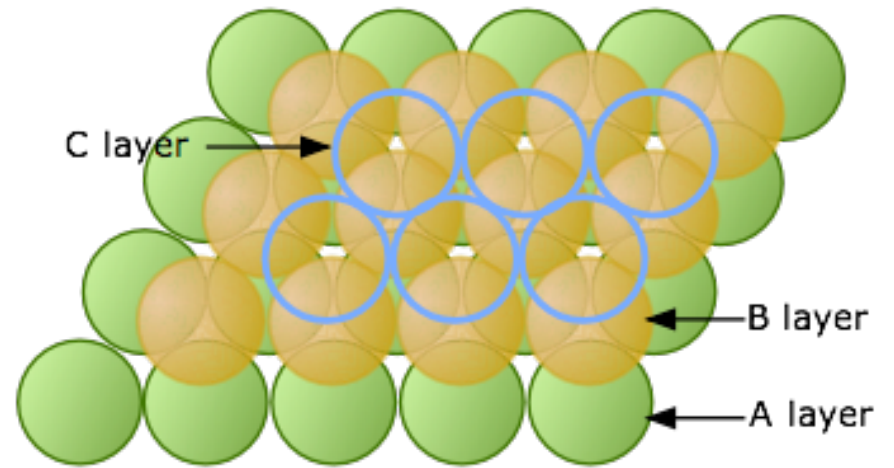
Packing – HCP vs. FCC

HCP

FCC

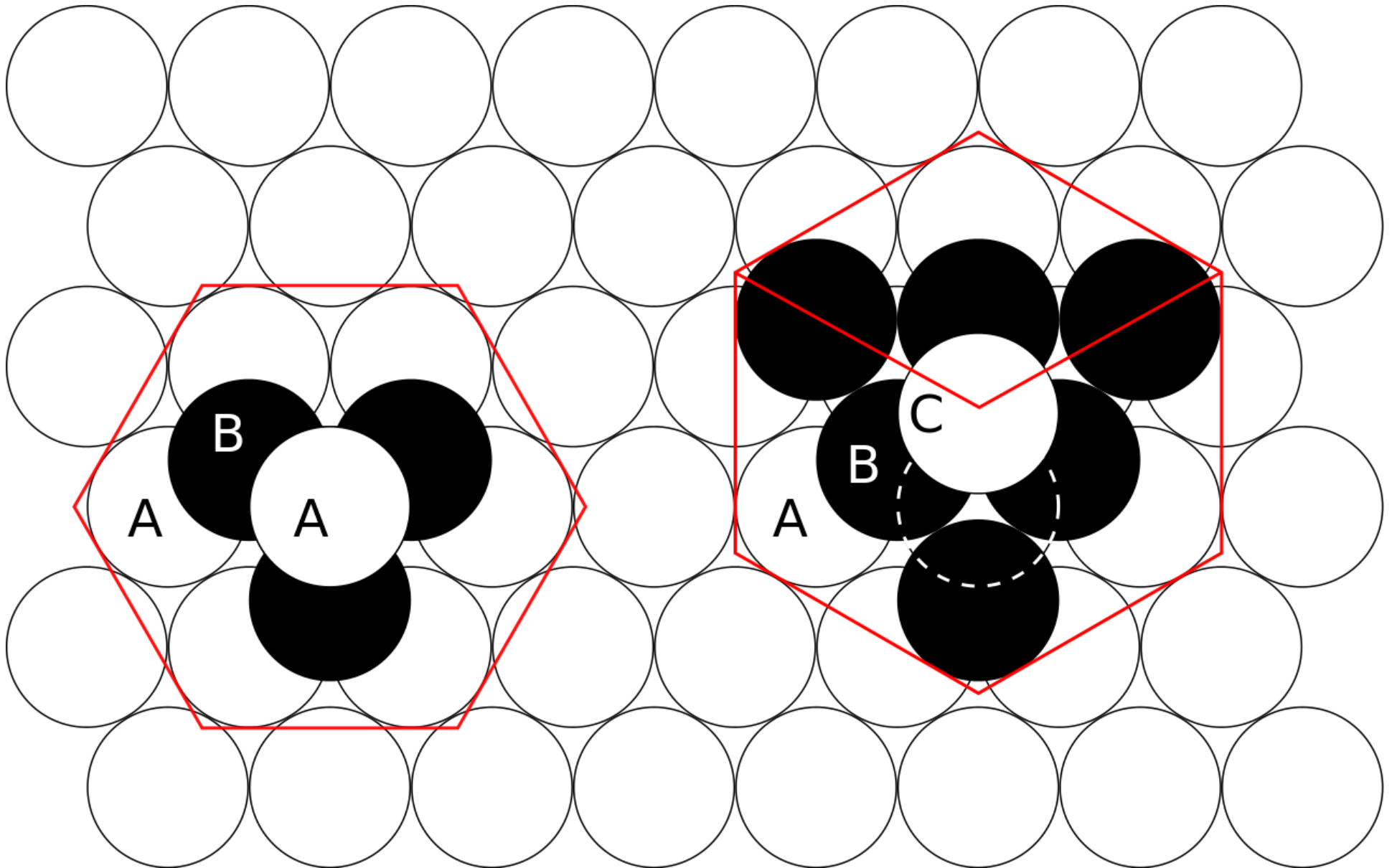


ABA hexagonal close packed

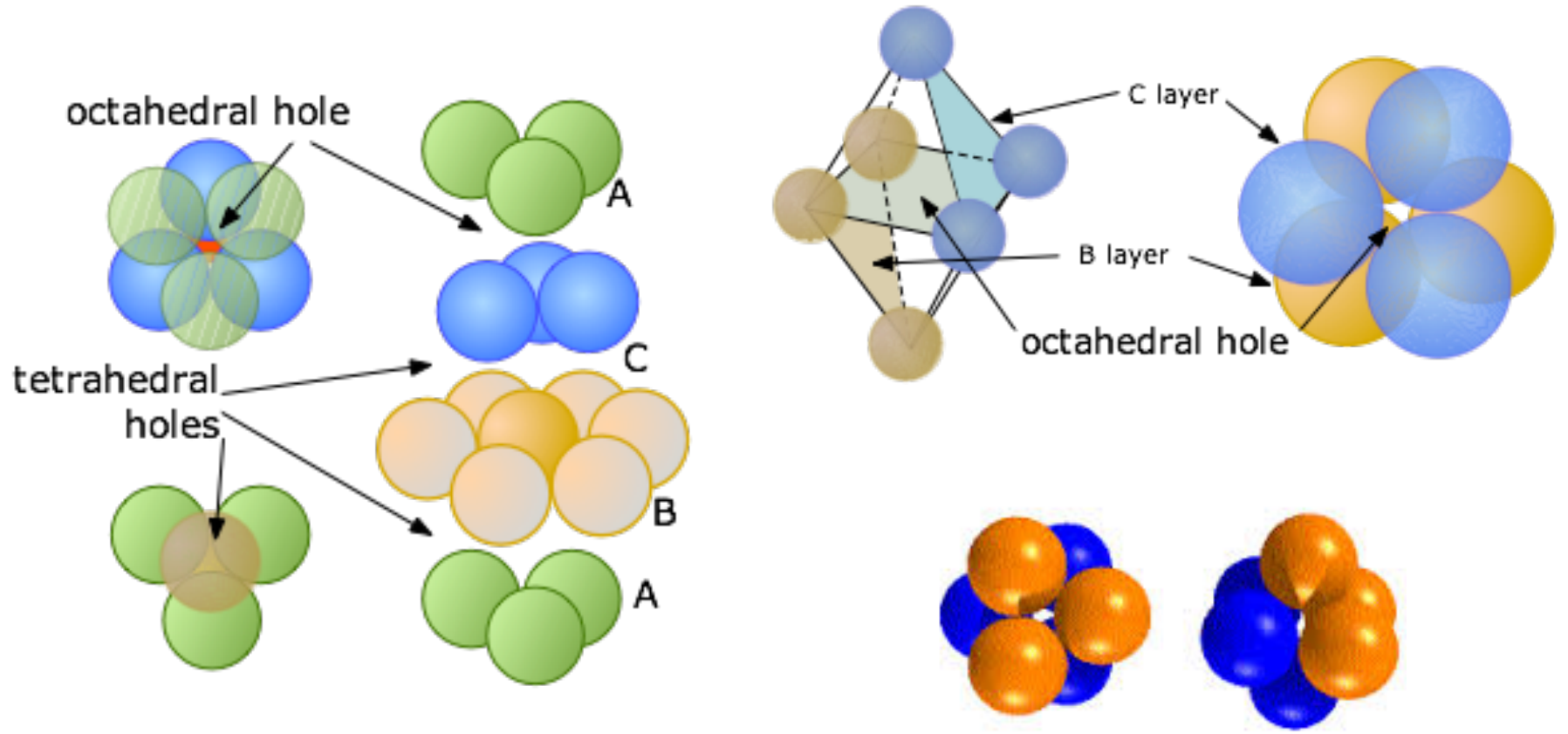


ABC face-centered cubic

Packing – HCP vs. FCC



Interstitial Sites



Pauling's Rules

- 1) The Radius Ratio Rule
- 2) The Electrostatic Valency Principle
- 3) Sharing of Polyhedrons
- 4) Crystals Containing Different Cations

Pauling's First Rule

"The Radius Ratio Rule"

Predict coordination with the radius ratio:

$$R_{\text{Cation}}/R_{\text{Anion}}$$

Cations are generally smaller than anions so begin with maximum ratio = 1.0

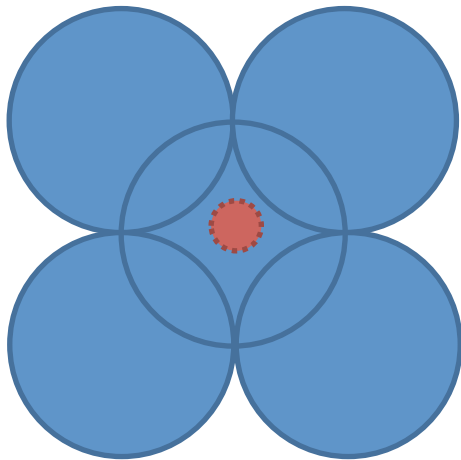
General Rule: Only cations that are large enough to not "rattle" around in the interstices and small enough to fit into the site are accepted.

Pauling's First Rule

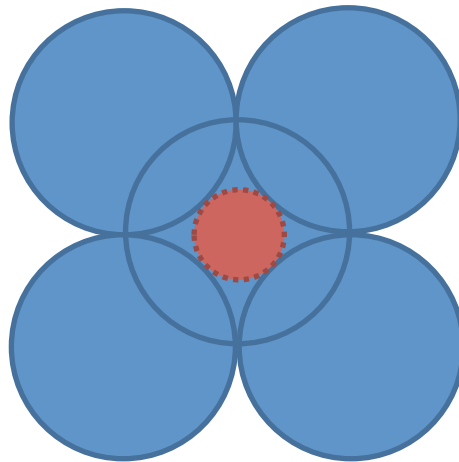
"The Radius Ratio Rule"

Around every cation, a coordination polyhedron of anions forms, in which the cation-anion distance is determined by the radius sums and the coordination number is determined by the radius ratio.

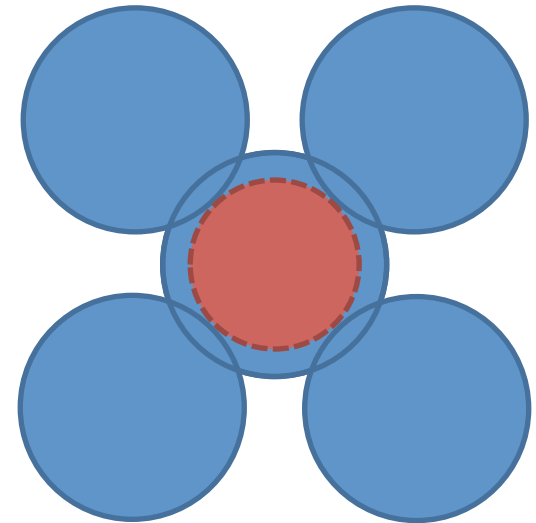
Unstable



Stability Limit



Stable



Red cation is coordinated by 6 blue anions (4 in the plane, 1 above and 1 below).
The stability limit here is at $r_C/r_A = 0.414$.

$R_{\text{cation}}/R_{\text{anion}}$	C.N.	Type
1.0	12	Hexagonal or Cubic Closest Packing
1.0 - 0.732	8	Cubic
0.732 - 0.414	6	Octahedral
0.414 - 0.225	4	Tetrahedral
0.225 - 0.155	3	Triangular
< 0.155	2	Linear

Ion	Coordination Number (C.N.)	Coordination Polyhedron	Ionic Radius, Å
K ⁺	8 – 12	cubic to closest	1.51 – 1.64
Na ⁺	8 – 6	cubic to octahedral	1.18 – 1.02
Ca ²⁺	8 – 6		1.12 – 1.00
Mn ²⁺	6	octahedral	0.83
Fe ²⁺	6		0.78
Mg ²⁺	6		0.72
Fe ³⁺	6		0.65
Ti ⁴⁺	6		0.61
Al ³⁺	6		0.54
Al ³⁺	4	tetrahedral	0.39
Si ⁴⁺	4		0.26
P ⁵⁺	4		0.17
S ⁶⁺	4		0.12
C ⁴⁺	3	triangular	0.08

Pauling's Second Rule

"The Electrostatic Valency Principle"

An ionic structure will be stable to the extent that the sum of the strengths of the electrostatic bonds that reach an ion equal the charge on that ion.

In other words, the bond valence of each ion should be approximately equal to its oxidation state.

$$\text{electrostatic bond strength} = \frac{\text{cation charge}}{\text{coordination number}}$$

$$s = Z/CN$$

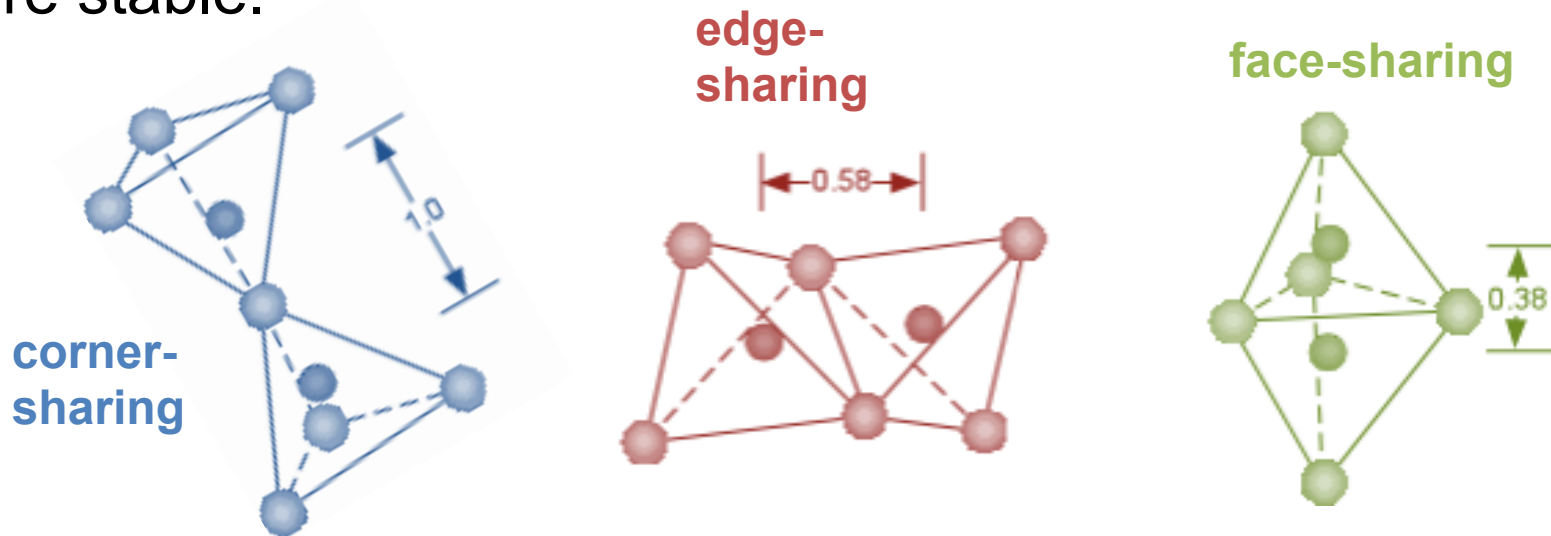
Pauling's Third Rule

"Sharing of Polyhedron Corners, Edges and Faces"

Shared edges, and particularly faces of two anion polyhedra in a crystal structure decreases its stability.

Sharing faces means the cations are closer together → less stable (cation-cation repulsion).

Sharing corners means the cations are further apart → more stable.



Pauling's Fourth Rule

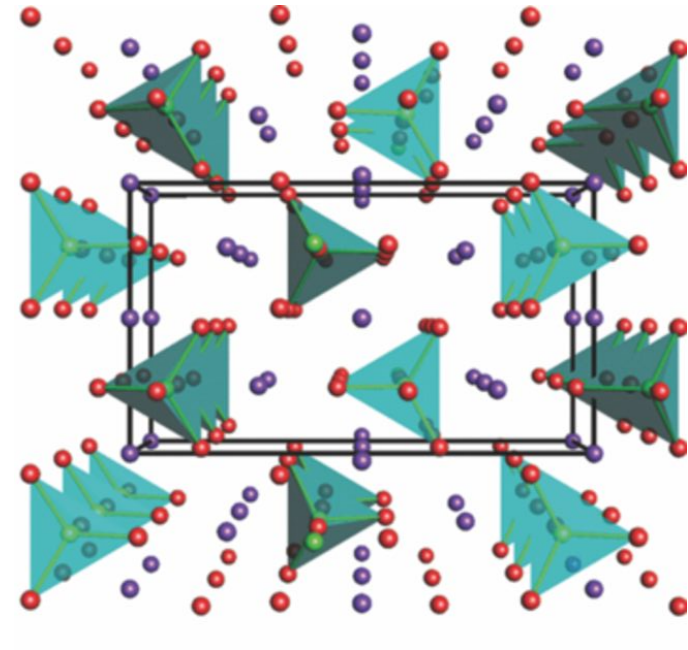
"Crystals Containing Different Cations"

In a crystal containing different cations, those with large valence and small CN tend not to share polyhedron elements with each other.

(Sharing polyhedra with cations of high charge will place cations close together so that they repel.)

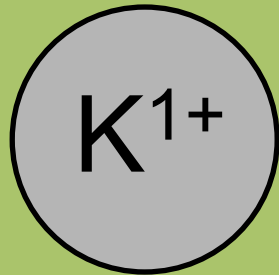
Olivine - $(\text{Mg,Fe})_2\text{SiO}_4$

- Isolated SiO_4 tetrahedra
 - small CN (4)
 - large valence (4)
- Contains both Mg^{2+} and Fe^{2+}



Cations of Similar Sizes

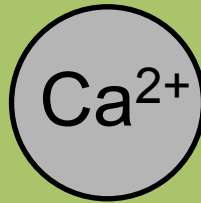
Examples



1.38 Å



1.02 Å



1.00 Å

Feldspars!

Orthoclase, KAlSi₃O₈

Albite, NaAlSi₃O₈

Anorthite, CaAl₂Si₂O₈



0.83 Å



0.78 Å



0.72 Å



0.65 Å

Double carbonates!

Dolomite, CaMg(CO₃)₂

Ankerite, CaFe(CO₃)₂

Kutnohorite, CaMn(CO₃)₂

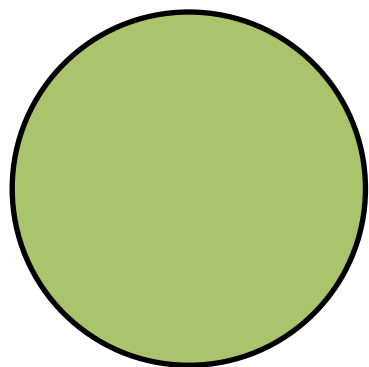


0.54 Å 0.40 Å 0.16 Å

Al^{3+} substitutes for Si^{4+} in silicates.

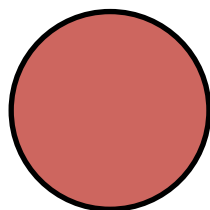
C^{4+} is the Si^{4+} analog in carbonates, except that it forms triangular groups instead of tetrahedra.

Effect of Charge on Anion Size



S^{2-}

1.84 Å



S^0

1.03 Å



S^{4+}

0.37 Å



S^{6+}

0.29 Å

(Sulfur has many oxidation states.)

Effect of Pressure

pressure	0	15 GPa	25 GPa
O			
Si			
depth	crust	410 km	660 km
coordination	tetrahedral (4)	octahedral (6)	cubic (8)

Goldschmidt's Rules

1. Ions of similar size can extensively substitute for each other in an ionic crystal.

If size difference is

- $< 15\%$: free substitution
- $15 - 30\%$: limited substitution
- $> 30\%$: little to no substitution

Goldschmidt's Rules

2. Ions whose charges differ by one unit substitute readily for one another, as long as electrical neutrality of the crystal is maintained.

If the charges differ by more than one unit, substitution is generally slight.

$\text{Fe}^{2+} \leftrightarrow \text{Fe}^{3+}$: very common

$\text{Na}^+ \leftrightarrow \text{Al}^{3+}$: extremely unlikely!

Goldschmidt's Rules

3. Ions with higher ionic potential form a stronger bond with surrounding anions.

Ionic potential = ratio of electric charge to the radius of an ion.

Thus, for ions of similar radii but different charges, the ion with the higher charge enters the crystal preferentially.

Ringwood's Modification of Goldshmidt's Rules (1955)

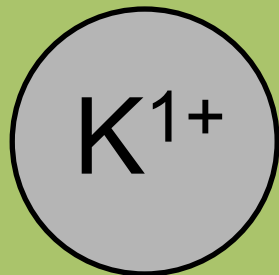
4. Substitutions may be limited, even when the size and charge criteria are satisfied, when the competing ions have *different electronegativities* and form bonds of *different ionic character*.

For example, Na^+ and Cu^+ have the same radius and charge, but do not substitute for one another.

Effect of Temperature

At ambient conditions, Na^+ and K^+ don't substitute for each other (ion difference of 25%), but at high temperatures, they will.

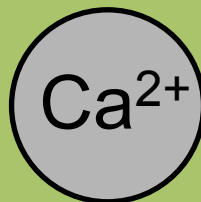
- Example: Alkali feldspars
- Degree of substitution gives us info about temperature of crystallization!



1.38 Å



1.02 Å



1.00 Å

Feldspars

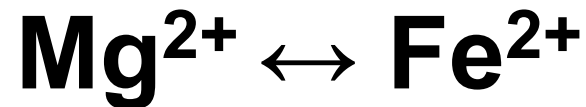
Orthoclase, **K** AlSi_3O_8

Albite, **Na** AlSi_3O_8

Anorthite, **Ca** $\text{Al}_2\text{Si}_2\text{O}_8$

Simple Substitution

Cations with identical charges:



Periclase-wüstite solid solution:



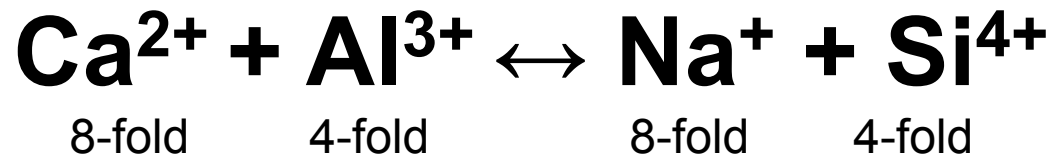
Olivine solid solution:



Coupled Substitution

Substitute atoms of different charges by coupling atoms that increase charge with those that reduces it.

Plagioclase feldspar solid solution series:



albite



anorthite

Ca^{2+} and Na^{+} occupy a distorted 8-fold coordination

Al^{3+} and Si^{4+} are tetrahedrally coordinated

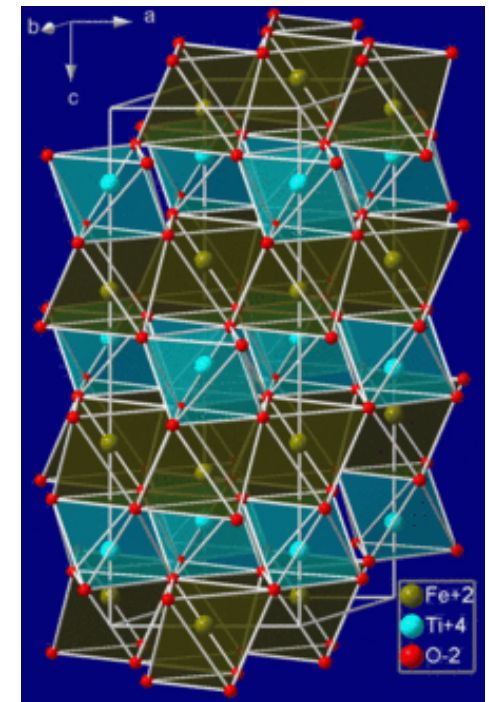
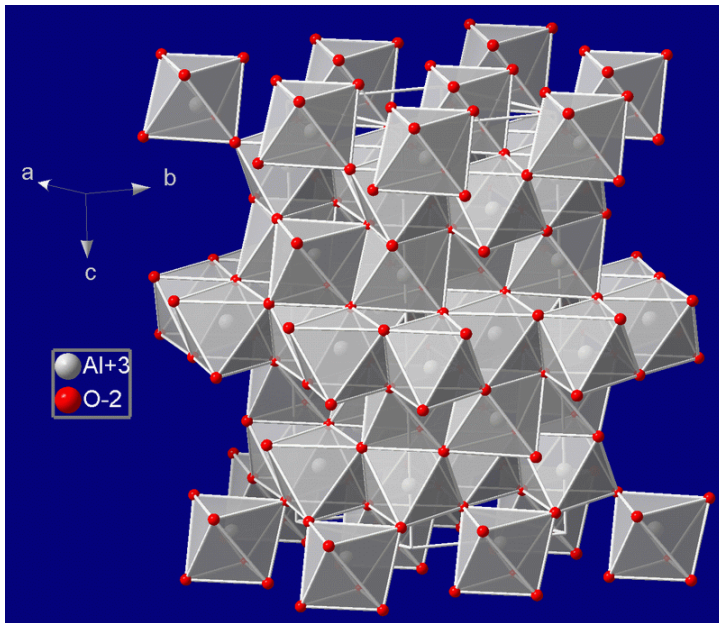
Coupled Substitution

Corundum – Ilmenite solid solution:



Al_2O_3
corundum

FeTiO_3
ilmenite



Omission Substitution

Substitute atoms of different charges and leave a site vacant, maintaining charge balance.



vacant site
normally
occupied by
 M^{n+}

Pyrrhotite:



ferrous
pyrrhotite

pyrrhotite with max Fe^{3+}

Omission Substitution

Chemical formulas for pyrrhotite:

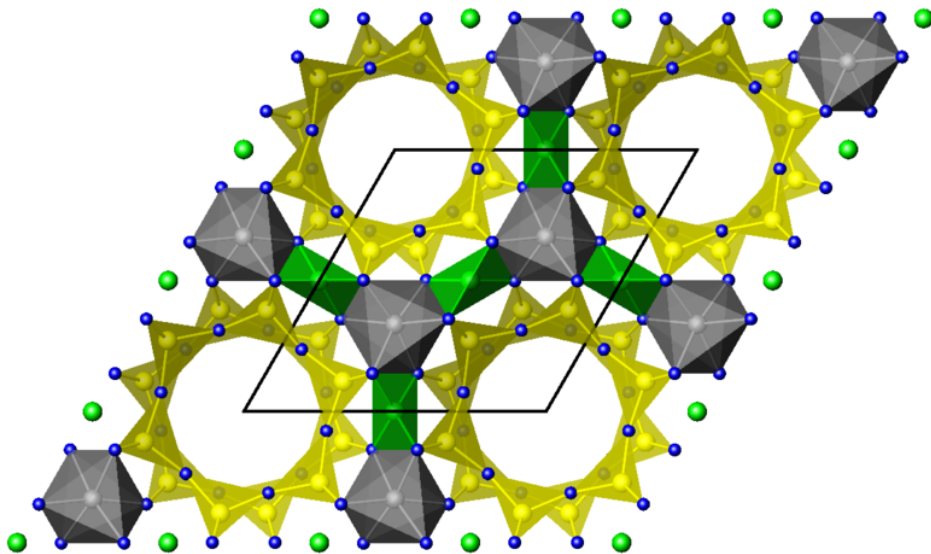


Rob Lavinsky

Interstitial Substitution

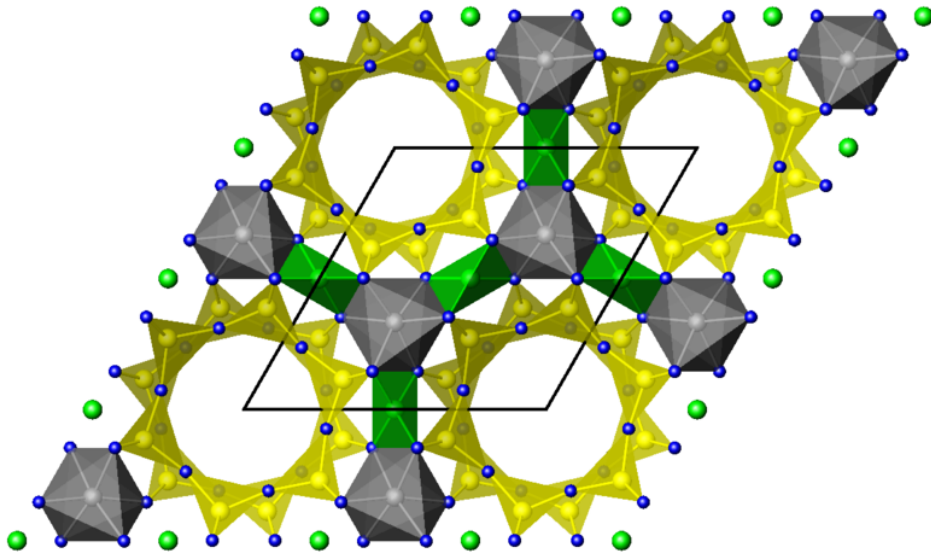
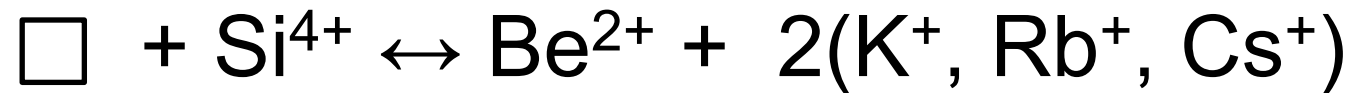
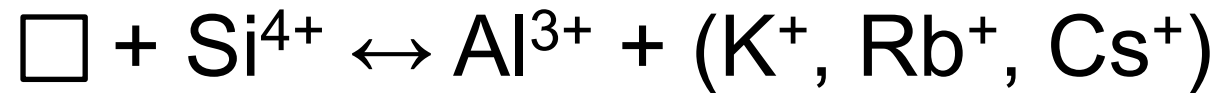
Charge balance is maintained by placing ions in sites that are normally vacant.

Beryl ($\text{Al}_2\text{Be}_3\text{Si}_6\text{O}_{18}$) is made of rings of silicon tetrahedra, creating channels.

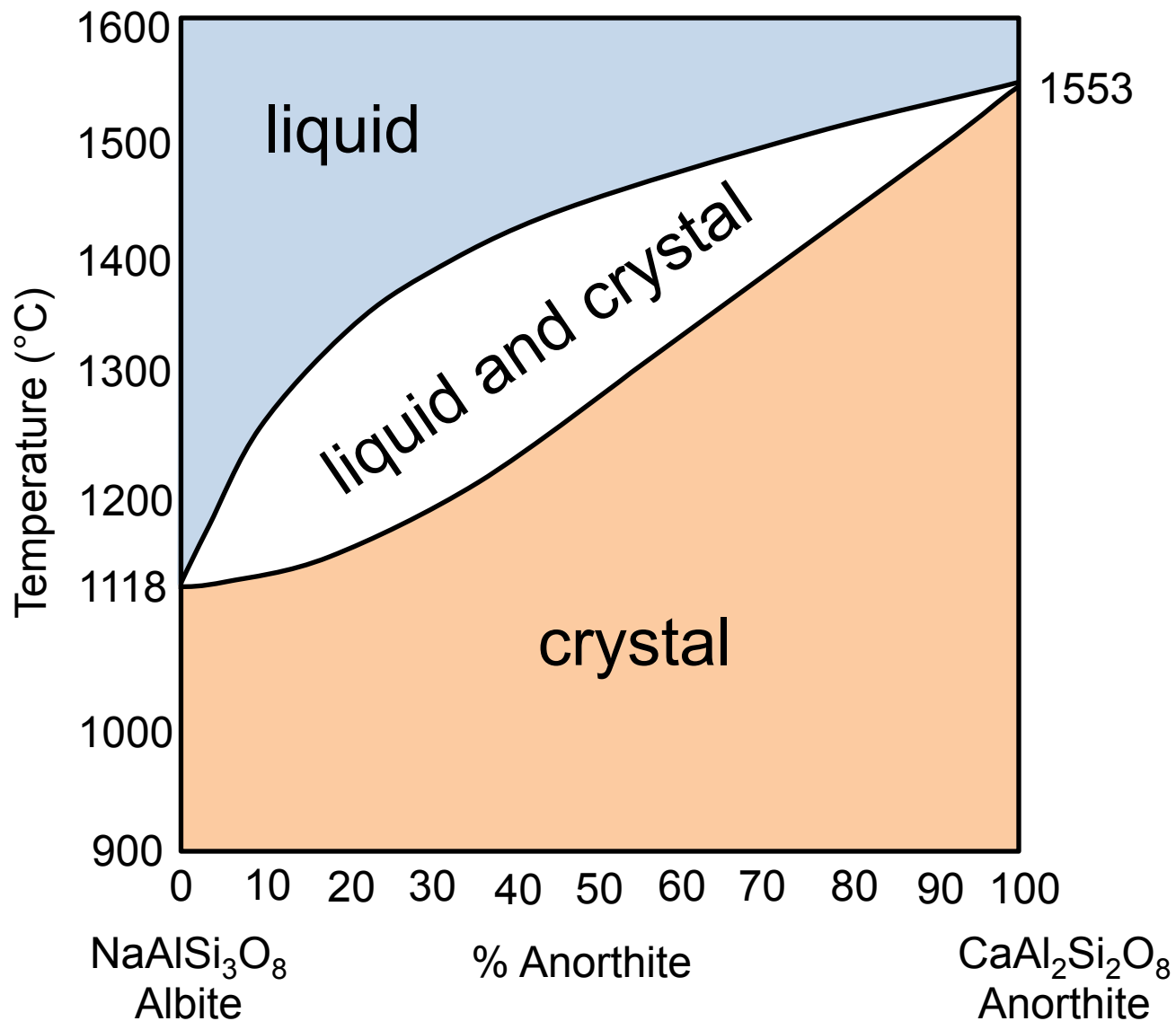


Interstitial Substitution

Monovalent cations can be inserted into these cavities.



Two-Component Phase Diagrams

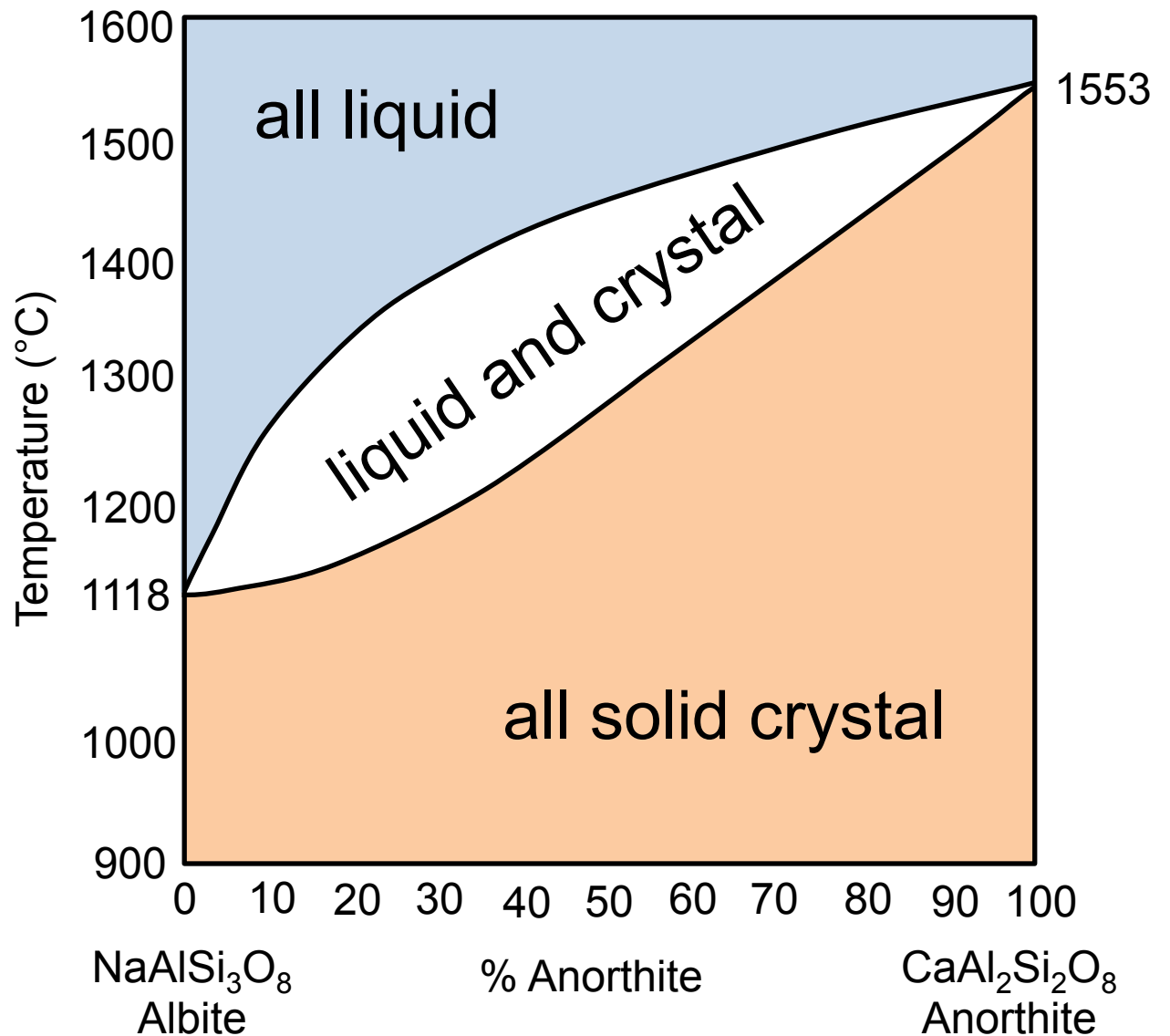


2-C Solid Solution Phase Diagram

Two phases:
plagioclase crystal
(orange) and melt
(blue)

The two phases
(liquid and crystal)
coexist in the
white region

Two components:
 $\text{NaAlSi}_3\text{O}_8$ and
 $\text{CaAl}_2\text{Si}_2\text{O}_8$

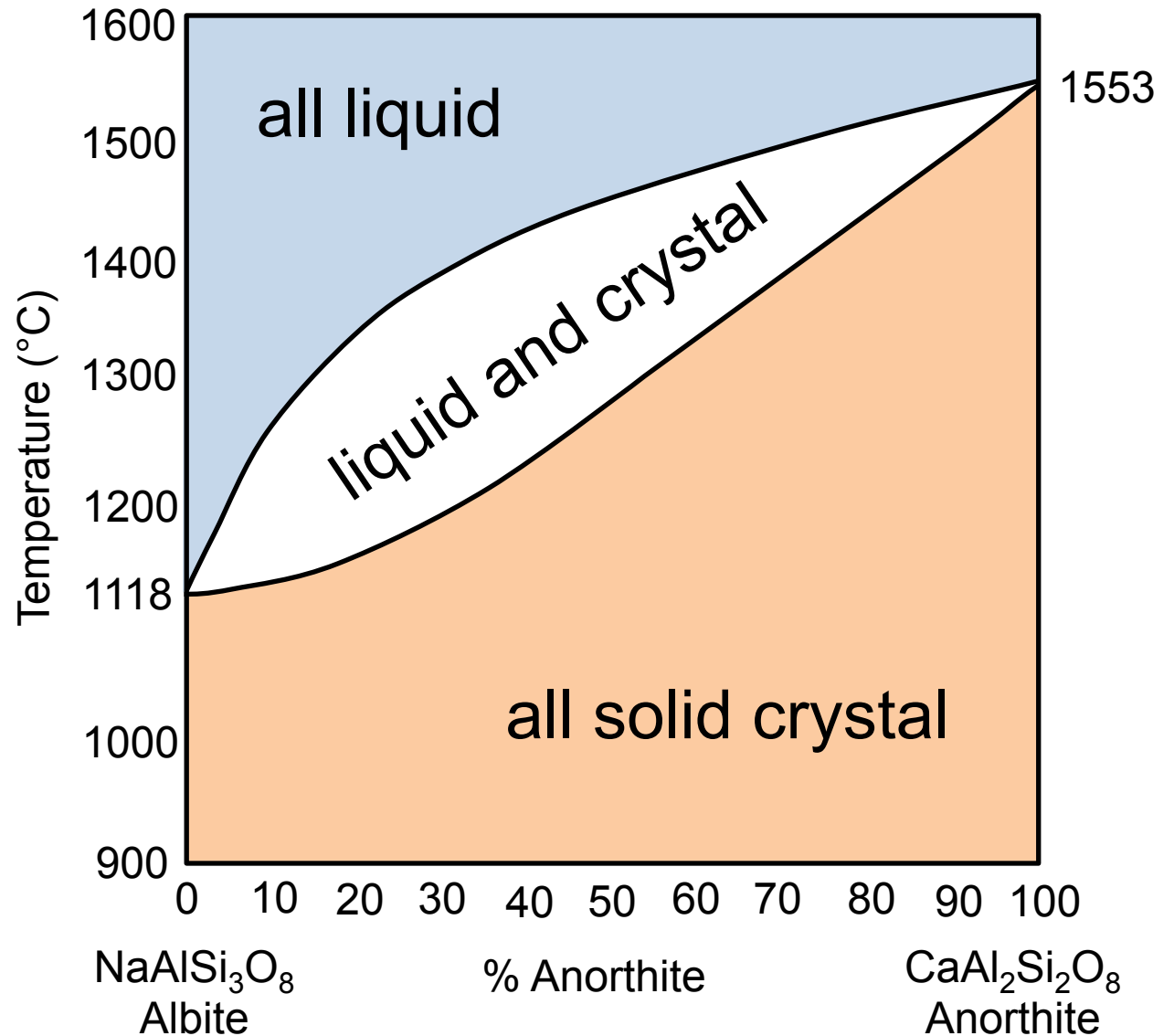


2-C Solid Solution Phase Diagram

Complete miscibility (mixability) in both liquid (magma) and crystal phases

The following terms will be used synonymously:

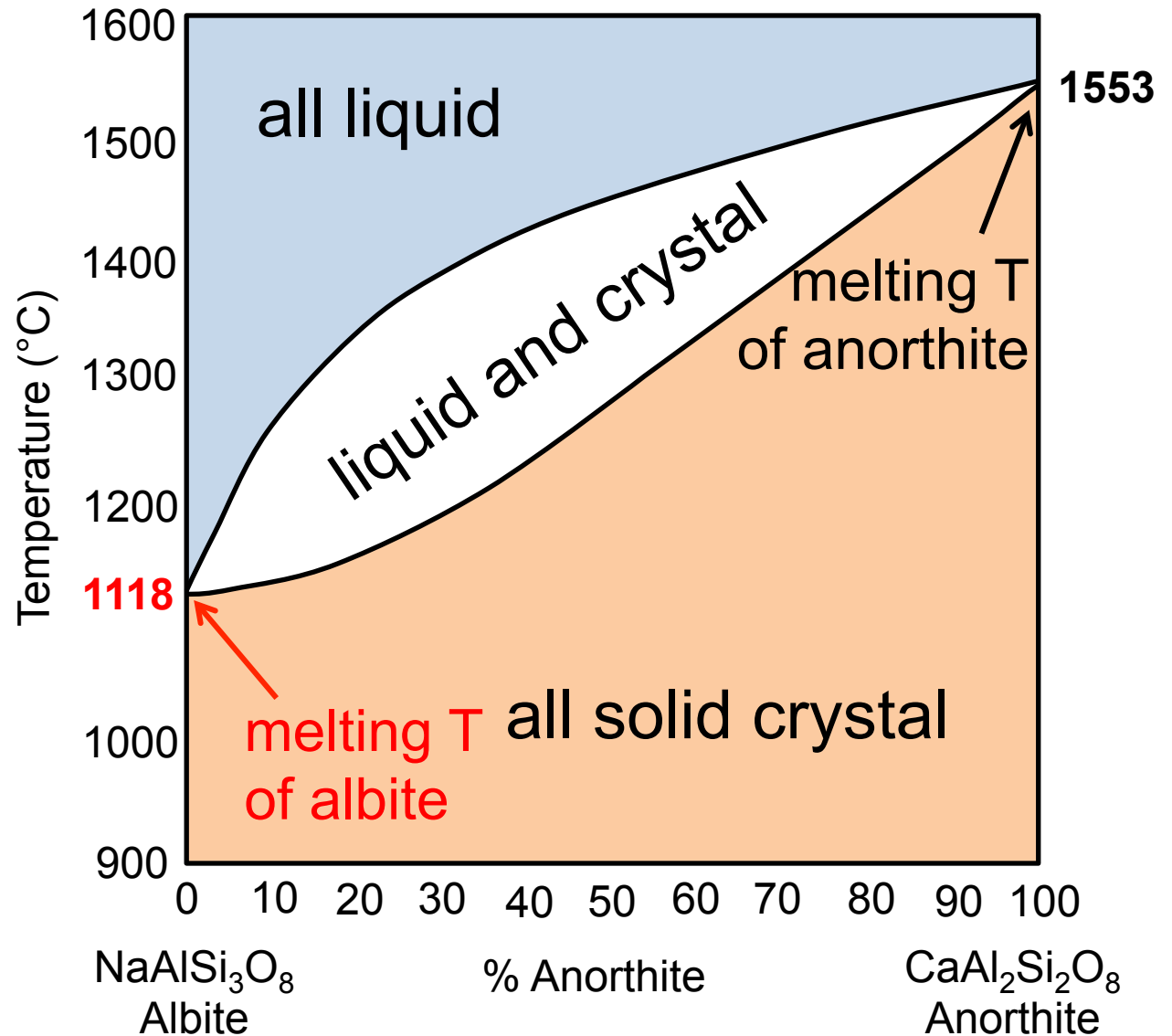
- 1) liquid, melt and magma
- 2) solid, crystal and plagioclase



2-C Solid Solution Phase Diagram

Pure albite melts at
1118° C

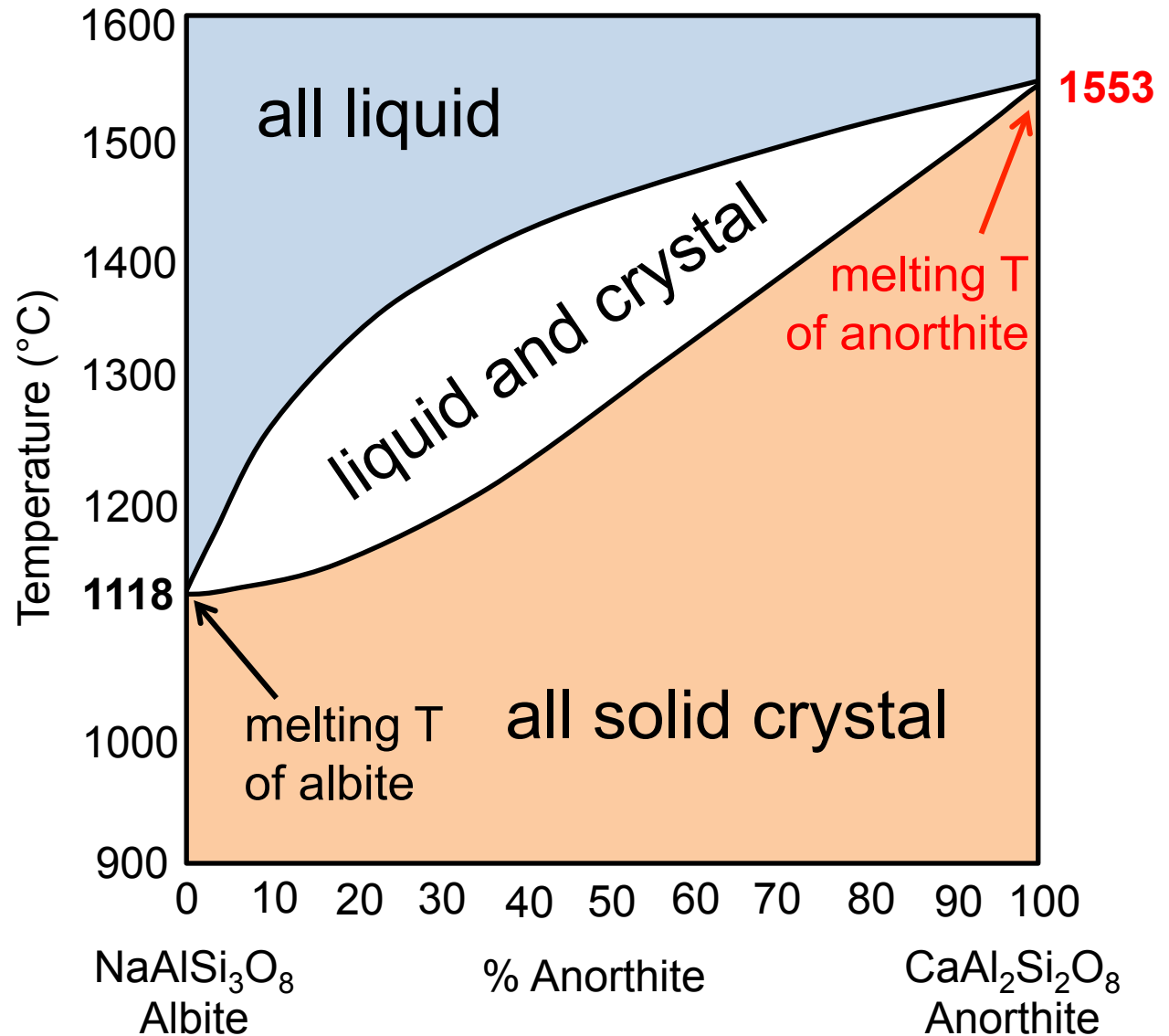
Pure anorthite melts
at 1553° C



2-C Solid Solution Phase Diagram

Pure albite melts at
1118° C

Pure anorthite melts
at 1553° C

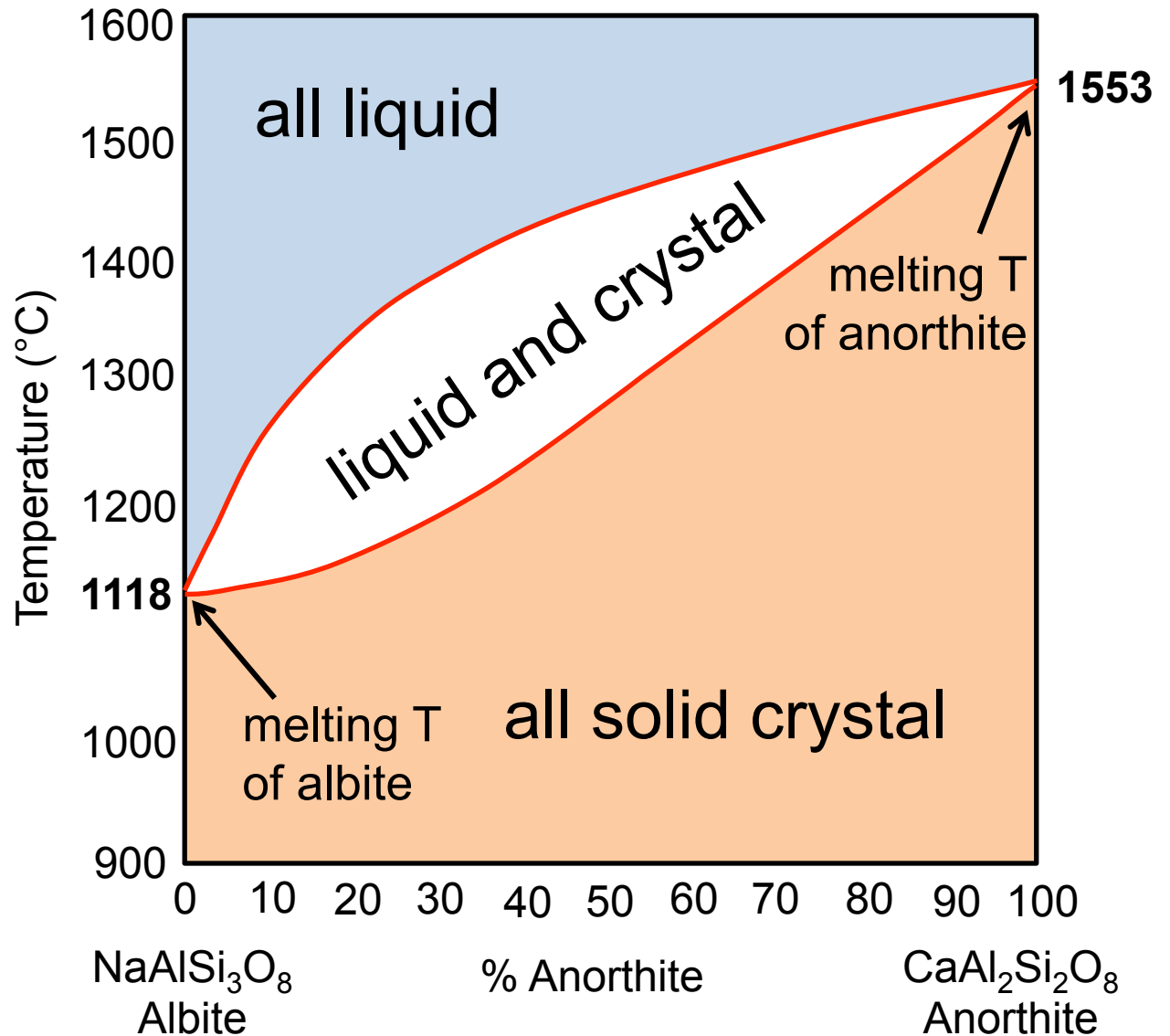


2-C Solid Solution Phase Diagram

Pure albite melts at
1118° C

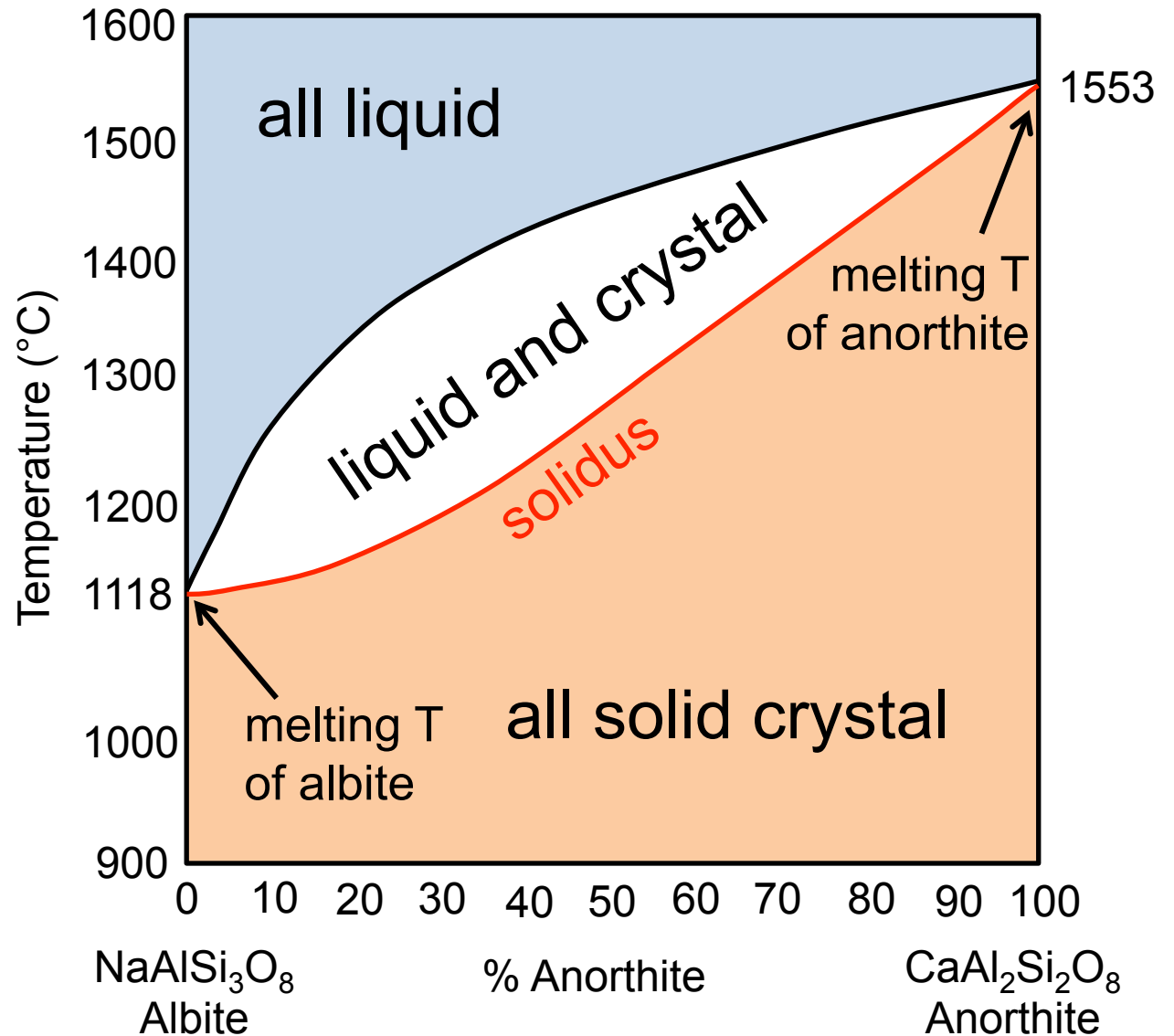
Pure anorthite melts
at 1553° C

Non endmembers
do not have one
melting temperature
– they melt over a
range of
temperatures



2-C Solid Solution Phase Diagram

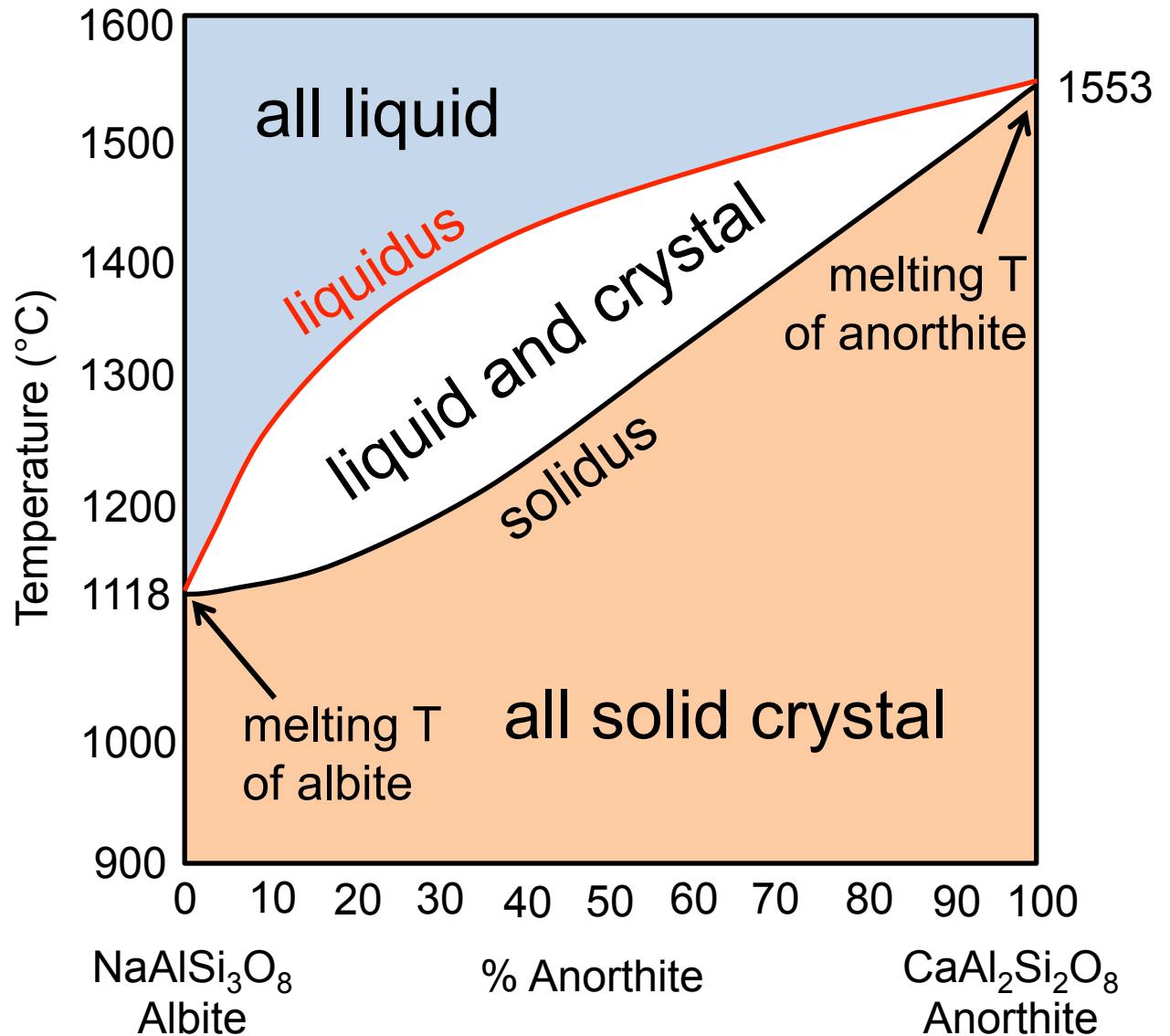
Solidus = line that separates all solid from liquid + solid



2-C Solid Solution Phase Diagram

Solidus = line that separates all solid from liquid + solid

Liquidus = line that separates all liquid from liquid + solid



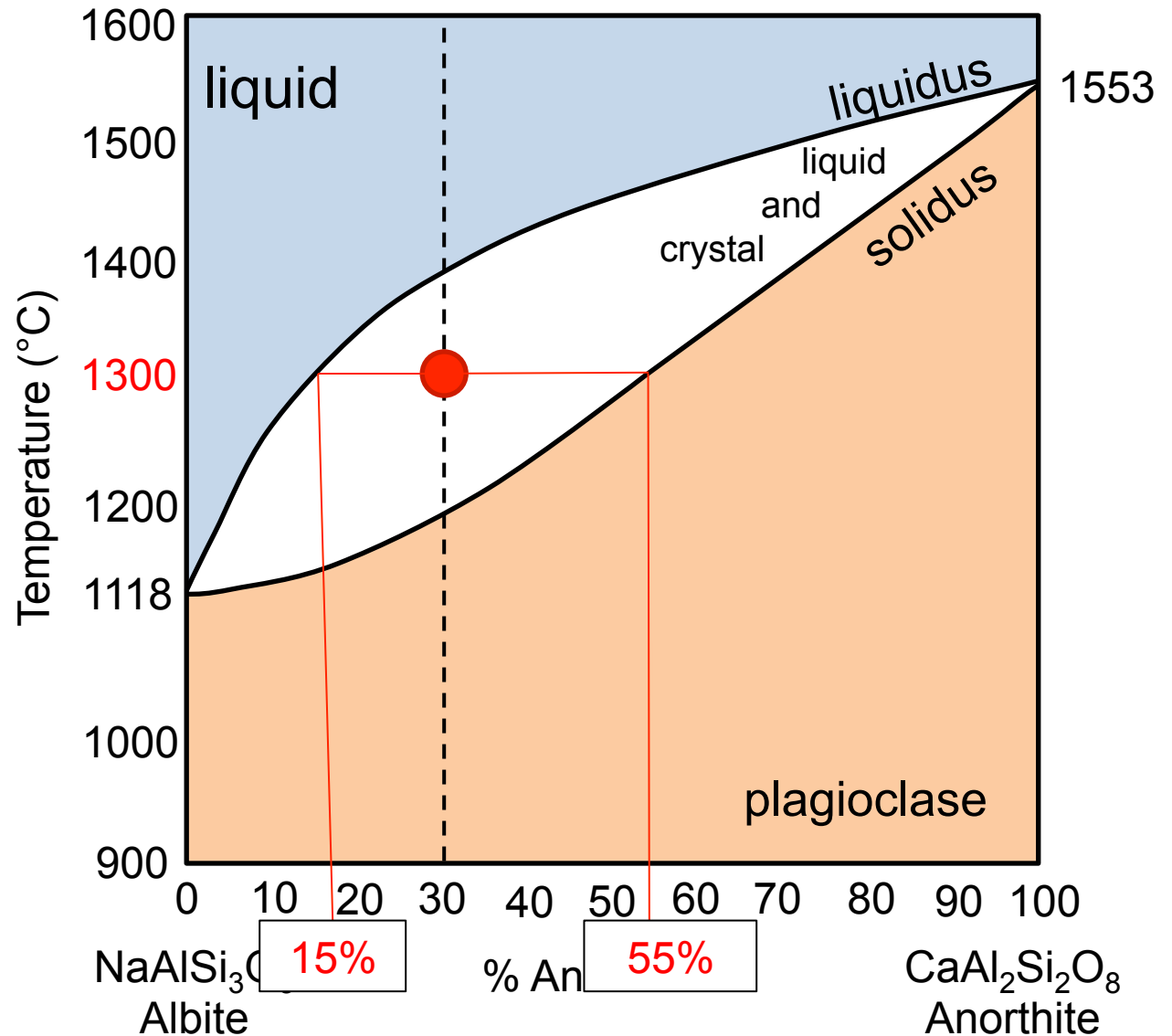
2-C Solid Solution Phase Diagram

Use the **liquidus** to determine the composition of the **melt**.

→ The melt is 15% anorthite.

Use the **solidus** to determine the composition of the **crystal**.

→ The crystal is 55% anorthite.



2-C Solid Solution Phase Diagram

The Lever Rule

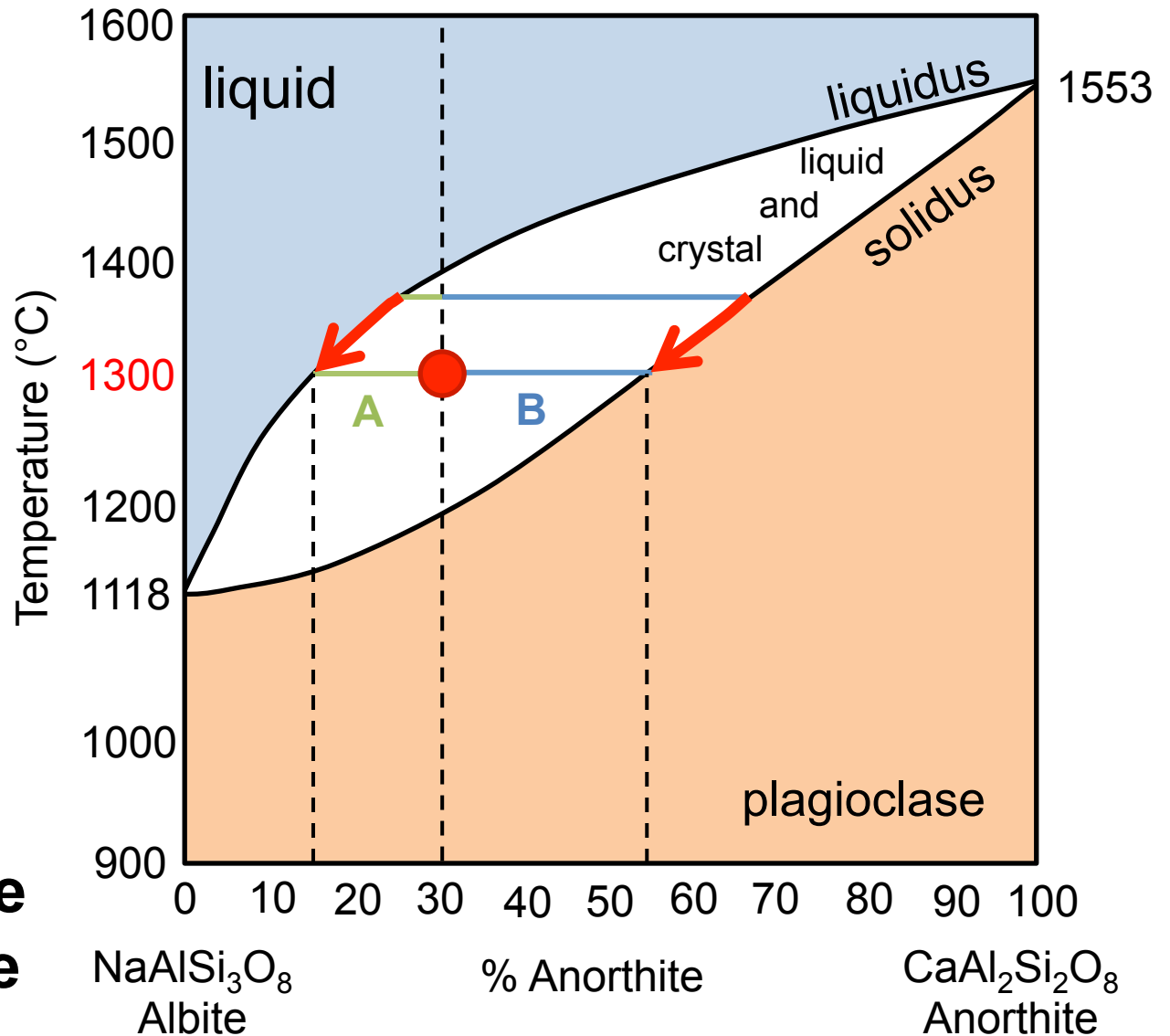
Melt fraction:

$$B/(A+B) = 25/(15+25) = 25/40 = \mathbf{0.625}$$

Crystal fraction:

$$A/(A+B) = 15/(15+25) = 15/40 = \mathbf{0.375}$$

**B decreases while
A increases as we
decrease T.**



Equilibrium vs. Fractional Melting

There are 2 ways to melt the mantle:

1) Equilibrium melting

occurs when the solid and liquid phases are kept together as melting progresses

2) Fractional melting

occurs if the liquid is removed from the solid as the solid melts

Equilibrium vs. Fractional Crystallization

There are 2 ways to crystallize solids from melt:

1) Equilibrium crystallization

occurs when the solid and liquid phases are kept together as crystallization progresses

2) Fractional crystallization

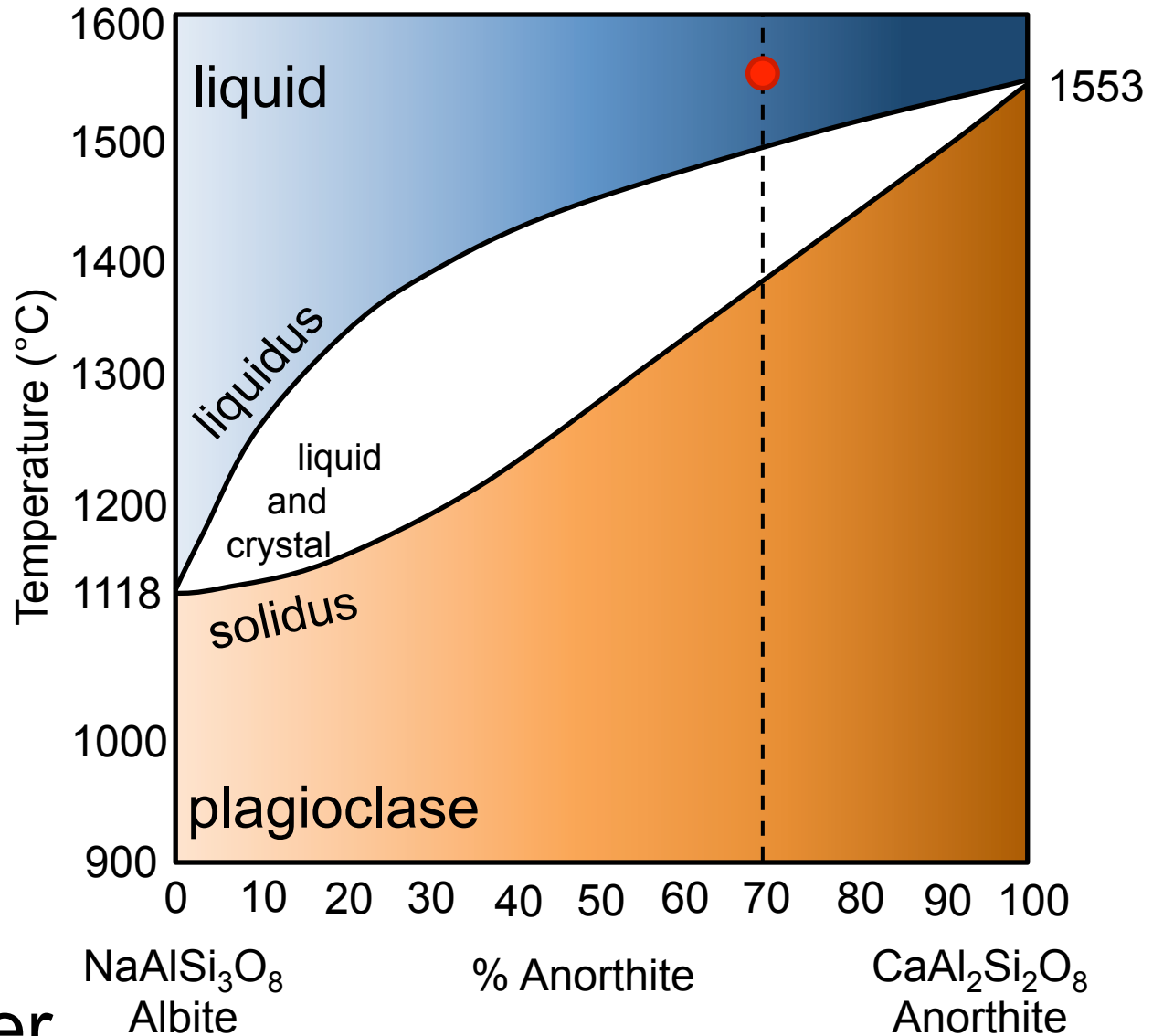
occurs if the solid is removed from the liquid as it crystallizes

Equilibrium Crystallization

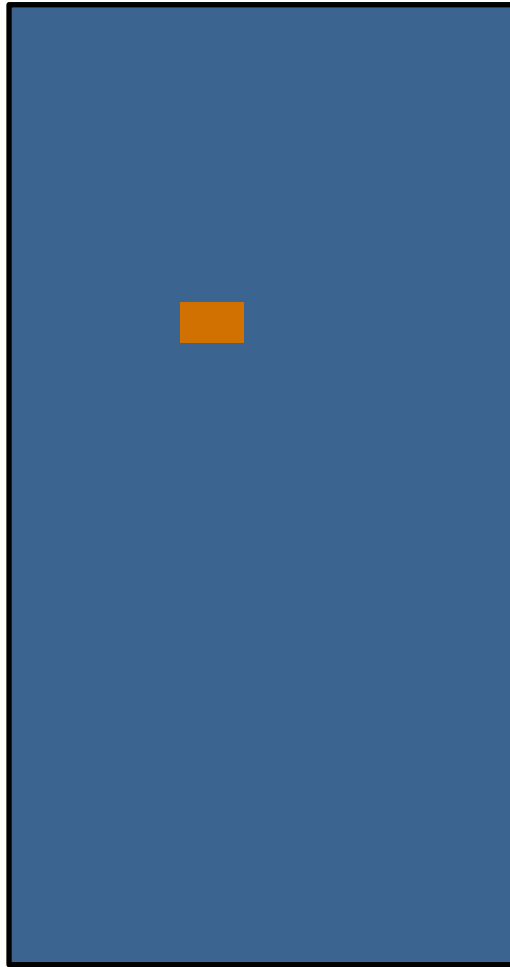
Dark colors = more anorthite rich.

Light colors = more albite rich.

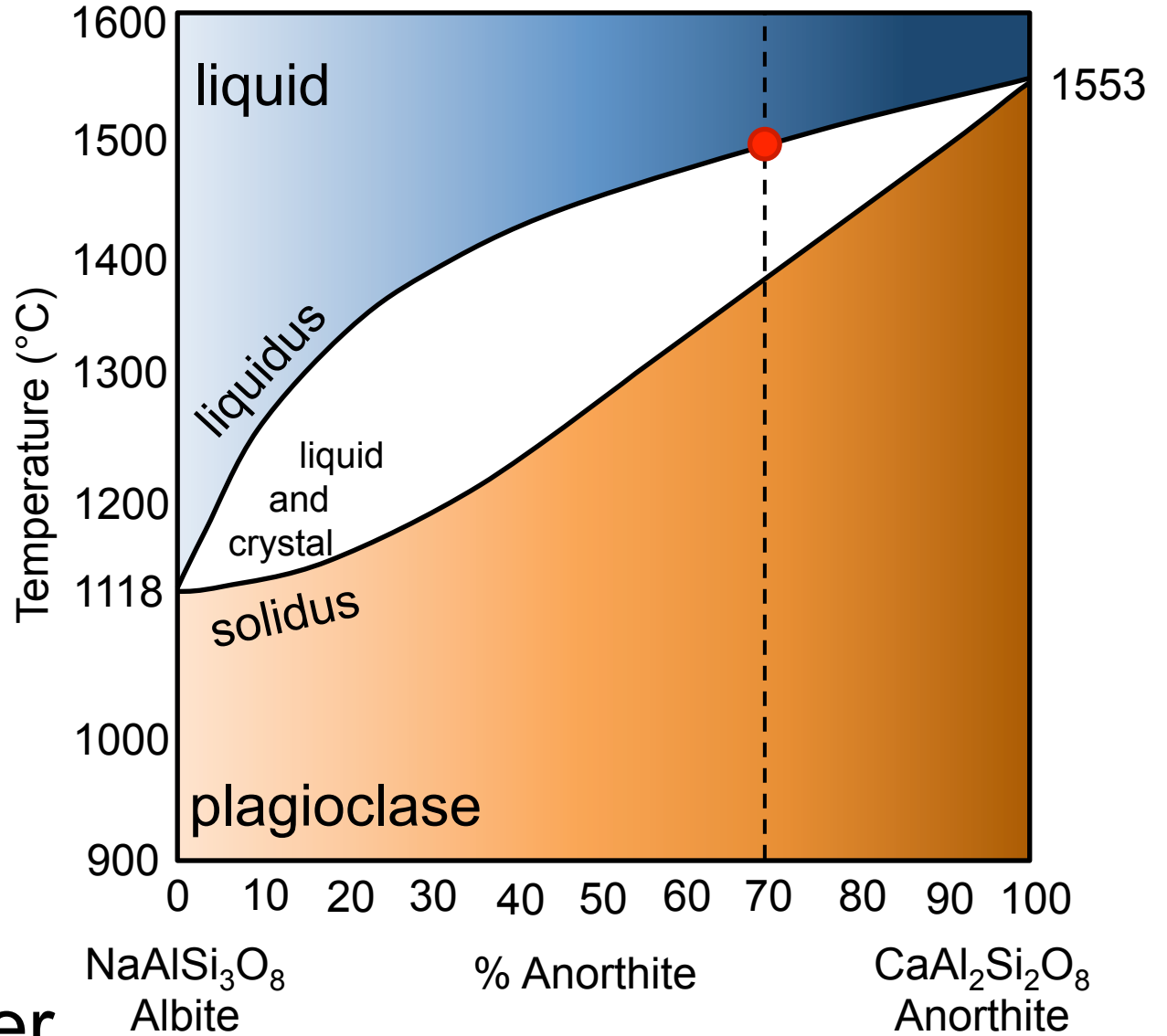
magma chamber



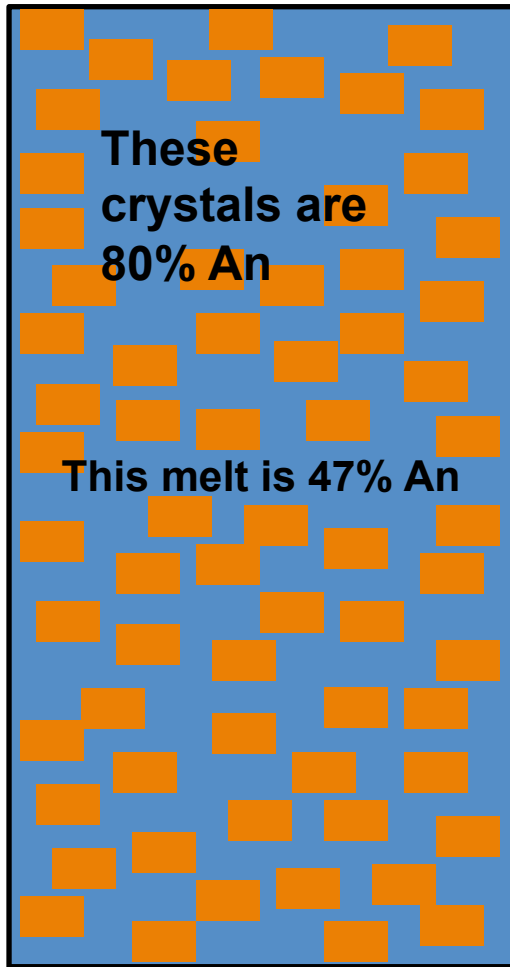
Equilibrium Crystallization



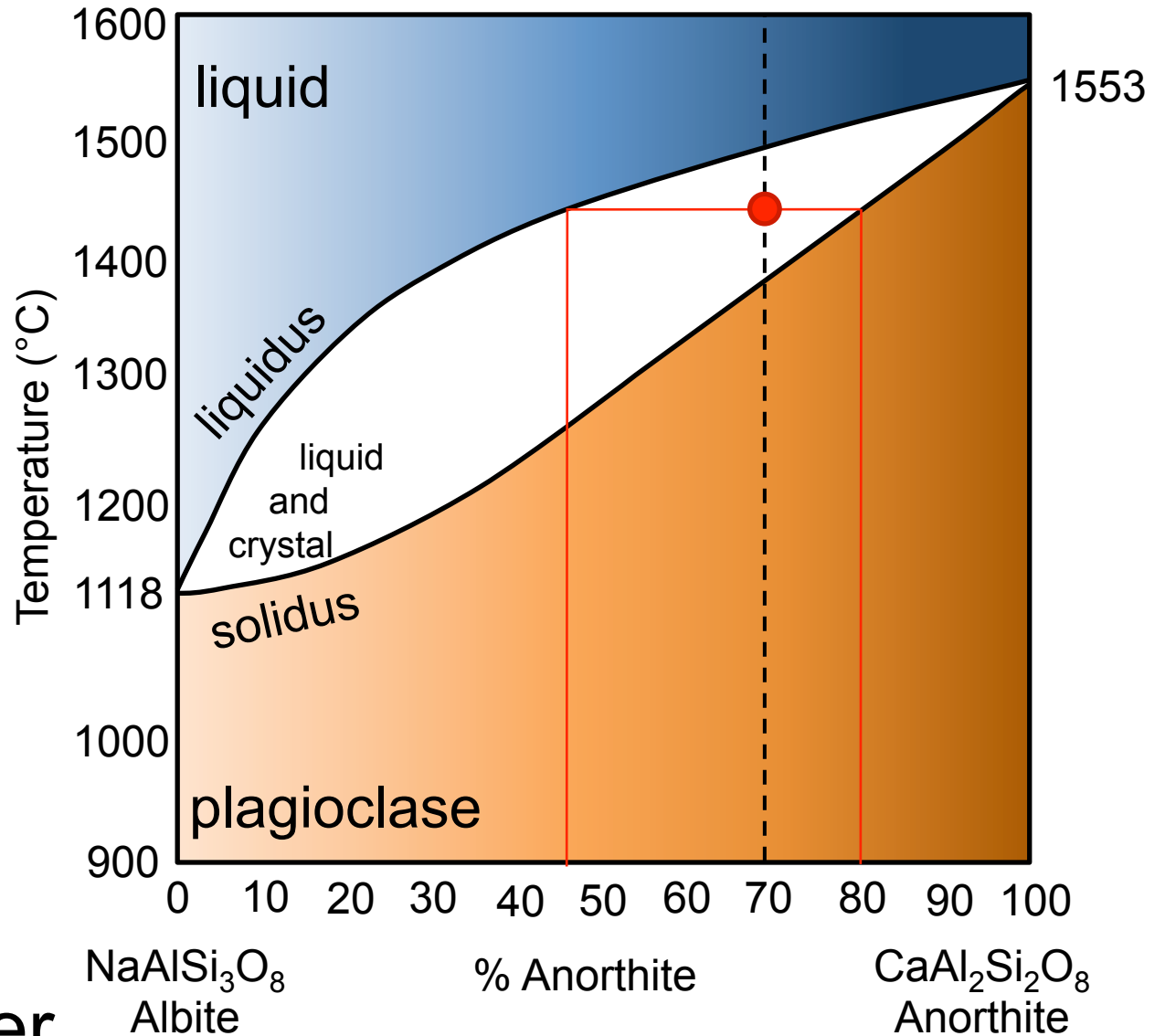
magma chamber



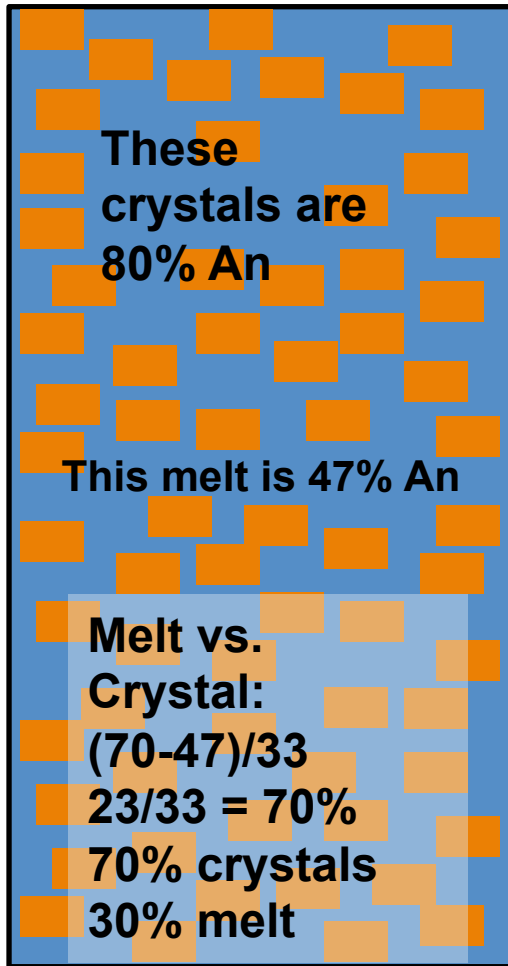
Equilibrium Crystallization



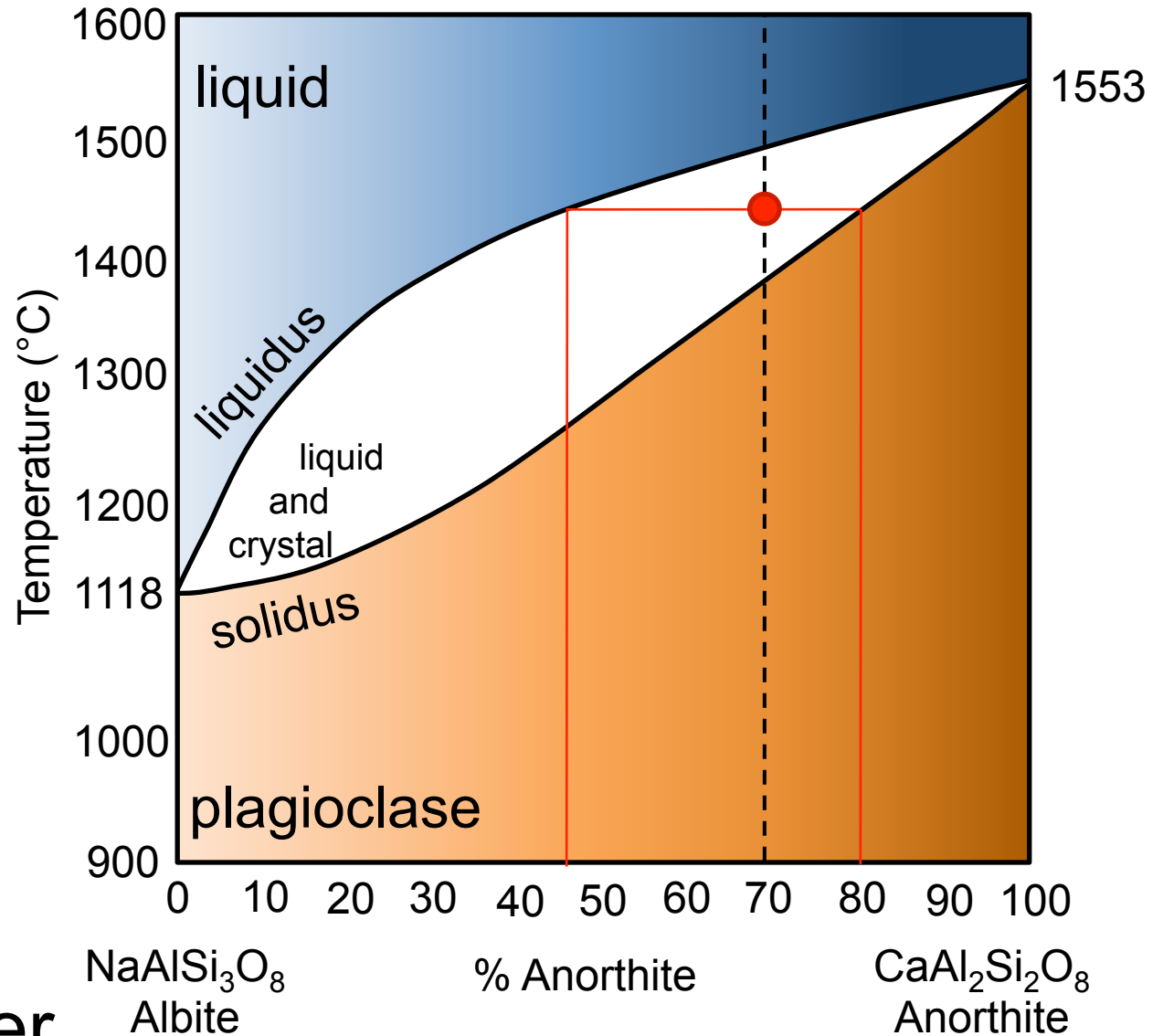
magma chamber



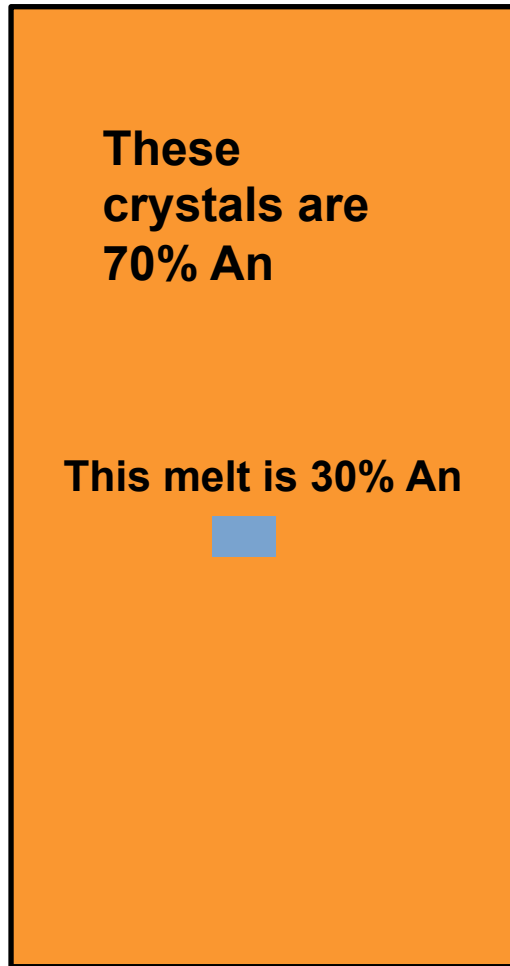
Equilibrium Crystallization



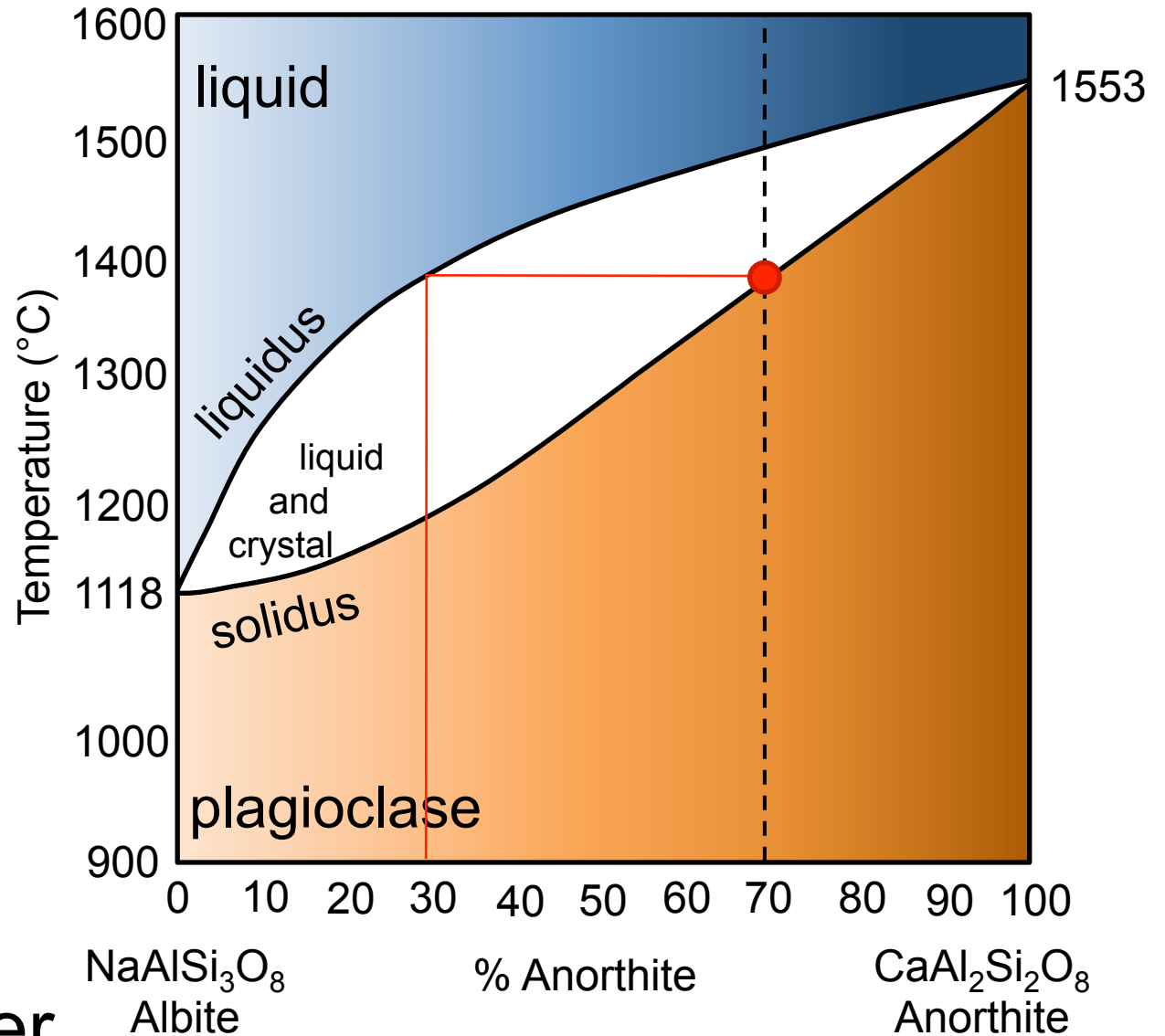
magma chamber



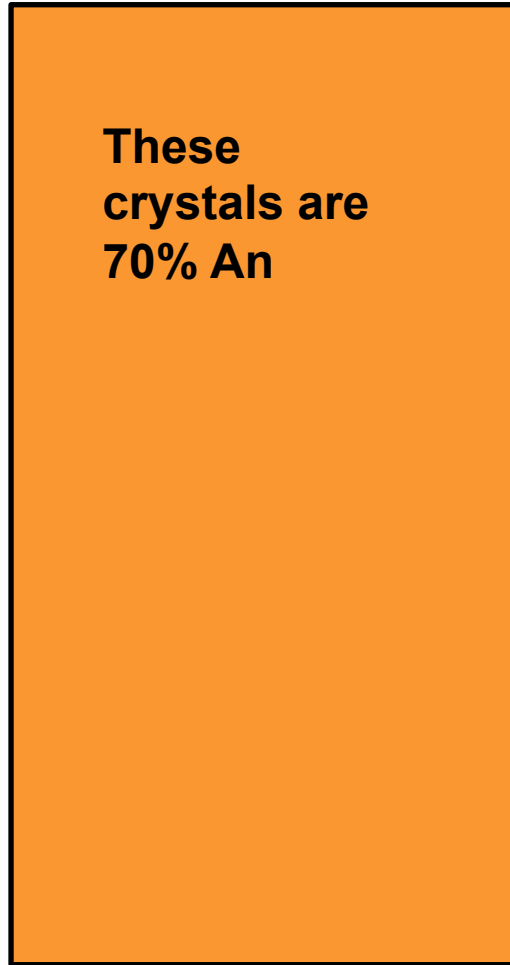
Equilibrium Crystallization



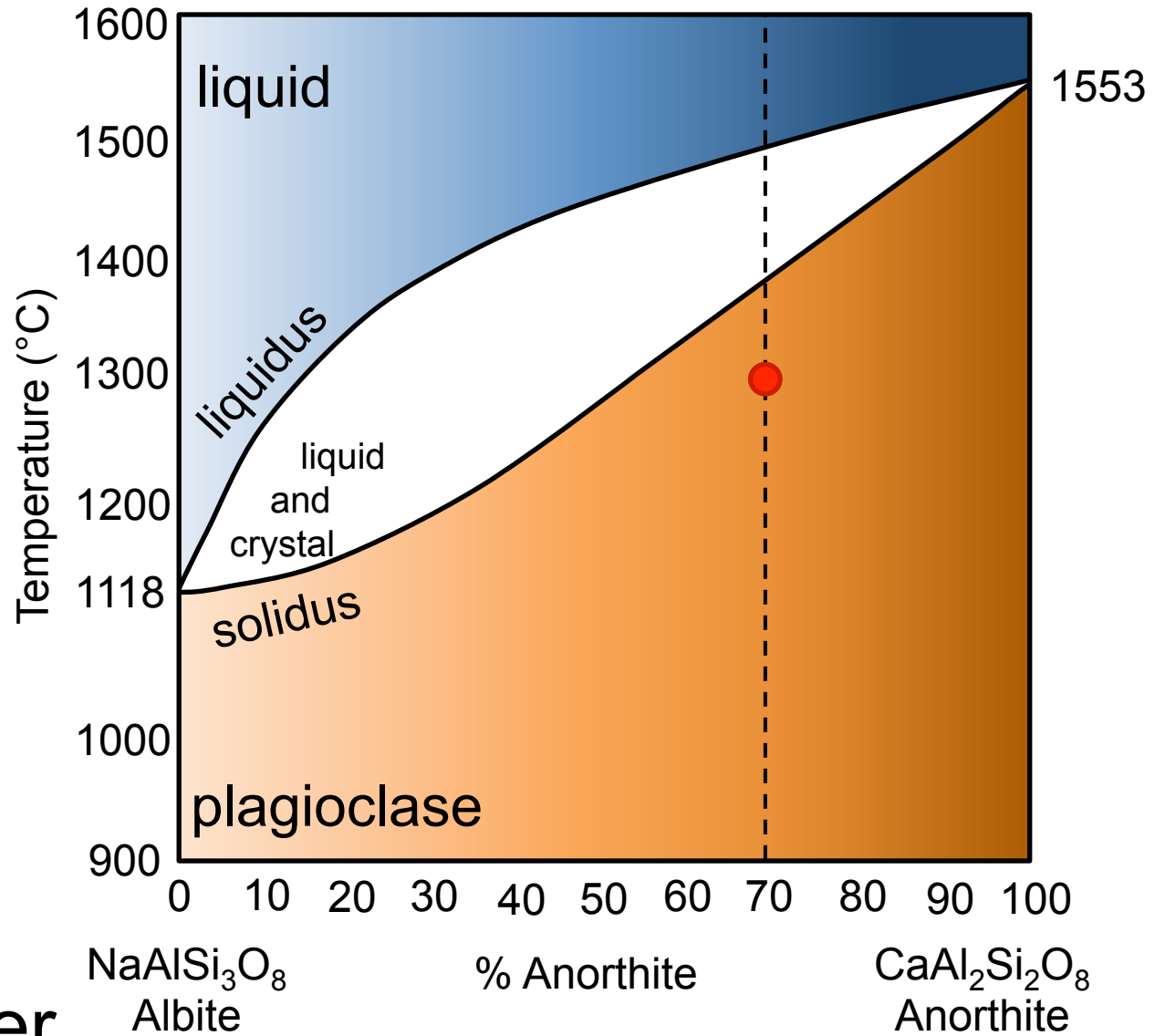
magma chamber



Equilibrium Crystallization



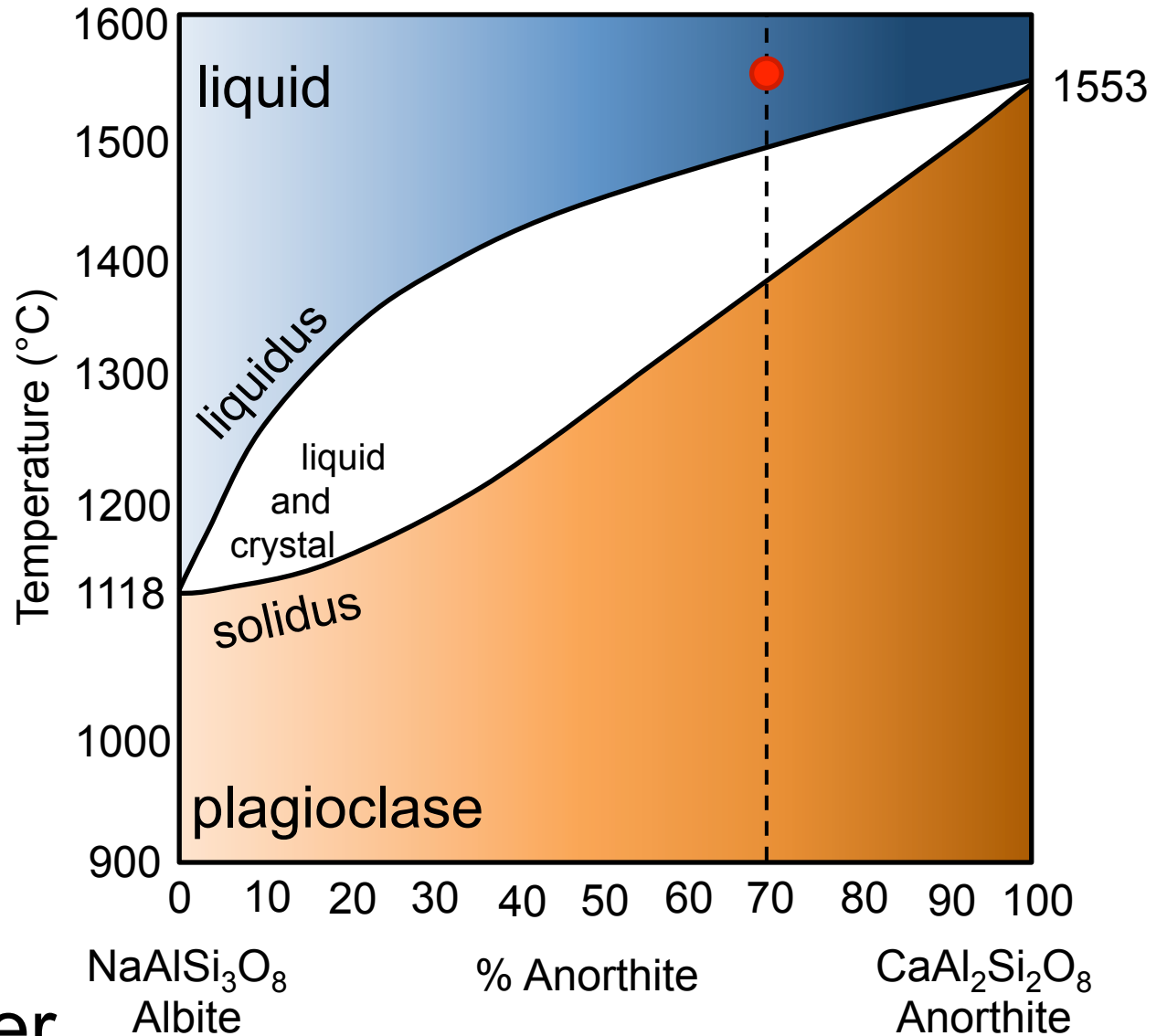
magma chamber



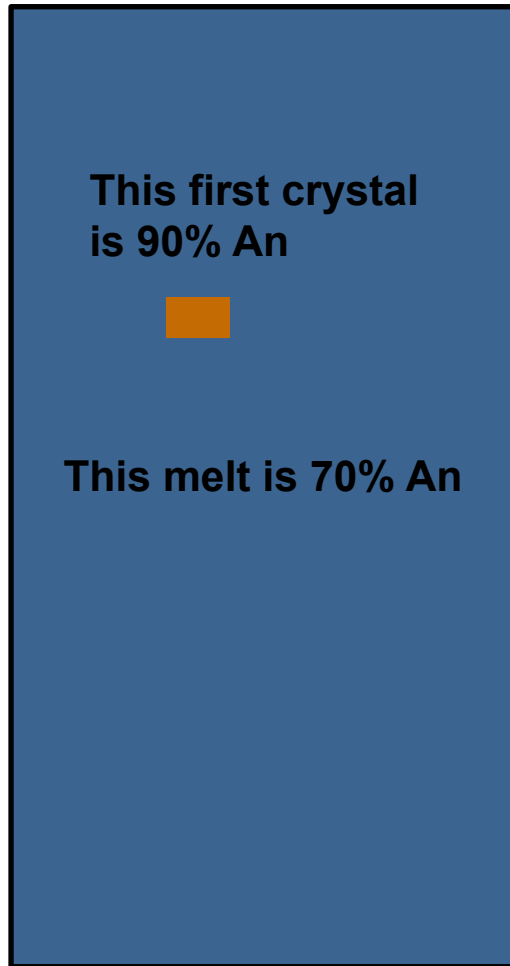
Fractional Crystallization

Example of fractional crystallization, where we will remove the crystals.

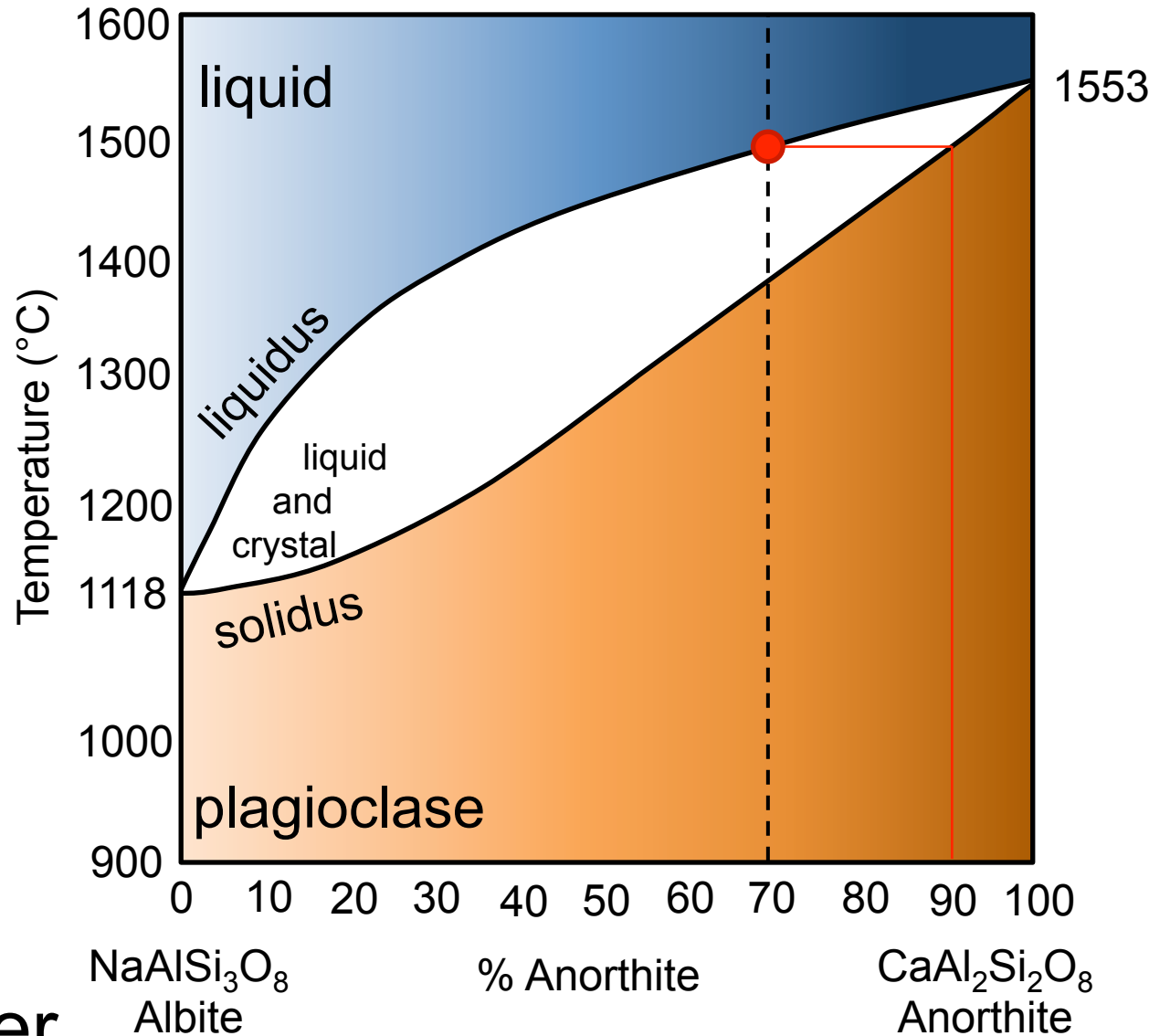
magma chamber



Fractional Crystallization



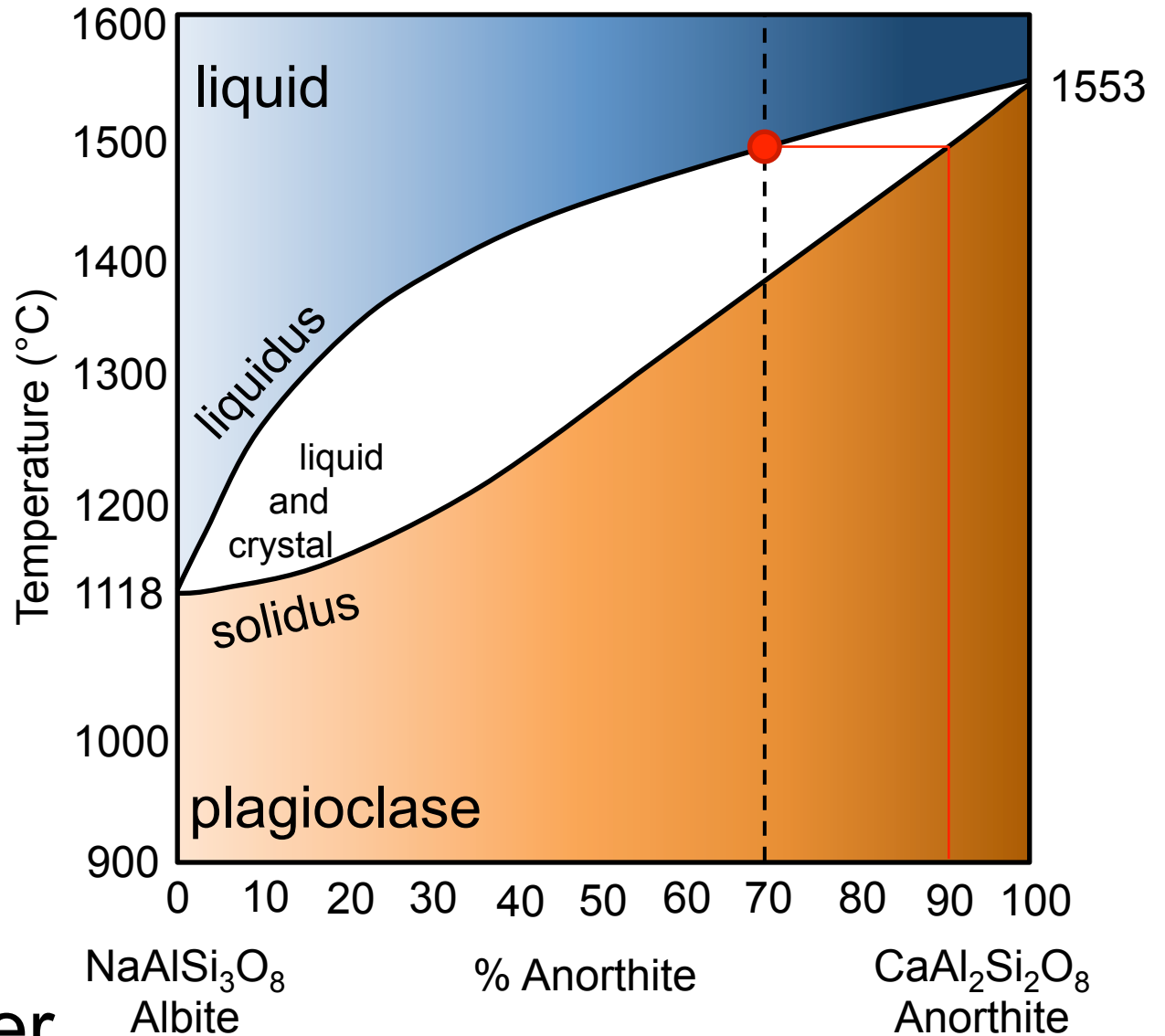
magma chamber



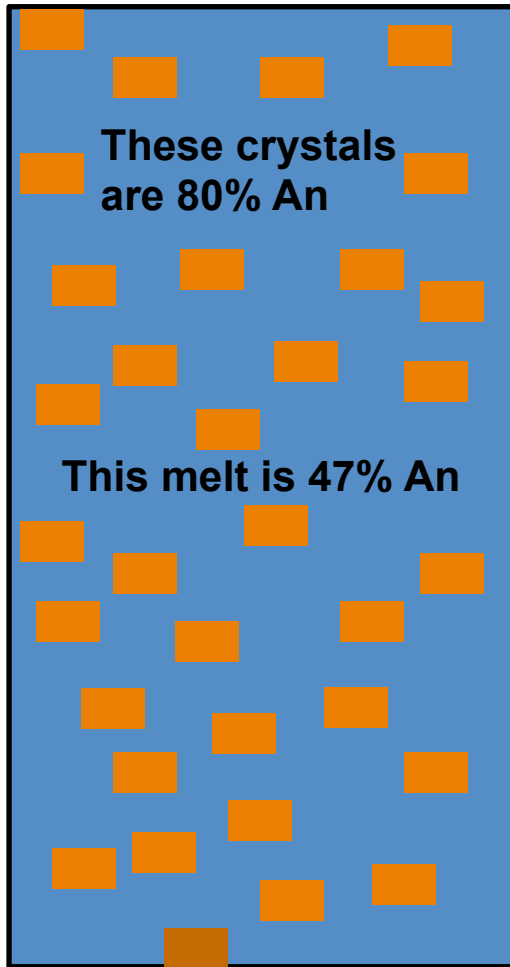
Fractional Crystallization



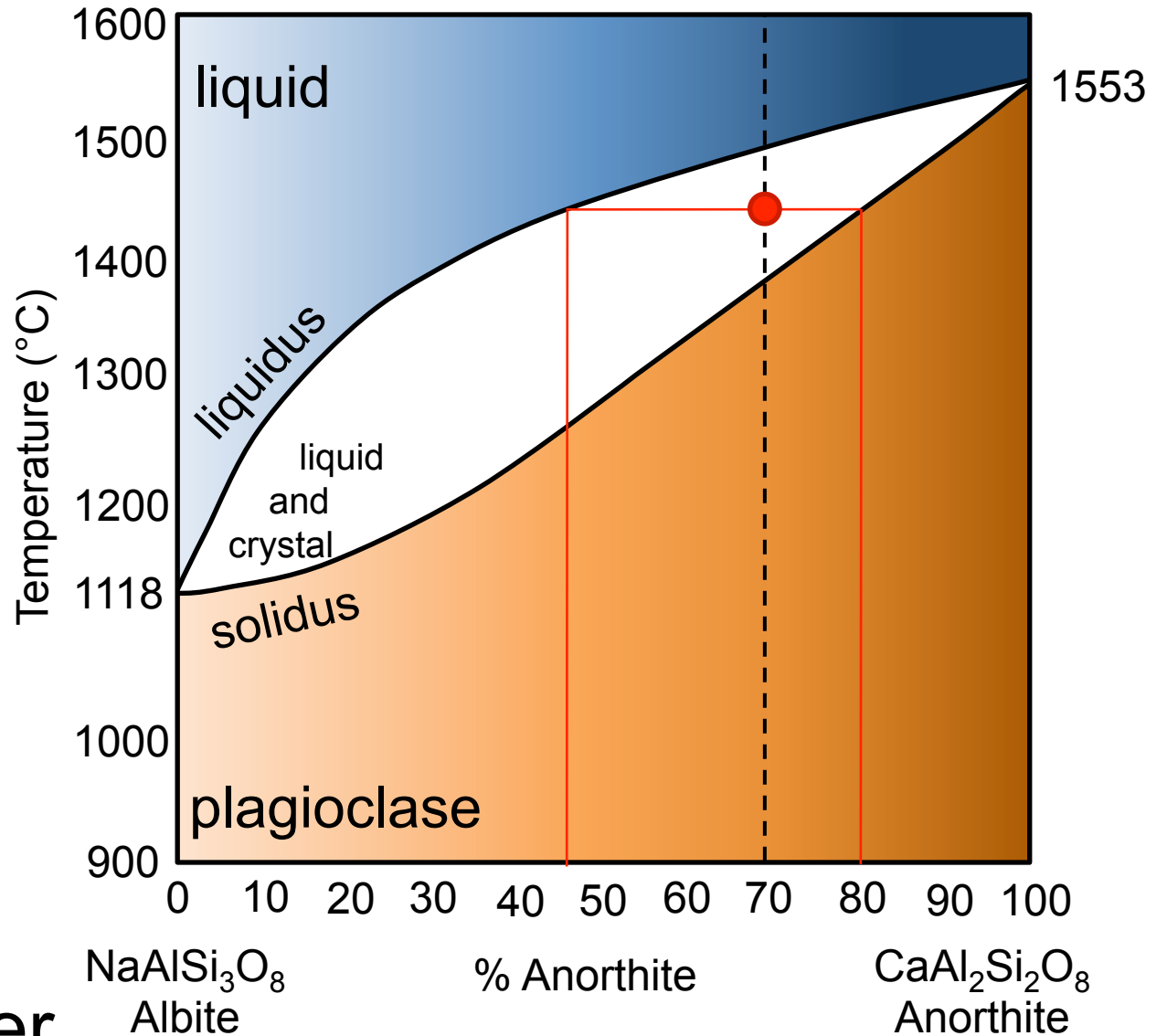
magma chamber



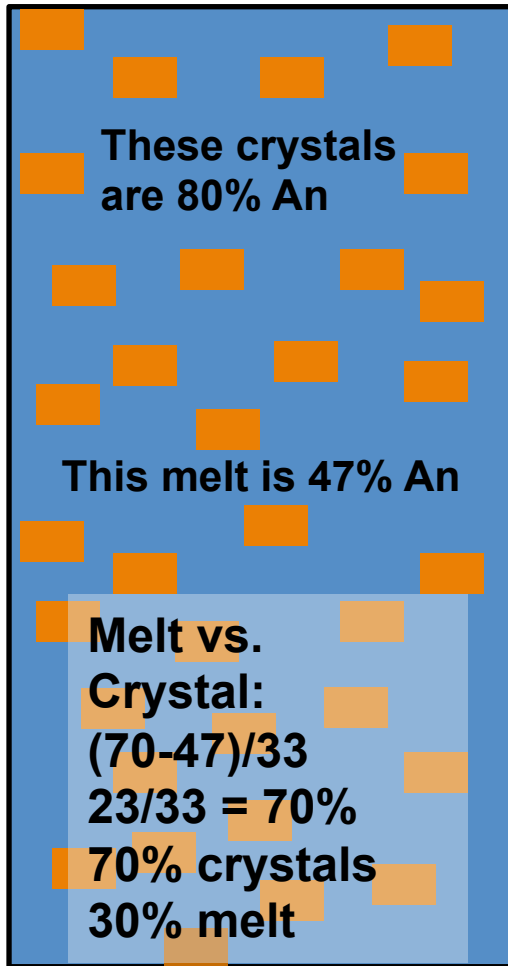
Fractional Crystallization



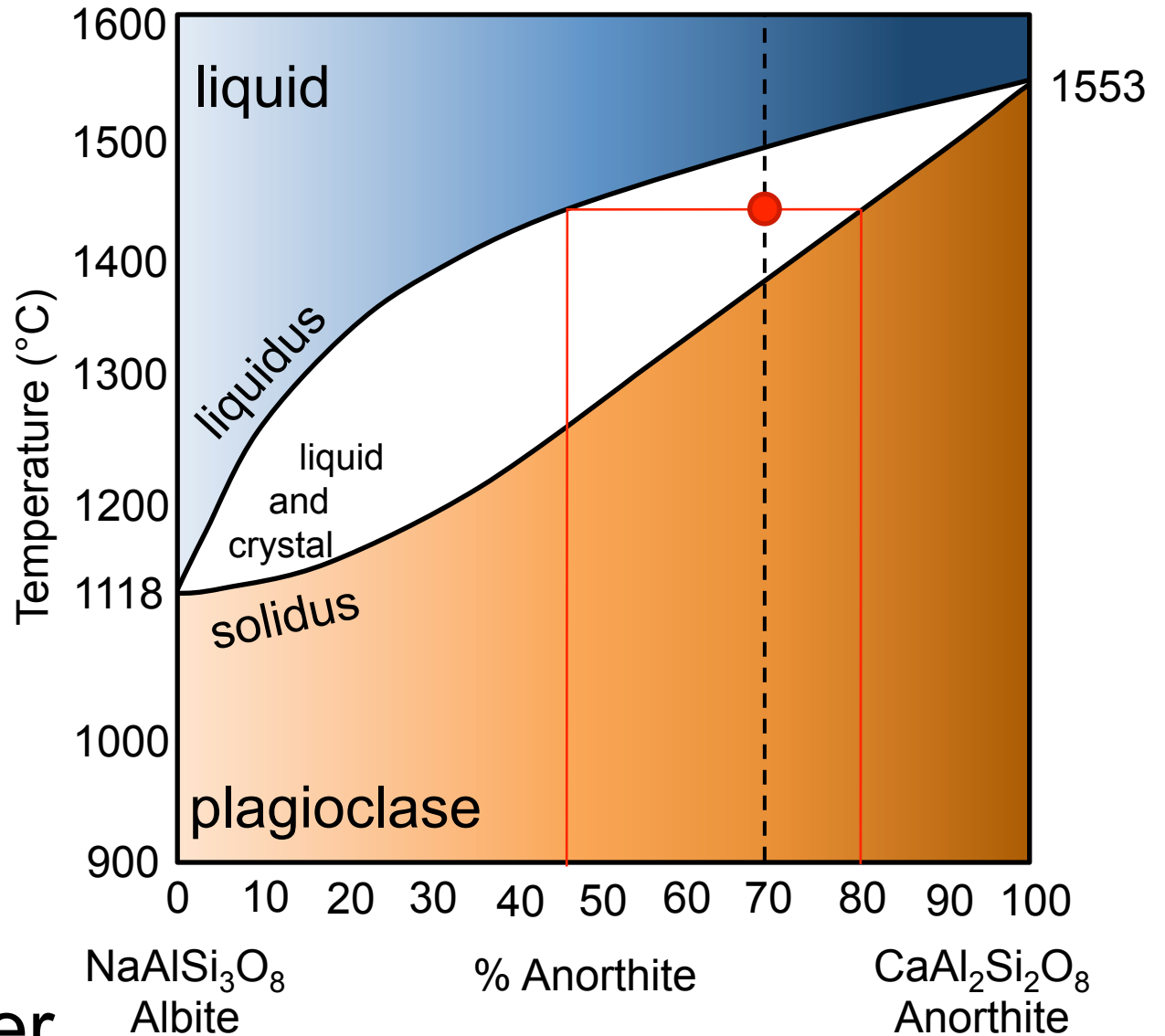
magma chamber



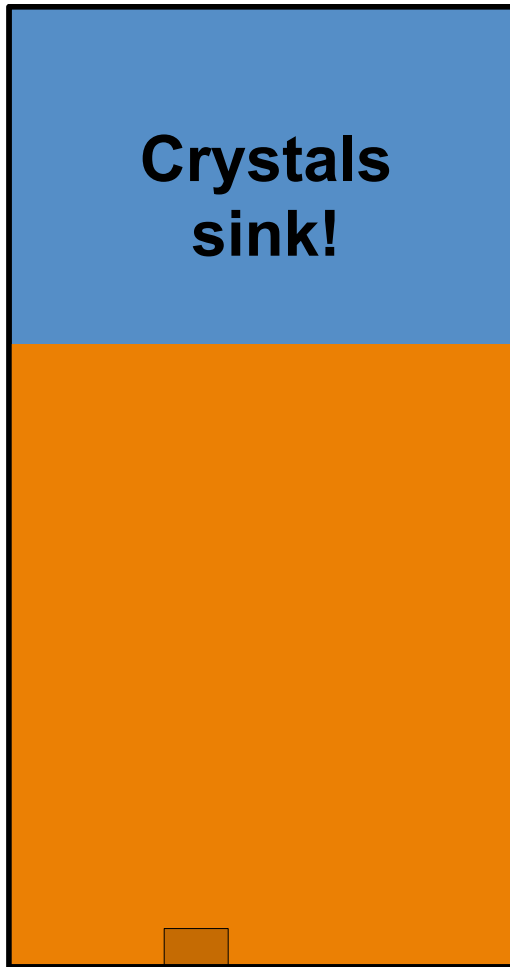
Fractional Crystallization



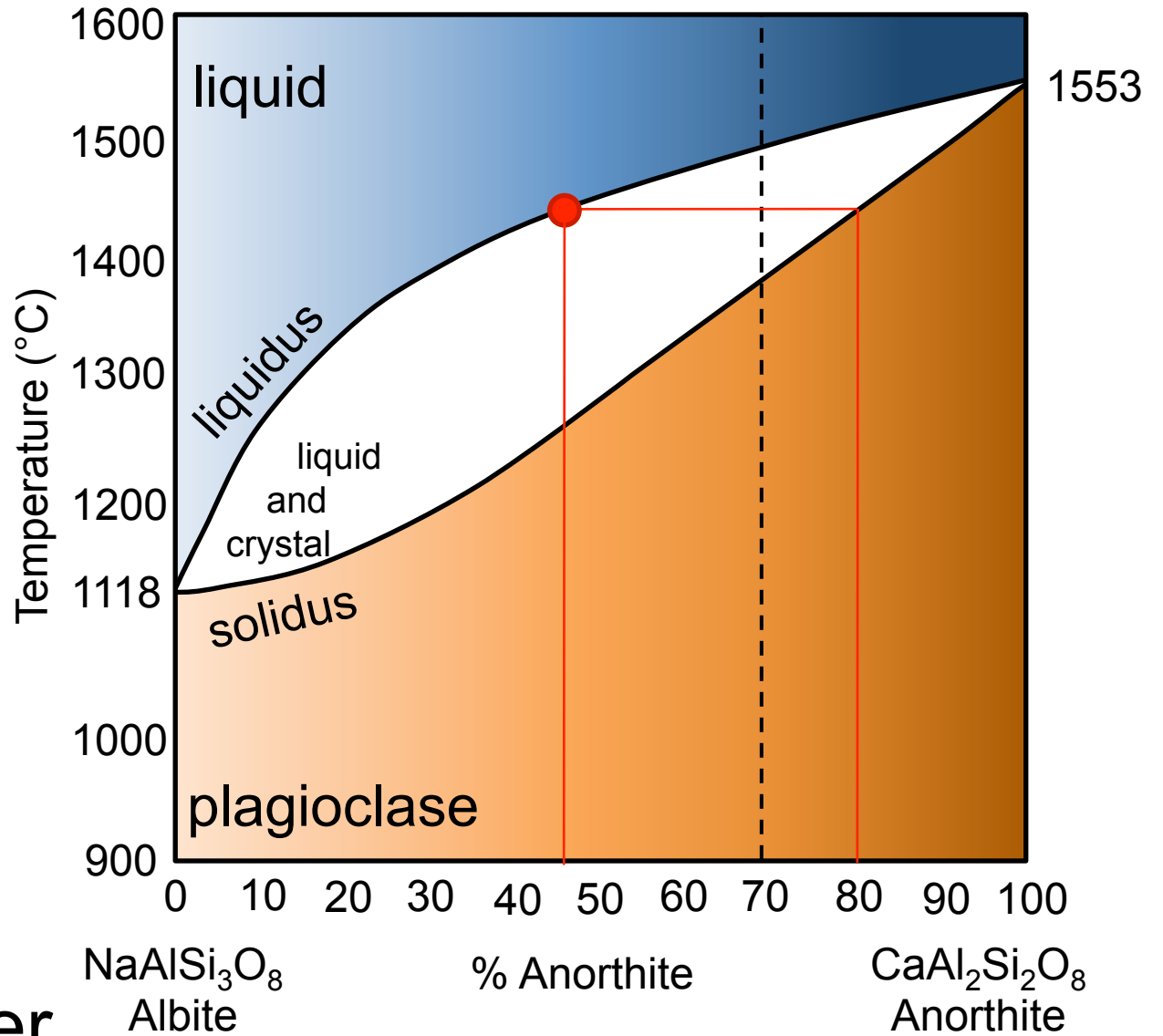
magma chamber



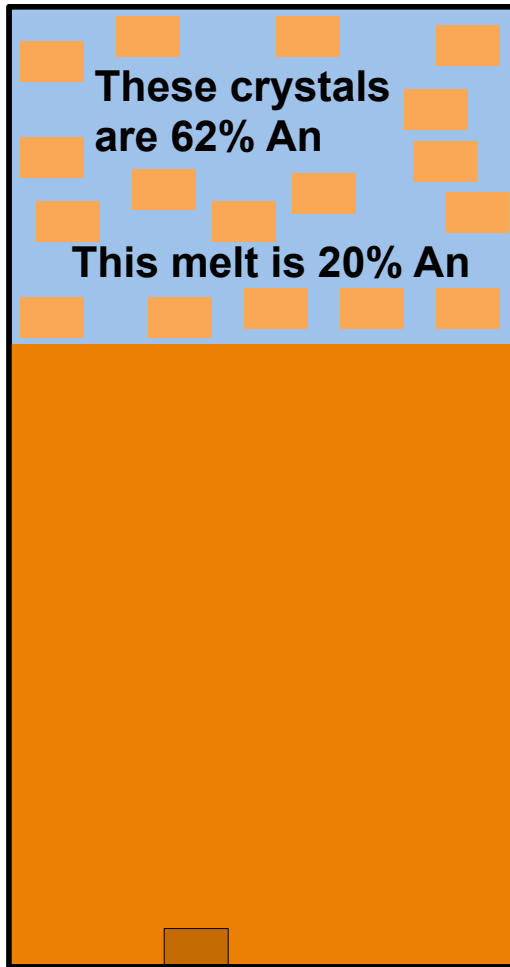
Fractional Crystallization



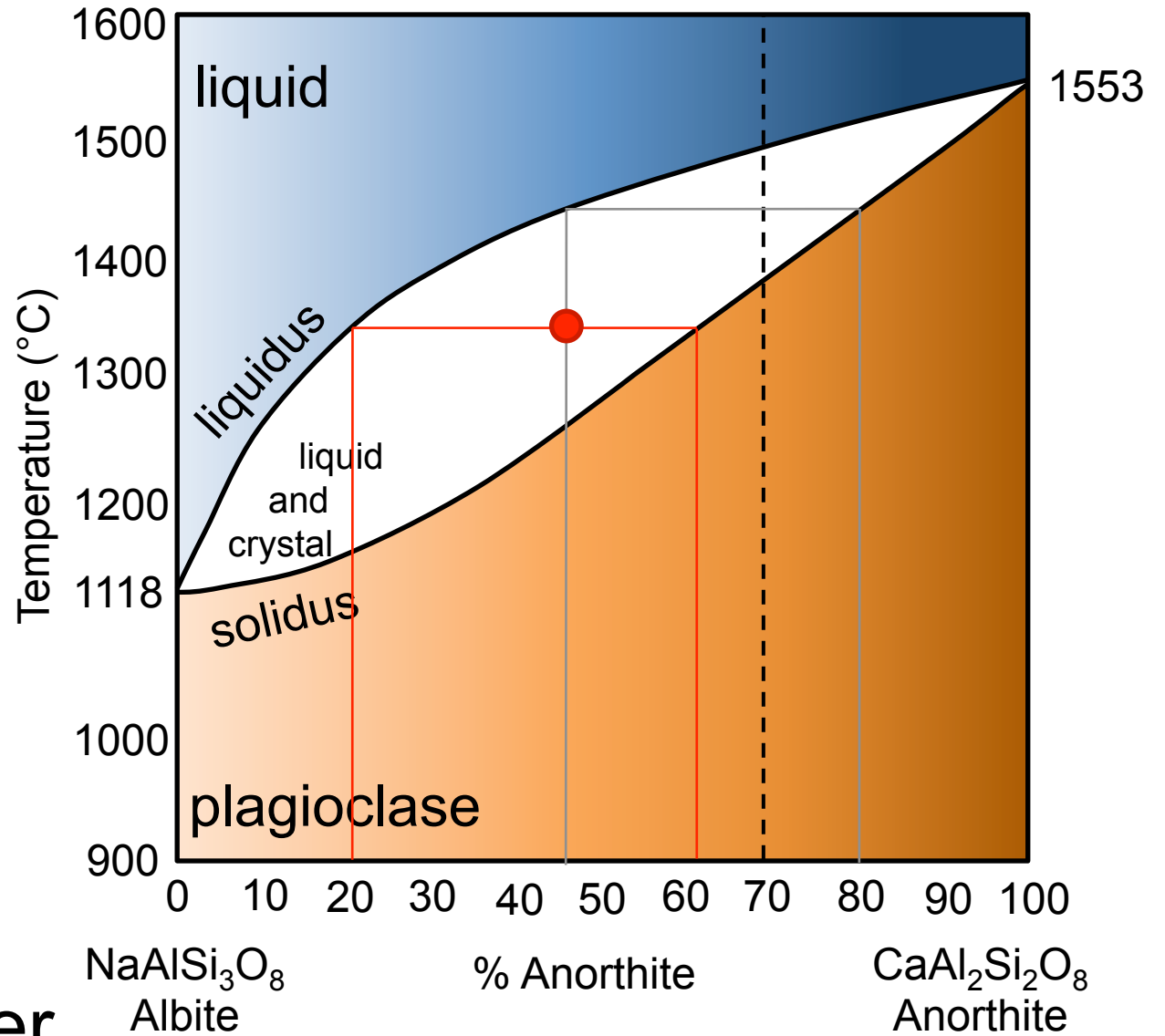
magma chamber



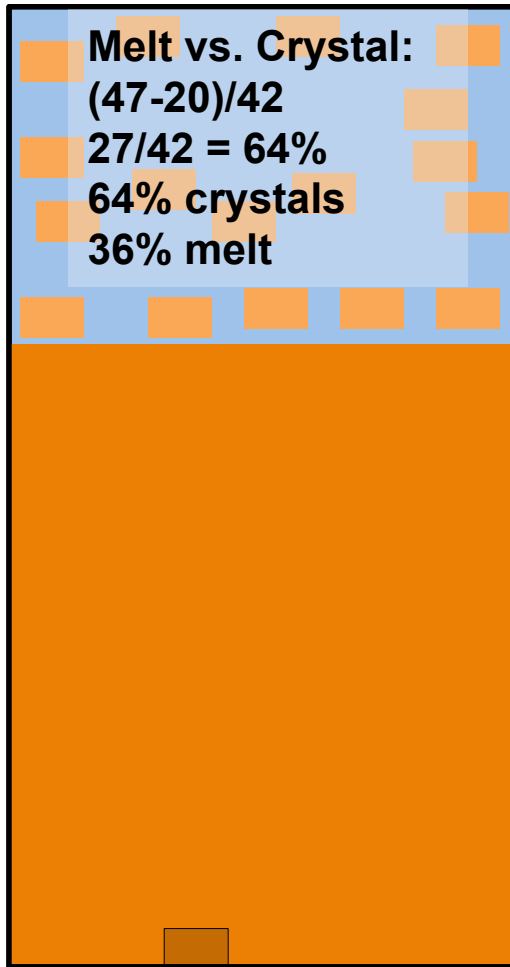
Fractional Crystallization



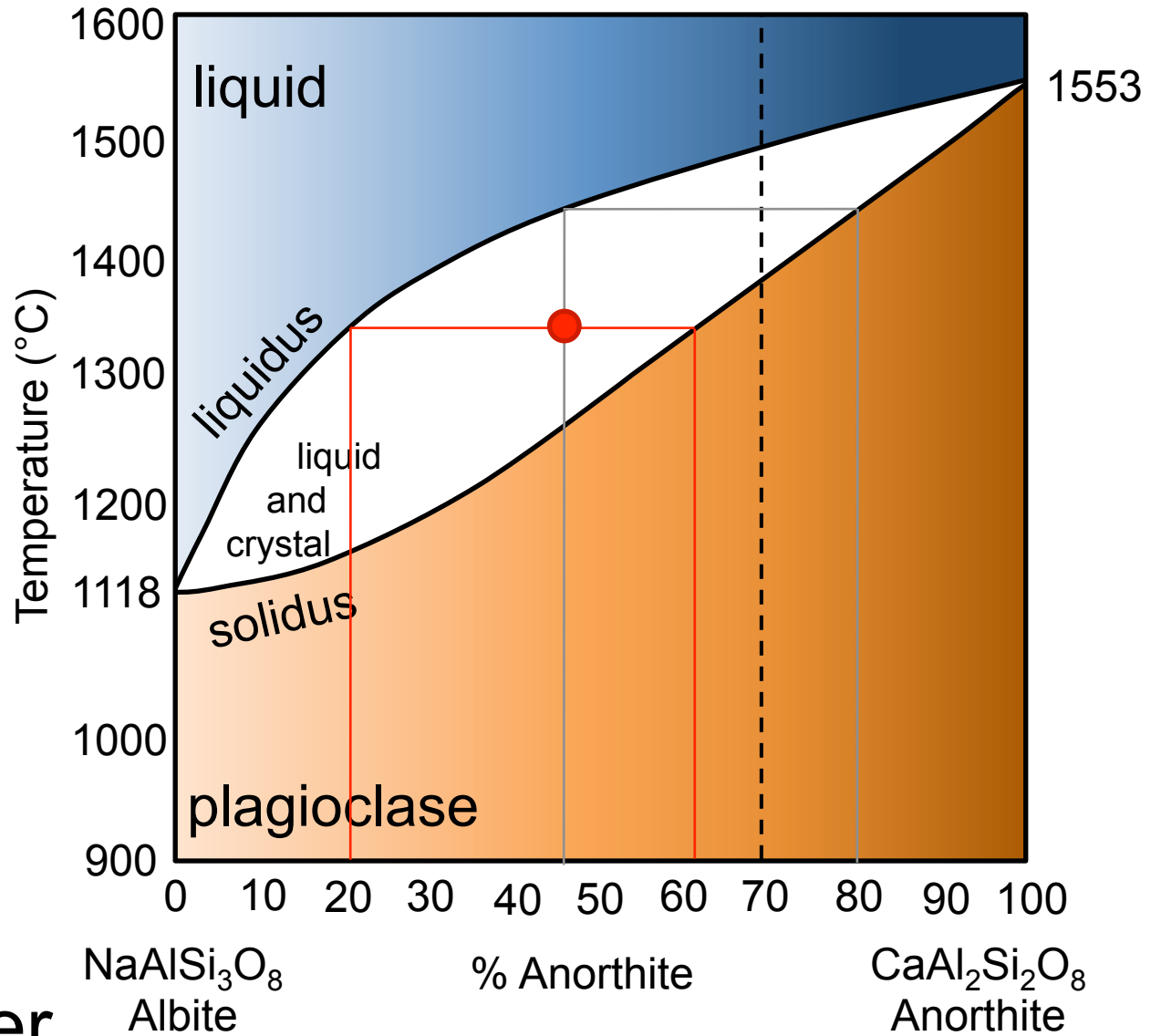
magma chamber



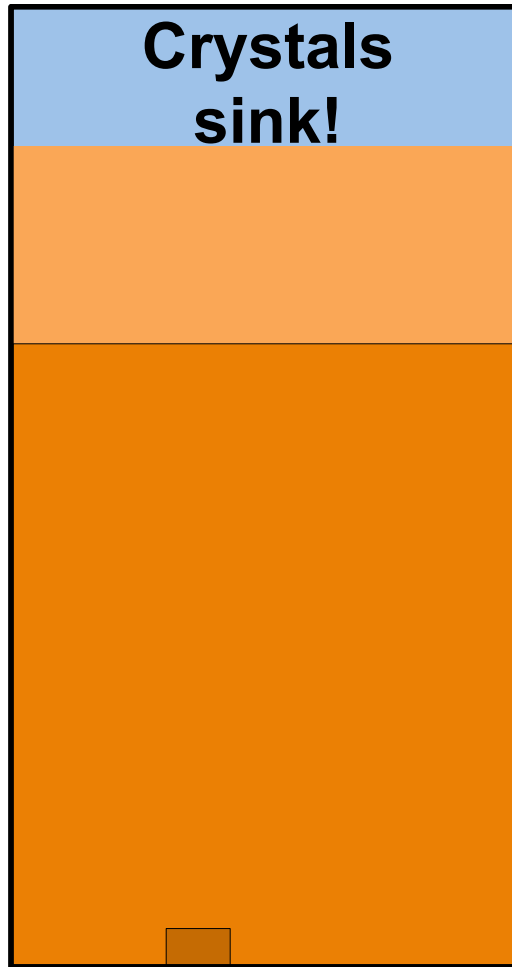
Fractional Crystallization



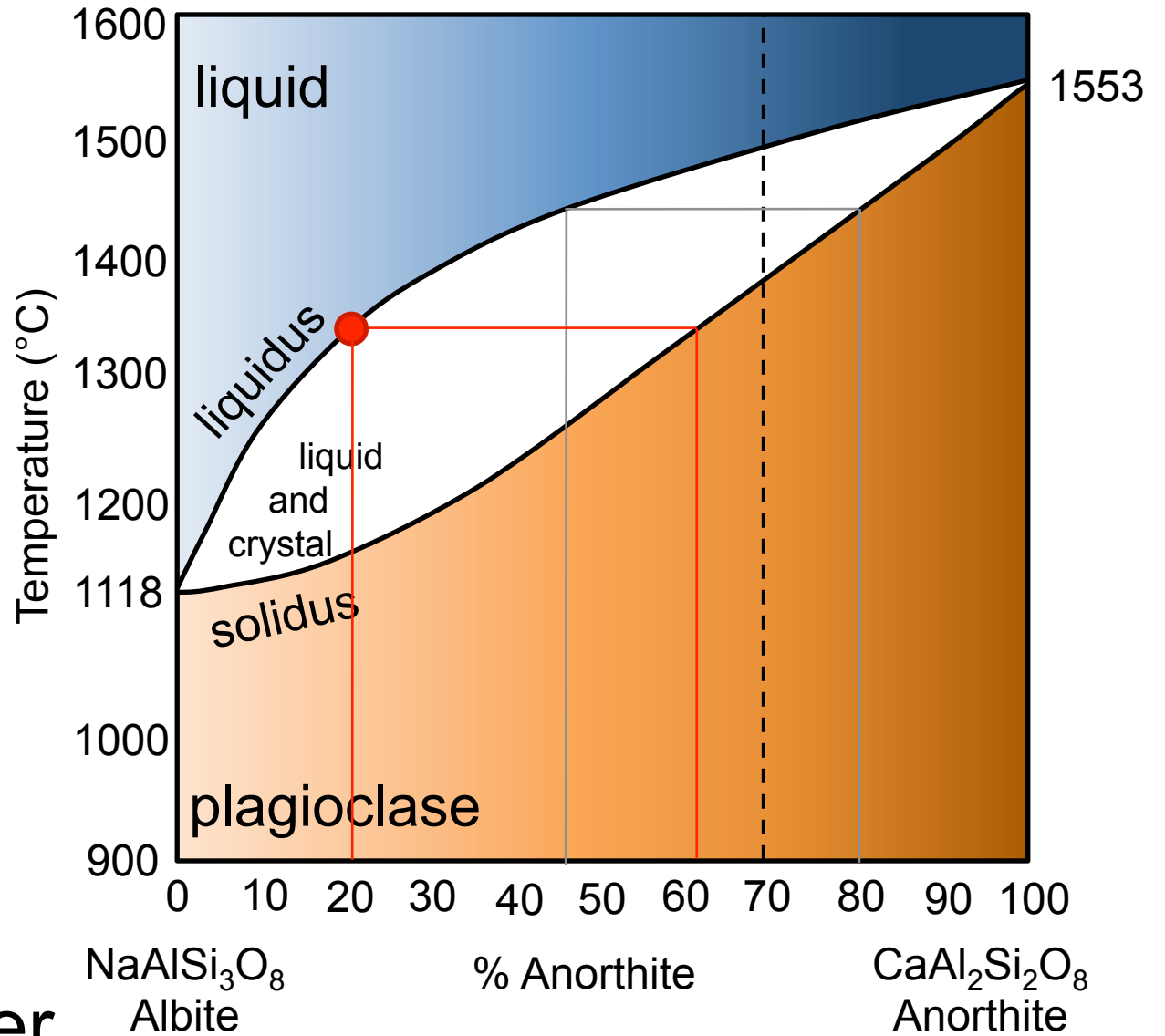
magma chamber



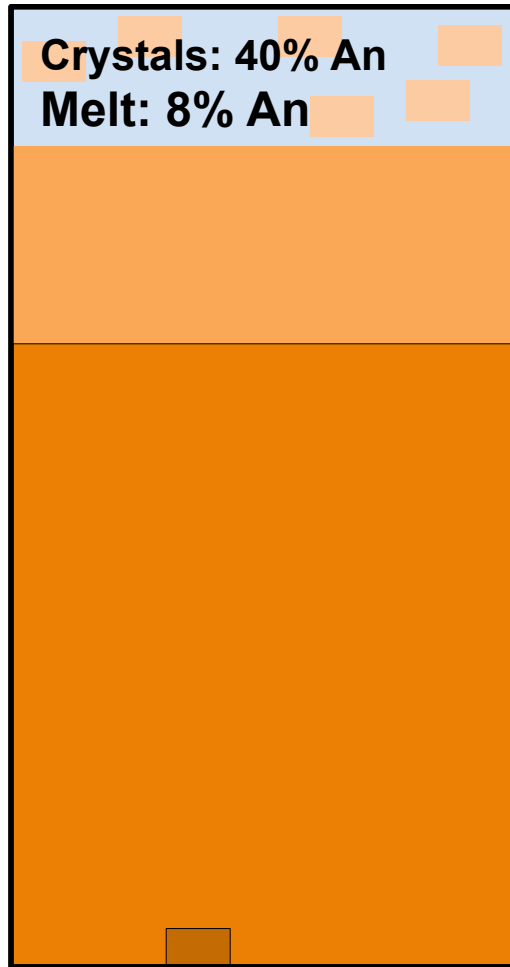
Fractional Crystallization



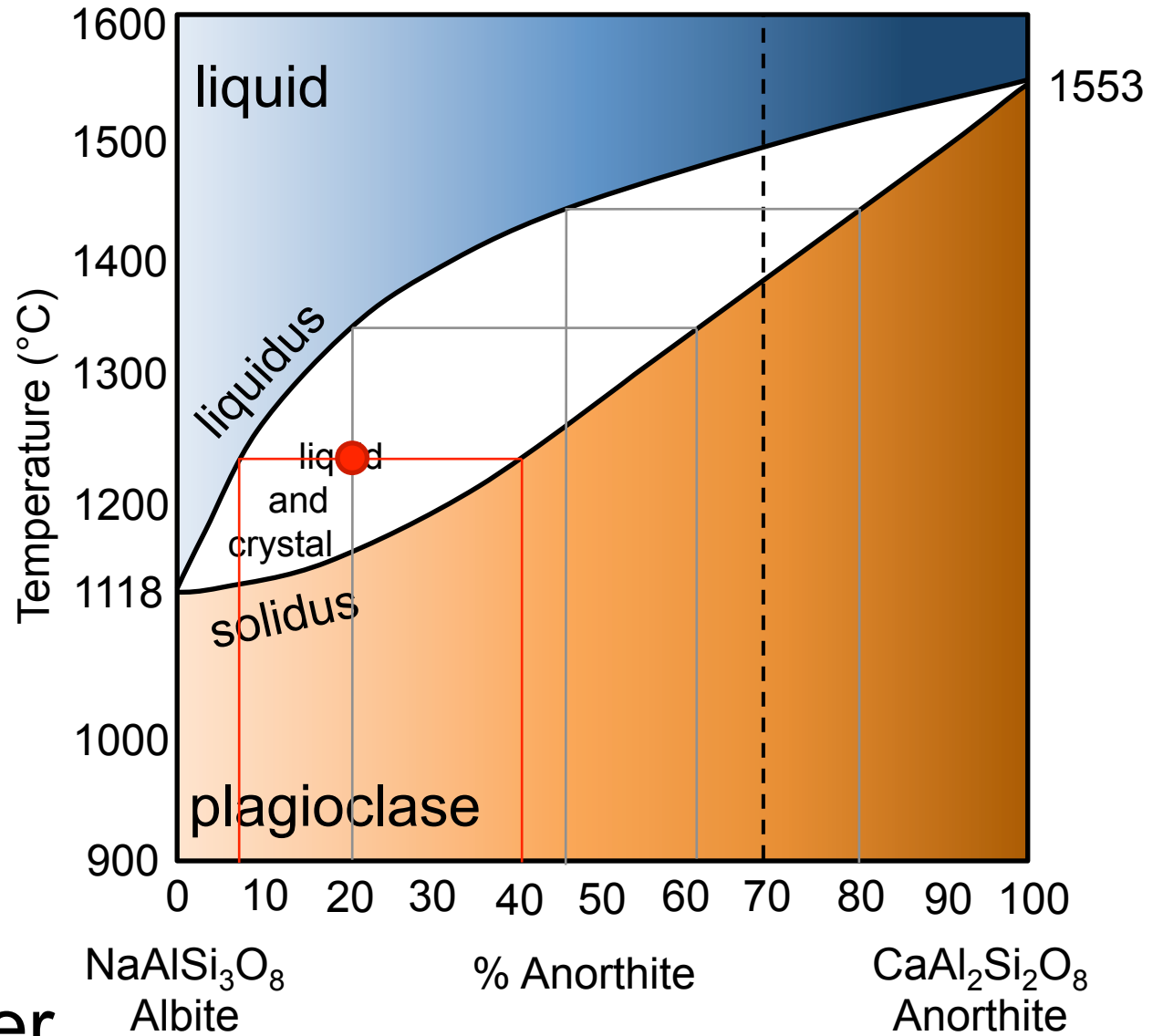
magma chamber



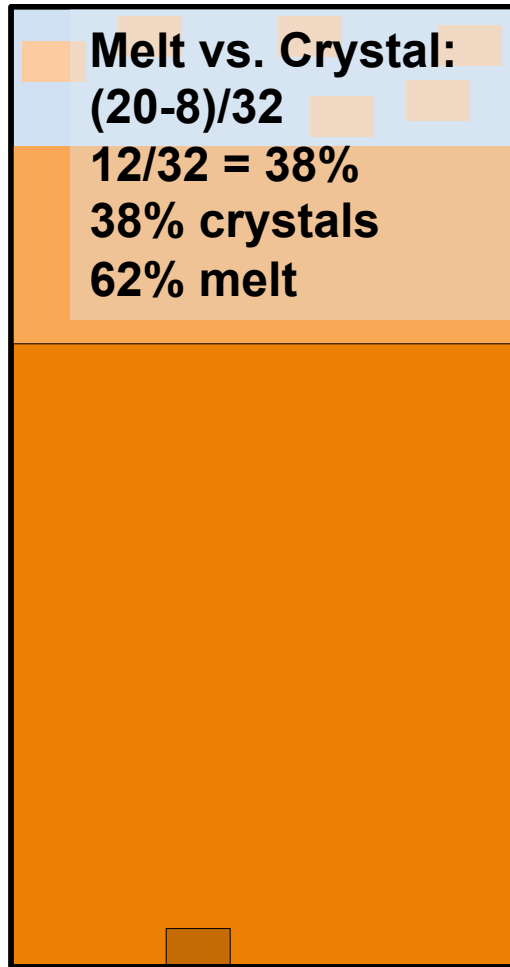
Fractional Crystallization



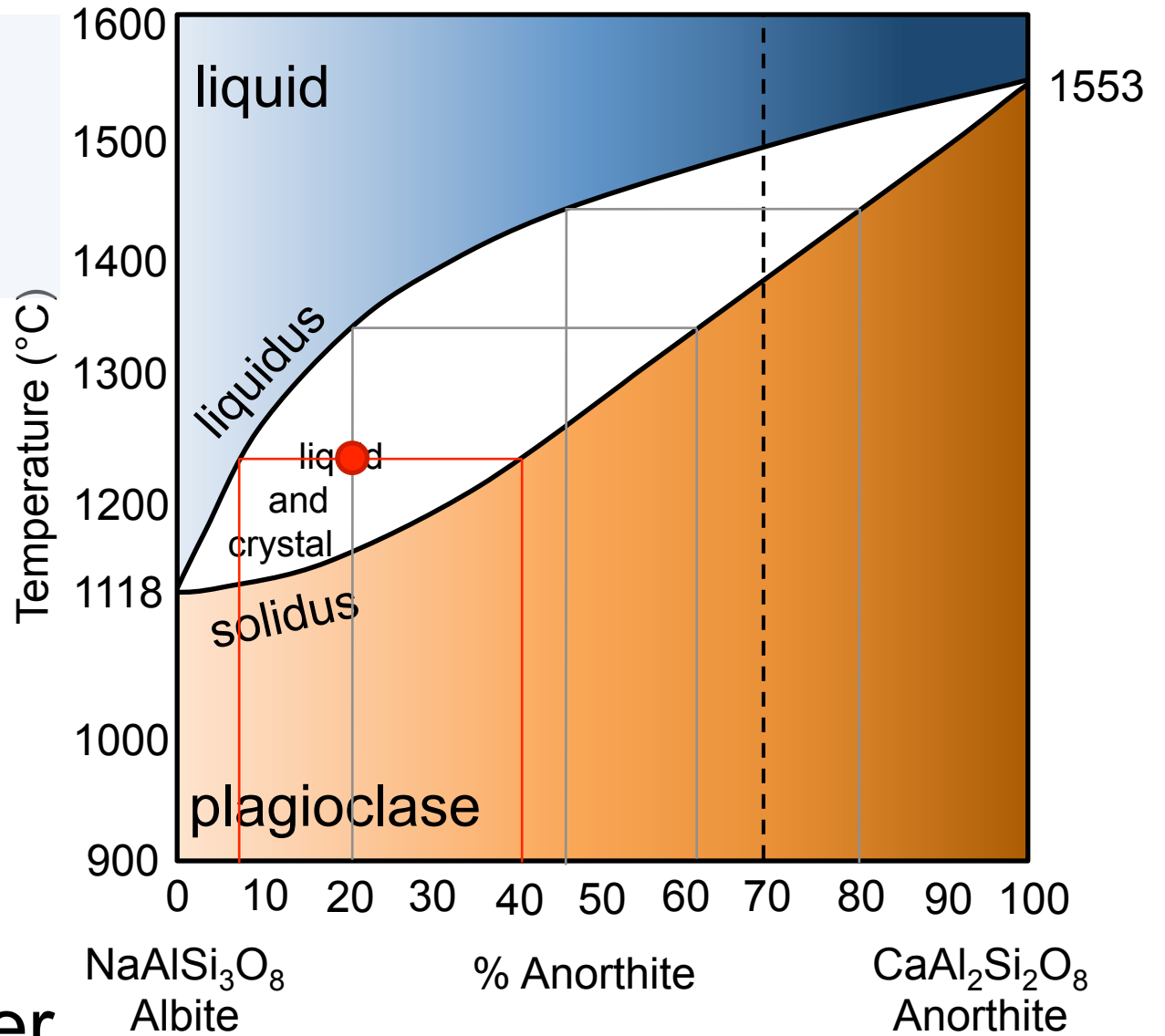
magma chamber



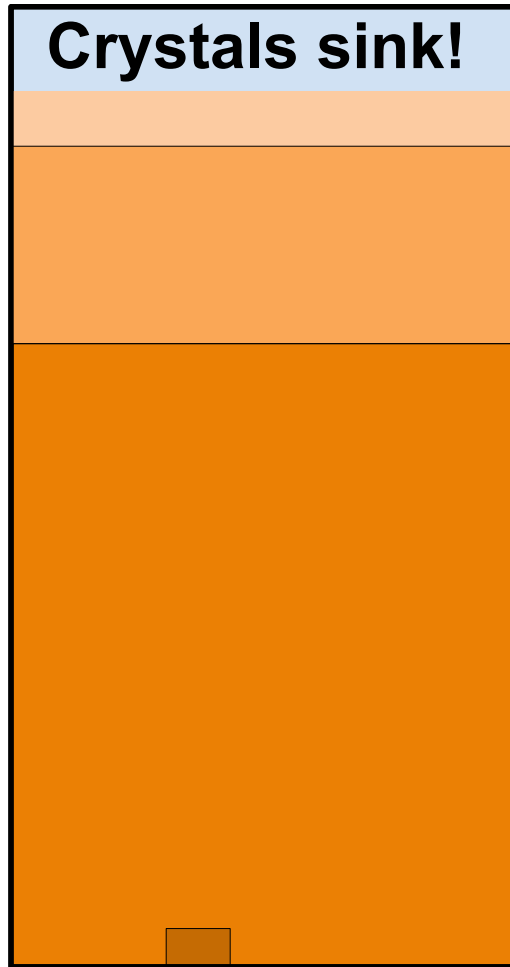
Fractional Crystallization



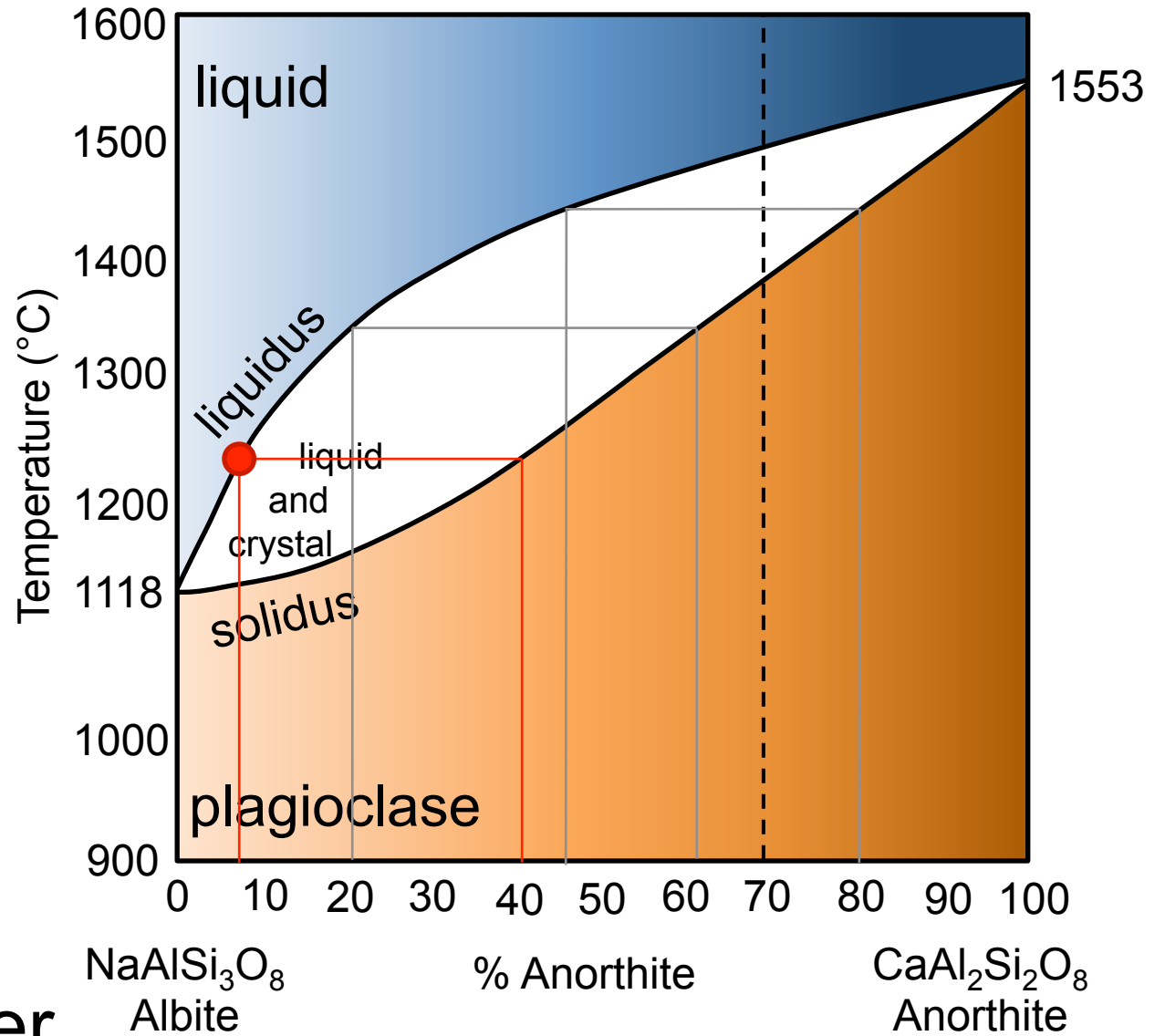
magma chamber



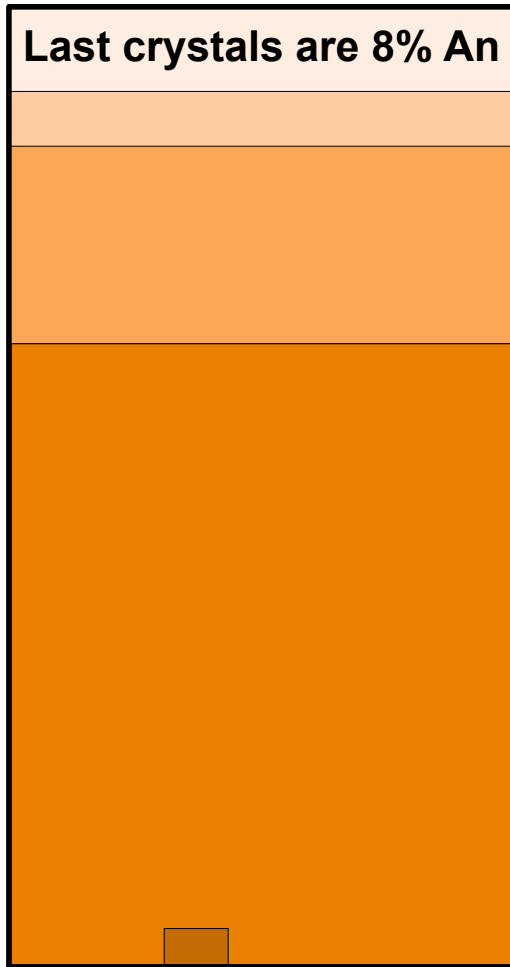
Fractional Crystallization



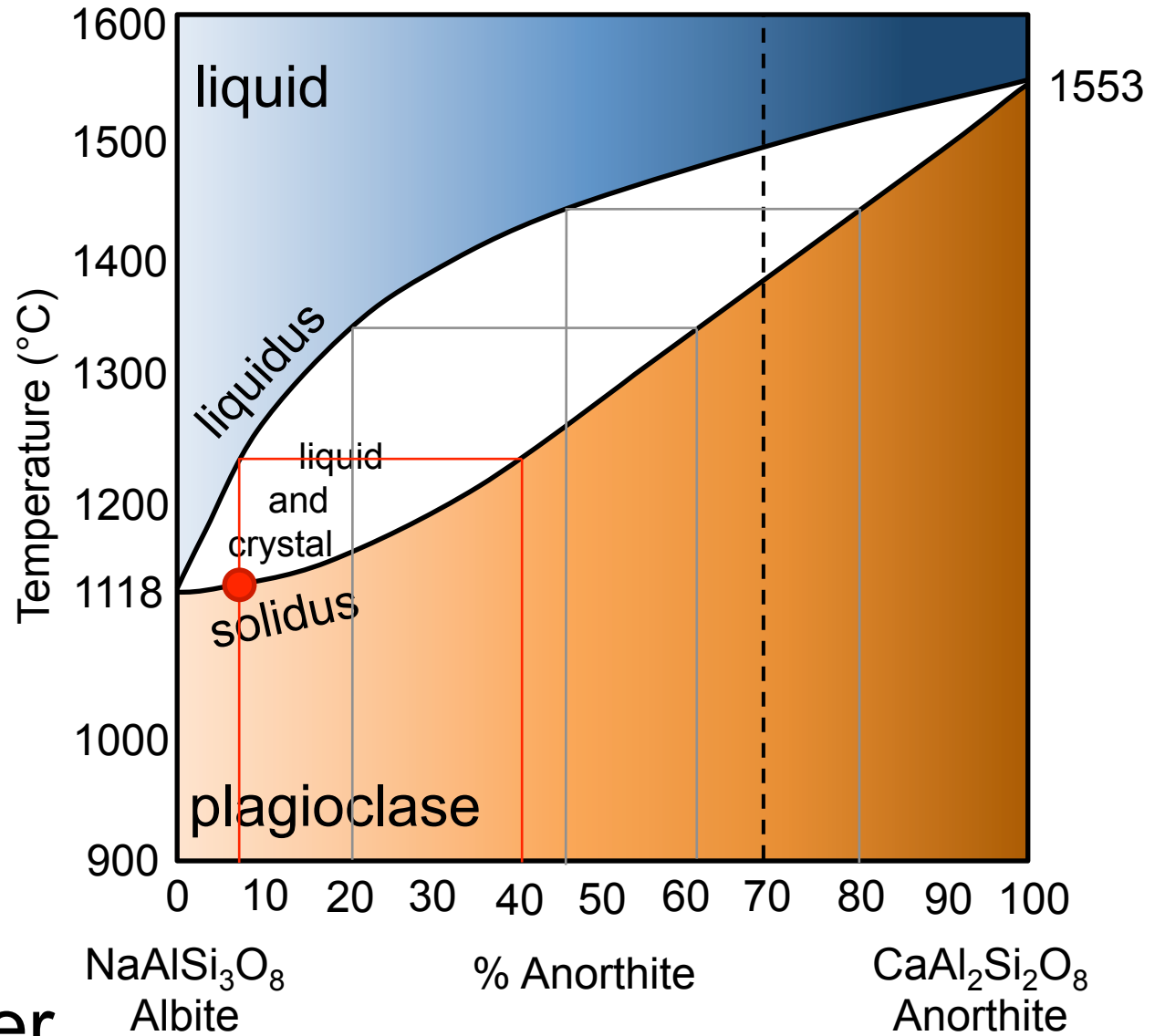
magma chamber



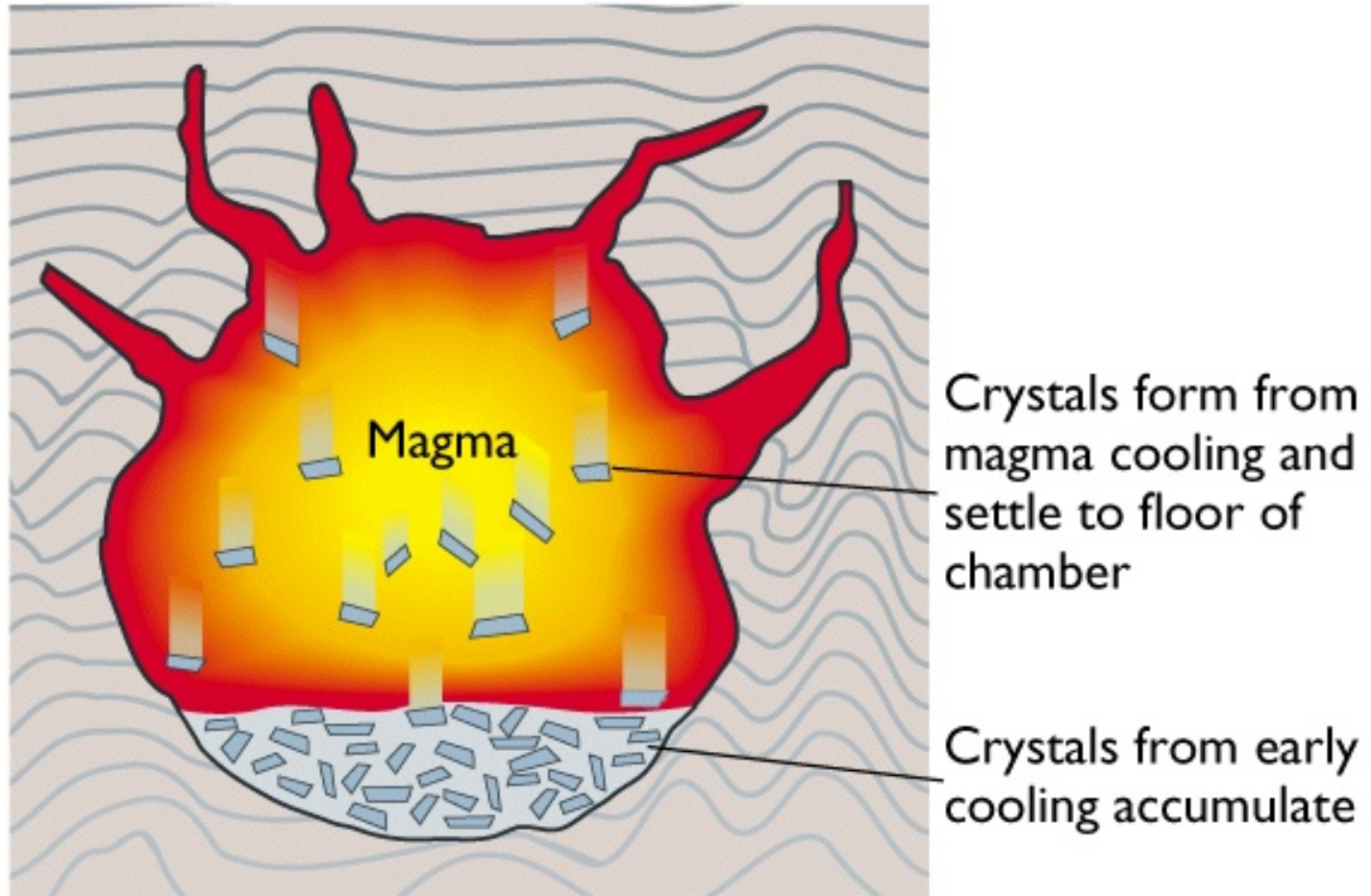
Fractional Crystallization



magma chamber



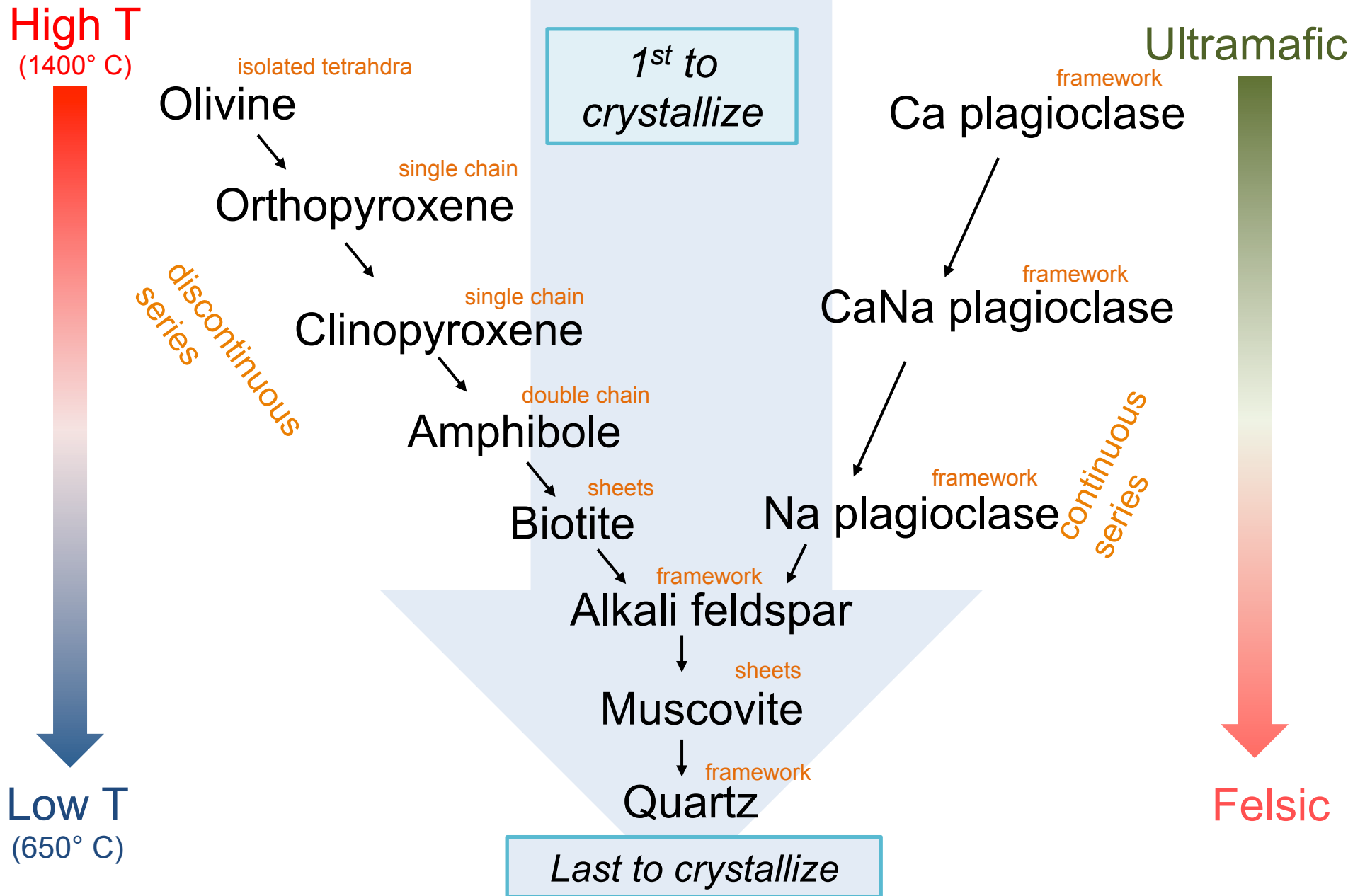
Fractional Crystallization



Early crystallization

Magma composition progressively changes as crystals are physically removed from the magma.

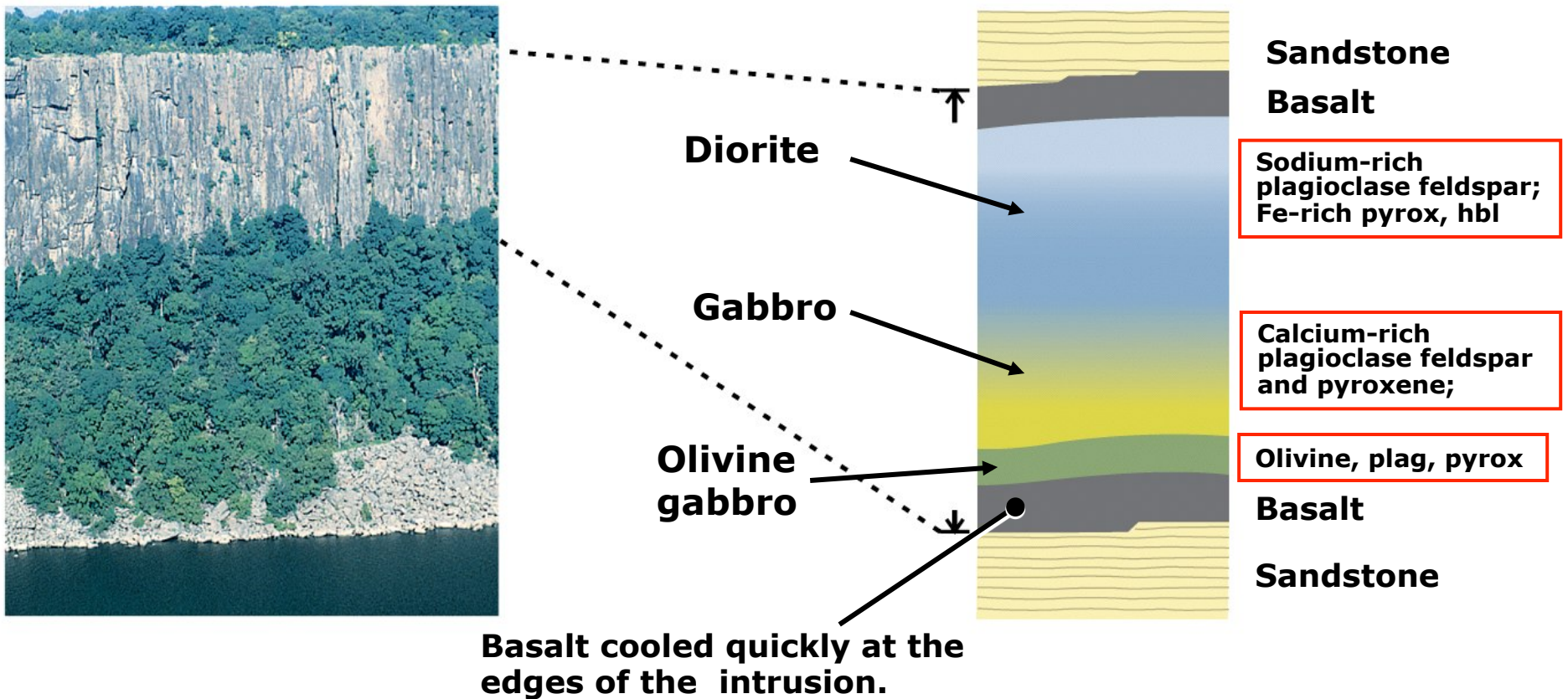
Bowen's Reaction Series



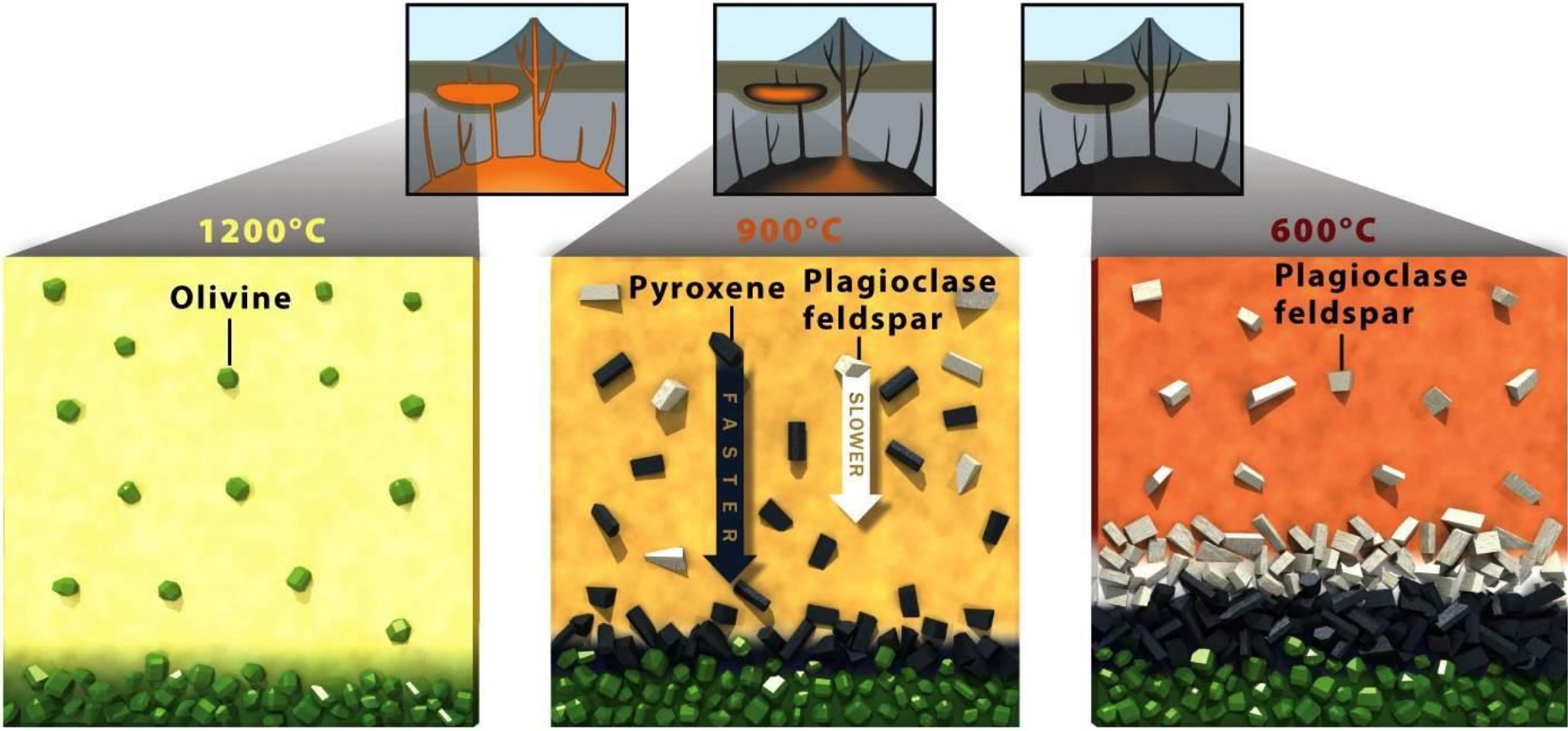
Fractional Crystallization

Palisades Sill (western shore of Hudson River, NJ)

Basaltic intrusion: 245–275 meters thick

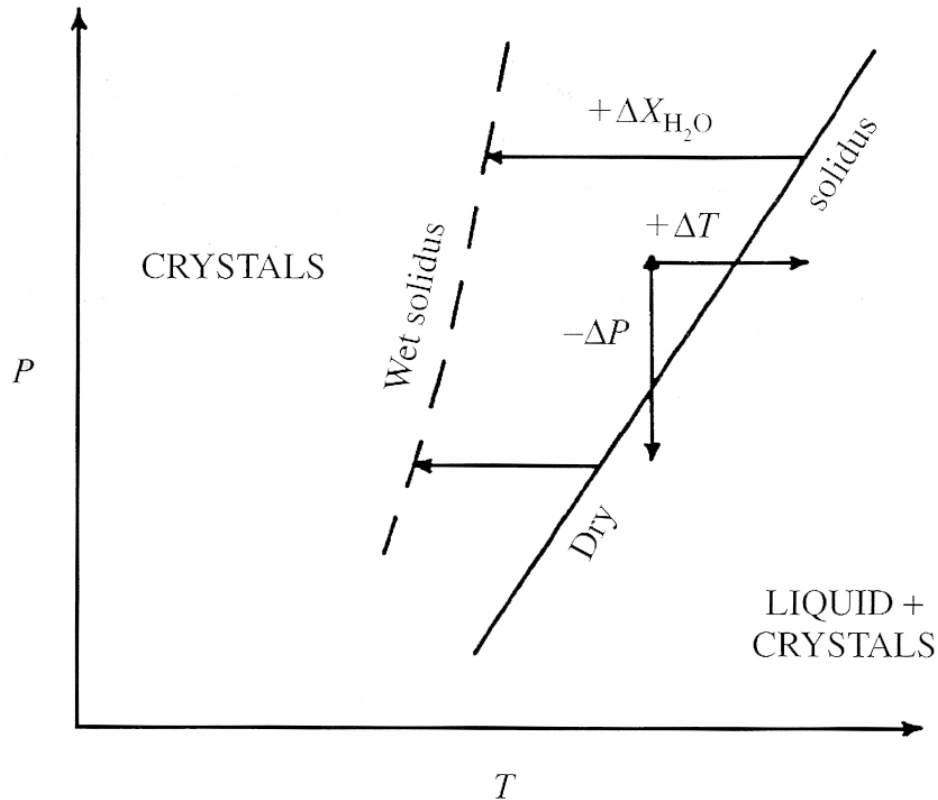


Fractional Crystallization

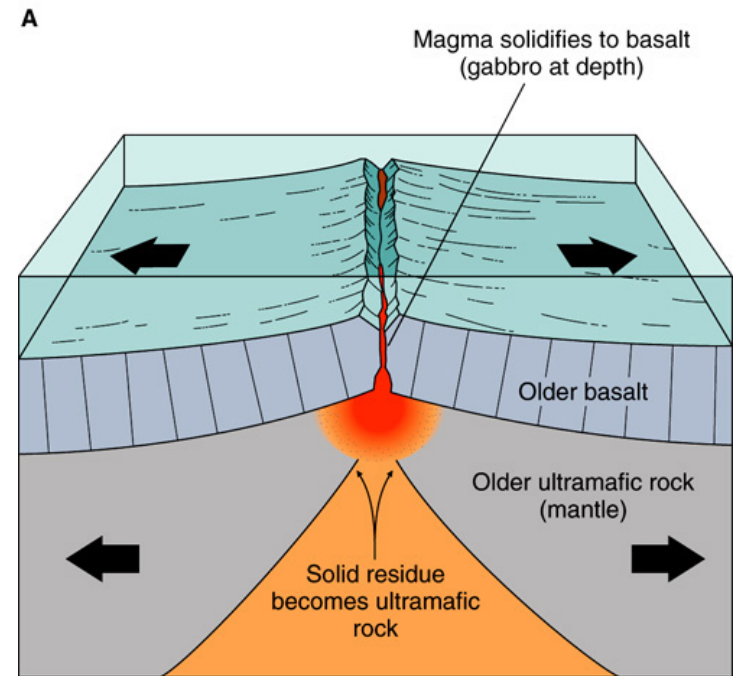
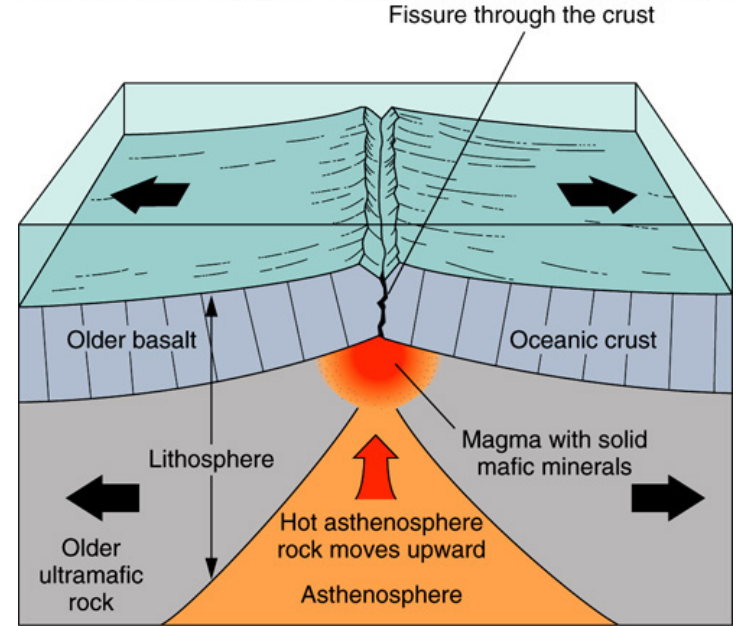


Decompression Melting

Decompression melting of mantle peridotite to produce primary basaltic magmas

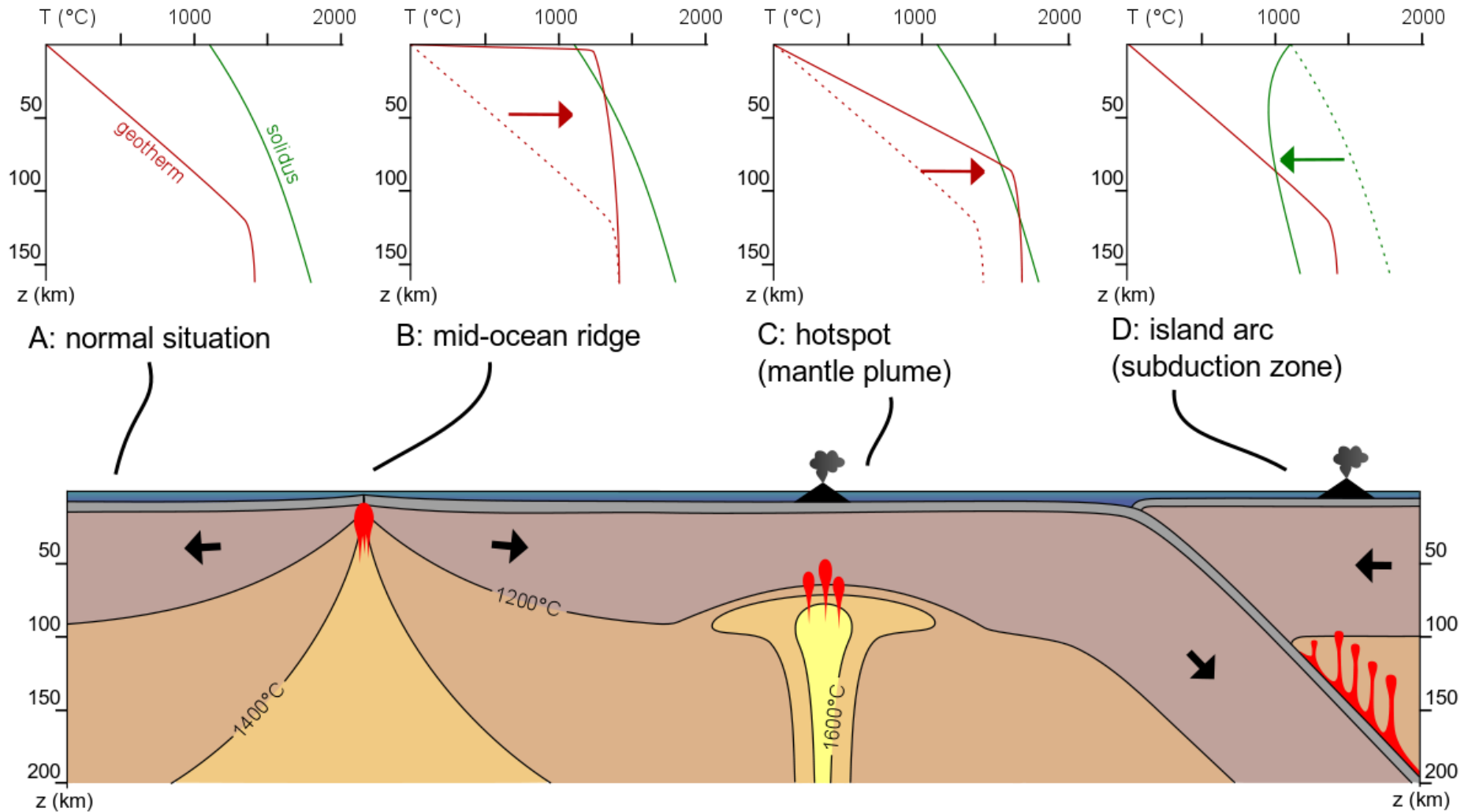


Copyright © McGraw-Hill Companies, Inc. Permission required for reproduction or display.

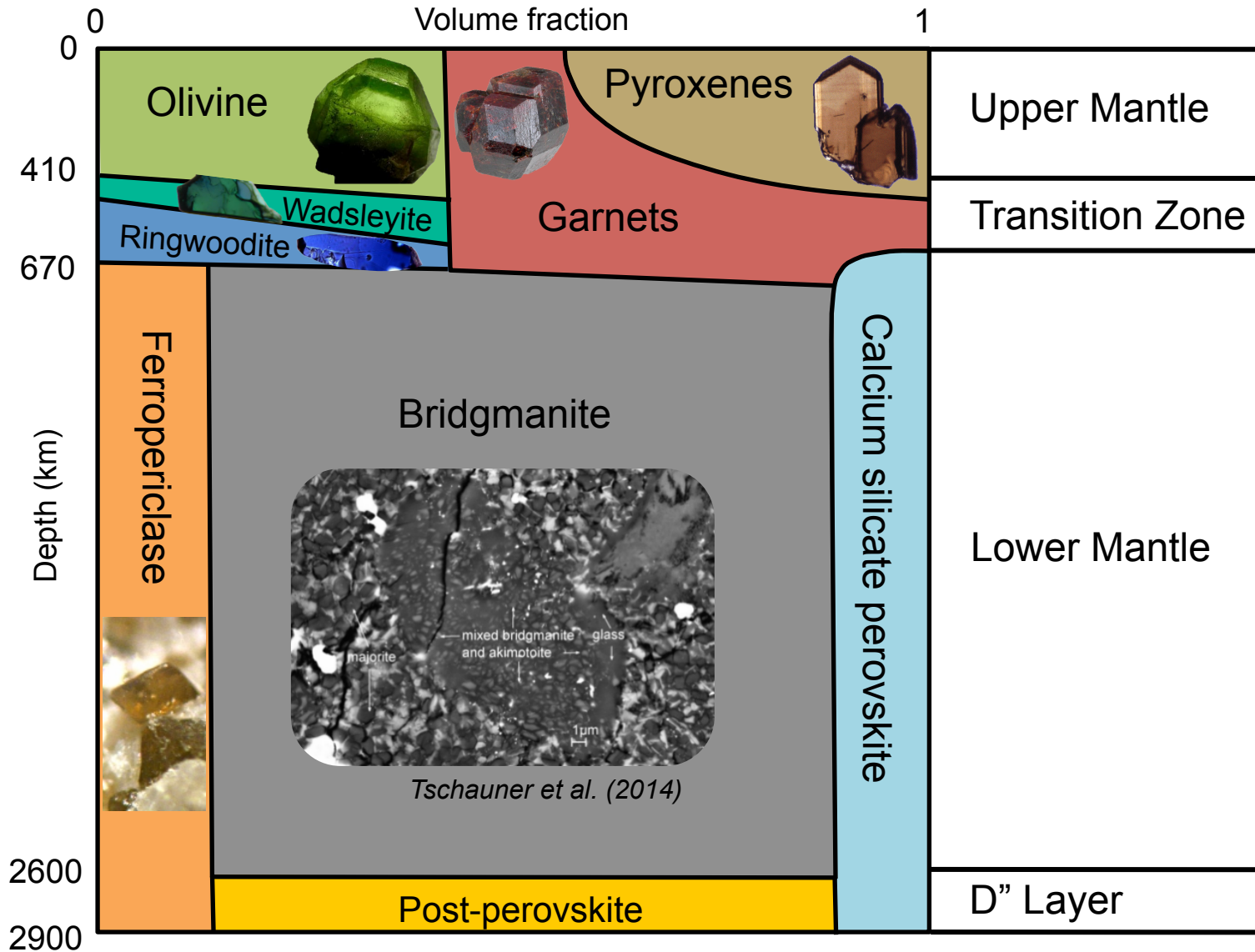


B

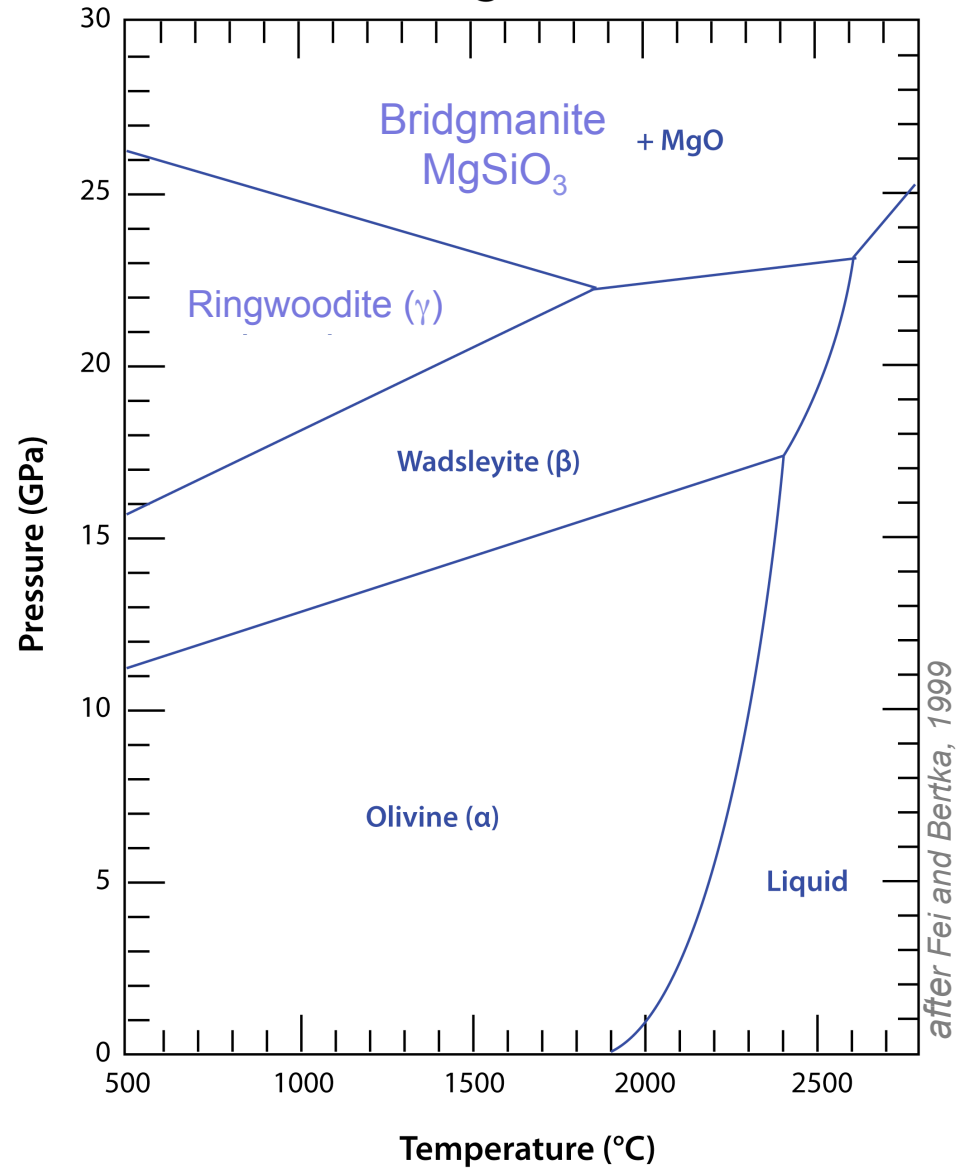
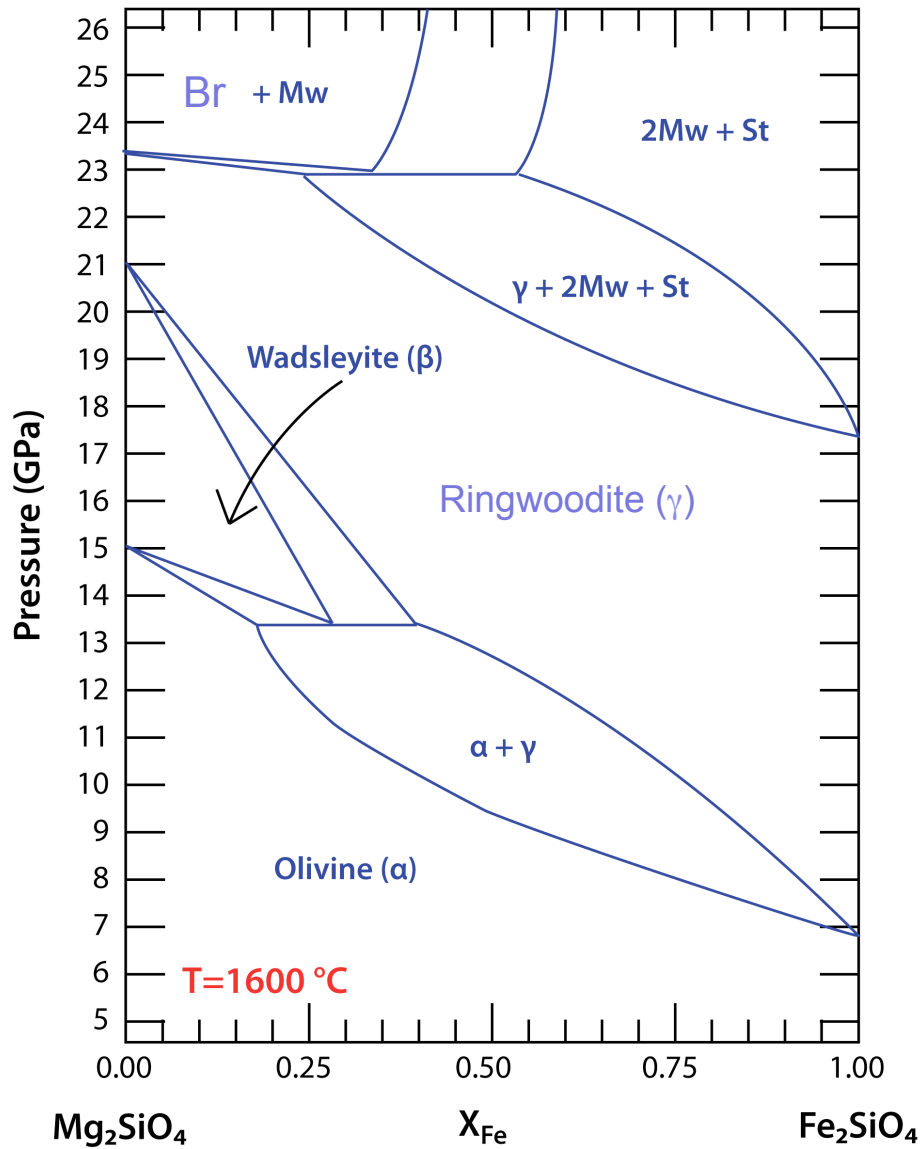
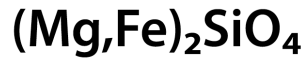
Melting the Mantle



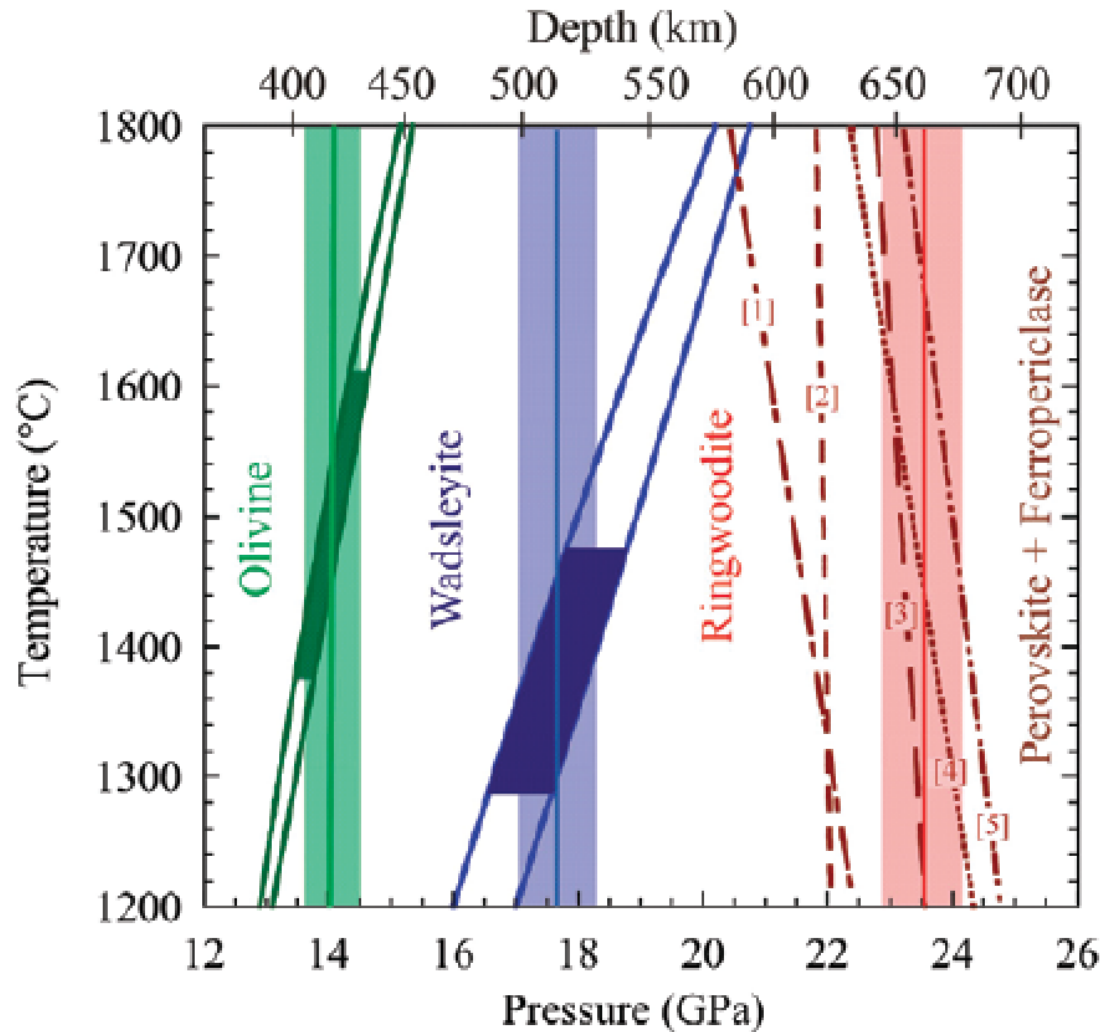
Mantle Mineralogy (Peridotitic)



olivine → wadsleyite → ringwoodite → (bridgmanite+periclase)

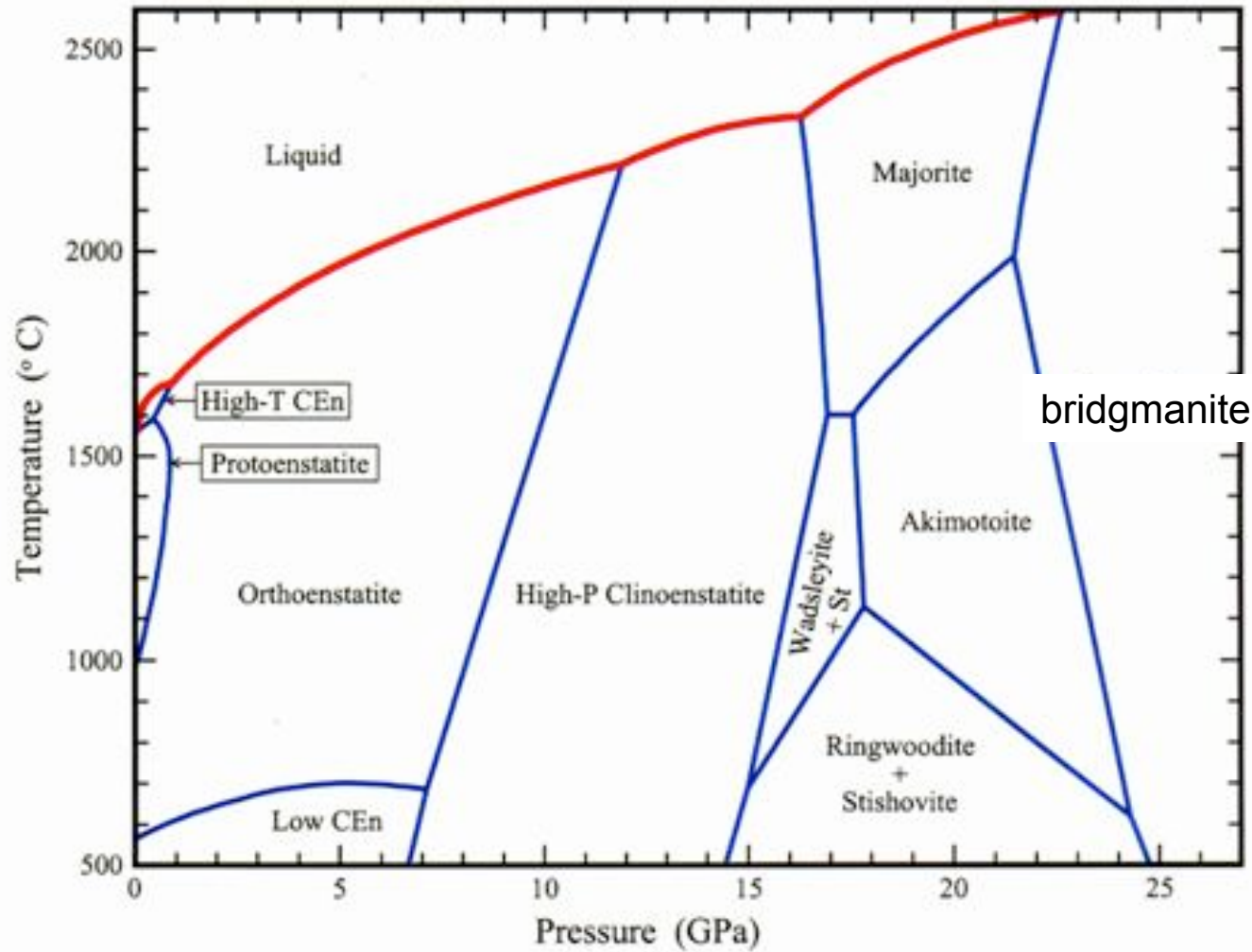


Phase transitions in the $(\text{Mg,Fe})_2\text{SiO}_4$ system and relationship to seismic discontinuities



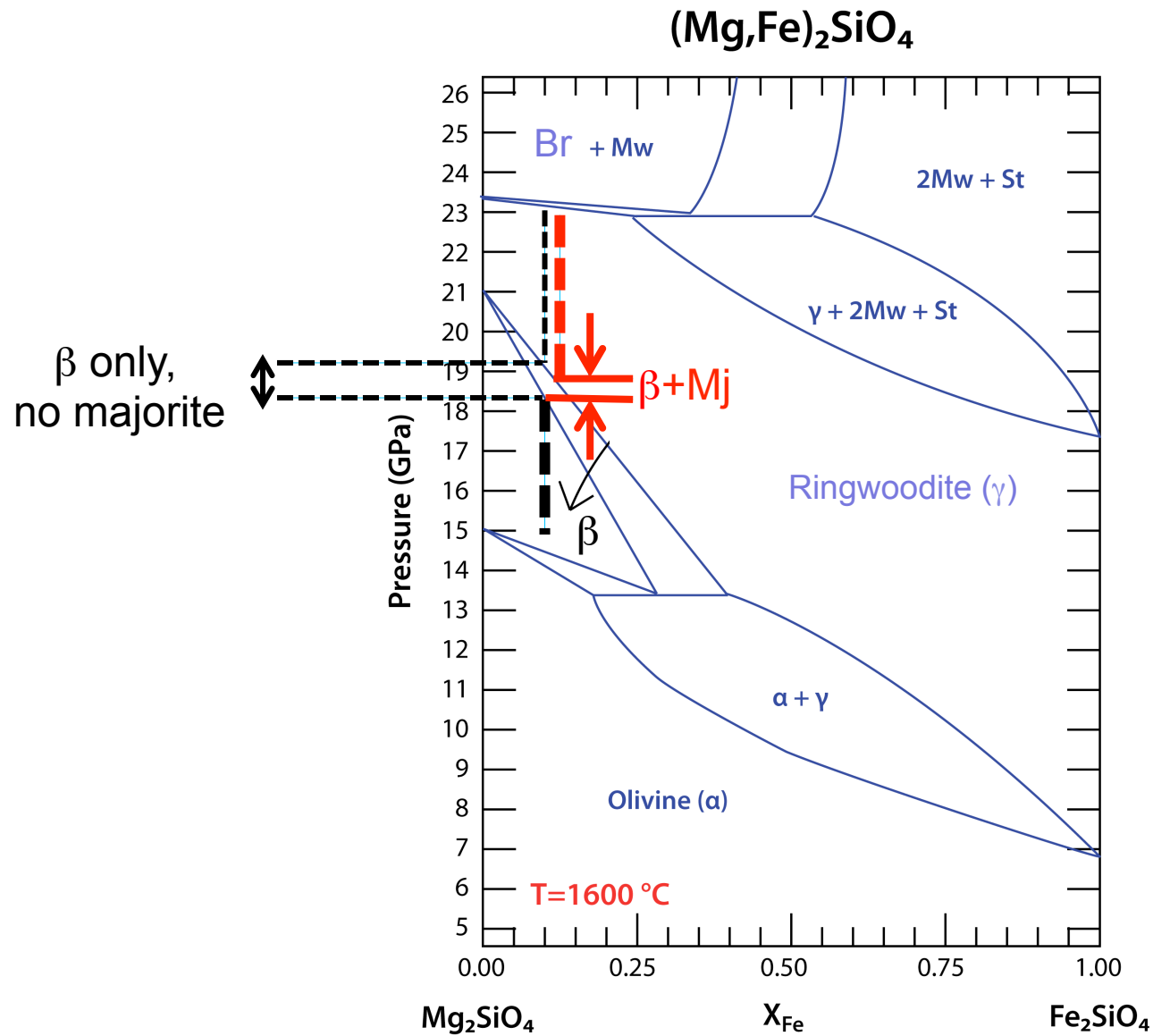
Review article: Frost, Elements (2008);
Shim et al. (2001)

MgSiO₃ : enstatite → (majorite/akimotoite) → bridgmanite

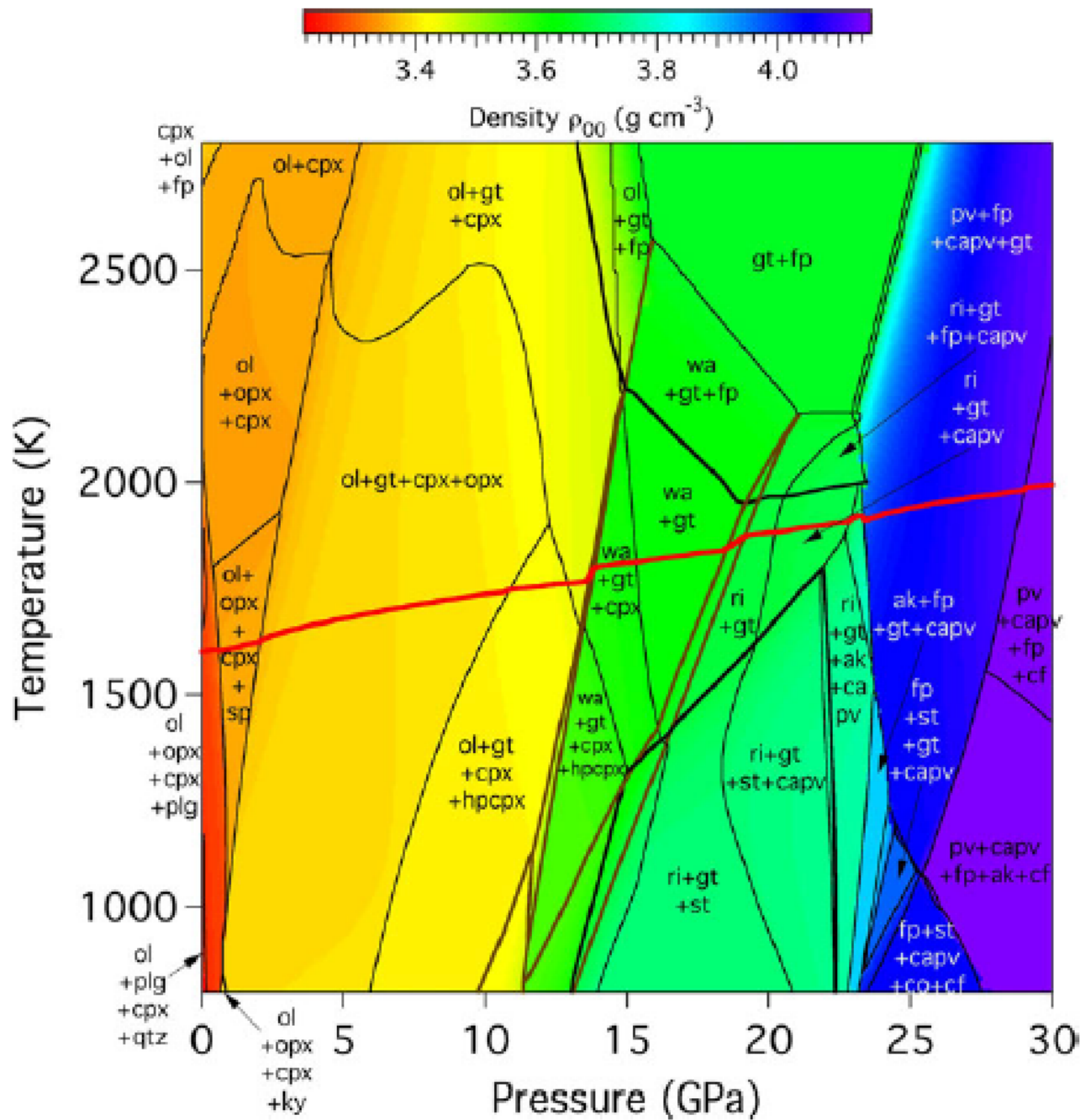


Fei and Bertka, 1999

Effect of majorite on the width & iron-partitioning of wadsleyite's phase transition



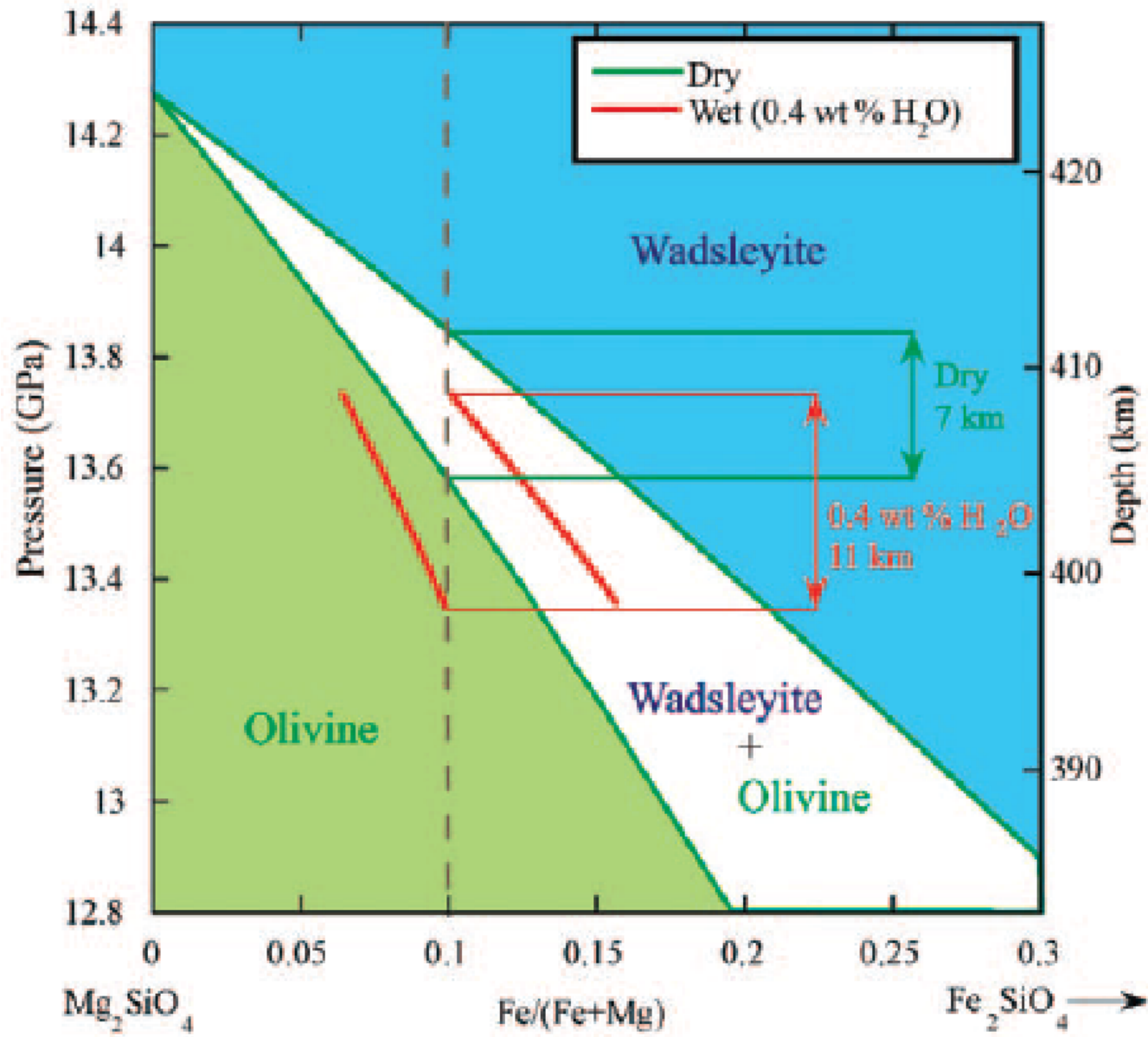
after Fei and Bertka, 1999



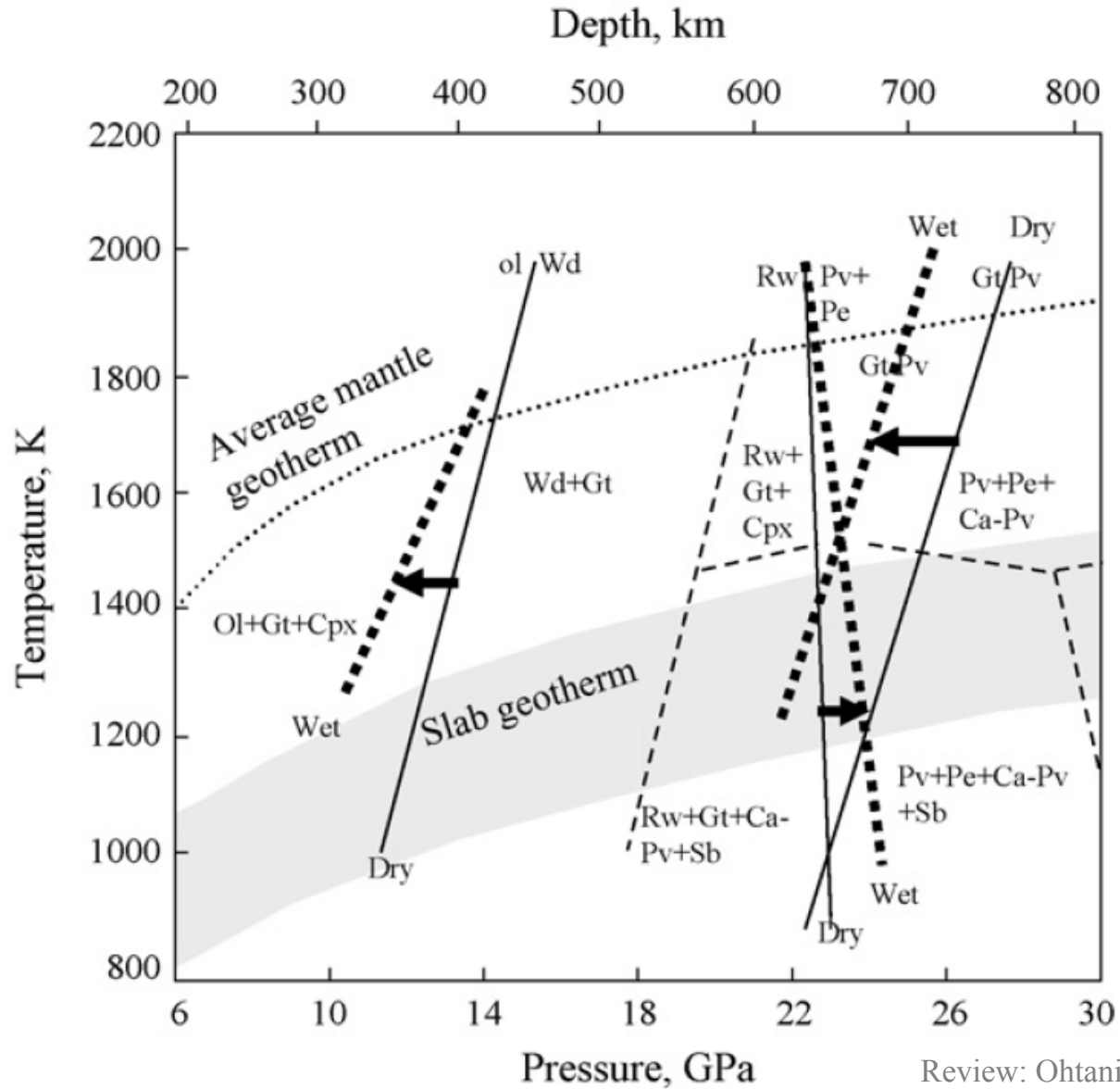
Phase diagram of a peridotitic mantle

Computed from first principles

Effect of hydroxyl (OH)⁻ on olivine's phase transition



Phase transitions in upper mantle mineral *assemblages*



Review: Ohtani & Sakai, PEPI (2008)

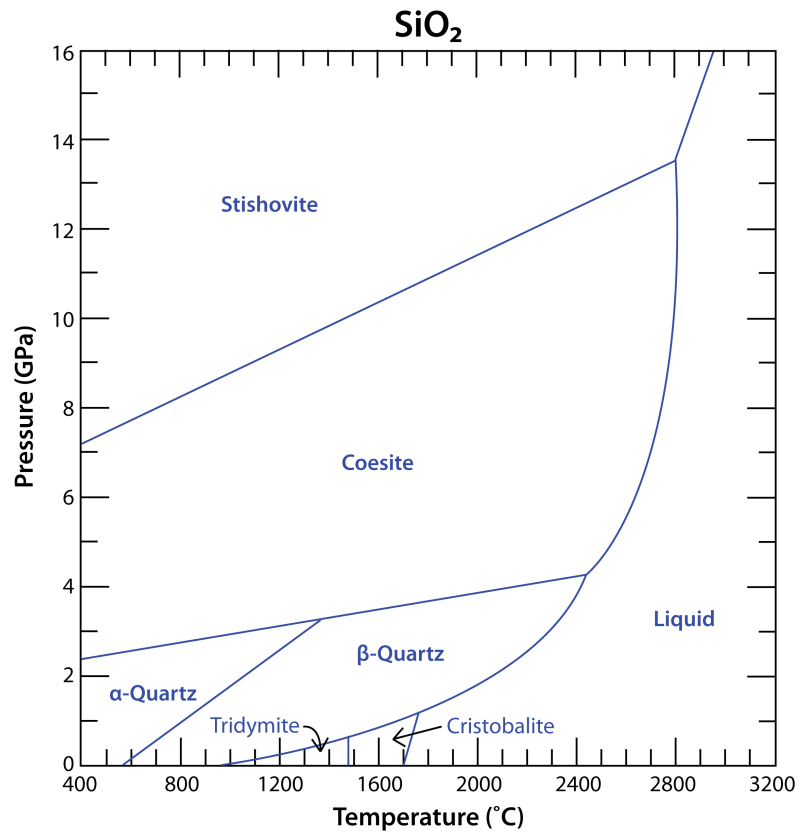
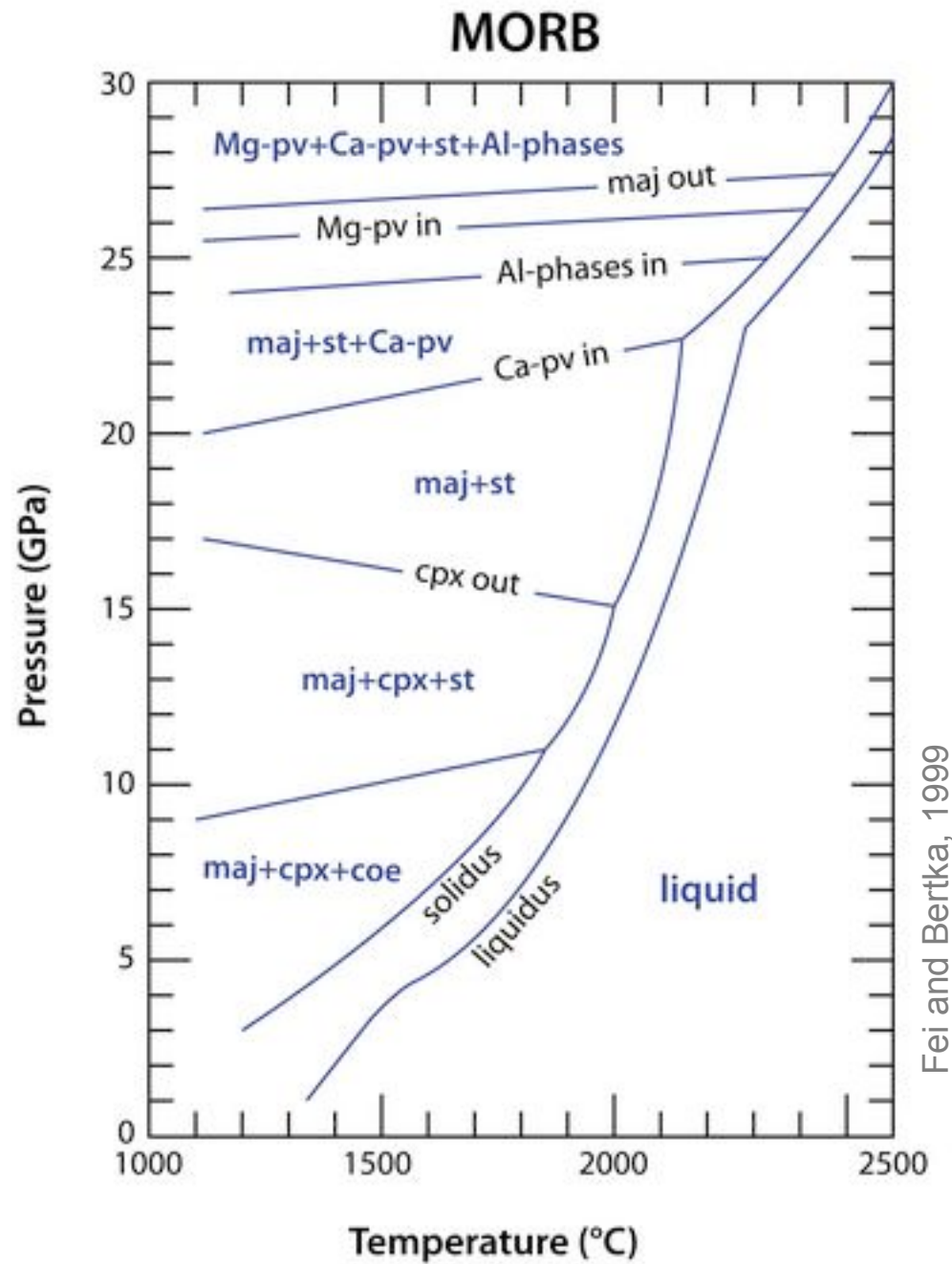


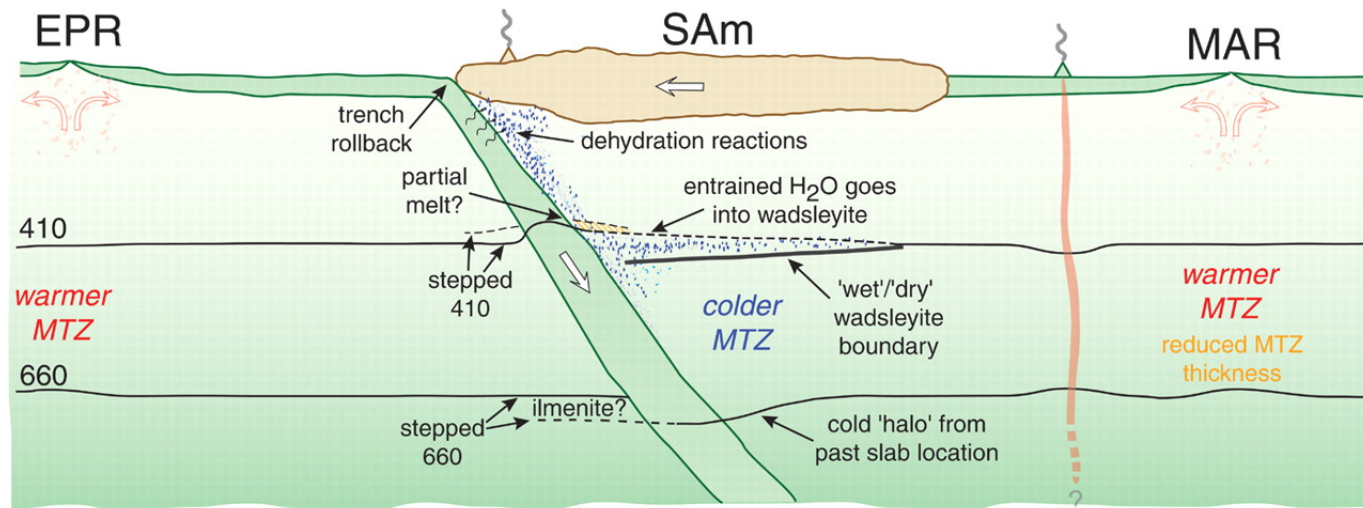
Figure modified from Fei and Bertka (1999) and Liu, L., and Bassett, W.A. (1986).

Exact chemistry of these minerals depends on phase equilibrium



Fei and Bertka, 1999

The upper mantle discontinuities



Schmerr & Garnero, Science (2007)

1. Temperature: decreases
transition pressure (α, β)

2. Presence of iron affects:

- * width of transition (increases)
- * transition pressure (typically decreases)

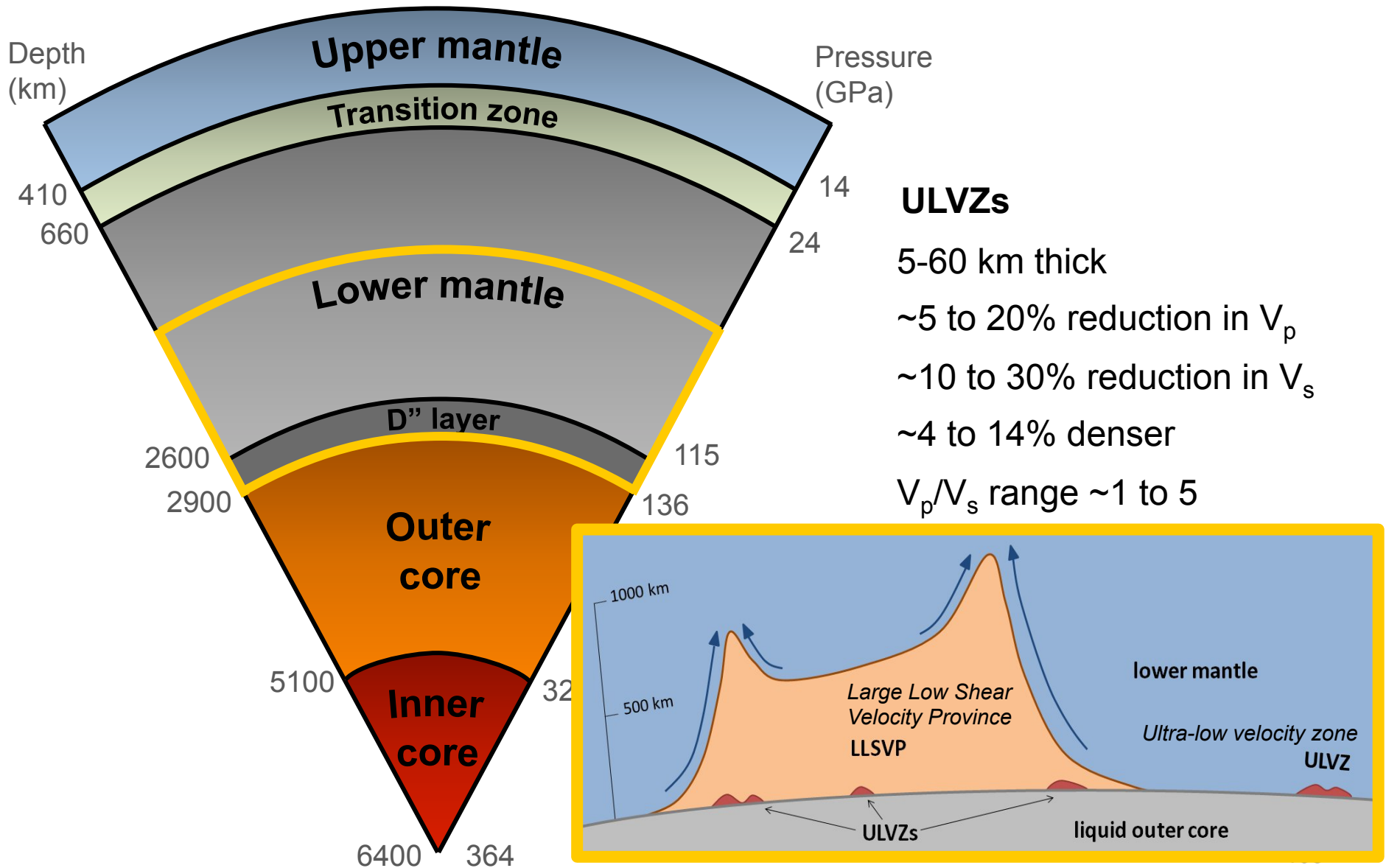
4. Adding OH to the system:

- *Decreases transition P
- *Widens the transition

3. Presence of garnet affects:

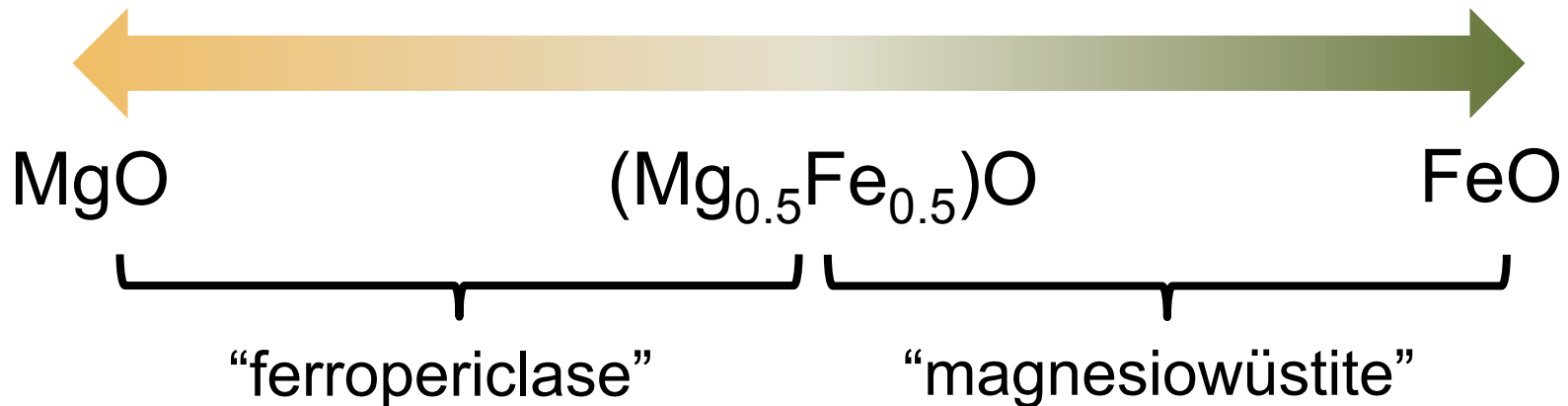
- * width (decreases, because of iron exchange)
- * transition pressure (increases, because of aluminum)
- * Clapeyron slope (dP/dT) (changes sign, from neg. to pos.)

Cross Section of Earth



Garnero and Helmberger (1996); Lay et al. (1998); Rost et al. (2005), Idehara et al. (2007), Idehara (2011); Thorne and Garnero (2004)

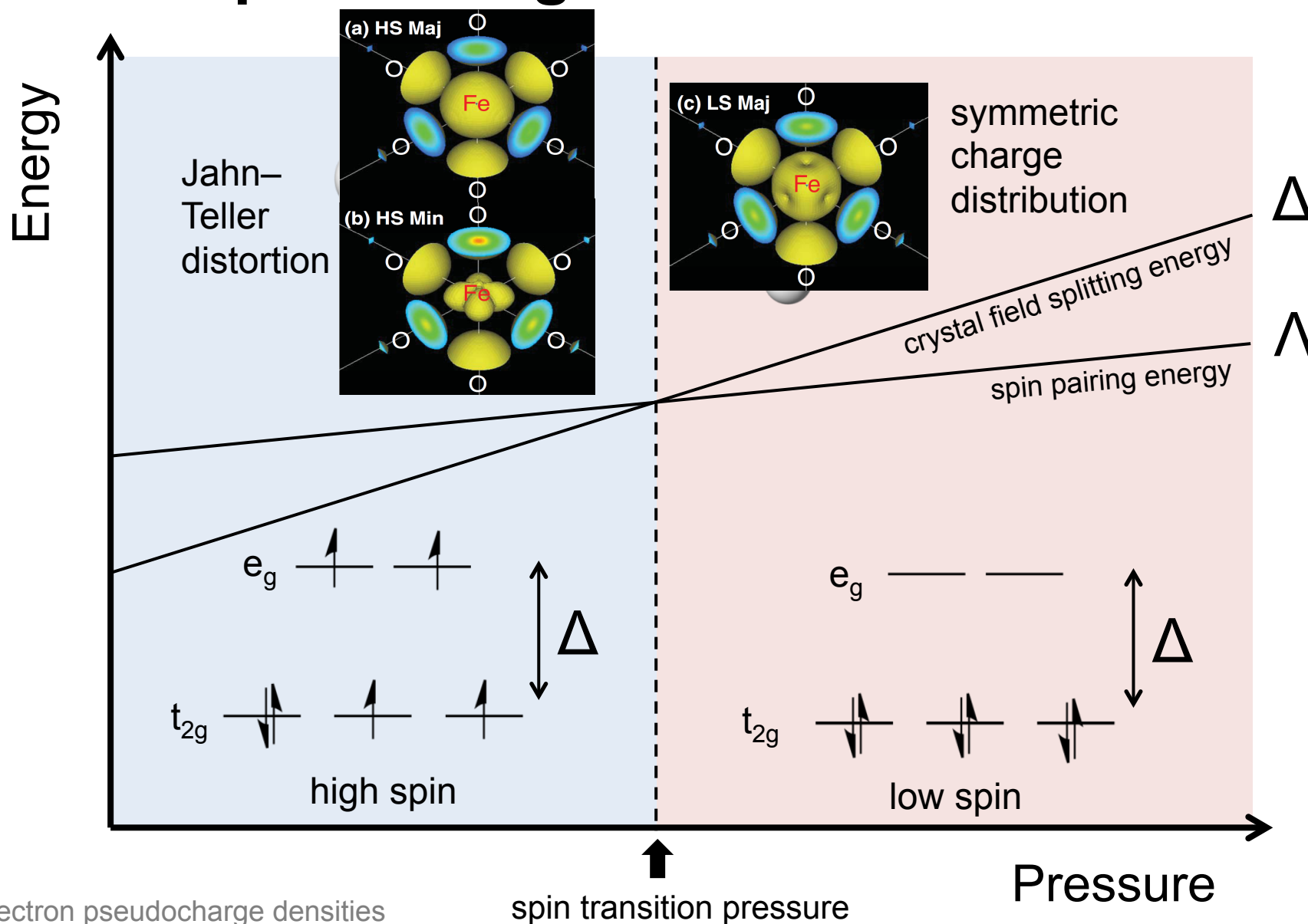
Periclase-Wüstite Solid Solution



Periclase remains in the rocksalt (B1) structure throughout lower mantle pressures.

Wüstite experiences a rhombohedral distortion around 17 GPa.

Spin Pairing in Octahedral Fe²⁺



3d-electron pseudocharge densities
 from Tsuchiya et al., PRL 96 (2006)

A Systematic Study

- Fit a spin crossover equation of state to previous pressure-volume data sets for compositions ranging from 10-60 mol% FeO, using either a neon pressure medium or laser-annealed ionic thermal insulator medium.
- Compare resulting equation of state parameters.
The logo for MINUTI features the word "MINUTI" in a bold, black, sans-serif font. Below the text is a colorful, abstract graphic composed of many small, overlapping circles in various colors (red, blue, green, yellow, purple). Below the graphic is the website address "www.nrixs.com" in a smaller, black, sans-serif font.

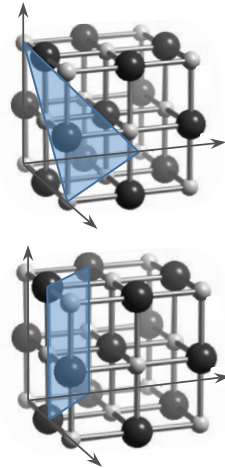
www.nrixs.com
- Directly compare to results from Mössbauer spectroscopy, which is sensitive to iron's spin state.

X-ray Diffraction Patterns

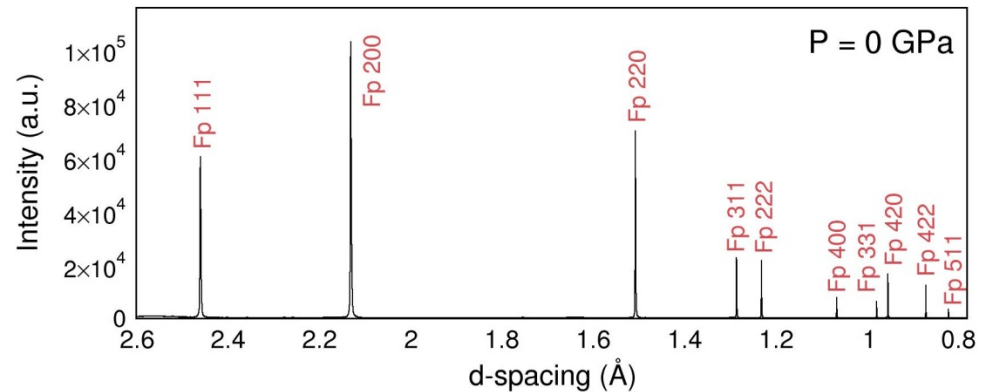
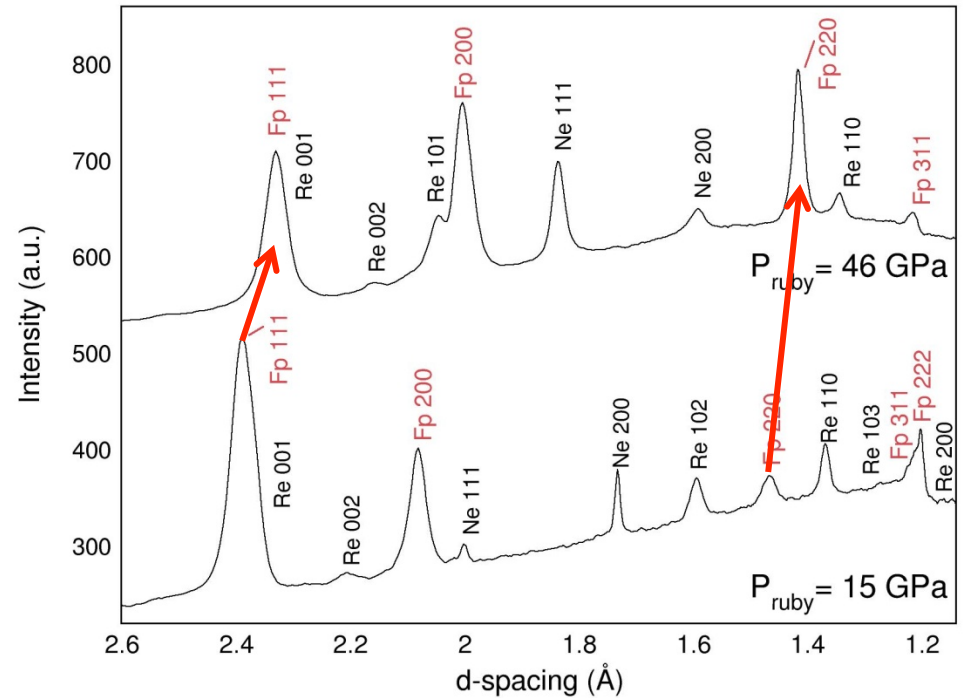
Integrated x-ray diffraction patterns for Fp48 at 0, 15 and 46 GPa at 300 K.

Rhombohedral distortion results in peak splitting:

$111 \rightarrow \begin{matrix} 101 \\ 003 \end{matrix}$
 $220 \rightarrow \begin{matrix} 110 \\ 104 \end{matrix}$



No peak splitting was observed.



Experimental Methods

Low-spin iron has a smaller ionic radius than high-spin iron. Thus, low-spin (Mg,Fe)O has a smaller volume than high-spin (Mg,Fe)O.



X-ray Diffraction Experiments

Observe volume change with pressure through the spin crossover region

The electronic environment of low-spin iron is more symmetrical than that of high-spin iron.

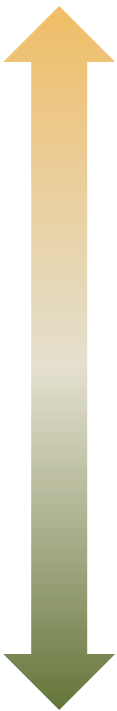


Synchrotron Mössbauer Spectroscopy

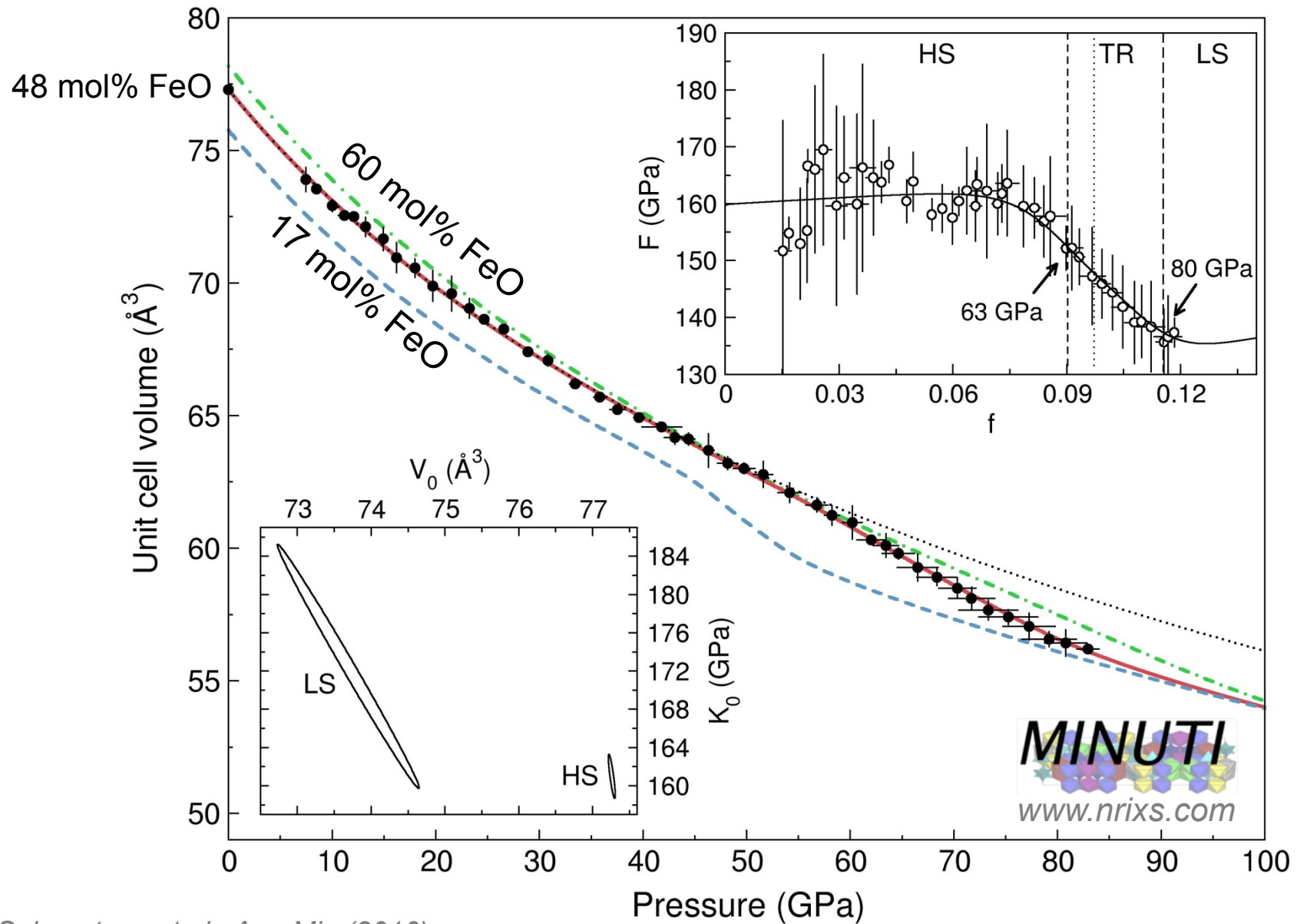
Direct access to the electronic environment of the iron atoms

+

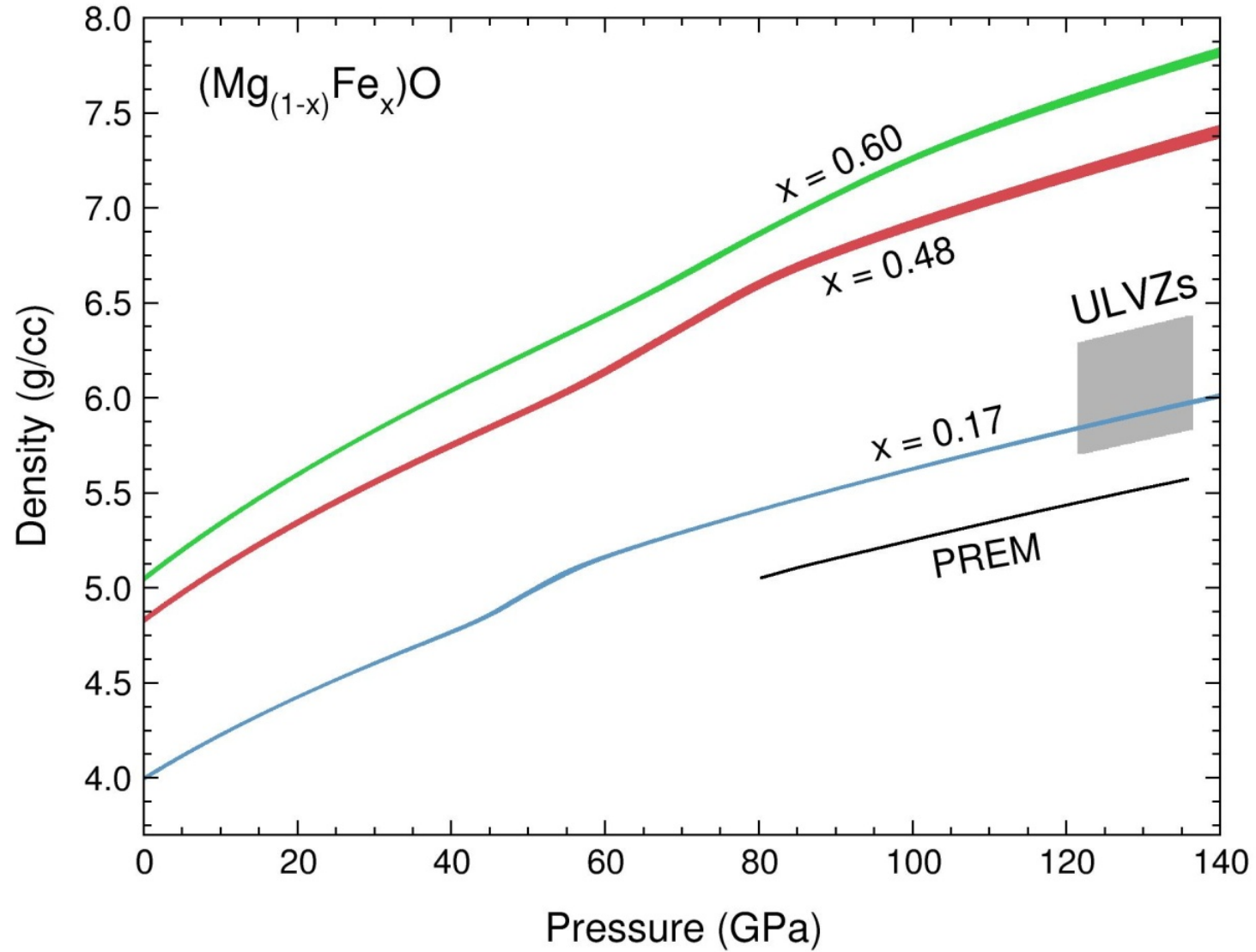
Previous Experiments on (Mg,Fe)O

FeO %	Methods	Pressure Mediums	Pressure Scales	Spin Transition Pressure
MgO  FeO	<ul style="list-style-type: none"> ○ Conventional Mössbauer ○ X-ray emission ○ Powdered x-ray diffraction ○ Single-crystal x-ray diffraction ○ Synchrotron Mössbauer ○ Optical absorption 	<ul style="list-style-type: none"> ○ None ○ Boron epoxy ○ NaCl ○ KCl ○ Ar ○ Alcohol mixtures ○ Ne ○ He 	<ul style="list-style-type: none"> ○ Ruby ○ NaCl ○ Pt ○ Au 	<ul style="list-style-type: none"> ○ 50% volume collapse ○ 50% low spin population ○ Spin pairing energy = crystal field splitting energy ○ Visual inspection of data

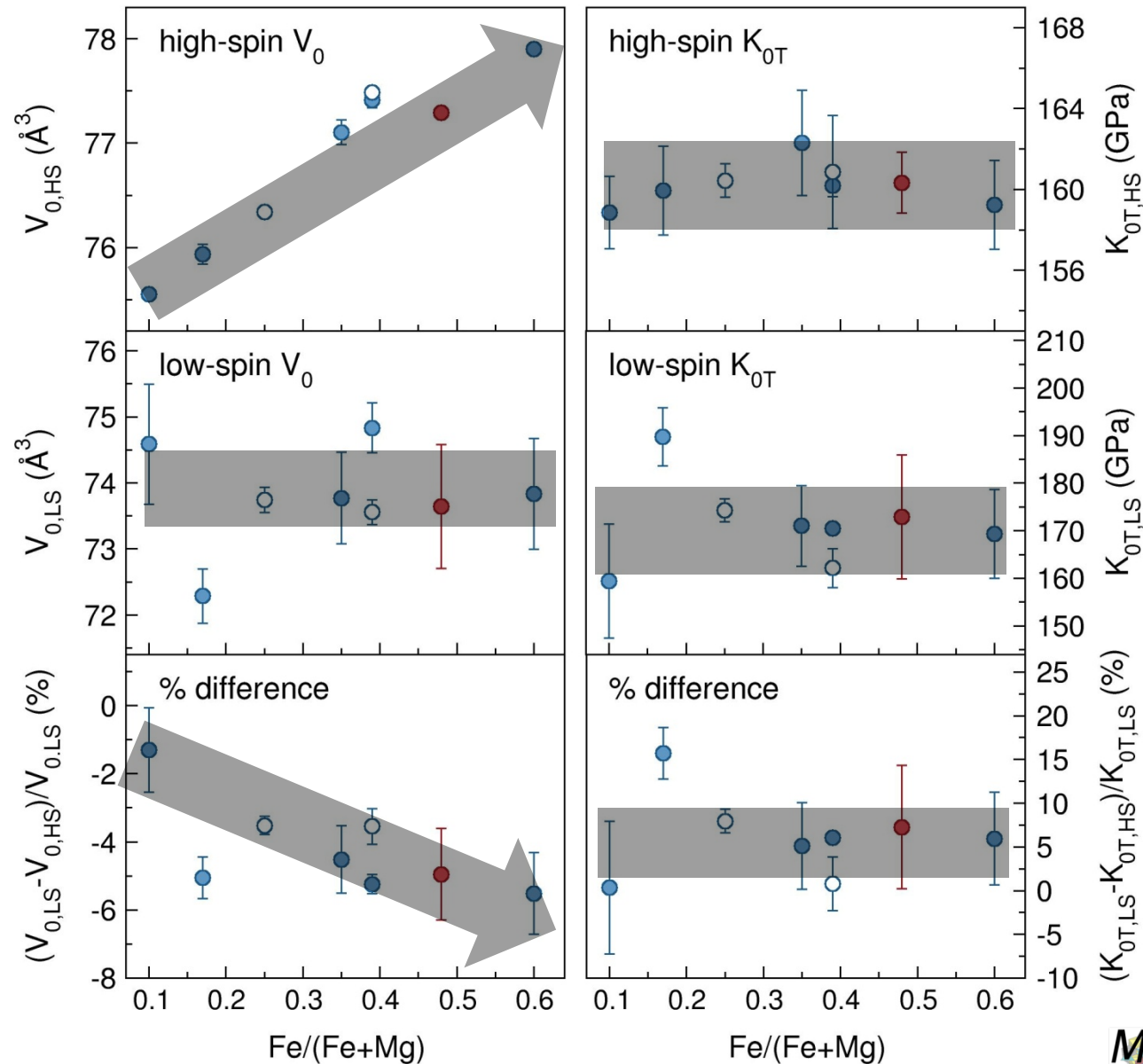
Spin Crossover Equation of State



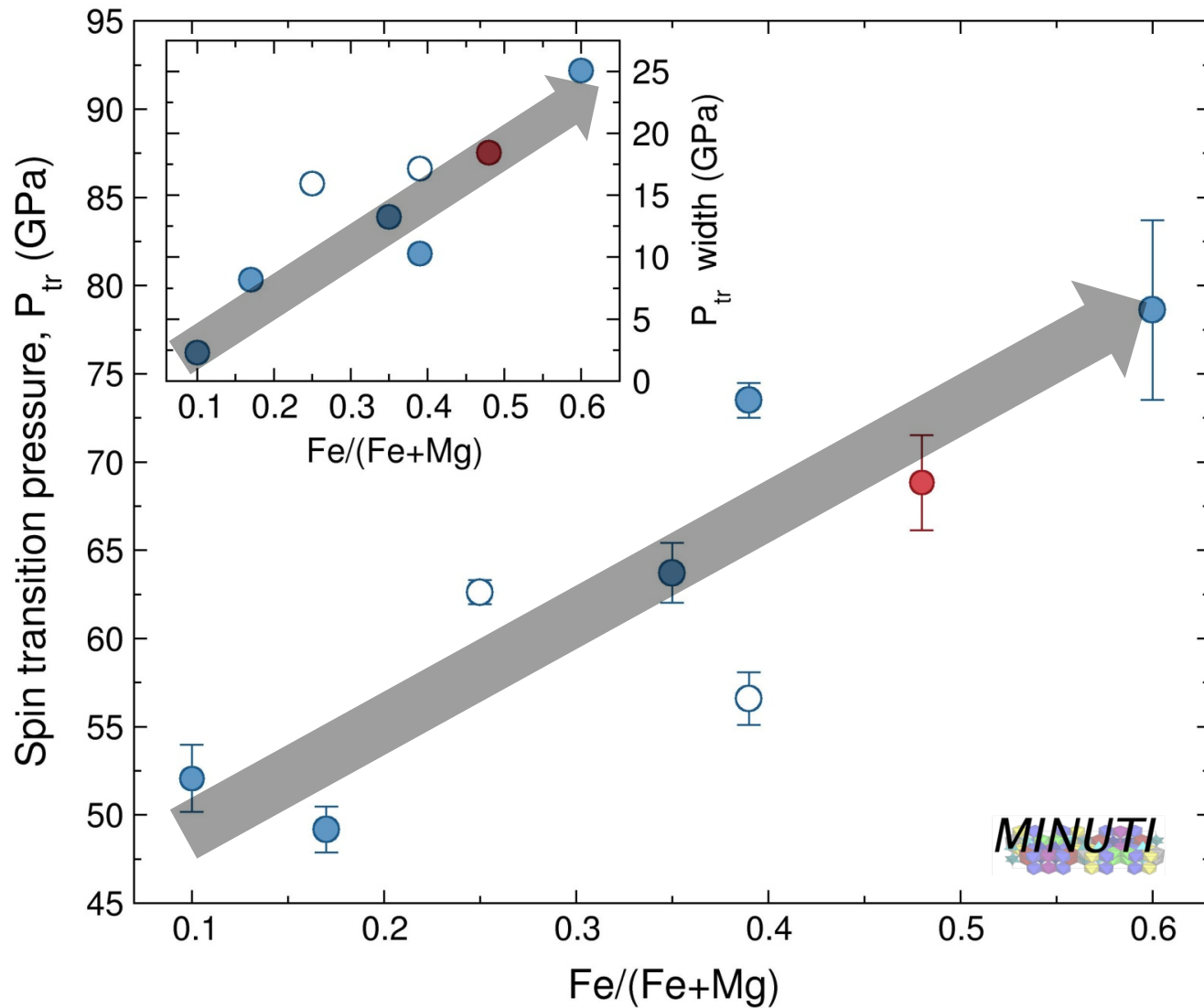
Density



Volume and Bulk Modulus of (Mg,Fe)O



Spin Transition Pressure and Width of (Mg,Fe)O

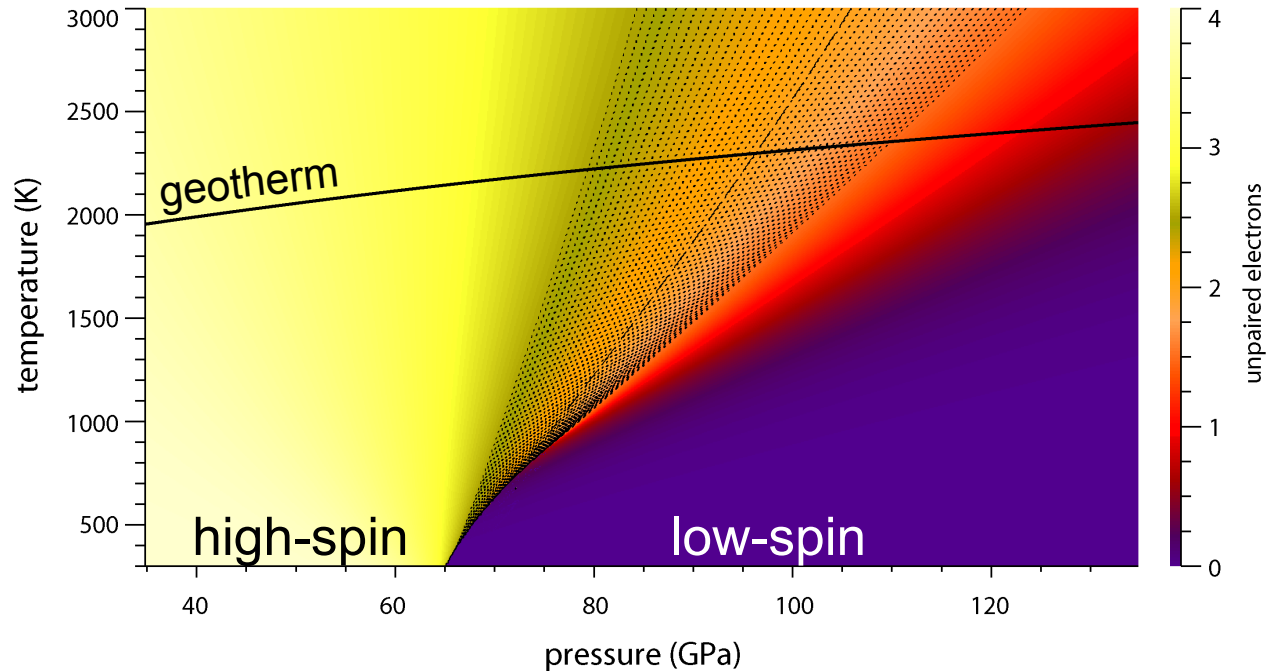


(Mg_(1-x)Fe_x)O with x=0.10 (Marquardt et al., 2009), x=0.17 (Lin et al., 2005), x=0.25 (Mao et al., 2011), x=0.35 (Chen et al., 2012), x=0.39 (Zhuravlev et al., 2010; Fei et al., 2007), x=0.48 (Solomatova et al. 2016), and x=0.60 (Lin et al., 2005). From Solomatova et al. (2016)

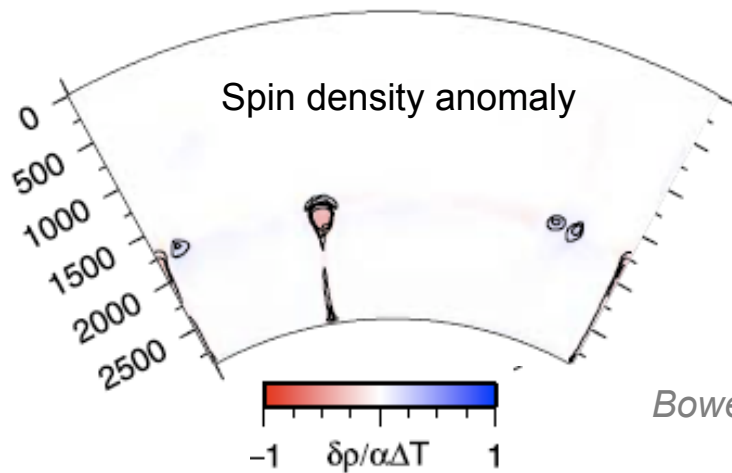
Spin Transition Width

- Core-mantle boundary temperatures:
 - 3300–4300 K
- Spin transition width is expected to increase with temperature.
- Spin transition width is larger for higher Fe content.
- There will be a fraction of high-spin population (positively buoyant) at the core-mantle boundary.

Influence of the continuous spin crossover on mantle dynamics



*Sturhahn, Jackson, Lin., GRL (2005)
First principles: e.g., Tsuchiya et al. (2006), Wentzcovitch et al. (2009)*

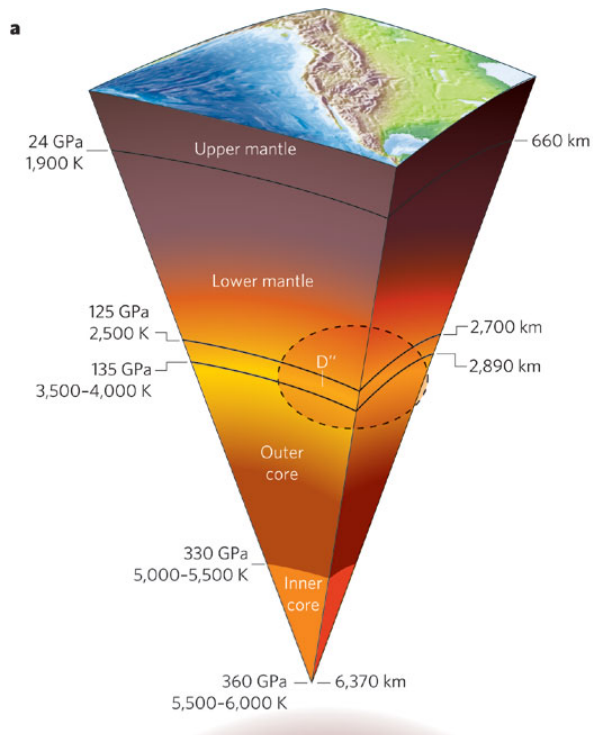


"Spin buoyancy"

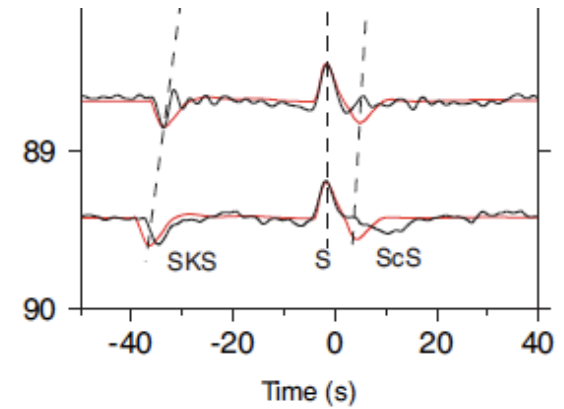
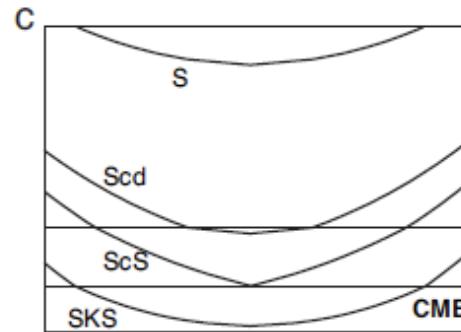
Bower, Gurnis, Jackson, Sturhahn. GRL (2009)

Advective heat transport more effective

The core-mantle boundary region, D''



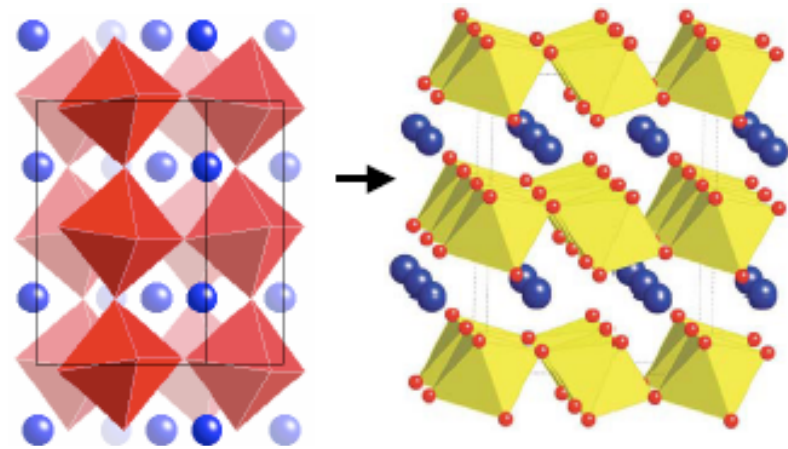
Duffy (2008)



Sidorin et al. (1999)

Seismic discovery that D'' layer could be a distinct boundary: Sidorin et al. (1999);

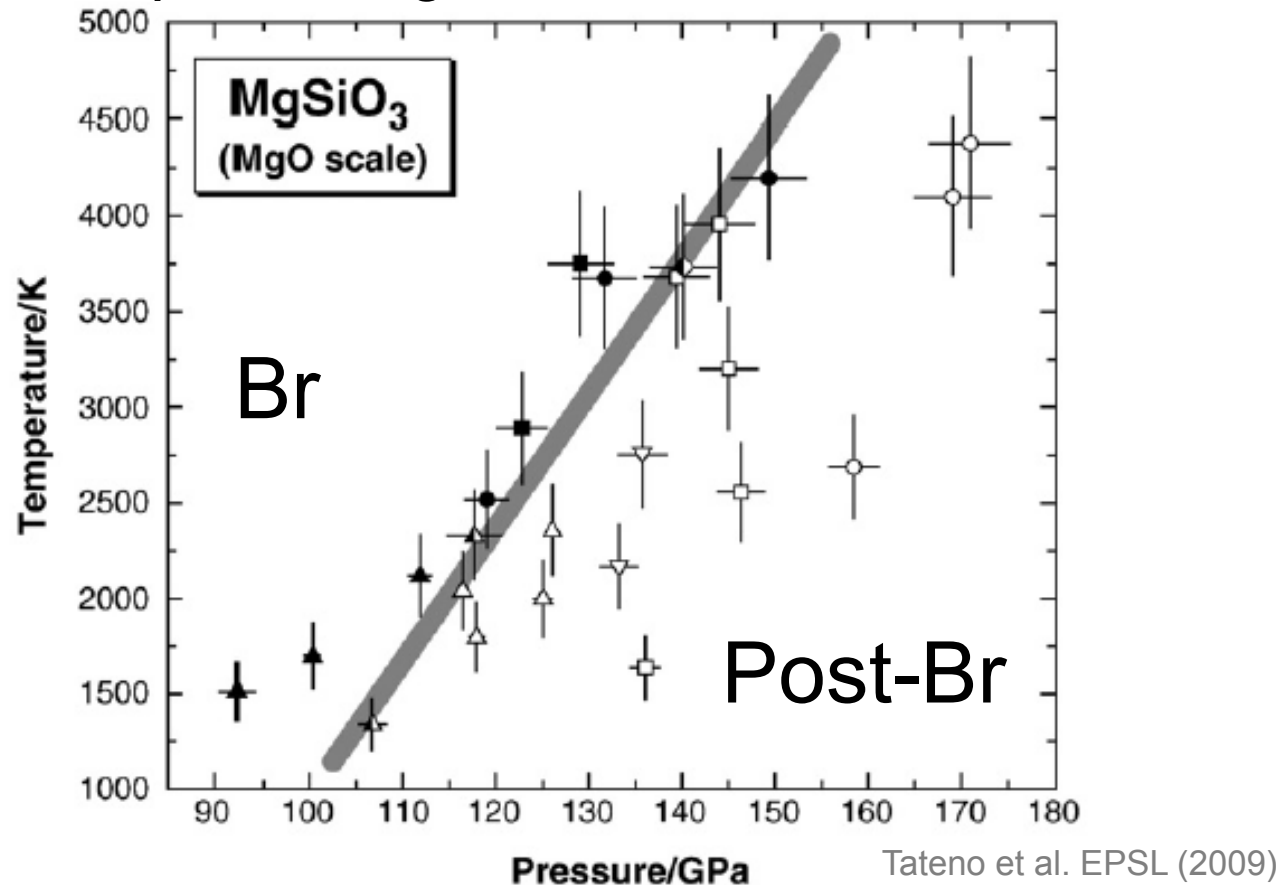
e.g., Helmberger et al. (2005);
 Hernlund et al. (2005);
 van der Hilst et al. (2007);
 dozens more since...



Bridgmanite ($Pbnm$) $MgSiO_3$ post-bridgmanite ($Cmcm$) $MgSiO_3$

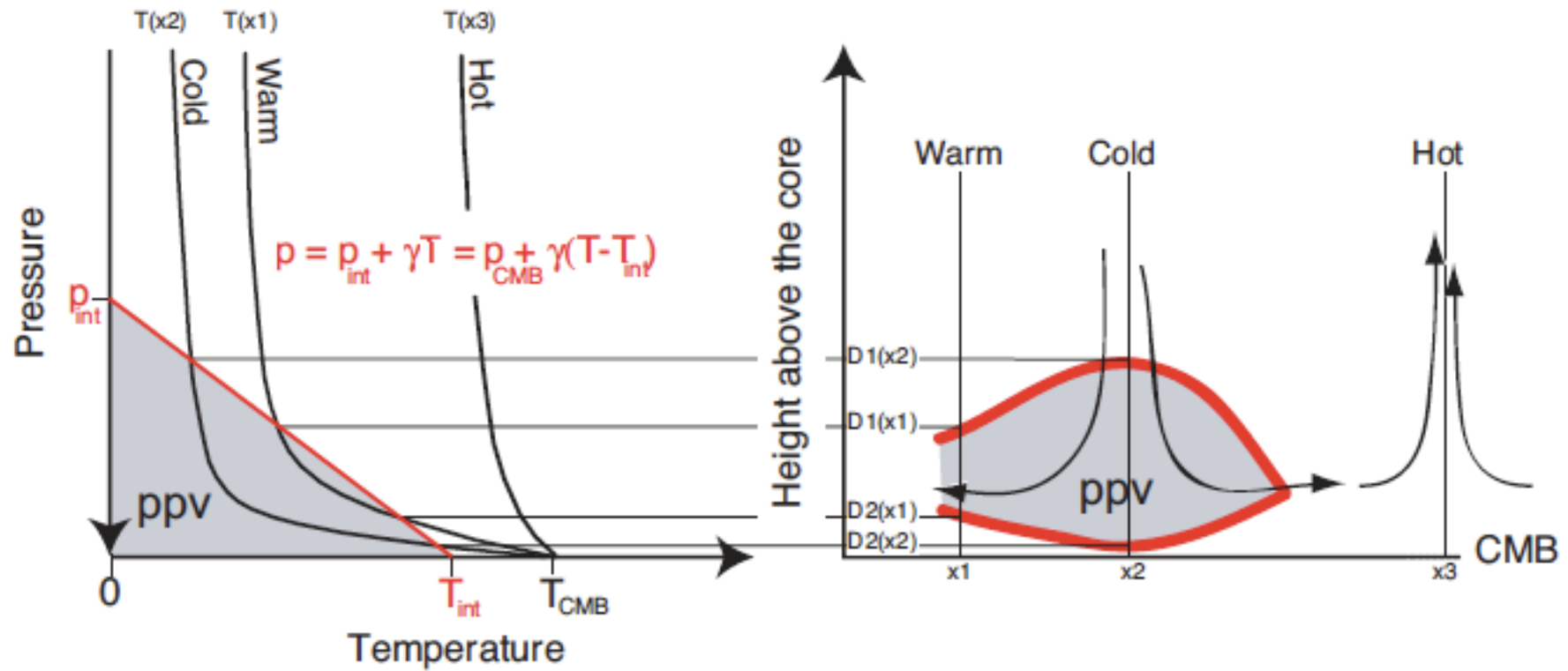
Murakami et al. (2004); Oganov & Ono (2004)

The Clapeyron slope ($dP/dT = dS/dV$) of the bridgmanite to post-bridgmanite transition



Negative molar volume and enthalpy changes of $0.4 \text{ cm}^3 \text{ mol}^{-1}$ and 11.8 kJ mol^{-1} for the Br to PBr transition at 0 K stabilize the PBr at low temperatures and high-P. Vibrational entropies calculated favor Br with increasing temperatures ($105.5 \text{ J K}^{-1} \text{ mol}^{-1}$ for Br vs. $99.2 \text{ J K}^{-1} \text{ mol}^{-1}$ for PBr at 298 K) (Stølen & Trønnes 2007).

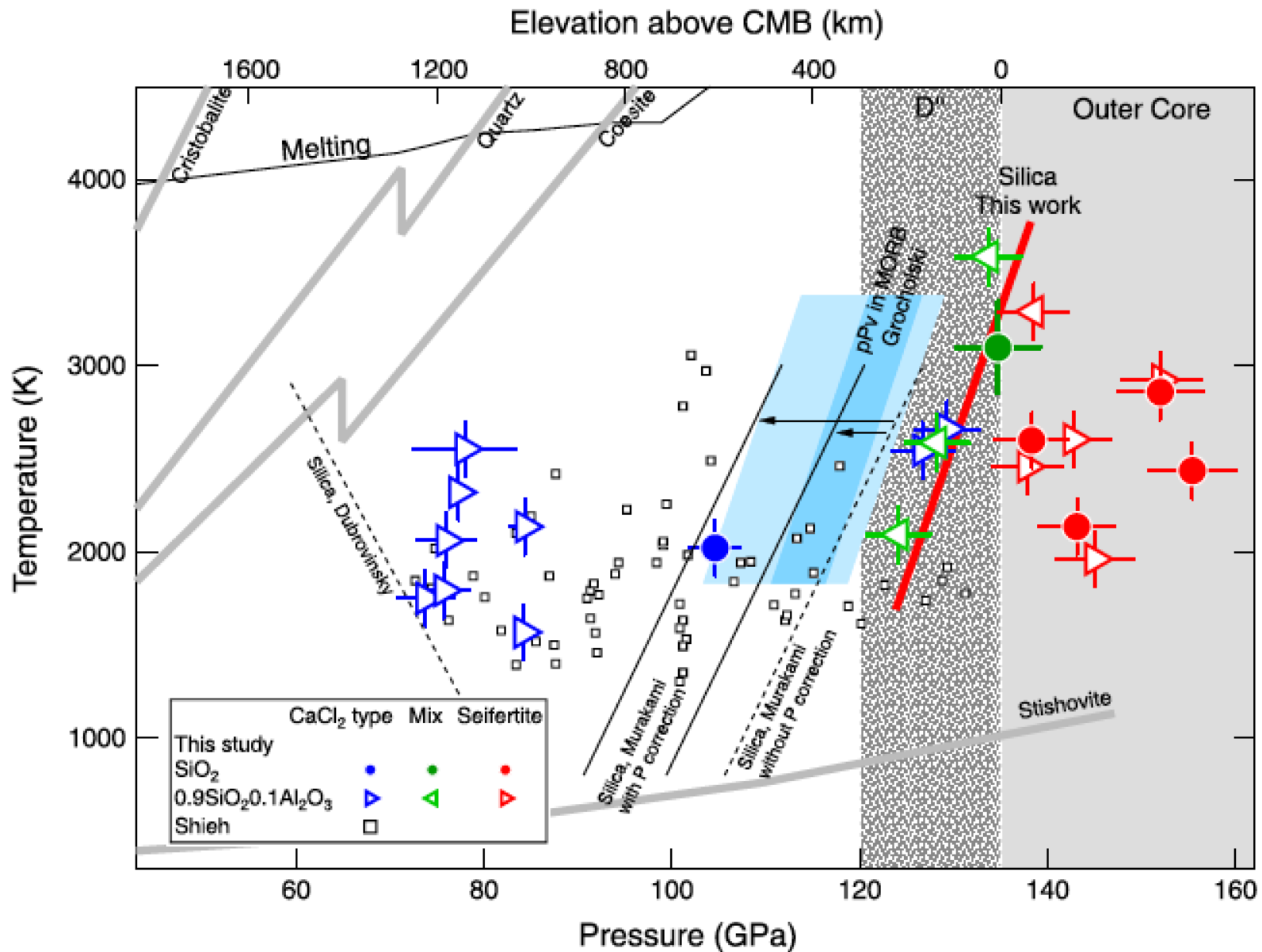
The Clapeyron slope of the bridgmanite to post-bridgmanite transition affects its presence/absence in Earth, because the temperature may be variable and the transition pressure is very close to CMB pressures on Earth.



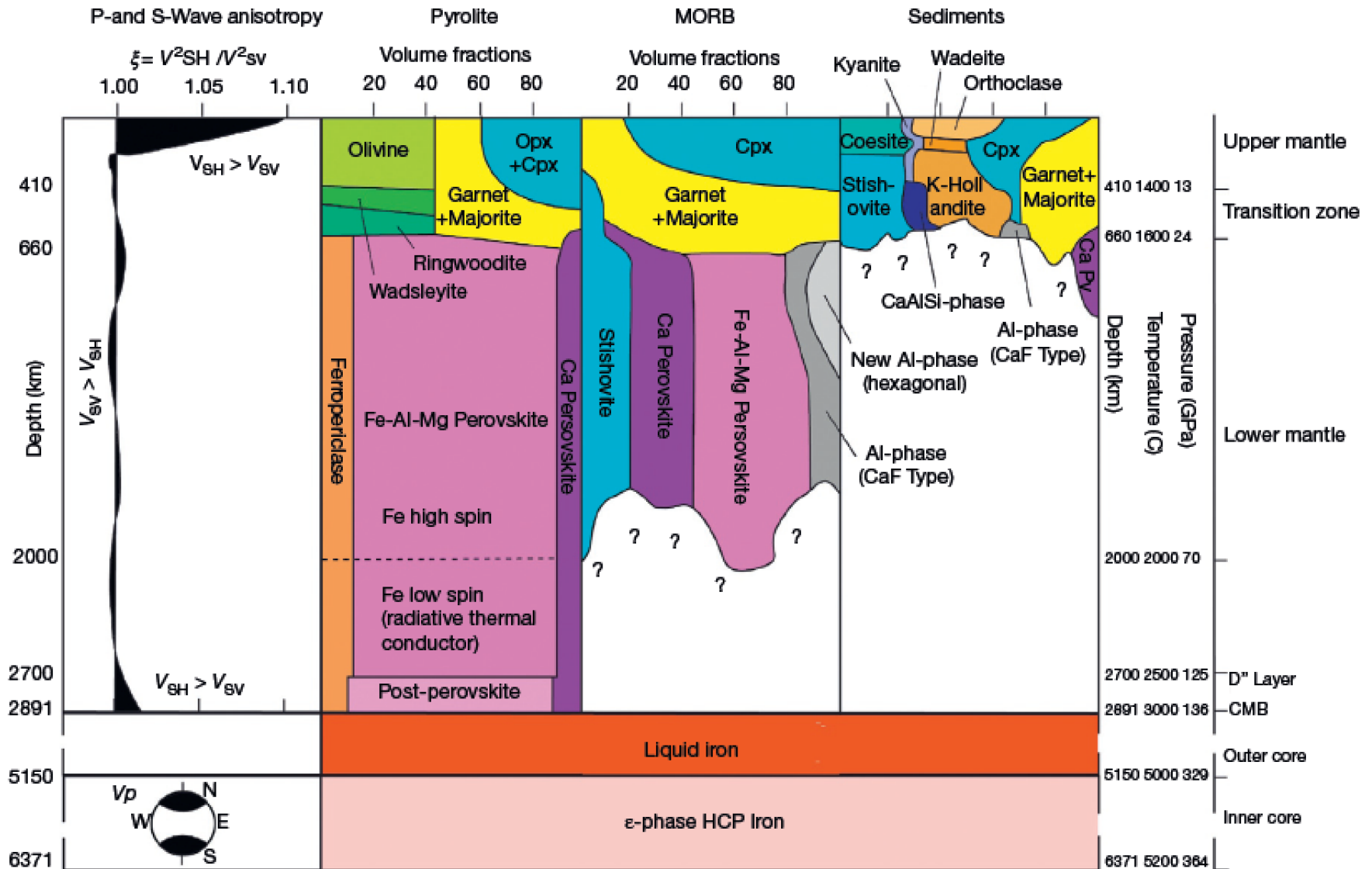
Implications for: phase relations, chemistry, and heat flow from the core

e.g., Hirose (2005); Lay et al., Science (2006); Monnereau & Yuen, PNAS (2007); Shim (2008)

Phase diagram of dense silica, SiO₂

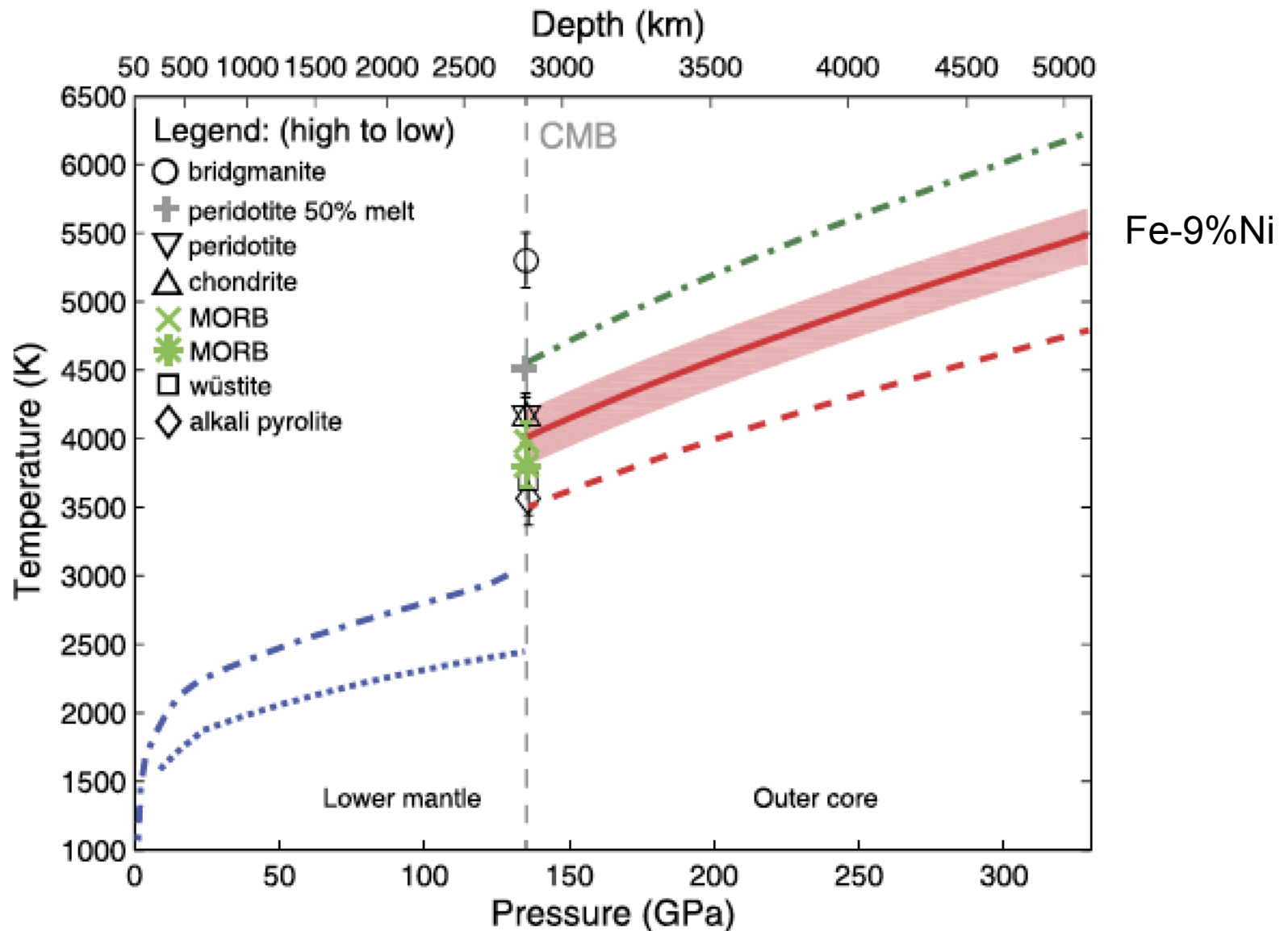


Each phase has its distinct (an)isotropic properties



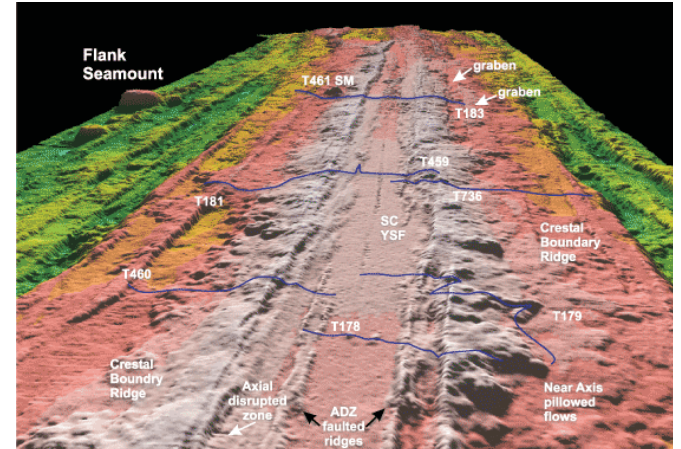
D. Mainprice, *Treatise of Geophysics* (2015)

Temperature of CMB dictates phase equilibrium



Zhang et al. EPSL (2016)

Summary



1. Basic Compositional Constraints
2. Building Minerals
3. Substitution Mechanisms

** Examples of minerals down to Earth's core*

4. Two Component Phase Diagrams, including Partial Melting

** Phase diagrams of mantle minerals*

** Spin crossover and width for (Mg,Fe)O*

5. *Each mineral will dictate differently the buoyancy, seismic wave speeds, thermal and electrical conduction, rheological behavior (flow). Collectively, assemblages can further be different*

Slides on single crystal
elasticity, isotropic averaging,
and equations of state

Jennifer M. Jackson
Caltech

Hooke's Law: $\sigma_{ij} = C_{ijkl} * \epsilon_{kl}$

$$\begin{array}{ccc}
 \sigma_{11} & \sigma_{12} & \sigma_{13} \\
 \sigma_{21} & \sigma_{22} & \sigma_{23} \\
 \sigma_{31} & \sigma_{32} & \sigma_{33}
 \end{array}
 =
 \begin{array}{cccccccc}
 C_{1111} & C_{1122} & C_{1133} & C_{1123} & C_{1113} & C_{1112} & C_{1133} & C_{1131} & C_{1121} \\
 C_{2211} & C_{2222} & C_{2233} & & & & & & \\
 C_{3311} & C_{3322} & C_{3333} & & & & & & \\
 C_{2311} & & & C_{2323} & & & & & \\
 C_{1311} & & & C_{1313} & & & & & \\
 C_{1211} & & & C_{1212} & & & & & \\
 C_{3211} & & & C_{3232} & & & & & \\
 C_{3111} & & & C_{3131} & & & & & \\
 C_{2111} & & & & & & & & C_{2121}
 \end{array}
 *
 \begin{array}{ccc}
 \epsilon_{11} & \epsilon_{12} & \epsilon_{13} \\
 \epsilon_{21} & \epsilon_{22} & \epsilon_{23} \\
 \epsilon_{31} & \epsilon_{32} & \epsilon_{33}
 \end{array}$$

One can fill in the empty spots of the tensor...

The single crystal elastic modulus tensor C_{ijkl} (4th rank) described the elastic energy density of a material. Hooke's law describes the static elasticity.

One can see how the single crystal elastic modulus tensor C_{ijkl} can reduce from 81 elements to 36 elements

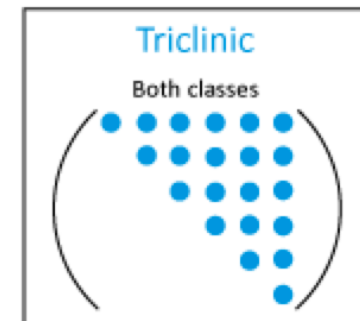
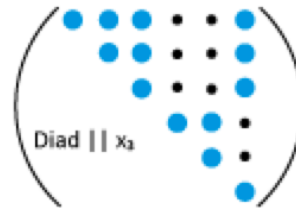
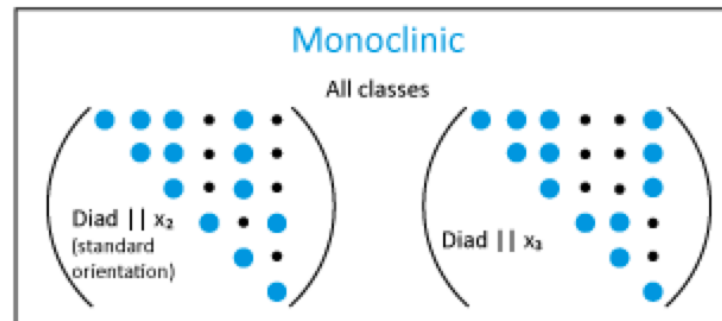
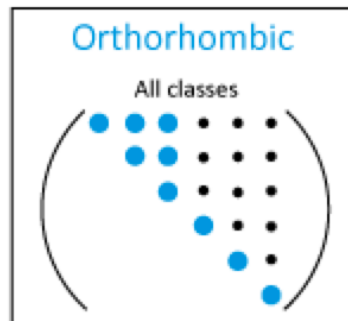
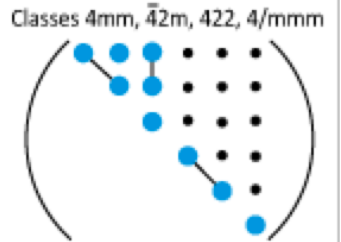
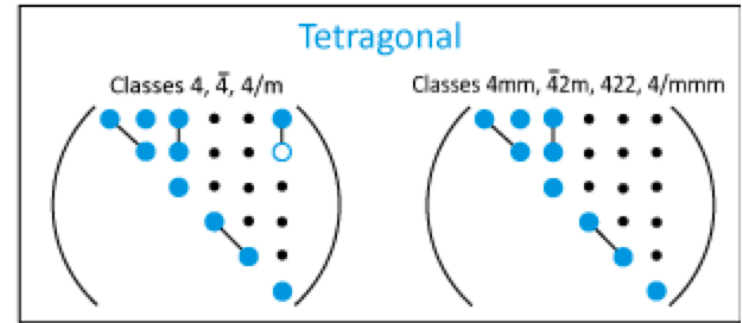
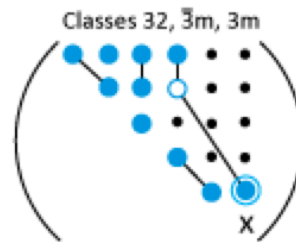
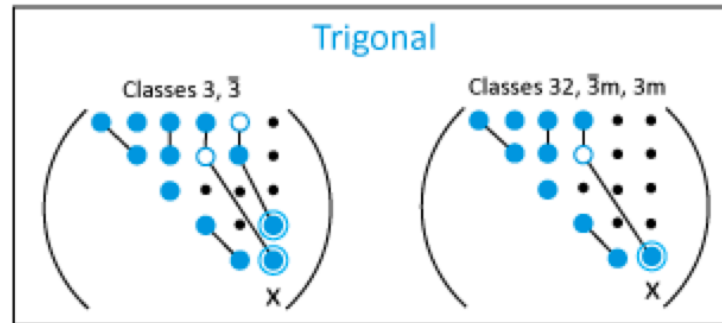
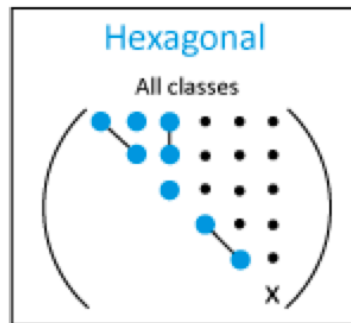
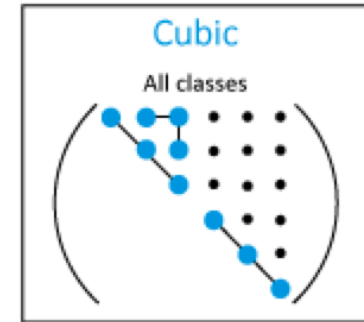
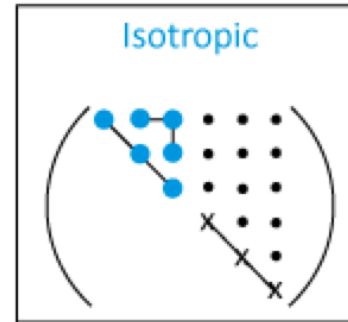
$$\mu = \frac{\textit{ShearStress}}{\textit{ShearStrain}}, \quad K = \frac{\textit{VolStress}}{\textit{VolStrain}} = -V \frac{dP}{dV}, \quad \textit{pressure} = -K \frac{\Delta V}{V}$$

Form of the (s_{ij}) and (c_{ij}) matrices

Key to notation

- zero component
- non-zero component
- equal components
- components numerically equal, but opposite in sign
- ⊙ twice the numerical equal of the heavy dot component to which it is joined (for s)
- ⊕ the numerical equal of the heavy dot component to which it is joined (for c)
- X $2(s_{11}-s_{12})$ (for s)
- X $\frac{1}{2}(c_{11}-c_{12})$ (for c)

All the matrices are symmetrical about the leading diagonal.



After Nye, 1959

Elastic waves in cubic crystals

Using Newton's equations of motion of a unit volume element in a continuum medium:

$$\rho \frac{\partial^2 \vec{u}}{\partial t^2} = \vec{F} \quad , \quad F_i = \sum_j \frac{\partial \sigma_{ij}}{\partial x_j}$$

\vec{u} = displacement
 ρ = specific mass
 \vec{F} = force that balances stress on a volume element

Christoffel equation: $|C_{ijkl} a_j a_l - \rho V^2 \delta_{ik}| = 0$

Simple cases, 1) Longitudinal wave propagating in the x_1 direction, displacement in "1" direction

$$\rho \frac{\partial^2 u}{\partial t^2} = C_{11} \frac{\partial^2 u_1}{\partial x_1^2} \quad C_{11} = \rho V_{P[100]}^2$$

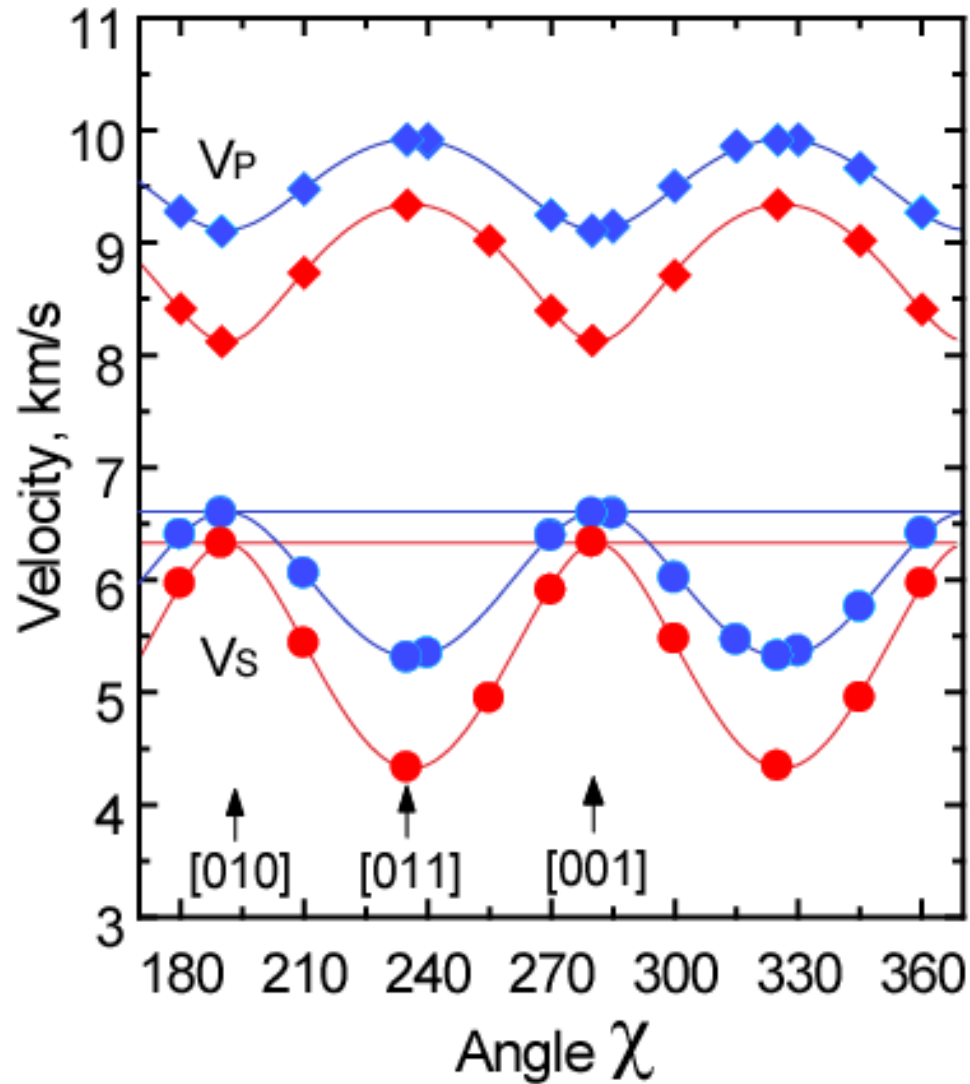
2) Shear wave propagating in the x_1 direction, with particle displacement in the "2" direction

$$\rho \frac{\partial^2 u}{\partial t^2} = C_{44} \frac{\partial^2 u_2}{\partial x_1^2} \quad C_{44} = \rho V_{SV,SH[100]}^2$$

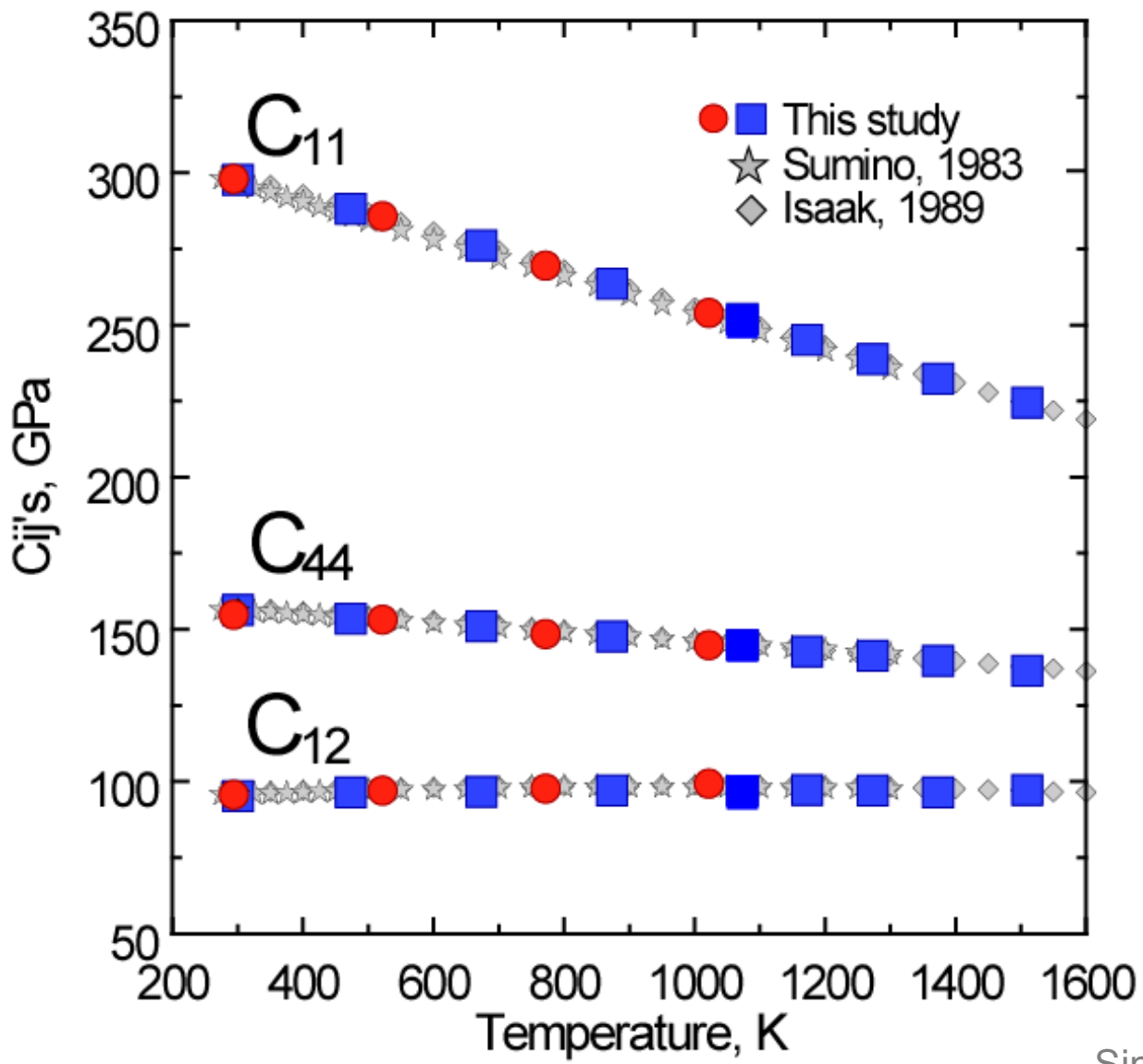
More complex cases that highlight dynamics involving waves: waves in the [110] plane

$$\frac{1}{2}(C_{11} + C_{12} + C_{44}) = \rho V_{P[110]}^2, \quad C_{44} = \rho V_{SV[110]}^2, \quad \frac{1}{2}(C_{11} - C_{12}) = \rho V_{SH[110]}^2$$

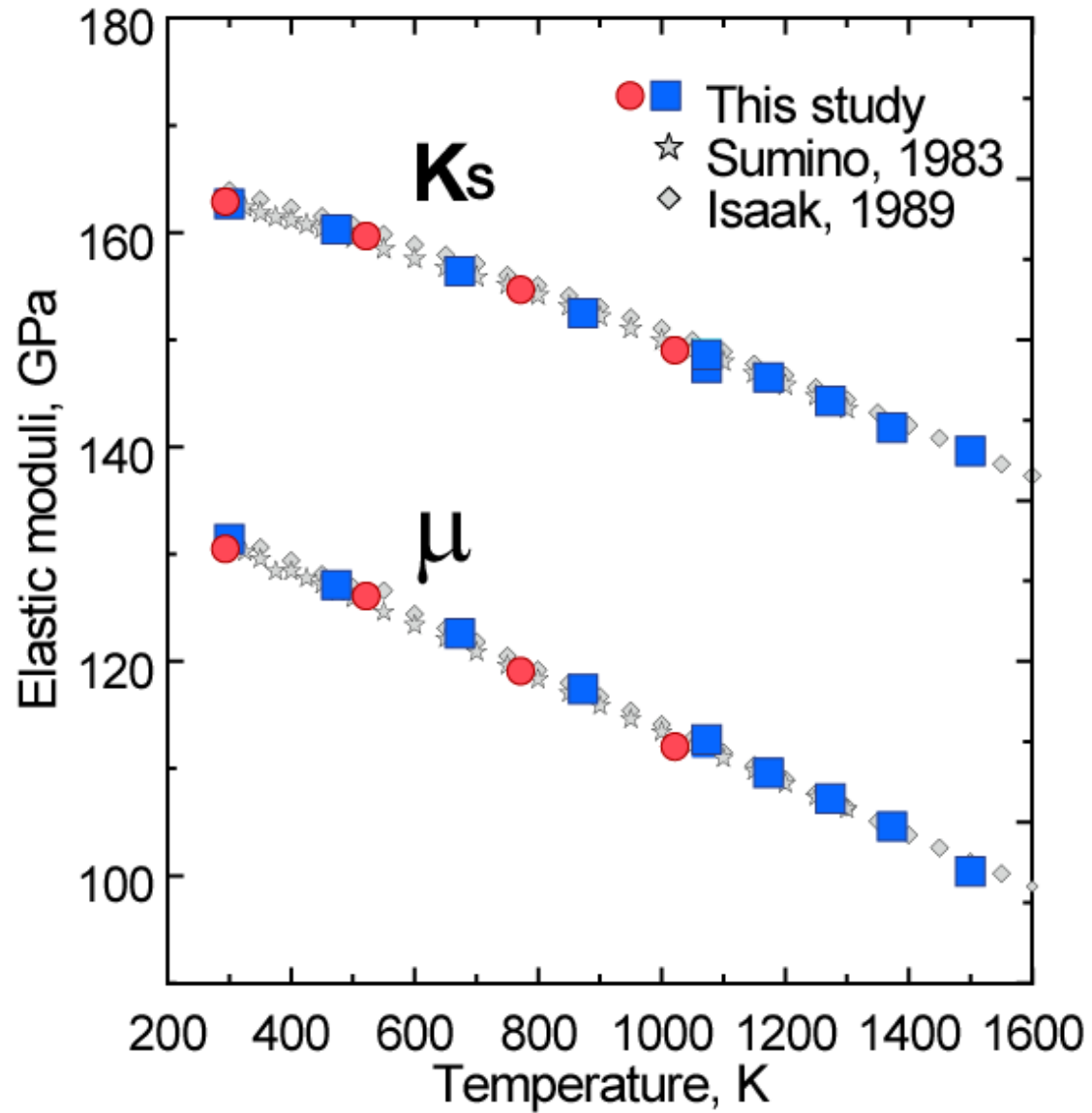
**Sound velocities in MgO
as a function of direction in (100) plane
at room temperature (blue) and 1500 K (red)**



Single-crystal Elastic Moduli of MgO as a function of temperature

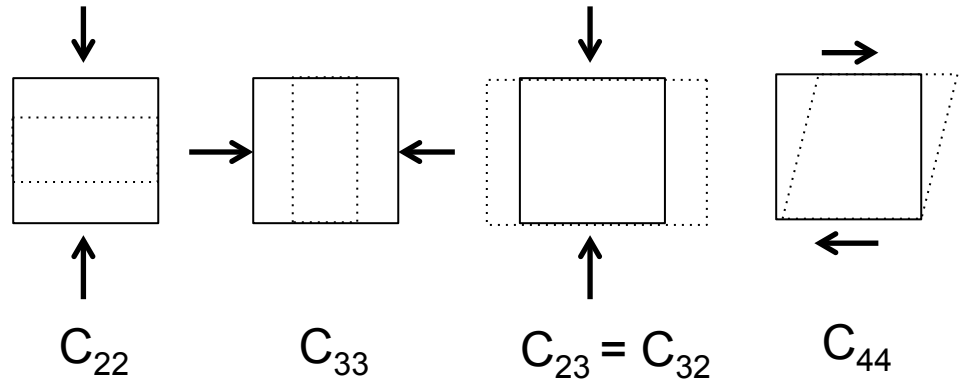
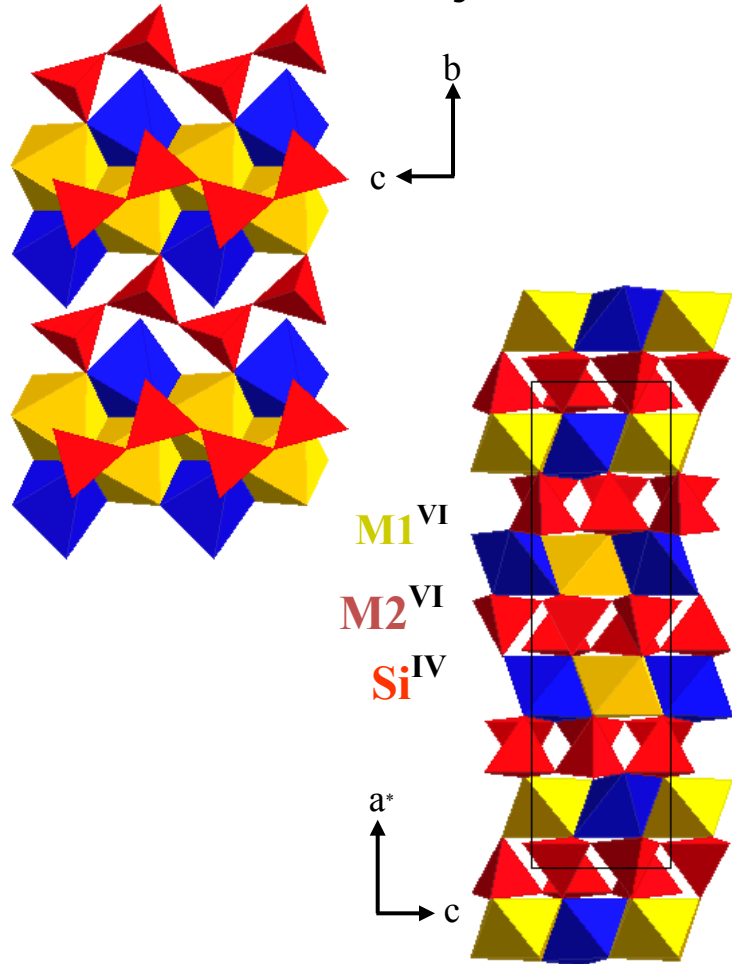


Aggregate Elastic Moduli in MgO as a function of temperature

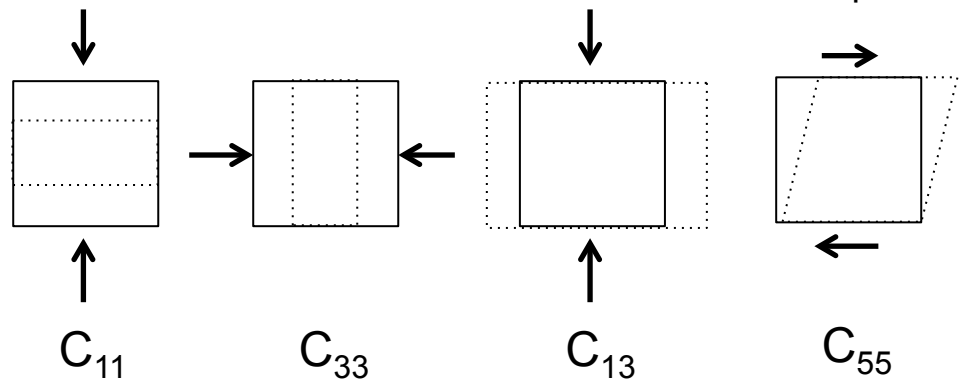


Single-crystal elastic moduli (C_{ij} 's) of $Mg_2Si_2O_6$ orthoenstatite

Orthoenstatite crystal structure:



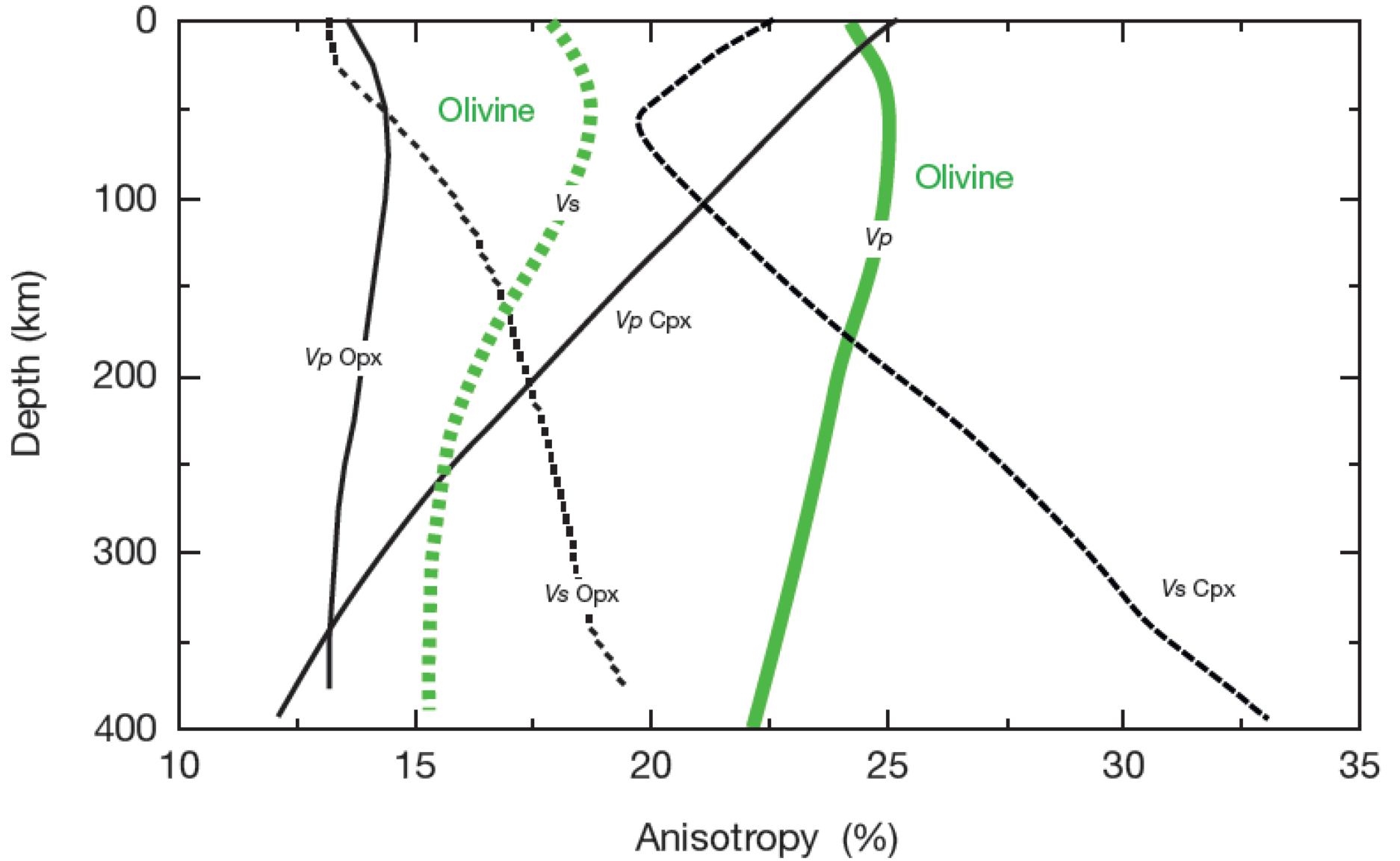
Propagation is along c , polarized in b -plane



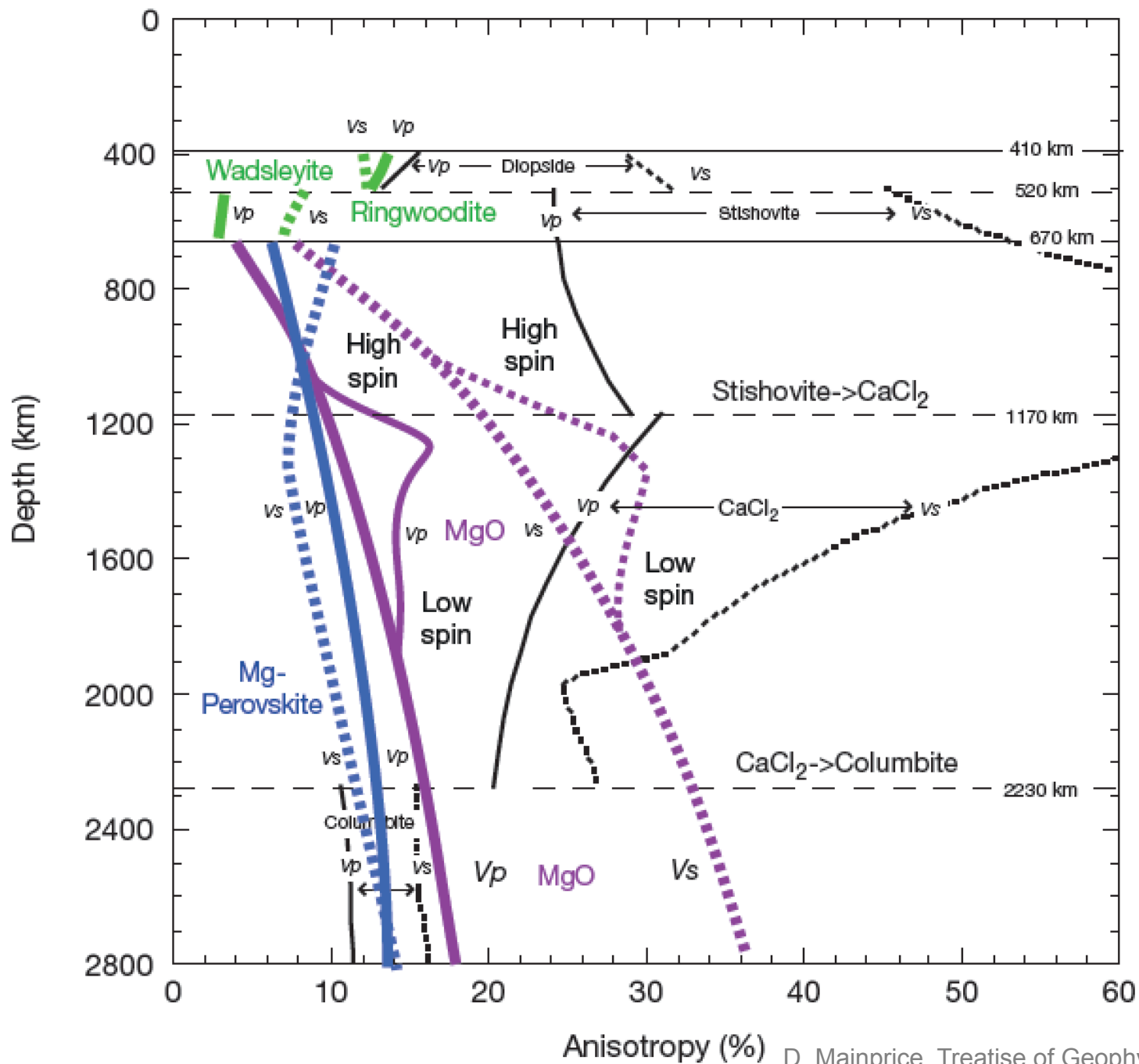
$$C_{33} = \rho(V_{P[001]})^2$$

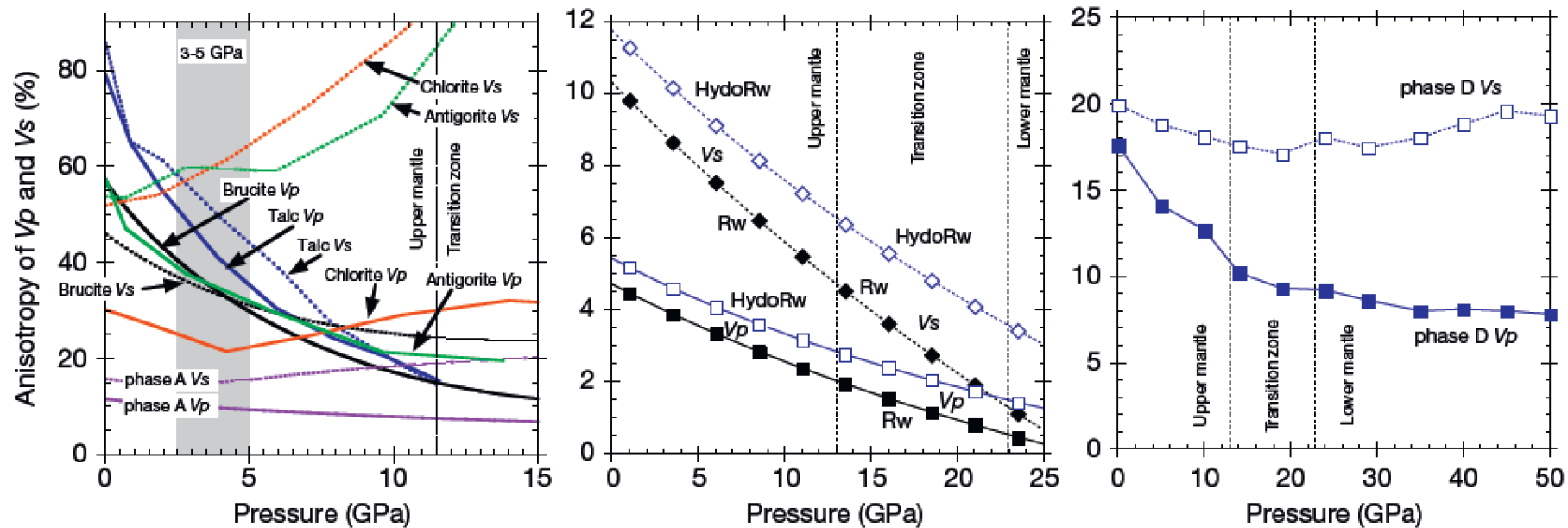
$$C_{55} = \rho(V_{S[-c,a\uparrow]})^2$$

Single crystal anisotropy : Upper mantle



Single crystal anisotropy : Transition zone and lower mantle





D. Mainprice, Treatise of Geophysics (2015)

Elastic properties of composite materials

- Starting point: single crystal elasticity
- Single crystal to polycrystalline aggregate of the same material
- Evaluate the boundary conditions of grain interaction

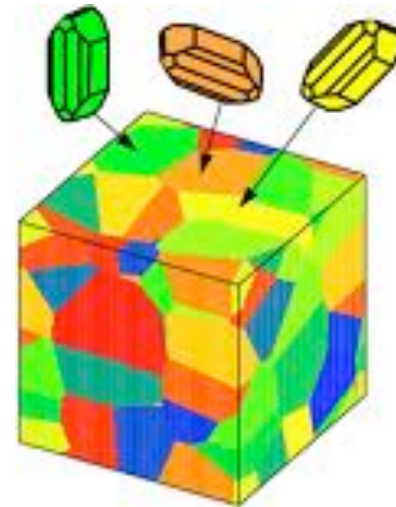


figure Phil Skemer

Voigt-Reuss-Hill bounds

- Obtaining aggregate elastic moduli (K , μ) from C_{ij} 's: Voigt and Reuss elasticity bounds on aggregates of the same crystallites (Nye 1959):
 - Voigt = uniform strain (isostrain), given in terms of single-crystal stiffnesses, C_{ij} 's.
 - Reuss = uniform stress (isostress), given in terms of the inverse of single-crystal compliances, S_{ij} 's⁻¹.
 - Voigt-Reuss-Hill = arithmetic average of Voigt and Reuss bounds.
 - Hill showed that the real value must be between these two bounds
- Compute the bounds for a monomineralic aggregate

Elastic Tensors of Mg end-member Upper Mantle Minerals

	ρ (g/cc)	C_{11} (GPa)	C_{22} (GPa)	C_{33} (GPa)	C_{44} (GPa)	C_{55} (GPa)	C_{66} (GPa)	C_{12} (GPa)	C_{13} (GPa)	C_{23} (GPa)
Gt, Py: $Mg_3Al_2Si_3O_{12}$	3.57	296			94			111		
Ol, Fo: Mg_2SiO_4	3.22	328	200	235	67	81	81	69	69	73
Opx, Oe n: $Mg_2Si_2O_6$	3.194	233	171	216	83	79	77	73	56	50

Cubic phases, such as garnet and periclase:

$$K_{S,R} = K_{S,V} \text{ (GPa)} = (C_{11} + 2C_{12})/3$$

$$\mu_V \text{ (GPa)} = (1/5)(C_{11} - C_{12} + 3C_{44}) \quad \sigma_{ij} = C_{ij} * \epsilon_{kl}$$

$$\mu_R \text{ (GPa)} = 15[(12/(C_{11} - C_{12})) + (9/C_{44})] \quad \epsilon_{kl} = S_{ij} * \sigma_{ij}$$

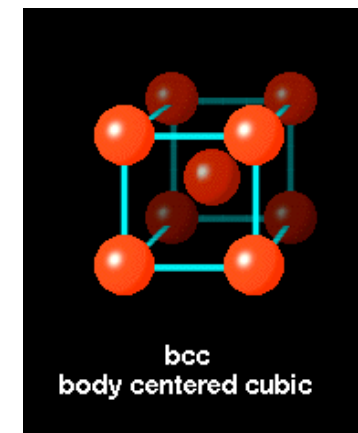
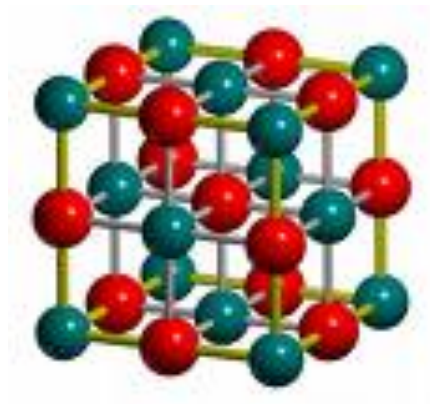
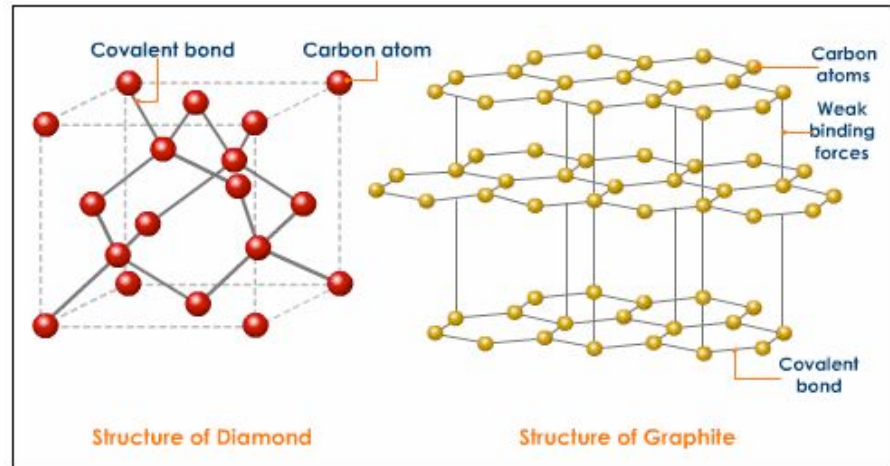
Voigt-Reuss-Hill bounds

Orthorhombic

- Voigt = uniform strain (isostrain), given in terms of single-crystal stiffnesses, C_{ij} 's.
 - $9K_V = C_{11} + C_{22} + C_{33} + 2(C_{12} + C_{13} + C_{23})$
 - $\mu_V = 1/15[(C_{11} + C_{22} + C_{33}) - (C_{12} + C_{13} + C_{23}) + 3(C_{44} + C_{55} + C_{66})]$
- Reuss = uniform stress (isostress), given in terms of the inverse of single-crystal compliances, S_{ij} 's⁻¹.
 - $1/K_R = (S_{11} + S_{22} + S_{33}) + 2(S_{12} + S_{13} + S_{23})$
 - $15/\mu_R = 4(S_{11} + S_{22} + S_{33}) - 4(S_{12} + S_{13} + S_{23}) + 3(S_{44} + S_{55} + S_{66})$
- Voigt-Reuss-Hill = arithmetic average of Voigt and Reuss bounds, applies to all symmetric classes.
 - $K_{VRH \text{ or } H} = 1/2(K_V + K_R)$
 - $\mu_{VRH \text{ or } H} = 1/2(\mu_V + \mu_R)$

Aggregate Elastic Properties: Polymorphs (allotropes), isostructures, metals

	ρ (g/cc)	K_S, μ_{VRH} (GPa)	μ_{VRH} (GPa)
graphite	2.26	160	109
diamond	3.5	443	536
NaCl	2.16	25	15
MgO	3.58	160	130
α -Fe	7.87	167	82



Comparing Aggregate Elastic Properties of Polymorphs

	Crystal class/form	ρ (g/cc)	$K_{S, VRH}$ (GPa)	μ_{VRH} (GPa)
MgSiO ₃	isotropic/glass	2.76	79	31
Mg ₂ Si ₂ O ₆	orthorhombic/orthoensatite	3.194	107.6	76.8
MgSiO ₃	Orthorhombic/bridgmanite	4.108	250	180
MgSiO ₃	orthorhombic/post-bridgmanite	4.25	230	136

Aggregate elastic properties of some major upper mantle minerals

	ρ (g/ cc)	$K_{S,V}$ (GPa)	$K_{S,R}$ (GPa)	$K_{S,VRH}$ (GPa)	μ_V (GPa)	μ_R (GPa)	μ_{VRH} (GPa)	$V_{P,VRH}$ (km/s)	$V_{S,VRH}$ (km/s)
Gt, Py: $Mg_3Al_2Si_3O_{12}$	3.57	172.7	172.7	172.7	92.2	92.2	92.2	9.09	5.08
Ol, Fo: Mg_2SiO_4	3.22	132	127	129.5	82.6	79.6	81.1	8.59	5.02
Opx, Oen: $Mg_2Si_2O_6$	3.19	108.6	106.6	107.6	77.2	76.4	76.8	8.11	4.90

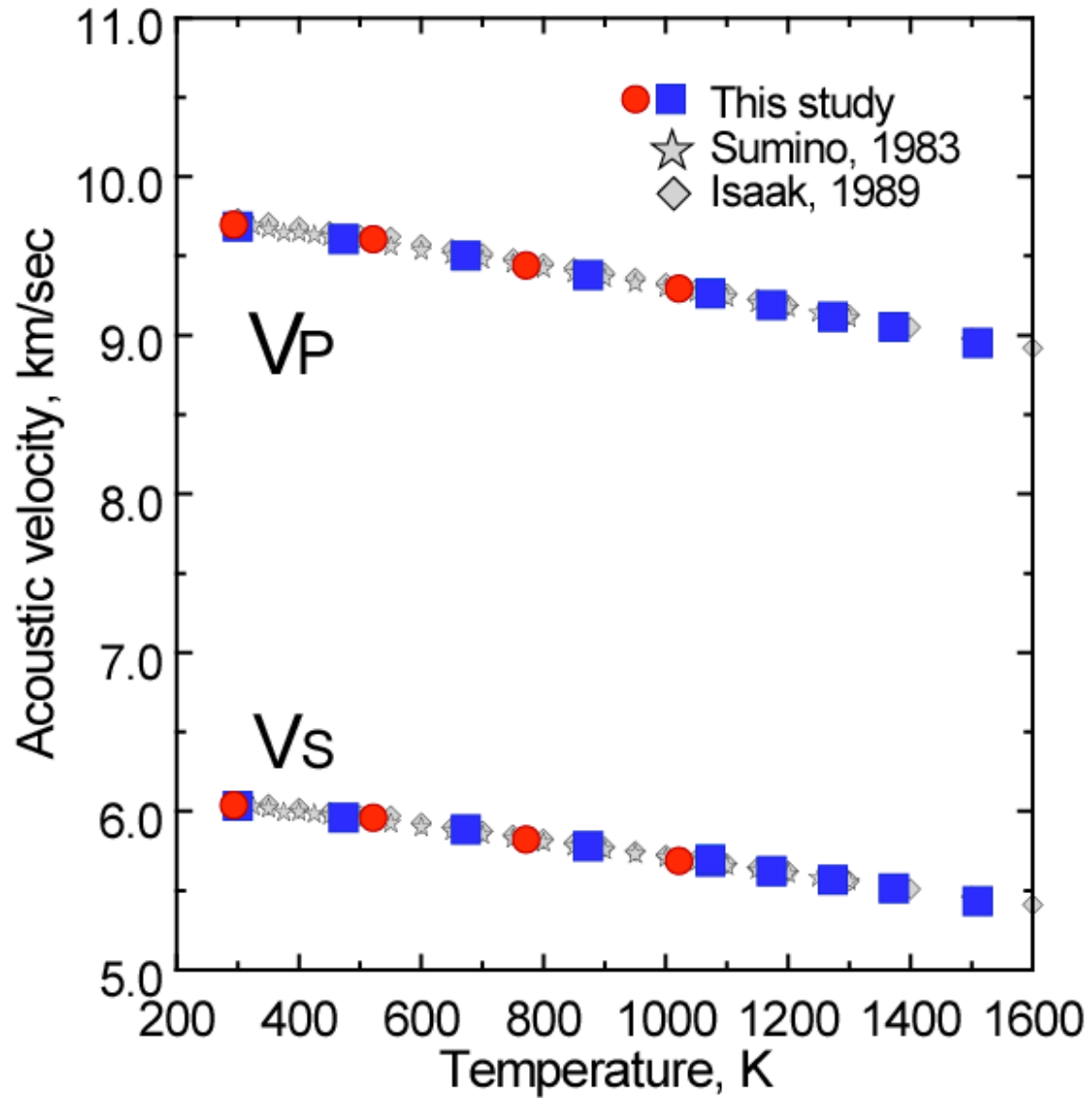
Other important elastic properties:

$$V_P^2 = \left(\frac{K_S + \frac{4}{3}\mu}{\rho} \right), \quad V_S^2 = \frac{\mu}{\rho}$$

$$V_\phi^2 = \frac{K_S}{\rho} = \left(V_P^2 - \frac{4}{3}V_S^2 \right)$$

$$\nu = \frac{\left(\frac{V_P}{V_S} \right)^2 - 2}{2 \left[\left(\frac{V_P}{V_S} \right)^2 - 1 \right]} = -\frac{\epsilon_{22}}{\epsilon_{11}}$$

Aggregate Sound Velocities in MgO as a function of temperature



Elasticity of composites made of heterogeneous materials



- Starting point: Aggregate isotropic properties of each component
- Add another component to the aggregate
- Compute V-R-H bounds for the multi-phase aggregate (rock)
- Calculate elastic properties of a multi-phase mixture (*Watt et al. 1976*):

$$M_R^* = \left(\sum_{i=1}^n \frac{v_i}{M_i} \right)^{-1} \leq M^* \leq \sum_{i=1}^n v_i M_i = M_V^*$$

Grüneisen parameter

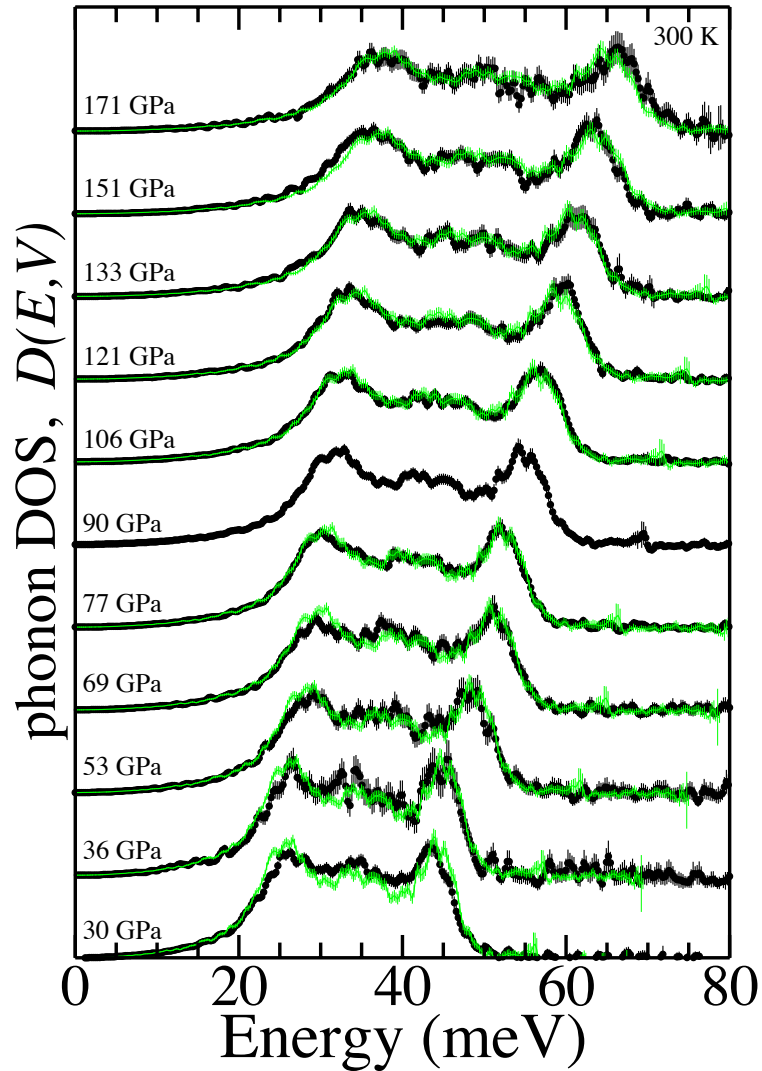
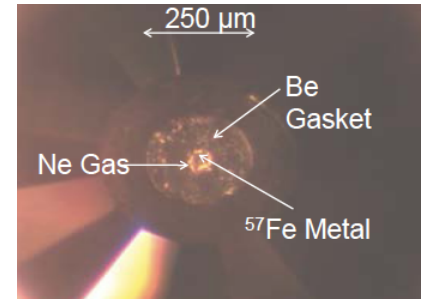
- Synthesis between thermal and elastic properties, provides the physical basis for thermoelastic coupling.
- **Thermoelastic** coupling: Bulk modulus (section 2.3, JPP). Two intensive variables (**T** and **stress**) depend only on two extensive variables (**S** and **strain**). Hydrostatic pressure (geophysically relevant), the chain rule, and definitions of the adiabatic and isothermal bulk moduli (Table 1.2):

$$K_S - K_T = \alpha K_T T \left(\frac{\alpha K_S V}{C_P} \right), \quad \gamma_{th} = \left(\frac{\alpha K_S V}{C_P} \right) = \left(\frac{\alpha K_S}{T} \right) \left(\frac{\partial T}{\partial P} \right)_S$$

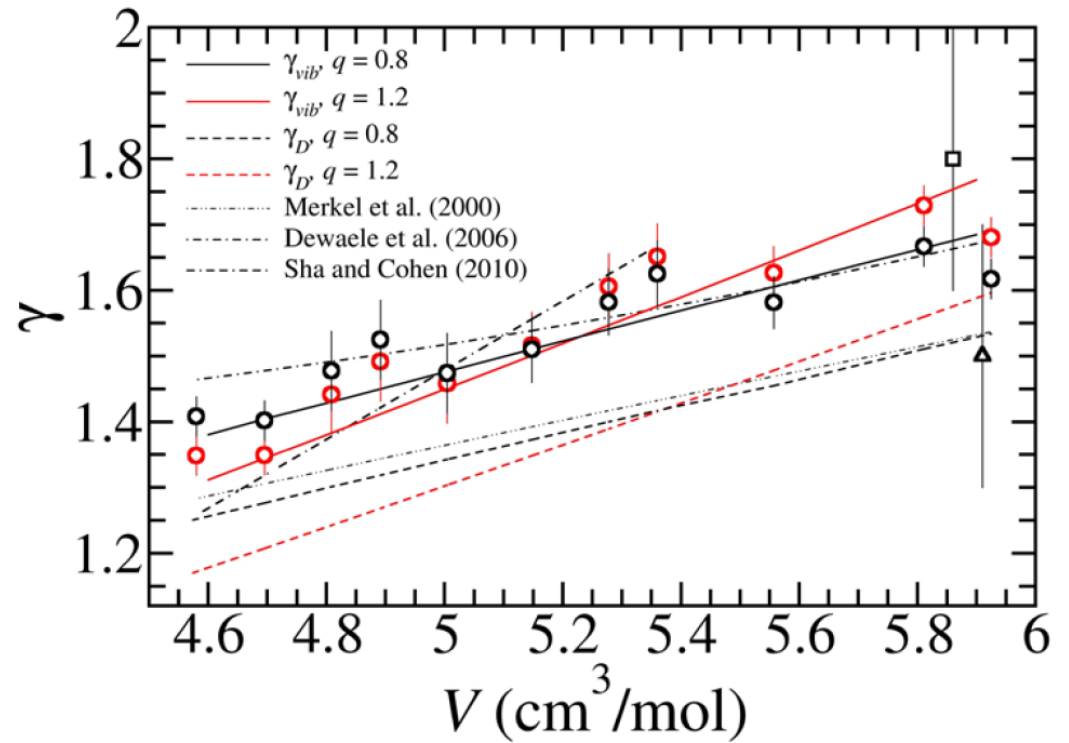
- The Grüneisen parameter describes the increase in internal pressure, caused by heating a material at constant volume. It is the coefficient relating thermal pressure to thermal energy per unit volume:

$$\Delta P_{th} = \gamma_{th} \left(\frac{\Delta U}{V} \right)$$

Phonon DOS for *hcp*-iron and the Grüneisen parameter



$$\Delta P_{vib} = \gamma_{vib} \left(\frac{\Delta U_{vib}}{V} \right)$$



Murphy *et al.* (*GRL* 2011; *PEPI* 2011);
Murphy *et al.* (*JGR* 2013)

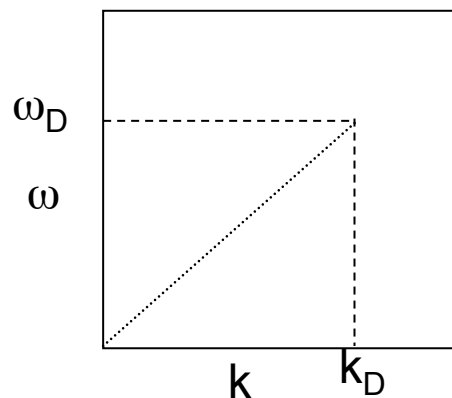
Approximations for vibrational energy (thermal pressure)

$$P = -\left(\frac{\partial F}{\partial V}\right)_T = -\left(\frac{\partial F_{elastic}}{\partial V}\right)_T - \left(\frac{\partial F_{phonon=vib}}{\partial V}\right)_T$$

□ Approximations to the phonon (“vib”) part:

□ Debye approximation (1912):

- Assumes all modes are acoustic: collapse DOS to one mode
- Max. radius corresponds to max cut-off frequency: $\omega_D = k_D v_D$
- Only considers monatomic case to determine k_D



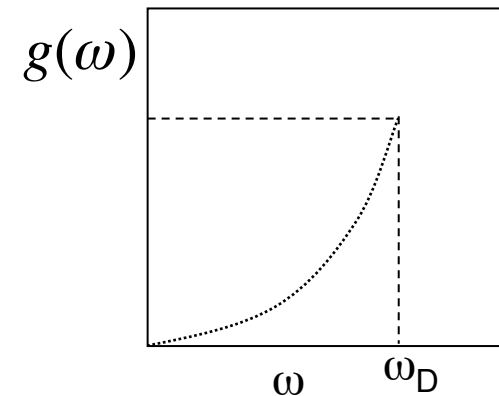
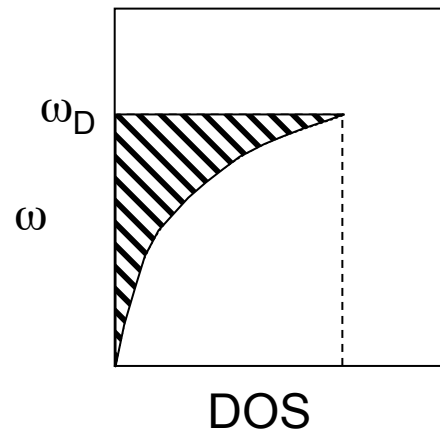
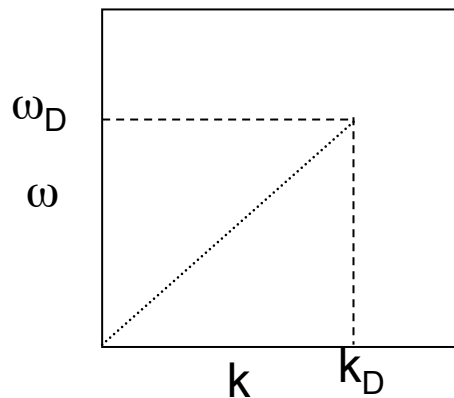
$$3/v_D^3 = 1/v_p^3 + 2/v_s^3$$

$$4/3 k_D^3 = (2\pi/a)^3$$

Debye approximation for vibrational energy

$$P_{\text{phonon=vibrational}} = F_{\text{vib}} = E_{\text{vib}} = \int_0^{\omega} \langle n \rangle \hbar \omega g(\omega) d\omega$$

- Assume 3D shape of Brillouin zone is spherical, with radius k_D



$$\text{DOS} = g(\omega) \approx B\omega_D^2/v_D^3$$

- Debye approximation to determine E_{vib} :

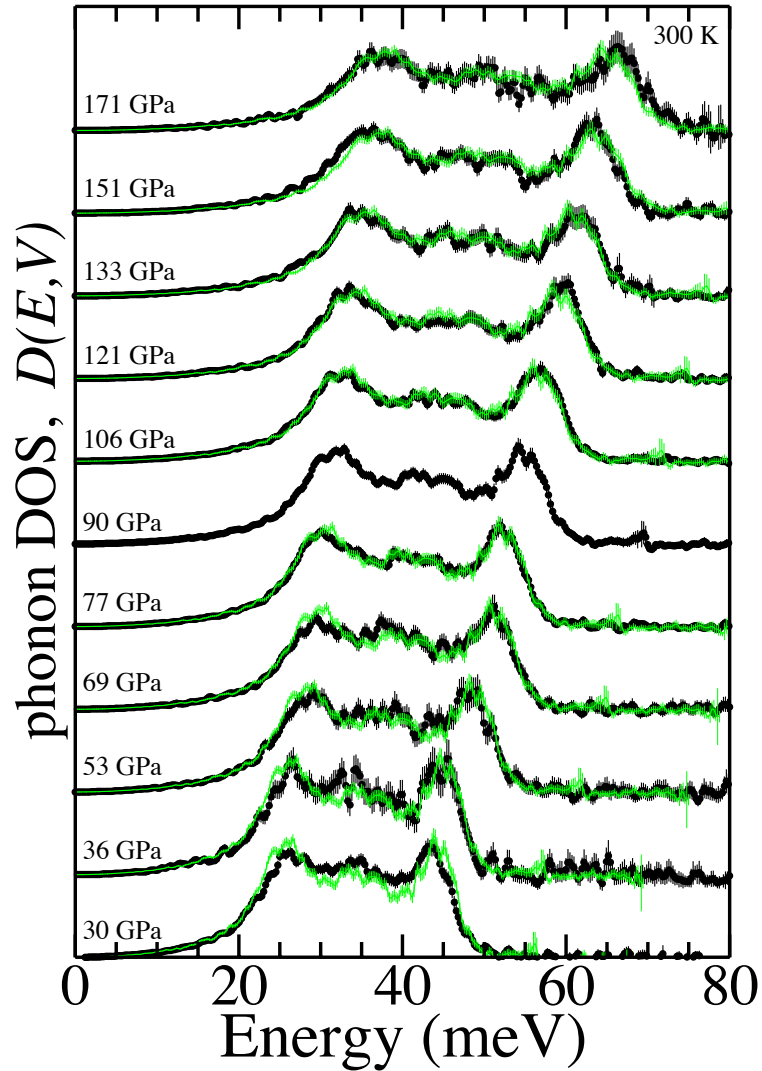
$$E_{\text{vib}} = 9nN_A k_B T x_D^{-3} \int_0^{x_D} x^3 / [\exp(x) - 1] dx, \text{ where}$$

$$x = \hbar \omega_D / k_B T$$

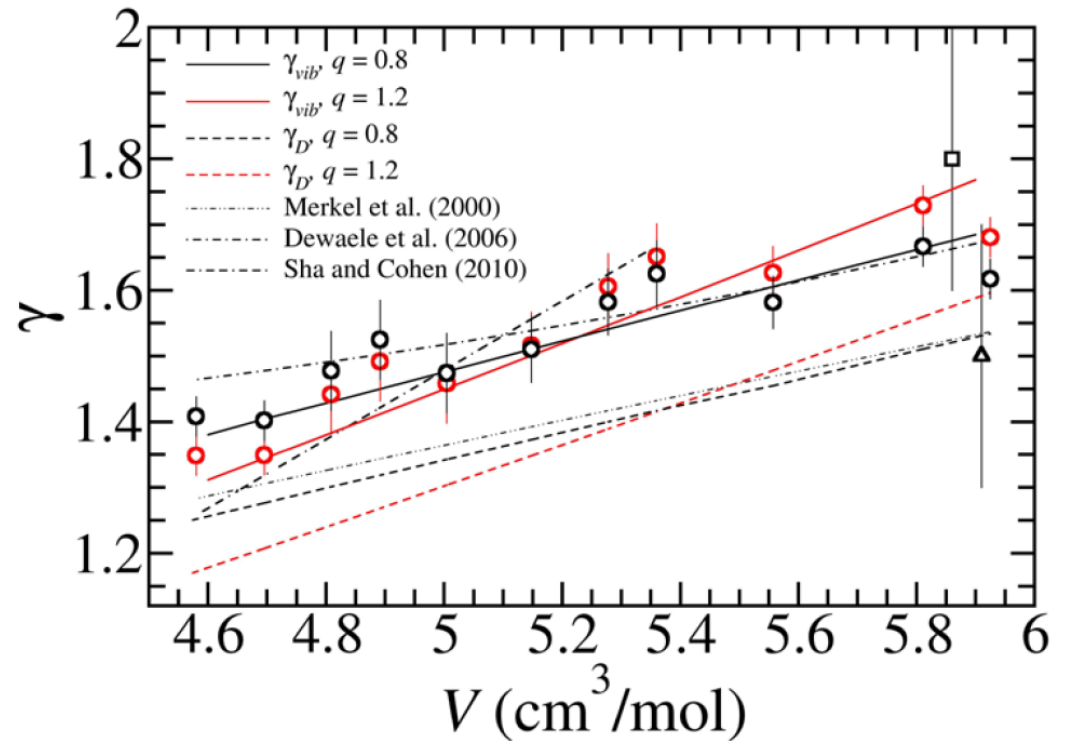
$$x_D = \theta_D / T$$

$$\theta_D = \hbar \omega_D / k_B = \text{“elastic Debye temperature”}$$

Phonon DOS for *hcp*-iron and the Grüneisen parameter



$$\gamma_{Debye} = \frac{1}{3} + \left(\frac{d \ln \left[\left(\frac{1}{v_P^3} + \frac{2}{v_S^3} \right) / 3 \right]^{-1/3}}{d \ln \rho} \right)$$



Obtaining Total Thermal Pressure (P_{th})

$$P_{th} = P_{vib} + P_{el} = - \left(\frac{\partial F_{vibrational}}{\partial V} \right)_T - \left(\frac{\partial F_{electronic}}{\partial V} \right)_T$$

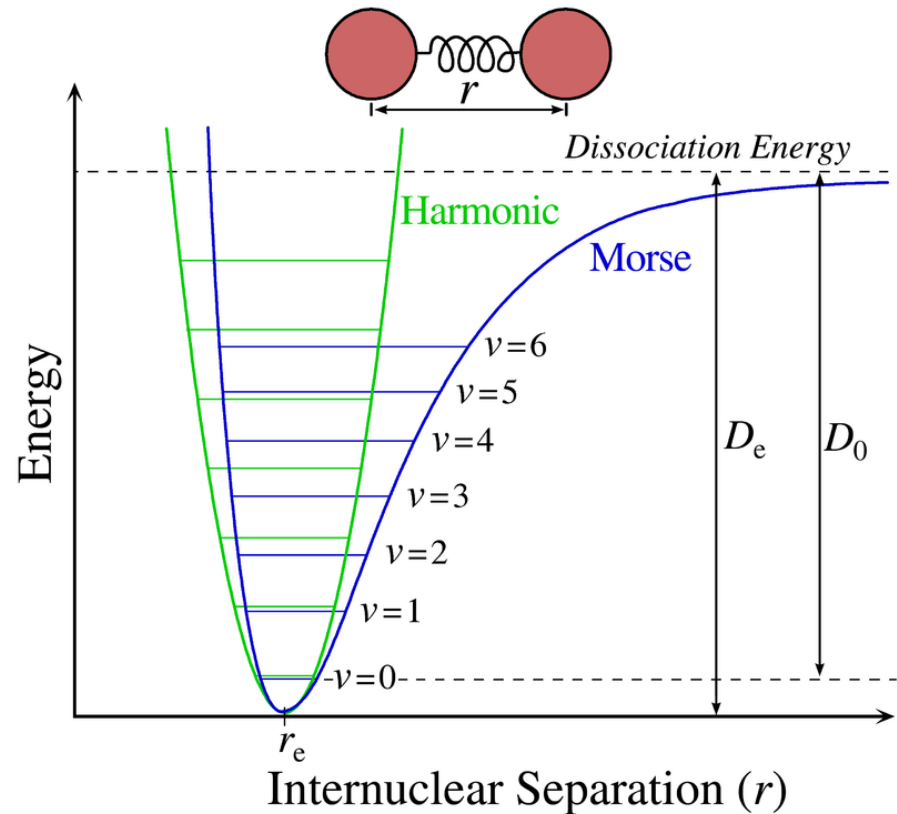
- **Phonon density of states:** provides total vibrational free energy: P_{th} and γ_{th} through volume dependence of the DOS. Requires a measurement of the phonon density of states and an electronic term. Or, estimate from Debye model.
- **Shock wave data:** one uses the conservation of energy & momentum in a shock experiment to determine the thermal pressure in the shock. Requires, in part, knowing the pressure and temperature accurately.
- **Density Functional Theory calculations:** predicts the phonon and electronic density of states for a material at different volumes. Requires the correct “functional” for all atoms.
- **PVT Measurements:** Measure volume as a function of pressure and temperature, then fit your data to a Mie-Grüneisen EOS to obtain P_{th} and γ_{th} . Less direct.

Harmonic, Anharmonic, Quasi-harmonic oscillators

- ❑ Perfect elastic material, independent of stress/strain: harmonic oscillatory
- ❑ $F=k(r-r_e)$, restoring force is proportional to elongation, and the symmetric interatomic pair potential (parabolic)
- ❑ Finite temperature: Not a perfect elastic bond. Does not obey simple harmonic motion: anharmonic.
- ❑ The mean bond length becomes longer than the equilibrium value.
- ❑ Cause of thermal expansion, Mie's potential:

$$E(r) = -\frac{a}{r^m} + \frac{b}{r^n}$$

- ❑ m: attractive force
- ❑ n: repulsive force



- ❑ Quasi-harmonic approximation: effect of T via volume change due to thermal expansion only, harmonic around around their new positions

Universal EoS

$$P = -\left(\frac{\partial F}{\partial V}\right)_T = -\left(\frac{\partial F_{elastic}}{\partial V}\right)_T - \left(\frac{\partial F_{phonon=vib}}{\partial V}\right)_T - \left(\frac{\partial F_{electronic,spin,etc}}{\partial V}\right)_T$$

- ❑ Anything with a volume term creates a pressure
- ❑ Elastic (static)
 - ❑ Describes equilibrium positions of material after it has undergone, for example: finite strain (Birch-Murnaghan)
 - ❑ Elastic = zero-energy exchange
 - ❑ Shear elasticity
 - ❑ No information on energy from vibrations (phonons) or electrons
- ❑ Vibrational (Temperature > 0 kelvin), P_{vib}
 - ❑ No information on where the equilibrium positions are
 - ❑ Describes dynamics of the system given by the phonons (PDOS)
 - ❑ deviation from equilibrium positions
 - ❑ harmonic, anharmonic
- ❑ Electronic
 - ❑ Dynamics of electronic states, e.g., conduction bands (EDOS)